



# **The Role of BCL3 in the Normal and Neoplastic Mammary Gland**

**Alison Wakefield**

**Thesis submitted for the award of PhD,  
2007-2011**



**School of Biosciences, Cardiff University, Museum Avenue, Cardiff, CF10 3US**

UMI Number: U585524

All rights reserved

INFORMATION TO ALL USERS

The quality of this reproduction is dependent upon the quality of the copy submitted.

In the unlikely event that the author did not send a complete manuscript and there are missing pages, these will be noted. Also, if material had to be removed, a note will indicate the deletion.



UMI U585524

Published by ProQuest LLC 2013. Copyright in the Dissertation held by the Author.  
Microform Edition © ProQuest LLC.

All rights reserved. This work is protected against  
unauthorized copying under Title 17, United States Code.



ProQuest LLC  
789 East Eisenhower Parkway  
P.O. Box 1346  
Ann Arbor, MI 48106-1346

# Table of Contents

<b>Table of Contents</b> .....	<b>i</b>
<b>Abstract</b> .....	<b>v</b>
<b>Acknowledgements</b> .....	<b>vi</b>
<b>Declaration</b> .....	<b>vii</b>
<b>List of Abbreviations</b> .....	<b>viii</b>
<b>Table of Figures</b> .....	<b>xii</b>
<b>Table of Tables</b> .....	<b>xv</b>
<b>Chapter 1: General Introduction</b> .....	<b>1</b>
<b>1.1 The mammary gland</b> .....	<b>2</b>
1.1.1 Introduction .....	2
1.1.2 The pregnancy cycle .....	4
1.1.3 Post-lactational mammary involution.....	4
<b>1.2 Breast Cancer</b> .....	<b>8</b>
1.2.1 Introduction .....	8
1.2.2 Breast cancer initiation and metastatic progression .....	8
1.2.3 Genetics of breast cancer.....	10
1.2.4 Gene expression profiling of breast cancer subtypes .....	11
1.2.5 Mouse models of breast cancer.....	12
1.2.6 Breast cancer stem cells.....	14
1.2.7 Treatment of breast cancer.....	16
<b>1.3 NF-<math>\kappa</math>B</b> .....	<b>19</b>
1.3.1 NF- $\kappa$ B family of transcription factors .....	19
1.3.2 NF- $\kappa$ B regulation and signalling pathways .....	20
1.3.3 Biological roles of NF- $\kappa$ B proteins .....	24
1.3.4 NF- $\kappa$ B in mammary gland development and breast cancer.....	24
<b>1.4 B-Cell Lymphoma 3</b> .....	<b>30</b>
1.4.1 Introduction .....	30
1.4.2 BCL3 structure .....	30
1.4.3 Regulation of BCL3 .....	30
1.4.4 Molecular functions of BCL3 .....	33
1.4.5 Physiological functions of BCL3.....	37
1.4.6 BCL3 and cancer .....	40
<b>1.5 Aims of this study</b> .....	<b>44</b>
<b>Chapter 2: Materials and Methods</b> .....	<b>45</b>
<b>2.1 Animal experiments</b> .....	<b>46</b>
2.1.1 Animals.....	46
2.1.2 Genotyping.....	46
2.1.3 Experimental procedures .....	49
<b>2.2 Tissue sampling and processing</b> .....	<b>50</b>
2.2.1 Removal and fixation of tissues .....	50
2.2.2 Tissue processing and sectioning for histology.....	51
<b>2.3 Histological analysis of tissue sections</b> .....	<b>52</b>

2.3.1	Haematoxylin and eosin (H&E) staining.....	52
2.3.2	Visualisation and quantification of H&E stained sections.....	52
<b>2.4</b>	<b>Immunohistochemistry (IHC).....</b>	<b>53</b>
2.4.1	Generic IHC protocol.....	53
<b>2.5</b>	<b>Cell culture maintenance and procedures.....</b>	<b>56</b>
2.5.1	Experimental cell lines.....	56
2.5.2	Maintenance of cell lines.....	57
2.5.3	Cell counting.....	57
2.5.4	Frozen storage of cells.....	57
2.5.5	Transient SiRNA transfection.....	58
2.5.6	CellTitre-blue cell viability assays.....	59
2.5.7	Trypan blue dye exclusion cell viability counts.....	59
2.5.8	Boyden chamber assays.....	60
2.5.9	Flow cytometry.....	61
2.5.10	Mammosphere assays.....	62
<b>2.6</b>	<b>Protein analysis by western blotting.....</b>	<b>63</b>
2.6.1	Protein extraction from cells.....	63
2.6.2	Protein extraction from tissues.....	63
2.6.3	Determination of protein concentrations.....	64
2.6.4	Western analysis.....	64
<b>2.7</b>	<b>Caspase assays.....</b>	<b>70</b>
2.7.1	Determination of caspase activity in mammary tissues.....	70
2.7.2	Determination of caspase activity in cells.....	70
<b>2.8</b>	<b>RNA analysis.....</b>	<b>71</b>
2.8.1	Isolation of RNA.....	71
2.8.2	Reverse transcription.....	71
2.8.3	Quantitative real-time polymerase chain reaction (QRT-PCR) & semi-quantitative PCR.....	72
<b>2.9</b>	<b>Microarray analysis.....</b>	<b>75</b>
<b>2.10</b>	<b>Statistical analysis.....</b>	<b>75</b>
<b>Chapter 3: Analysis of BCL3 Deficiency in the Murine Mammary Gland.....</b>		<b>76</b>
<b>3.1</b>	<b>Introduction.....</b>	<b>77</b>
<b>3.2</b>	<b>Results.....</b>	<b>79</b>
3.2.1	Gross mammary epithelial morphology is unaffected by the absence of BCL3 in virgin glands and during pregnancy and lactation.....	79
3.2.2	<i>Bcl3</i> displays a transient increase in expression during early involution that is dependent on STAT3.....	81
3.2.3	<i>Bcl3</i> <sup>+/-</sup> glands exhibit increased numbers of apoptotic bodies in comparison to both <i>Bcl3</i> <sup>+/+</sup> and <i>Bcl3</i> <sup>-/-</sup> glands at 18 hours involution.....	84
3.2.4	Selection of a cohort to analyse <i>Bcl3</i> <sup>+/-</sup> phenotype at the molecular level.....	88
3.2.5	<i>Bcl3</i> <sup>-/-</sup> glands display significantly less caspase 3/7 activity at 18 hours involution than <i>Bcl3</i> <sup>+/-</sup> glands.....	91
3.2.6	The percentage and distribution of NF-κB p50 and p52 subunits is unaltered in <i>Bcl3</i> <sup>-/-</sup> glands compared to <i>Bcl3</i> <sup>+/-</sup> glands at 18 hours involution.....	93
3.2.7	<i>Bcl3</i> <sup>-/-</sup> glands have the same protein levels of key regulators of involution in comparison to <i>Bcl3</i> <sup>+/-</sup> glands.....	97

3.2.8	Analysis of the expression of components of the extrinsic apoptosis pathway in <i>Bcl3</i> <sup>-/-</sup> and <i>Bcl3</i> <sup>-/-</sup> mammary glands.....	99
<b>3.3</b>	<b>Discussion.....</b>	<b>101</b>
3.3.1	Summary .....	103
<b>Chapter 4: Analysis of BCL3 Deficiency in Two <i>Neu</i> Transgenic Mouse Models .....</b>		<b>104</b>
<b>4.1</b>	<b>Introduction.....</b>	<b>105</b>
<b>4.2</b>	<b>Results.....</b>	<b>107</b>
4.2.1	BCL3 deficiency significantly delays the onset of <i>MMTV/N<sub>2</sub></i> but not <i>MMTV/NK</i> mammary adenocarcinomas .....	107
4.2.2	BCL3 deficiency does not reduce NEU (ERBB2) or EGFR protein levels.....	111
4.2.3	BCL3 depletion has no effect on tumour growth rates in <i>MMTV/N<sub>2</sub></i> or <i>MMTV/NK</i> mice ....	112
4.2.4	BCL3 deficiency does not reduce tumour burden in <i>MMTV/N<sub>2</sub></i> or <i>MMTV/NK</i> mice .....	114
4.2.5	Proliferation and apoptosis in <i>MMTV/N<sub>2</sub></i> tumours is unaffected by BCL3 deficiency .....	116
4.2.6	<i>Bcl3</i> <sup>-/-</sup> / <i>MMTV/N<sub>2</sub></i> mice develop pre-neoplastic hyperplasias that are histologically comparable to those formed in <i>Bcl3</i> <sup>+/+</sup> / <i>MMTV/N<sub>2</sub></i> mice.....	118
4.2.7	BCL3 deficiency has no effect on NF-κB p50 and p52 protein levels .....	121
4.2.8	BCL3 deficiency reduces the size and occurrence of lung metastases in ERBB2-driven tumours.....	124
4.2.9	BCL3 deficiency has a small but significant effect on the proliferation and apoptosis of <i>MMTV/N<sub>2</sub></i> metastatic lesions .....	130
<b>4.3</b>	<b>Discussion.....</b>	<b>132</b>
4.3.1	BCL3 promotes the initiation of <i>MMTV/N<sub>2</sub></i> tumours .....	132
4.3.2	BCL3 promotes the metastatic progression of <i>MMTV/N<sub>2</sub></i> tumours.....	133
4.3.3	Summary .....	134
<b>Chapter 5: Investigation into the Cell Autonomous Effects of BCL3 on ERBB2-driven Carcinogenesis.....</b>		<b>135</b>
<b>5.1</b>	<b>Introduction.....</b>	<b>136</b>
<b>5.2</b>	<b>Results.....</b>	<b>138</b>
5.2.1	<i>Bcl3</i> is highly expressed in ERBB2-positive murine mammary cancer cell lines .....	138
5.2.2	Optimisation of <i>Bcl3</i> SiRNA in MG1361 cells .....	140
5.2.3	Suppression of <i>Bcl3</i> does not affect the proliferation or apoptosis of MG1361 cells in adherent conditions.....	142
5.2.4	<i>Bcl3</i> suppression reduces the ability of MG1361 cells to metastasize to the lungs in a cell autonomous manner.....	144
5.2.5	<i>Bcl3</i> suppression reduces both the migratory and invasive capacity of MG1361 cells <i>in vitro</i> .....	146
5.2.6	Loss of <i>Bcl3</i> does not affect the anchorage-independent survival of MG1361 cells .....	148
5.2.7	Suppression of <i>Bcl3</i> does not alter epithelial-to-mesenchymal transition markers <i>in vitro</i> or <i>in vivo</i> .....	150
5.2.8	Suppression of <i>Bcl3</i> does not alter the self-renewing tumour cell population in MG1361 cells .....	152
5.2.9	Identification of BCL3 gene targets potentially involved in the metastatic process .....	161
5.2.10	QRT-PCR validation of microarray targets in MG1361 cells.....	163
5.2.11	QRT-PCR analysis of gene targets potentially regulated by BCL3 in <i>MMTV/N<sub>2</sub></i> tumours .....	165
5.2.12	Loss of BCL3 does not alter the mRNA or protein expression of Caveolin 1 in <i>MMTV/N<sub>2</sub></i> tumours.....	167

<b>5.3</b>	<b>Discussion.....</b>	<b>169</b>
5.3.1	The metastatic defect in BCL3 deficient tumour cells is due to a cell autonomous effect involving motility rather than changes in EMT or the stem/progenitor cell population.....	169
5.3.2	Gene expression profiling of <i>Bcl3</i> -deficient tumour cells reveals a combination of differentially expressed motility and invasion related genes .....	172
5.3.3	Summary .....	173
<b>Chapter 6: Analysis of BCL3 Deficiency in Human Breast Cancer Cell Lines .....</b>		<b>174</b>
<b>6.1</b>	<b>Introduction.....</b>	<b>175</b>
<b>6.2</b>	<b>Results.....</b>	<b>177</b>
6.2.1	<i>BCL3</i> is highly expressed in ERBB2-positive human breast cancer cell lines .....	177
6.2.2	Optimisation of <i>BCL3</i> SiRNA in human breast cancer cell lines .....	179
6.2.3	Suppression of <i>BCL3</i> reduces the viability of human breast cancer cell lines in adherent growth conditions .....	182
6.2.4	<i>BCL3</i> inhibition reduces the motility of human ERBB2-positive and negative breast cancer cell lines.....	184
6.2.5	Suppression of BCL3 results in a reduction in the anchorage-independent survival of ZR-75-1 cells.....	187
6.2.6	<i>BCL3</i> suppression does not alter the expression of epithelial-to-mesenchymal transition markers in MDA-MB-231 cells .....	189
6.2.7	Analysis of motility-related gene targets potentially regulated by BCL3.....	190
<b>6.3</b>	<b>Discussion.....</b>	<b>195</b>
6.3.1	<i>BCL3</i> suppression reduces the viability and migratory capacity of both EGFR- and ERBB2-positive human breast cancer cell lines .....	195
6.3.2	Summary .....	196
<b>Chapter 7: General Discussion.....</b>		<b>198</b>
<b>7.1</b>	<b>General Discussion.....</b>	<b>199</b>
<b>7.2</b>	<b>The role of BCL3 during the murine pregnancy cycle .....</b>	<b>199</b>
<b>7.3</b>	<b>The role of BCL3 in breast carcinogenesis.....</b>	<b>200</b>
7.3.1	<i>BCL3</i> and murine ERBB2-driven mammary tumour initiation .....	200
7.3.2	<i>BCL3</i> and murine ERBB2-driven metastatic progression .....	204
7.3.3	<i>BCL3</i> and human breast cancer.....	206
7.3.4	<i>BCL3</i> and the transcriptional regulation of TIMPs .....	207
<b>7.4</b>	<b>Future perspectives: targeting BCL3 as a therapeutic treatment in breast cancer? .....</b>	<b>207</b>
<b>Appendices.....</b>		<b>209</b>
<b>Bibliography .....</b>		<b>216</b>

## Abstract

The NF- $\kappa$ B family of transcription factors have previously been shown to be elevated in many malignant diseases including breast cancer. NF- $\kappa$ B activation is strongly associated with signalling downstream of the epidermal growth factor (EGF) family of receptors in both aggressive EGFR-positive and ERBB2-positive breast cancer subtypes. These observations have led to much interest in the use of NF- $\kappa$ B inhibitors to suppress tumour progression in breast cancer patients. However, as NF- $\kappa$ B controls numerous functions in homeostasis there are significant risks associated with sustained global inhibition of NF- $\kappa$ B signalling. This investigation therefore aimed to determine whether inhibition of the NF- $\kappa$ B co-factor, B-Cell Lymphoma 3 (BCL3), would block the pro-tumourigenic function of NF- $\kappa$ B, while allowing it to retain its physiological functions in normal tissues.

Deletion of BCL3 had no effect on the gross morphology or function of the mammary gland during the pregnancy cycle, although a subtle BCL3 dose-dependent effect was observed during involution whereby *Bcl3*<sup>+/-</sup> mice had increased apoptotic bodies in comparison with both *Bcl3*<sup>+/+</sup> and *Bcl3*<sup>-/-</sup> mice. Loss of BCL3 in the context of ERBB2-driven murine mammary carcinogenesis resulted in a significant delay in both the initiation and metastatic progression of mammary adenocarcinomas. Further *in vitro* investigation revealed that *Bcl3* suppression by siRNA in a murine mammary ERBB2-positive cell line reduced both the migratory and invasive capacity of cells, indicating that BCL3 was able, at least in part, to exert a pro-metastatic effect in a cell autonomous manner. In addition, siRNA suppression of *BCL3* reduced both the proliferative and migratory capacity of both ERBB2-positive and EGFR-positive human breast cancer cell lines. Collectively, these results suggest that targeting BCL3 may be an effective therapeutic strategy in the treatment of both ERBB2- and EGFR-positive breast cancers.

# Acknowledgements

Firstly, all my thanks and praise goes to God for His amazing grace, goodness and unfailing love. He is my refuge and salvation. I thank Him for the countless blessings in my life, including providing me with all of the people listed below, plus many more, who have supported and encouraged me through the last three and a half years. May this work bring Him glory.

I would like thank my supervisor, Dr. Richard Clarkson. He has provided invaluable support and advice throughout my PhD for which I will always be hugely grateful. It has been a great privilege to work in his lab and I will miss it very much. I am also extremely thankful to all of the past and present members of the Clarkson Lab, in particular Dawn Croston for her technical expertise and friendship in my first year, Nuria Marquez-Almuina for her help with QRT-PCR experiments and for introducing me to all things Spanish, Nader Omidvar for his scientific advice and for sharing his extensive knowledge on most things, Luke Piggott for his assistance with FACs analysis and being generally entertaining, Syn Kok Yeo for always being willing to help with anything and James Knight for helping me to understand chemistry just a little bit more. I would also like to thank Hannah Jones and Amelie Montagne for their assistance with immunohistochemical analysis and for being great students.

I am extremely thankful to Derek Scarborough in the Biosciences Histology Unit for processing all tissue samples and to Kirsty Richardson for her help with FACs experiments. In addition, I would like to thank all of the staff in the animal facility at Cardiff University who expertly looked after my mice on a day to day basis. I am especially grateful to Helen Read for being such an efficient animal technician and for her extensive technical expertise from which I have greatly benefited. I would also like to thank Andrew Stuart for teaching me how to perform tail vein experiments which was not an easy task.

I would like to thank everyone on the fourth and fifth floor of Biosciences 3 for all of their technical advice, for their willingness to share equipment and for generally making my time as a PhD student such an enjoyable experience. I will very much miss working with them all.

I would like to thank my fantastic friends for all their support throughout my PhD. I have been overwhelmed by their kindness to me, particularly in the last few months of writing up. The coffee, cereal and chocolate deliveries have been greatly appreciated and I am looking forward to thanking each one of my friends personally 'post PhD'. I am particularly thankful to Adam Fairman or 'Mr. Excel' for giving up his time to teach me some serious Excel skills.

Finally, I am hugely grateful to my Mum and Dad who have always supported me in all that I have done. I am incredibly privileged to have such wonderful parents and am deeply thankful to God for them.

# Declaration

## DECLARATION

This work has not previously been accepted in substance for any degree and is not concurrently submitted in candidature for any degree.

Signed ..... *A. Vesterfeld* ..... (candidate) Date ..... *08/08/2011* .....

## STATEMENT 1

This thesis is being submitted in partial fulfillment of the requirements for the degree of PhD.

Signed ..... *A. Vesterfeld* ..... (candidate) Date ..... *08/08/2011* .....

## STATEMENT 2

This thesis is the result of my own independent work/investigation, except where otherwise stated. Other sources are acknowledged by explicit references.

Signed ..... *A. Vesterfeld* ..... (candidate) Date ..... *08/08/2011* .....

## STATEMENT 3

I hereby give consent for my thesis, if accepted, to be available for photocopying and for inter-library loan, and for the title and summary to be made available to outside organisations.

Signed ..... *A. Vesterfeld* ..... (candidate) Date ..... *08/08/2011* .....

## List of Abbreviations

ABC	Avidin-Biotin Complex
ALDH1	Aldehyde dehydrogenase 1
AML	Acute Myeloid Leukaemia
AP1	Activator protein 1
ARD	Ankyrin Repeat Domains
ARHGDI2	Rho GDP dissociation inhibitor 2
BAFF	B-cell-activating factor of the TNF family
BAR1	BRCA1-associated RING domain protein 1
BCL2	B-cell Lymphoma 2
BCL3	B-cell Lymphoma 3
BLG	$\beta$ -lactoglobulin
BSA	Bovine serum albumin
C/EBP $\delta$	CCAAT/enhancer-binding protein $\delta$
cAMP	Cyclic adenosine monophosphate
CAV1	Caveolin 1
CBP	cAMP response element protein
CC3	Cleaved caspase 3
cDNA	complementary deoxyribonucleic acid
c-FLIP	Cellular FLICE inhibitory protein
c-flip	Cellular FLICE-inhibitory protein
ChIP	Chromatin immunoprecipitation
c-IAP	Cellular inhibitor of apoptosis
CMF	Cyclophosphamide, Methatrexate, Fluorouracil
Co-IP	Co-immunoprecipitation
COX2	Cyclooxygenase
CREB	cAMP response element-binding
Ct	Cycle thresholds
CtBP	C-terminal binding protein
CXCL1	Chemokine (C-X-C motif) ligand 1
DAB	3,3'-diaminobenzidine
DCIS	Ductal Carcinoma In Situ
DD	Death domain
DEAB	Diethylaminobenzaldehyde
dH <sub>2</sub> O	Distilled H <sub>2</sub> O
ddH <sub>2</sub> O	Double distilled H <sub>2</sub> O
DHMEQ	Dehydroxymethylepoxyquinomicin
DMBA	Dimethyl benzanthracene
DMEM	Dulbecco's modified Eagle's medium
DMSO	Dimethyl sulfoxide
DNA	Deoxyribonucleic Acid
dNTPs	Deoxyribonucleic triphosphates
DPX	Di-n-butylPhthalate in Xylene
DR	Death receptor
EBV	Epstein-Barr virus
ECM	Extracellular Matrix
EDTA	Ethylene diamine tetraacetic acid
EGF	Epidermal growth factor
EGFR	Epidermal growth factor receptor
EGTA	Ethylene glycol tetraacetic acid

ELAM- 1	Endothelial leukocyte adhesion molecule 1
EMT	Epithelial-to-mesenchymal transition
Epo	Erythropoietin
ER	Oestrogen receptor
ERBB2-4	v-erb-b2 erythroblastic leukemia viral oncogene homolog 2-4
ERK	Extracellular signal-regulated kinase
Ets	E-twenty six
FACS	Fluorescence activated cell sorting
FAIM	Fas apoptotic inhibitory molecule
FBS	Foetal bovine serum
FEC	Fluorouracil, Epirubicin, Cyclophosphamide
FITC	Fluorescein isothiocyanate
FOXA1	Forkhead box protein A1
GAB1	GRB2-associated-binding protein
G-CSF	Granulocyte colony-stimulating factor
GM-CSF	Granulocyte-macrophage colony-stimulating factor
GRB7	Growth factor receptor bound-protein 7
GSK3	Glycogen synthase kinase 3
H&E	Haematoxylin and eosin
HATs	Histone acetyl transferases
HDAC	Histone deacetylase
HER2	Human epidermal growth factor receptor 2
HGF	Hepatocyte growth factor
HRP	Horseradish peroxidase
ICAM-1	Intercellular adhesion molecule 1
IGF-1	Insulin-like growth factor-1
IGF1R	Insulin-like growth factor 1 receptor
IGFBP	Insulin-like growth factor binding protein
IHC	Immunohistochemistry
IKK	Inhibitor of KappaB Kinase
IL	Interleukin
INF $\gamma$	gamma interferon
I $\kappa$ B	Inhibitors of NF- $\kappa$ B
JAB1	Jun activating binding protein
JAK-STAT	Janus kinase and signal transducer and activator of transcription
K14	Cytokeratin 14
LIF	Leukaemia inhibitory factor
LMP1	Latent membrane protein-1
LPS	Lipopolysaccharide
LT $\beta$	Lymphotoxin $\beta$
LZ	Leucine zipper
mAb	Monoclonal antibody
MAPK	Mitogen-activated protein kinase
MEBM	Mammary epithelial basal medium
MEEBO	Mouse Exonic Evidence Based Oligonucleotide
MEK	Mitogen-activated protein kinase kinase
MET	Mesenchymal –to-epithelial transition
MiRNAs	Micro-RNAs
MMPs	Matrix metalloproteinases
MMTV	Mouse mammary tumour virus
MMTV-LTR	Mouse mammary tumour virus long terminal repeat

mRNA	Messenger Ribonucleic acid
mTOR	Mammalian target of rapamycin
MYC	Myelocytomatosis
N2	Wild-type Neu transgene
NCBI	National Centre for Biotechnology Information
NEMO	NF- $\kappa$ B essential modifier
NF- $\kappa$ B	Nuclear factor binding to the intronic kappa-light-chain enhancer element in B cells
NIK	NF- $\kappa$ B inducing kinase
NK	Activated Neu transgene
NLS	Nuclear localisation sequence
NME1-4	Non-metastatic cells 1-4
NOS	Nitric oxide synthases
pAb	Polyclonal antibody
PBS	Phosphate buffered saline
PCR	Polymerase chain reaction
PE	Phycoerythrin
PET	Polyethylene terephthalate
PI3K	Phosphatidylinositol 3-kinase
PLL	Poly-L-lysine
PPAR $\gamma$	Peroxisome proliferator-activated receptor gamma
PR	Progesteron receptor
PSMB1	Proteasome subunit $\beta$ type-1
PVDF	Polyvinylidene difluoride
PyVT	Polyoma middle T oncogene
QRT-PCR	Quantitative real-time polymerase chain reaction
RAB21	Ras-related protein
RHD	REL Homology Domain
RIPA	Radioimmunoprecipitation assay
RM3(E)	Rat and Mouse No.3 Expanded
RXR	Retinoid X receptor
Sca-1	Stem cell antigen
SDS	Sodium dodecyl sulphate
SDS-PAGE	Sodium dodecyl sulphate polyacrylamide gel electrophoresis
SEM	Standard error of the mean
siRNA	Small interfering RNA
SLP1	Synaptotagmin-like protein 1
SPHK2	Sphingosine kinase 2
SRC-1	Steroid receptor co-activator 1
STAT	Signal transducer and activator of transcription
TAD	Transactivation domain
TAM	Tumour associated macrophages
TBE	Tris-Borate-EDTA
TBLR1	Transducin $\beta$ -like 1X-related protein 1
TBP	TATA binding protein
TCFAP2	Transcription factor AP-2 gamma
TCR	T-cell receptor
TEBs	Terminal end buds
TEMED	N'N'N'N' tetra methyl ethylene diamine
TFIIA-B	Transcription factor IIA-B
TGF	Transforming growth factor
TIC	Tumour initiating cells

TIMPs	Tissue inhibitors of metalloproteinases
TIP60	60 kDa Tat-interactive protein
TKI	Tyrosine kinase inhibitor
TLR	Toll-like receptor
TNFR	Tumour necrosis factor receptor
TNF $\alpha$	Tumour necrosis factor $\alpha$
TWEAK	TNF-like Weak inducer of apoptosis
VCAM-1	Vascular cell adhesion molecule 1
VEGF	Vascular endothelial growth factor
WAP	Whey acidic protein
Wnt	Wingless-int
WT	Wild-type
XIAP	X-linked inhibitor of apoptosis protein

# Table of Figures

Figure 1.1: Development of the adult virgin murine mammary gland.....	3
Figure 1.2: Stages of the murine mammary gland pregnancy cycle .....	5
Figure 1.3: Signalling events during involution .....	6
Figure 1.4: Stages of metastatic progression .....	9
Figure 1.5: EGFR and ERBB2-driven signalling pathways and target-based agents in development for breast cancer treatment.....	17
Figure 1.6: Structural domains of the NF-κB and IκB family of proteins.....	19
Figure 1.7: Canonical and non-canonical NF-κB signalling pathways.....	21
Figure 1.8: NF-κB target genes involved in the pathogenesis of cancer .....	26
Figure 1.9: Targets of NF-κB inhibitors .....	29
Figure 1.10: Structure of the BCL3 protein.....	31
Figure 3.1: Loss of BCL3 has no effect on the gross morphology of the mammary gland .....	80
Figure 3.2: <i>Bcl3</i> expression transiently increases in response to STAT3 signalling at 18 hours involution	83
Figure 3.3: Histological analysis of <i>Bcl3</i> <sup>+/+</sup> , <i>Bcl3</i> <sup>+/-</sup> and <i>Bcl3</i> <sup>-/-</sup> glands at 12, 18, 24 and 48 hours involution	85
Figure 3.4: <i>Bcl3</i> <sup>+/-</sup> glands display increased apoptotic bodies in comparison to <i>Bcl3</i> <sup>+/+</sup> and <i>Bcl3</i> <sup>-/-</sup> glands at 18 hours involution.....	86
Figure 3.5: <i>Bcl3</i> <sup>+/-</sup> glands exhibit significantly more apoptotic bodies at 18 hours involution in comparison to <i>Bcl3</i> <sup>-/-</sup> glands .....	87
Figure 3.6: Milk stasis grading scale .....	89
Figure 3.7: <i>Bcl3</i> <sup>-/-</sup> glands have significantly less shed apoptotic bodies at 18 hours involution than <i>Bcl3</i> <sup>+/-</sup> glands from the chosen cohort.....	90
Figure 3.8: <i>Bcl3</i> <sup>-/-</sup> mammary glands have significantly less caspase 3/7 activity than <i>Bcl3</i> <sup>+/-</sup> glands .....	92
Figure 3.9: The distribution and percentage of p50 and p-p50 <sup>ser337</sup> positively stained epithelial cells is unchanged in <i>Bcl3</i> <sup>-/-</sup> glands compared to <i>Bcl3</i> <sup>+/-</sup> glands.....	95
Figure 3.10 The distribution and percentage of p52 and p-p52 <sup>ser222</sup> positively stained epithelial cells is unchanged in <i>Bcl3</i> <sup>-/-</sup> glands compared to <i>Bcl3</i> <sup>+/-</sup> glands.....	96
Figure 3.11: <i>Bcl3</i> <sup>-/-</sup> glands exhibit comparable protein levels of key initiators of involution to <i>Bcl3</i> <sup>+/-</sup> glands .....	98
Figure 3.12: <i>Bcl3</i> <sup>-/-</sup> mammary glands have significantly increased Faim expression in comparison to <i>Bcl3</i> <sup>+/-</sup> glands.....	100
Figure 4.1: Loss of BCL3 has no effect on the latency or histology of <i>MMTV/NK</i> induced mammary adenocarcinomas .....	109
Figure 4.2: Loss of BCL3 results in the delayed onset of <i>MMTV/N<sub>2</sub></i> mammary adenocarcinomas.....	110

Figure 4.3: Loss of BCL3 does not reduce NEU or EGFR protein levels .....	111
Figure 4.4: Loss of BCL3 has no effect on the growth rates of <i>MMTV/N<sub>2</sub></i> or <i>MMTV/NK</i> mammary adenocarcinomas .....	113
Figure 4.5: BCL3 deficiency has no effect on the tumour burden of <i>MMTV/NK</i> or <i>MMTV/N<sub>2</sub></i> mice .....	115
Figure 4.6: Proliferation and apoptosis is unaffected by BCL3 deficiency in <i>MMTV/N<sub>2</sub></i> tumours .....	117
Figure 4.7: Loss of BCL3 does not affect the formation of pre-neoplastic hyperplasias.....	119
Figure 4.8: Loss of BCL3 does not affect the proliferation of pre-neoplastic tissues.....	120
Figure 4.9: Loss of BCL3 does not affect the expression of p50 or p52 in the nuclear or cytoplasmic fractions of <i>MMTV/N<sub>2</sub></i> tumours.....	123
Figure 4.10: BCL3 deficiency reduces the size and occurrence of lung metastases.....	126
Figure 4.11: BCL3 deficiency does not alter the gross histology of <i>MMTV/N<sub>2</sub></i> driven lung metastases ...	127
Figure 4.12: BCL3 deficiency does not significantly reduce the size or number of <i>MMTV/NK</i> driven lung metastases.....	128
Figure 4.13: BCL3 deficiency does not affect the gross histology of <i>MMTV/NK</i> driven lung metastases.	129
Figure 4.14: Loss of BCL3 reduces the rates of proliferation and apoptosis in <i>MMTV/N<sub>2</sub></i> metastatic lesions .....	131
Figure 5.1: <i>Bcl3</i> expression is highest in ERBB2-positive murine mammary cancer cell line.....	139
Figure 5.2: <i>Bcl3</i> SiRNA efficiently suppresses <i>Bcl3</i> mRNA expression in MG1361 cells .....	141
Figure 5.3: Suppression of <i>Bcl3</i> does not affect the proliferation or apoptosis of murine MG1361 cancer cell lines in adherent growth conditions .....	143
Figure 5.4: <i>Bcl3</i> deficient cells are less able to seed in the lungs in an experimental metastases model	145
Figure 5.5: <i>Bcl3</i> suppression reduces the migratory and invasive capacity of MG1361 murine mammary cancer cells .....	147
Figure 5.6: <i>Bcl3</i> suppression does not affect the anchorage-independent survival of MG1361 murine mammary cancer cells.....	149
Figure 5.7: Loss of <i>Bcl3</i> does not alter markers of EMT .....	151
Figure 5.8: <i>Bcl3</i> suppression has no effect on the formation of primary or secondary mammospheres.	155
Figure 5.9: Loss of <i>Bcl3</i> results in an insignificant reduction in the ALDH1-positive population in MG1361 murine mammary cancer cells .....	158
Figure 5.10: The CD24+/SCA1- population enriches for mammospheres in MG1361 cells.....	159
Figure 5.11: <i>Bcl3</i> suppression increases the CD24+ population in MG1361 cells.....	160
Figure 5.12: Selection of MG1361 RNA samples for microarray analysis .....	162
Figure 5.13: BCL3 regulates the transcription of a variety of motility- and invasion-related genes.....	164
Figure 5.14: QRT-PCR analysis of motility- and invasion- related genes in <i>MMTV/N<sub>2</sub></i> tumours.....	166

Figure 5.15: BCL3 does not regulate Caveolin 1 in late stage <i>MMTV/N<sub>2</sub></i> tumours .....	168
Figure 6.1: <i>BCL3</i> expression correlates with high ERBB2 rather than EGFR protein levels.....	178
Figure 6.2: <i>BCL3</i> SiRNA efficiently suppresses <i>BCL3</i> mRNA expression in MDA-MB-231 cells .....	180
Figure 6.3: <i>BCL3</i> SiRNA efficiently suppresses <i>BCL3</i> expression in HCC1954, ZR-75-1 and SKBR3 cells ...	181
Figure 6.4: <i>BCL3</i> suppression reduces the viability of MDA-MB-231, ZR-75-1 and SKBR3 cells .....	183
Figure 6.5 <i>BCL3</i> suppression reduces the migratory capacity of ERBB2-negative, EGFR-positive human breast cancer cell lines .....	185
Figure 6.6: <i>BCL3</i> suppression reduces the migratory capacity of SKBR3 cells but not HCC1954 cells.....	186
Figure 6.7: <i>BCL3</i> suppression results in a significant reduction in the viability of ZR-75-1 cells in anchorage-independent conditions .....	188
Figure 6.8: <i>BCL3</i> suppression has no effect on the expression EMT markers in MDA-MB-231 cells.....	189
Figure 6.9: QRT-PCR analysis of <i>NME</i> genes in <i>BCL3</i> suppressed human breast cancer cell lines.....	192
Figure 6.10: <i>BCL3</i> suppression increases the mRNA expression of <i>TIMP</i> genes in human breast cancer cell lines.....	193
Figure 6.11: QRT-PCR analysis of motility-related genes in <i>BCL3</i> suppressed human breast cancer cell lines.....	194
Figure 7.1: Proposed model for the BCL3 mediated effects on breast cancer initiation and progression .....	203

# Table of Tables

Table 1.1: Promoters used to drive oncogenes to the mammary epithelium.....	12
Table 1.2: Examples of inducers of BCL3 expression.....	31
Table 2.1: PCR cycling conditions.....	48
Table 2.2: Genotyping primers and product sizes.....	48
Table 2.3: PCR reaction components (N2, NK, Stat3, Blg/Cre).....	49
Table 2.4: PCR reaction components (Bcl3).....	49
Table 2.5: Immunohistochemistry antibodies and conditions.....	55
Table 2.6: SiRNA reagents and concentrations.....	58
Table 2.7: Volumes and concentrations used for SiRNA transfections.....	59
Table 2.8: Seeding densities for SiRNA transfections and CellTitre Blue assays.....	59
Table 2.9: Composition of polyacrylamide gels.....	65
Table 2.10: Composition of solutions used in western analysis.....	67
Table 2.11: Western antibodies and conditions.....	68
Table 2.12: Western antibodies and conditions continued.....	69
Table 2.13: Reaction mix components for reverse transcription.....	72
Table 2.14: QRT-PCR and semi-quantitative PCR reaction components.....	73
Table 2.15: QRT-PCR primer sequences.....	74
Table 3.1: The percentage of glands displaying a high degree of stasis is the same in <i>Bcl3</i> <sup>+/-</sup> and <i>Bcl3</i> <sup>-/-</sup> mice.....	90
Table 5.1: Motility and invasion related genes regulated by BCL3.....	162
Appendix 1: Top 100 largest fold increases in gene expression following <i>Bcl3</i> suppression.....	212
Appendix 2: Top 100 largest fold decreases in gene expression following <i>Bcl3</i> suppression.....	215

# **Chapter 1:**

## **General Introduction**

## 1.1 The mammary gland

### 1.1.1 Introduction

The mammary gland is a highly complex and specialised tissue with the primary function of producing milk to provide both nutrition and immune factors to the mother's offspring. The gland achieves this function by developing an extensive network of secretory alveolar cells, interconnected by epithelial ducts, which transport milk via the nipple to the suckling young. The developmental cycle of the human and rodent mammary gland can be classified into three main stages: embryonic, pubertal and adult (reviewed in Watson and Khaled 2008). In the mouse embryo, mammary gland development occurs between embryonic day (E) 10.5 and E18 and involves the formation of a rudimentary ductal tree that originates from the nipple and extends into an adipocyte-rich stroma known as the mammary fat pad (Figure 1.1A). During the first 3 weeks after birth, terminal end buds (TEBs) appear at the tips of the ducts and invade the mammary fat pad at a rate that corresponds to body growth. At the onset of puberty, serum oestrogen levels rise and initiate extensive proliferation within the TEBs, which results in ductal elongation and branching into the fat pad. This continues until about 10-12 weeks of age, when the ducts reach the limits of the fat pad and the TEBs disappear, resulting in the formation of a complete adult virgin mammary gland.

The adult virgin murine mammary gland is composed of a variety of different cell types: epithelial cells, which form the ductal system of the gland; adipocytes, which make up the mammary fat pad in which the ductal system is embedded; stromal cells; vascular endothelial cells; and a variety of immune cells (reviewed in Richert, Schwertfeger et al. 2000). The ductal network consists of two layers of epithelial cells, luminal and basal. The luminal cells line the ducts and form the secretory alveoli, whereas the basal epithelium, composed mainly of myoepithelial cells, forms an outer layer that is in direct contact with the surrounding stroma (Figure 1.1B). The mammary gland maintains this structure until the initiation of pregnancy when it undergoes further development in preparation for providing all the nutritional and immunological support required to sustain the mother's new-born offspring.

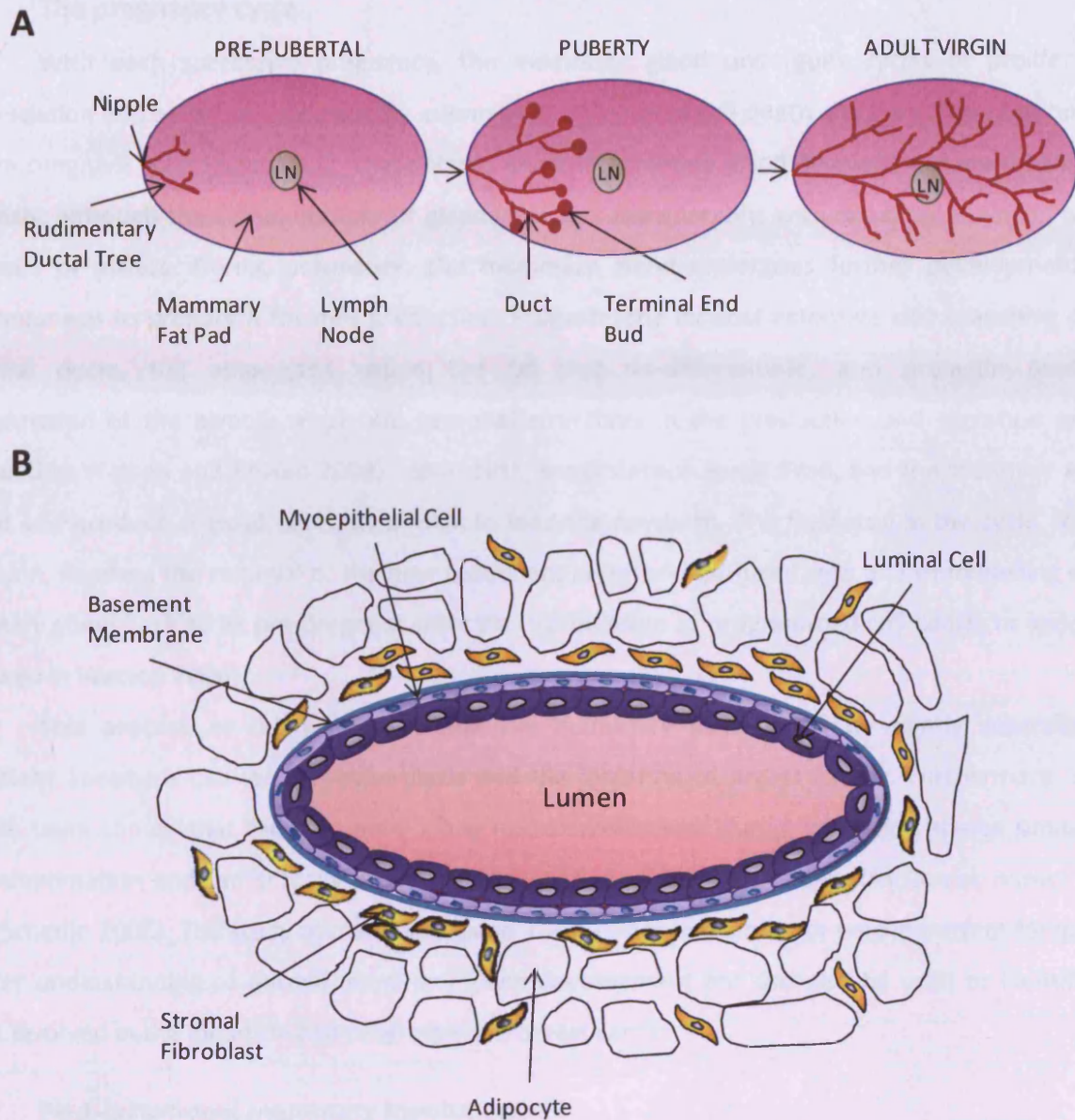


**Figure 1.1: Development of the adult virgin murine mammary gland**

Schematic of the development of the adult virgin murine mammary gland (A). The rudimentary ductal tree extends into the fat pad during puberty as a result of an increase in oestrogen and the extensive proliferation of the terminal end buds (figure adapted from Watson and Khaled 2008). Schematic representation of a cross-section through a mammary duct (B). The luminal epithelial cells line the ducts while the myoepithelial cells form an outer layer that is in contact with the surrounding stroma (figure adapted from Visvader 2009).

### 1.1.2 The pregnancy cycle

With each successive pregnancy, the mammary gland undergoes cycles of proliferation, differentiation and secretion, followed by extensive programmed cell death and de-differentiation back to a pre-pregnant state (Figure 1.2). These stages of adult mammary gland development are similar in all mammals, although the actual number of glands can vary considerably, with mice, for example, having five pairs of glands. During pregnancy, the mammary gland undergoes further development and morphogenesis to prepare it for milk production. Progesterone induces extensive side branching of the epithelial ducts, the adipocytes within the fat pad de-differentiate, and prolactin promotes differentiation of the alveoli, which are essential structures in the production and secretion of milk (reviewed in Watson and Khaled 2008). Upon birth, progesterone levels drop, and the secretory alveoli expand and produce copious amounts of milk to feed the newborn. The final step in the cycle, termed involution, involves the removal of the now redundant secretory epithelial cells and re-modelling of the mammary gland back to its pre-pregnant state via the initiation of programmed cell death, or apoptosis (reviewed in Watson 2006).

This process of cell removal within the mammary gland must be tightly controlled as insufficient apoptosis can lead to hyperplasia and the initiation of breast cancer. Furthermore, it has recently been shown that the mammary gland microenvironment during involution shares similarities with inflammation and can actually promote the metastatic properties of cells (McDaniel, Rumer et al. 2006; Schedin 2006). The study of mammary gland involution is therefore not only important for gaining a better understanding of normal mammary gland development but can also be used to identify key events involved in the initiation and progression of breast cancer.

### 1.1.3 Post-lactational mammary involution

Forced weaning studies have demonstrated that murine mammary gland involution involves two discrete stages that are characterised by the expression of specific genes (Figure 1.3) (Lund, Romer et al. 1996). The first phase lasts for 48 hours after pup removal and is reversible, allowing pups to be returned to the mother and to continue feeding. This phase is characterised by shedding of the now redundant secretory epithelial cells into the lumen of the alveoli. The second, longer phase involves the expression of a gene set that initiates the re-modelling of the gland back to an almost pre-pregnant state. During this phase, apoptosis continues and is accompanied by re-modelling of the surrounding stroma as well as re-differentiation and filling of adipocytes. Re-modelling of the gland is largely due to the activity of a specific set of matrix metalloproteinases (MMPs) that are inhibited during the first phase by tissue inhibitors of metalloproteinases (TIMPs) (Green and Lund 2005).

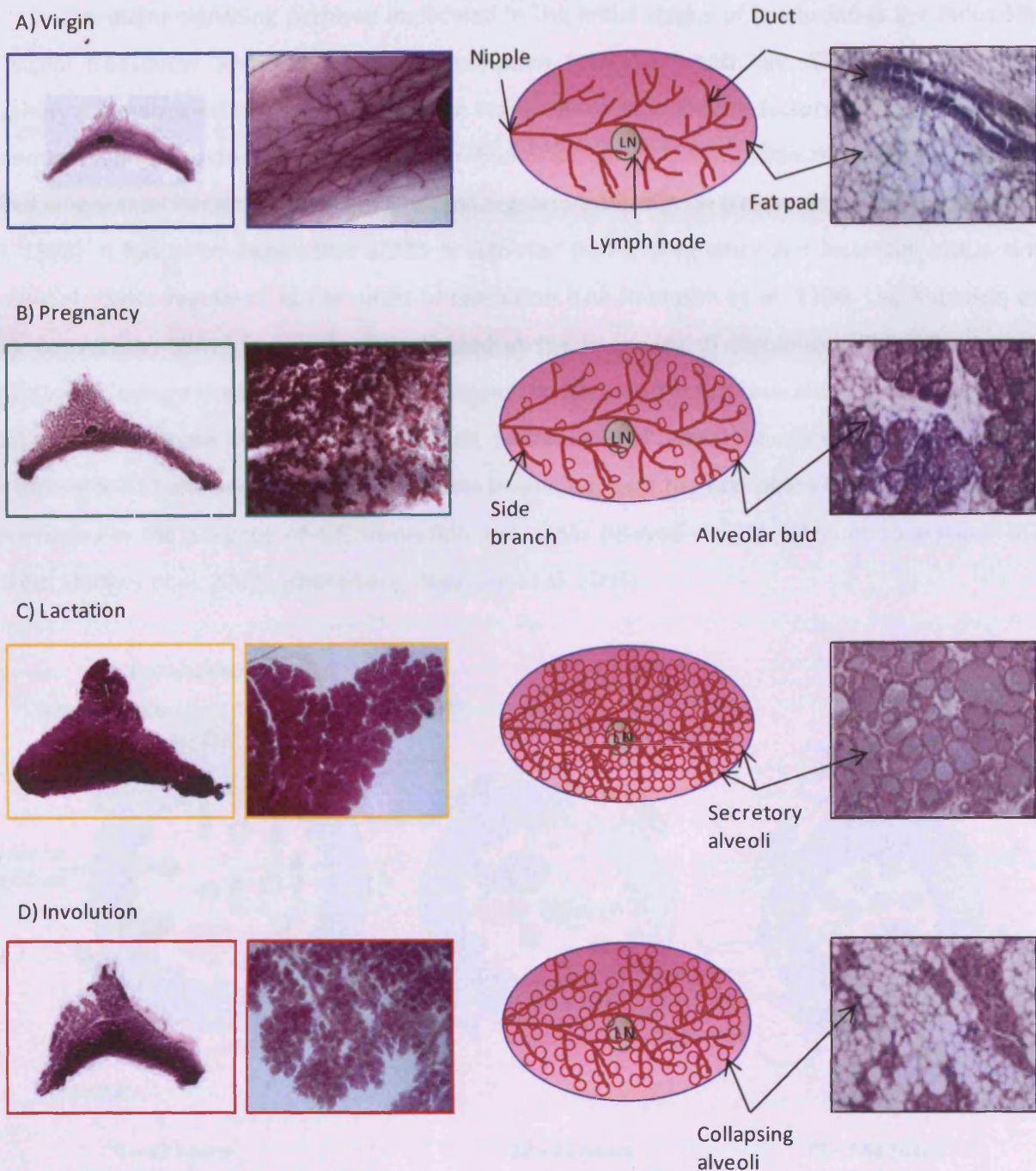


**Figure 1.2: Stages of the murine mammary gland pregnancy cycle**

Left two columns = mammary gland wholemounts, middle column = schematic representation of the mammary gland, right column haematoxylin and eosin (H&E) stained sections. The adult virgin mammary gland consists of a ductal network spread throughout the mammary fat pad (A). Epithelial ducts undergo extensive proliferation during pregnancy to form side branches and alveolar buds (B). Lactation involves the expansion of secretory epithelial cells and the production of milk (C). During involution the alveoli collapse and the redundant secretory epithelial cells undergo apoptosis (D) (figure adapted from Watson 2006).

The major signalling pathway implicated in the initial stages of involution is the Janus kinase and signal transducer and activator of transcription (JAK-STAT) pathway. STATs are activated by phosphorylation on specific tyrosine residues in response to many growth factors and cytokines such as leukaemia inhibitory factor (LIF). This results in homo- or hetero-dimerisation and translocation to the nucleus where they interact with target DNA and regulate transcription (reviewed in Heinrich, Behrmann et al. 1998). It has been shown that STAT5 is activated during pregnancy and lactation, but is almost immediately down-regulated at the onset of involution (Liu, Robinson et al. 1996; Liu, Robinson et al. 1997). Conversely, STAT3 is specifically activated at the beginning of involution (Philp, Burdon et al. 1996). Studies using a mammary-specific, conditional knock-out of *Stat3* have shown that it is critical for initiating the first phase of involution (Chapman, Lourenco et al. 1999; Humphreys, Bierie et al. 2002). Mice lacking STAT3 showed a substantial delay in involution, with the first phase being all but abolished. Furthermore, in the absence of LIF, involution was again delayed due to a failure to activate STAT3 (Kritikou, Sharkey et al. 2003; Schere-Levy, Buggiano et al. 2003).

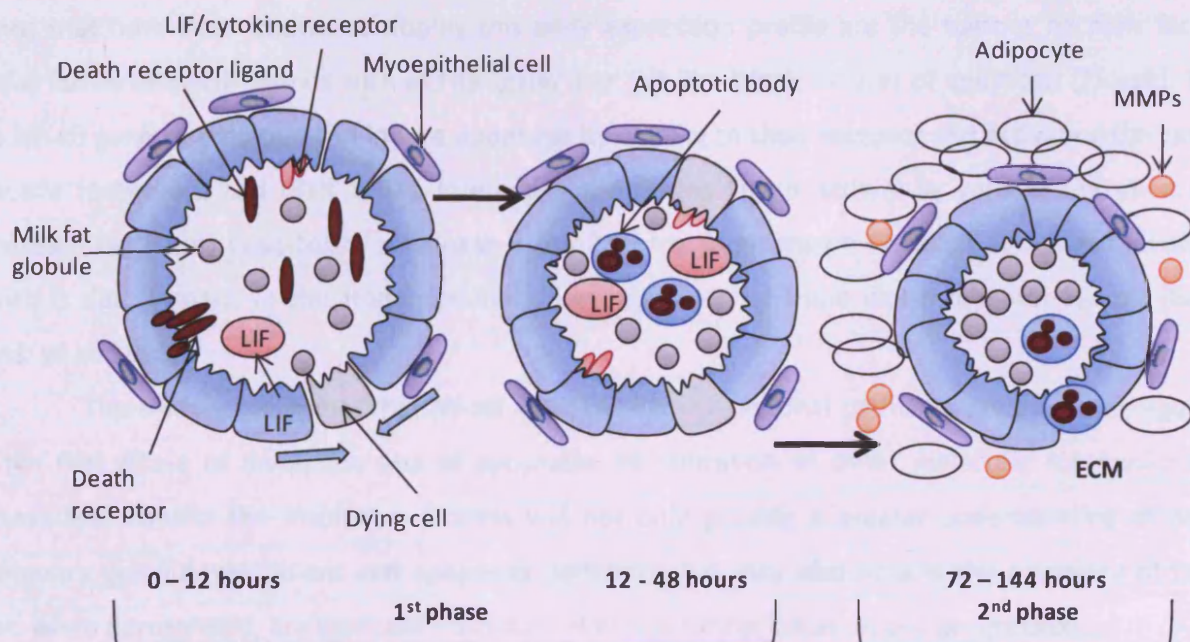


**Figure 1.3: Signalling events during involution**

Schematic of a collapsing alveoli during involution. The first phase is reversible. Milk stasis induces the secretion of LIF within 12 hours of forced weaning. This results in the phosphorylation and activation of STAT3 which induces apoptosis and the shedding of dying cells into the alveolar lumen. Neighbouring cells migrate together to fill the gap. At the same time, members of the death receptor ligand family and their receptors are up-regulated and induce apoptosis via caspase 8 activation. Transition to the second, irreversible, stage occurs by the activation of downstream targets of these pathways. MMPs break down the surrounding ECM, resulting in detachment-induced apoptosis and total collapse of the alveoli. The gland is then re-modelled back to the pre-pregnant state by the re-differentiation of adipocytes. ECM, extracellular matrix; MMP, matrix metalloproteinase, (figure adapted from Watson 2006).

Several downstream targets of STAT3 such as IGFBP-5 (insulin-like growth-factor-binding protein 5) and C/EBP $\delta$  (CCAAT/enhancer-binding protein  $\delta$ ) have been implicated in mammary gland apoptosis and involution (Tonner, Barber et al. 2002; Thangaraju, Rudelius et al. 2005), which is further evidence of the importance of the STAT3 signalling pathway in this process. Interestingly, AKT/PROTEIN KINASE B, which is normally down-regulated during involution, has been shown to provide a dominant survival signal and cause delayed involution when it is constitutively active in the mammary gland (Schwertfeger, Richert et al. 2001). The transcription factor, NF- $\kappa$ B (see section 1.3 for a detailed description of NF- $\kappa$ B), has also been shown to be up-regulated during murine mammary gland involution. This signalling pathway is activated within 1 hour of pup removal and shows maximum activation at about 3 days involution (Clarkson, Heeley et al. 2000), suggesting that it also plays an important role in the involution process.

Microarray analysis of the lactation-to-involution switch revealed a number of other genes that are up-regulated early in the onset of involution (Clarkson, Wayland et al. 2004; Stein, Morris et al. 2004). Many of these genes are either STAT3 and/or NF- $\kappa$ B transcriptional targets. An important group of genes that have been shown to display this early expression profile are the tumour necrosis factor  $\alpha$  (*Tnfa*) family of death ligands such as Fas ligand and TNF-like Weak inducer of apoptosis (*Tweak*). These are NF- $\kappa$ B gene targets that can induce apoptosis by binding to their receptor and activating the caspase cascade (Ashkenazi and Dixit 1998). Interestingly, reducing NF- $\kappa$ B activity by genetic alteration of its upstream regulator, Inhibitor of  $\kappa$ B Kinase  $\beta$  (*Ikk-2/ $\beta$* ) has been shown to result in delayed involution, which is due, in part, to the transcriptional down-regulation of these death receptor ligands (Baxter, Came et al. 2006).

The evidence suggests that NF- $\kappa$ B and STAT3 transcriptional pathways are essential regulators of the first phase of involution and of apoptosis. Identification of other molecular mechanisms and factors that control the involution process will not only provide a greater understanding of normal mammary gland development and apoptosis pathways, but may also help in the discovery of factors that, when deregulated, are essential mediators of breast cancer initiation and progression.

## 1.2 Breast Cancer

### 1.2.1 Introduction

Cancer is initiated via a multistage process involving the acquisition of oncogenic signals that accumulate through genetic and epigenetic mutations in gene expression and/or function. Hanahan & Weinberg (2000) proposed that there are six essential alterations in cell physiology that determine malignant cell growth. These so-called 'hallmarks of cancer' are defined as self-sufficiency in growth signals, insensitivity to growth-inhibitory signals, evasion of apoptosis, limitless replicative potential, sustained angiogenesis, and tissue invasion and metastases (Hanahan and Weinberg 2000). As the cell acquires each of these novel capabilities during tumour development, it is able to successfully overcome the anticancer defence mechanisms that are intrinsic to every cell and tissue.

Breast cancer is an important disease not only because it is now the most common female malignancy in the U.K., with more than 44,000 women being diagnosed each year (CancerResearchUK 2007), but also because of its biological complexity and heterogeneity. Although the early detection and treatment of breast cancer has improved considerably, still about 50% of patients eventually die of the disease (reviewed in Caldas and Aparicio 2002). In most cases, death is due to resistance to therapy and the formation of metastases.

### 1.2.2 Breast cancer initiation and metastatic progression

The majority of cancers originate from the epithelium lining the mammary ducts or lobules and are histologically classified as mammary ductal or lobular carcinoma (Bombonati and Sgroi 2011). Several linear models of breast cancer initiation and progression exist. The model for the ductal subtype proposes that neoplasia initiates in the normal ductal epithelium, progresses to flat epithelial atypia, advances to atypical ductal hyperplasia, followed by ductal carcinoma *in situ*, and culminates as invasive ductal carcinoma (Wellings, Jensen et al. 1975; Wellings and Jensen 1973; Oyama, Maluf et al. 1999; Oyama, Iijima et al. 2000). A similar multi-stage model has been proposed for mammary lobular carcinoma and involves the progression from normal lobular epithelium, to atypical lobular hyperplasia, followed by lobular carcinoma *in situ* which finally results in invasive lobular carcinoma (Page, Dupont et al. 1985).

Primary breast tumours are currently being treated with increasing degrees of success. However, many tumours are not completely eradicated by local and systemic therapy, and will relapse, often leading to the development of invasive metastatic carcinoma. Metastatic disease is a complex phenomenon in which cells must detach from the primary tumour, invade the surrounding stroma, and enter and survive in the vasculature before extravasating out of the circulation and colonising at distant sites (Figure 1.4). Metastatic progression is aided by the process of epithelial-to-mesenchymal transition

(EMT), a type of cell plasticity whereby epithelial cells acquire a more mesenchymal morphology with an increased capacity to migrate (for review, see Thiery 2002). Secondary metastatic sites in breast cancer may differ between subtypes of the disease, but are most commonly found in the lung, pleura, liver and bone (Lee 1983).

Breast cancer initiation and metastatic progression depends upon the activation and inhibition of numerous signalling pathways and their downstream targets, many of which are currently poorly understood. A great deal of research is focused on elucidating these signalling pathways to enable therapeutic targeting of the underlying cellular mechanisms involved in the pathogenesis of the disease.

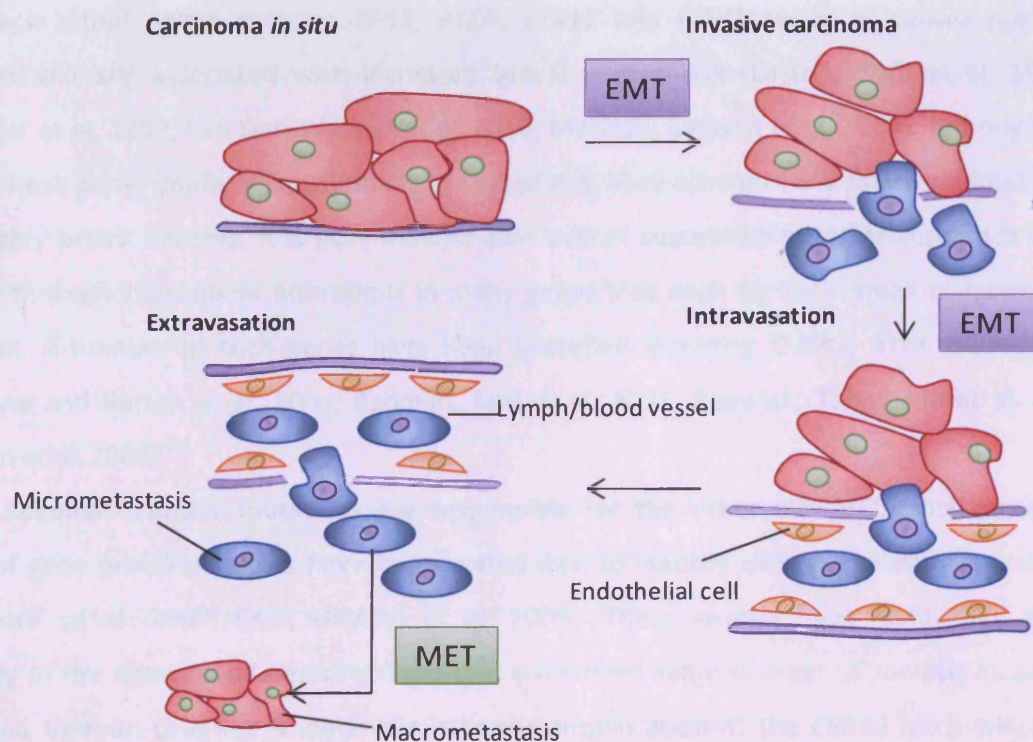


**Figure 1.4: Stages of metastatic progression**

Carcinoma *in situ* is maintained locally by the surrounding basement membrane. Alterations, such as EMT, whereby epithelial cells acquire a more mesenchymal morphology, lead to the detachment of carcinoma cells from the primary tumour, through the basement membrane and into the surrounding stroma. Cells are then able to intravasate through blood vessel walls and into the bloodstream, which allows their passive transport to distant organs. At secondary sites, solitary cancer cells can extravasate out of the circulation and remain solitary (micrometastasis), or they can undergo MET, the reversion back to an epithelial morphology, and form a new carcinoma. EMT, epithelial-to-mesenchymal transition; MET, mesenchymal-to-epithelial transition (figure adapted from Thiery 2002).

### 1.2.3 Genetics of breast cancer

A number of risk factors for the disease, including early menarche, late menopause, nulliparity and a positive family history have been identified (Claus, Risch et al. 1990). It is estimated that hereditary breast cancers make up 5-10% of all cases of the disease and are generally attributable to high-penetrance susceptibility genes including *BRCA1* and *BRCA2* (Miki, Swensen et al. 1995; Easton, Ford et al. 1993). Disease-causing mutations in either of these two genes result in inactivation of the encoded proteins which, when functioning normally, are involved in metabolic processes such as DNA damage repair and cell cycle control (Venkitaraman 2002; Bertwistle and Ashworth 1998). Mutations in *BRCA1* and *BRCA2* genes account for approximately 16% of the hereditary breast cancer risk. Germline mutations in other genes such as *TP53*, *PTEN*, *STK11* and *CDH1* result in cancer pre-disposition syndromes and are associated with increased breast cancer risk (Easton, Ford et al. 1993; Lynch, Ostermeyer et al. 1997; van Lier, Wagner et al. 2010; Masciari, Larsson et al. 2007). Although mutations in any of these genes confer a substantially increased risk, they account for a relatively small proportion of hereditary breast cancers. It is now thought that overall susceptibility to the disease is likely to be mediated through subsequent alterations in many genes that each confer a small to moderate breast cancer risk. A number of such genes have been identified including *CHEK2*, *ATM*, *BRIP1*, and *PALB2* (Nevanlinna and Bartek et al. 2006; Rahman, Seal et al. 2007; Renwick; Thompson et al. 2006; Seal, Thompson et al. 2006).

Acquired somatic mutations are responsible for the other 90% of breast cancer cases. A number of gene profiling studies have been undertaken to identify clinically relevant mutations (Chin, Teschendorff et al. 2007; Chin, DeVries et al. 2006). These studies have highlighted the genetic complexity of the disease and demonstrated that a relatively large number of somatic mutations drive each breast tumour. One key somatic aberration is amplification of the *ERBB2* locus which occurs in approximately 20% of all human breast cancers and leads to a clinically aggressive subtype of the disease (Paik, Hazan et al. 1990). Further sequencing studies have identified a large number of point mutations that are present in breast tumours (Greenman, Stephens et al. 2007; Wood, Parsons et al. 2007). These include high-frequency mutations in *TP53* (53%), *PIK3CA* (26%) and *CDH1* (21%) and less common mutations in genes such as *IKBKB*, *IKBKA*, *CHD5*, *STK11*, *STK6* and *BRAF*. Interestingly, multiple somatic mutations have now been found to be enriched in signalling pathways that have previously been identified as being pathogenic in breast cancer (Lin, Gan et al. 2007; Chittenden, Howe et al. 2008). Thus, the overall genetic complexity of breast cancer is only just beginning to emerge, and elucidation of the growing number of disease-causing mutations will aid in the discovery of improved treatments and eventual cures for the disease.

#### 1.2.4 Gene expression profiling of breast cancer subtypes

Gene expression profiling of breast cancer has recently identified the presence of multiple molecular subtypes of the disease. Microarrays were performed to characterise gene expression patterns in a set of 65 specimens of human breast tumours from 42 different individuals (Perou, Sorlie et al. 2000). This revealed that the phenotypic diversity of breast tumours was associated with corresponding diversity in gene expression. These gene expression profiles were subsequently used to subdivide breast cancers into five different molecular groups: the oestrogen receptor (ER)-positive luminal A and luminal B tumours and the ER-negative basal-like, ERBB2-positive and normal breast tumours (Perou, Sorlie et al. 2000; Sorlie, Perou et al. 2001). The luminal A and luminal B cancers over-express ER, oestrogen-responsive genes and genes that are characteristically expressed in luminal epithelial cells (Perou, Sorlie et al. 2000). The luminal A cancers often express the transcription factors, GATA-3 and FOXA1, and the progesterone receptor (PR) (Sorlie, Tibshirani et al. 2003; Badve, Turbin et al. 2007), whereas luminal B cancers have a less well understood molecular phenotype, but are known to be PR-negative and express higher levels of the proliferation marker Ki67 and possibly the tyrosine kinase receptor ERBB2 (Cheang, Chia et al. 2009). The ERBB2-positive tumours over-express ERBB2 and neighbouring genes such as growth factor receptor-bound protein-7 (*GRB7*); they lack ER expression and generally have high levels of NF- $\kappa$ B activation (Sorlie, Perou et al. 2001; Bertucci, Borie et al. 2004; Biswas and Iglehart 2006). Basal-like tumours over-express a range of genes that characterise basal epithelial cells (Perou, Sorlie et al. 2000). These tumours are often also denoted as 'triple negative' due to their general lack of ER, PR and ERBB2 (Perou, Sorlie et al. 2000). However, although the majority of basal-like tumours are also 'triple negative', this is not always the case as some basal-like tumours can express ERBB2 (Rouzier, Perou et al. 2005) and conversely some 'triple negative' tumours do not express basal markers (Tischkowitz, Brunet et al. 2007; Tan, Marchio et al. 2008). The normal breast-like tumours resemble normal breast tissue samples and over-express many genes that characterise non-epithelial mammary cells and lack luminal epithelial cell markers, but have strong expression of basal epithelial genes (Perou, Sorlie et al. 2000; Sorlie, Perou et al. 2001). Notably, these different subtypes can be used to predict clinical outcome, with luminal A cancers having the best prognosis and ERBB2-positive and basal-like tumours being more aggressive with a worse prognosis (Sorlie, Tibshirani et al. 2003; Sotiriou, Neo et al. 2003).

### 1.2.5 Mouse models of breast cancer

Transgenic mouse models of human breast cancer are an important research tool for understanding the basic biology of the disease and for pre-clinical testing of novel therapeutic targets and treatments. Their value, however, is dictated by how accurately they recapitulate the circumstances that lead to the initiation and progression of the human disease. Furthermore, as breast cancer is such a heterogeneous disease, it is essential to use a model that most accurately represents the disease subtype that the investigation is aiming to target.

A number of promoters have been used to drive the expression of known oncogenes to mammary epithelium (Table 1.1). Many recognised oncogenes, including *ERBB2/Neu*, *Ha-Ras*, Polyoma middle T antigen, *TGF- $\alpha$* , *Wnt-1* and *c-Myc* have been expressed under the control of these promoters to initiate or modulate breast carcinogenesis in mice.

Promoter	Origin	Expression	Activation	Strengths	Weaknesses	Reference
<b>MMTV</b>	Mouse Mammary Tumour Virus	Mammary epithelial cells, several other tissues	Steroid hormones	Strong promoter	Requires pregnancy for strong expression, expressed in other tissues	(Muller, Sinn et al. 1988)
<b>WAP</b>	Whey acidic protein	Secretory mammary epithelial cells	Lactogenic hormones	Mammary gland specific	Requires pregnancy	(Schoenenberger, Andres et al. 1988; Lipnik, Petznek et al. 2005)
<b>BLG</b>	Bovine $\beta$ -lactoglobulin	Mammary epithelial cells – mostly luminal, salivary gland	Pregnancy and lactation	Mammary gland specific	Requires pregnancy	(Ali and Clark 1988; Bortner and Rosenberg 1997; Molyneux, Geyer et al. 2010)
<b>K14</b>	Cytokeratin 14	Basal mammary epithelial cells, skin, salivary gland, thymus	N/A	Does not require pregnancy	Expressed in other tissues	(Turksen, Kupper et al. 1992; Molyneux, Geyer et al. 2010)

**Table 1.1: Promoters used to drive oncogenes to the mammary epithelium**  
(Table adapted from Jonkers and Derksen 2007)

The vast majority of this thesis focuses on understanding the role of the NF- $\kappa$ B transcriptional co-factor, BCL3, in breast cancer initiation and progression (for a detailed description of NF- $\kappa$ B and BCL3, see sections 1.3 and 1.4 respectively). NF- $\kappa$ B activation has been shown to be strongly associated with ERBB2 signalling in breast cancer (Biswas, Cruz et al. 2000; Biswas, Shi et al. 2004; Biswas and Iglehart 2006; further highlighted in section 1.3.4.2). It was therefore appropriate to use a model driven by this oncogene in this study. A number of transgenic mouse models that recapitulate the initiation and

progression of ERBB2-positive disease have been generated to provide insight into the molecular mechanisms behind the potent transforming ability of this oncogene in breast cancer (for review, see Ursini-Siegel, Schade et al. 2007). A detailed description of the two ERBB2-driven models utilised in this thesis is presented below.

#### 1.2.5.1 *MMTV/NK and MMTV/N<sub>2</sub> mouse models*

In 1988, the first ERBB2 transgenic mouse model expressing an activated form of *Neu*, the rat homologue of *ErbB2*, under the transcriptional control of the mammary-specific mouse mammary tumour virus long terminal repeat (*MMTV-LTR*) promoter was generated (Muller, Sinn et al. 1988).

These transgenic mice (herein referred to as *MMTV/NK*) were derived by the microinjection of a recombinant plasmid composed of the entire *MMTV-LTR* and a cDNA encoding the activated NEU protein into one-cell mouse embryos. Five founder lines containing the activated *Neu* transgene were generated. The best characterised line was shown to uniformly express the *Neu* transgene in all mammary epithelial cells. These mice presented with numerous hyperplastic lesions early in mammary epithelial development, leading to multifocal tumours covering the entire mammary gland with an average latency of 3 months. Other lines expressing the transgene in a less uniform manner developed more sparsely distributed tumours that correlated with the expression pattern of the transgene. These tumours were also infrequently shown to metastasize to the lungs. Given that tumours arose comparatively rapidly, and no morphologically normal mammary epithelium was present in lines where the transgene was uniformly expressed, it was suggested that over-expression of an activated variant of the NEU protein requires few, if any, further genetic events for transformation of the primary mammary epithelium to occur (Muller, Sinn et al. 1988).

This pioneering model of ERBB2-driven breast cancer effectively demonstrated that over-expression of activated *Neu* alone is sufficient to transform mammary epithelial cells *in vivo*. However, this model is limited with respect to recapitulating the human disease as there is no evidence for comparable *ERBB2*-activating mutations in primary human ERBB2-positive cancers (Lemoine, Staddon et al. 1990). Furthermore, clinical studies have demonstrated that over-expression of wild-type *ERBB2* in human breast cancers is primarily due to gene amplification (Slamon, Clark et al. 1987).

To overcome this limitation, a second transgenic model was generated that over-expressed unactivated *Neu* in the mammary epithelium (Guy, Webster et al. 1992), also under the control of the *MMTV* promoter (herein referred to as *MMTV/N<sub>2</sub>*). These mice were shown to develop focal mammary tumours that often metastasized to the lungs with a much longer latency period of approximately 7 months. Tumours were surrounded by *Neu*-over-expressing hyperplastic mammary epithelium, indicating that, unlike the *MMTV/NK* model, expression of the unactivated *Neu* alone is not sufficient for mammary tumourigenesis (Guy, Webster et al. 1992). This model is now often used to explore the

potential effects of genetic alteration of other potential oncogenes or tumour suppressors in ERBB2-positive breast cancer (Cao, Luo et al. 2007; Ju, Katiyar et al. 2007).

Both the *MMTV/NK* and *MMTV/N<sub>2</sub>* transgenic mouse models have been used extensively in this thesis to gain a greater understanding of the role of the NF- $\kappa$ B co-factor, BCL3, in breast cancer initiation and progression.

### 1.2.6 Breast cancer stem cells

The classic models of carcinogenesis propose that cancer arises via a series of stochastic events whereby, given the right combination of mutations, any cell within an organ is able to be transformed and produce tumours containing cells that are all equally malignant (Nowell 1976). Recently, however, a fundamentally different model for describing the initiation and maintenance of cancers has been proposed. The 'cancer stem cell hypothesis' states that cancers originate from only stem or progenitor cells (reviewed in Reya, Morrison et al. 2001). Stem cells are characterised by their ability to undergo both self-renewal and multi-lineage cell differentiation. The process of self-renewal can be either symmetrical, whereby the cell produces two daughter stem cells, or asymmetrical, whereby the cell produces one daughter stem cell and one cell that is able to differentiate along one of a variety of lineages. The cancer stem cell hypothesis proposes that de-regulation of these normally tightly controlled processes of self-renewal gives rise to heterogeneous tumours that are driven by a small subset of cells referred to as cancer stem cells or tumour-initiating cells (reviewed in Wicha, Liu et al. 2006).

Evidence for the existence of cancer stem cells was first found in acute myelogenous leukaemia (Bonnet and Dick 1997). Here, leukaemic stem cells were identified on the basis of their ability to initiate human Acute Myeloid Leukaemia (AML) when transplanted into immunocompromised mice. A similar approach has now been utilised to demonstrate the existence of breast cancer stem cells. Al-Hajj et al. (2003) demonstrated that, when grown in immunocompromised mice, only a small minority of human breast cancer cells were able to grow tumours. Furthermore, they showed that human breast cancers contain a small cellular population characterised by the expression of certain cell surface markers, which display stem cell-like properties. When as few as 100 of these cells were transplanted into immunocompromised mice, they were able to form tumours. In accordance with the cancer stem cell hypothesis, the tumours formed in these mice had the same phenotypic heterogeneity as the initial tumour, suggesting that they were driven by multipotent cells. Furthermore, cells from these tumours were able to generate new tumours after transplantation into new recipient mice, demonstrating the self-renewal ability of the cells. In contrast, transplantation of up to 20,000 cells not expressing these surface markers failed to form tumours at all (Al-Hajj, Wicha et al. 2003).

Elucidation of signalling pathways that regulate self-renewal has become of prime importance for gaining further understanding of how de-regulation of this process can lead to carcinogenesis. Recent evidence suggests that key oncogenic pathways such as those mediated by ERBB2, NOTCH and NF- $\kappa$ B signalling regulate breast stem cell behaviour (Dontu, Jackson et al. 2004; Korkaya, Paulson et al. 2008; Liu, Sakamaki et al. 2010; Wang, Kao et al. 2010) and as such may provide excellent targets for breast cancer therapy.

#### 1.2.6.1 Functional Identification of breast cancer stem cells

Advances in cell culture techniques have been important in the identification and study of both normal mammary and breast cancer stem cells. The *in vitro* study of mammary stem cells has been based on work from the neuronal field in which a cell culture assay, known as the neurosphere assay, was developed to identify neural stem cells (Reynolds and Weiss 1992; Rietze and Reynolds 2006). Similar cell culture conditions have since been adopted to aid in the identification of both normal mammary and breast cancer stem cells (Dontu, Abdallah et al. 2003; Ponti, Costa et al. 2005). Initially Dontu et al. (2003) demonstrated that when normal human mammary epithelial cells are plated on non-adherent surfaces and grown in serum-free medium containing a specific set of growth factors, they form spherical colonies termed mammospheres. These mammosphere colonies were shown to be enriched for cells that exhibit functional characteristics of stem/progenitor cells such as multipotency and self-renewal (Dontu, Abdallah et al. 2003). The mammosphere-forming assay is now routinely used to identify key mediators of stem cell behaviour in both human and rodent cell populations (Dontu, Jackson et al. 2004; Fillmore and Kuperwasser 2008; Bhat-Nakshatri, Appaiah et al. 2010; Tao, Roberts et al. 2011).

The use of flow cytometry for isolating breast cancer stem cells on the basis of cell surface markers has also been crucial in studying these populations. Both limiting dilution transplant experiments and analysis of cell surface markers in mammosphere cultures identified human breast cancer stem cells as being CD44<sup>+</sup>/CD24<sup>-</sup> (Al-Hajj, Wicha et al. 2003; Ponti, Costa et al. 2005). More recently, aldehyde dehydrogenase 1 (ALDH1), an enzyme responsible for the oxidation of aldehydes to carboxylic acids, has been shown to be over-expressed in human breast cancer stem cells (Ginestier, Hur et al. 2007) and is now routinely used in the identification of this cell population (Korkaya, Paulson et al. 2008; Aktas, Tewes et al. 2009; Morimoto, Kim et al. 2009; Tanei, Morimoto et al. 2009; Charafe-Jauffret, Ginestier et al. 2010).

In murine breast tumours, the appropriate cell surface marker to use depends heavily on the model of breast cancer that is being evaluated. For example, the mammary luminal progenitor marker, integrin  $\beta$ -3 (CD61), has been shown to define an enriched breast cancer stem cell population in *MMTV-Wnt-1* and *p53<sup>+/-</sup>* tumour models (Vaillant, Asselin-Labat et al. 2008), whereas, in accordance with human breast cancers, breast cancer stem cells in *Brca1*-deficient mouse mammary tumours are enriched in the

CD44+/CD24- population (Wright, Calcagno et al. 2008). In the *MMTV/Neu* models of breast cancer, Stem cell antigen 1 (Sca-1) and CD24-positive populations have been shown to enrich for breast cancer stem cells in tumours driven by the activated and unactivated forms of the *Neu* transgene, respectively (Liu, Deng et al. 2007; Grange, Lanzardo et al. 2008). In addition to cell surface markers, ALDH1 activity, as detected by an enzymatic 'Aldefluor' assay or immunohistochemistry, has also been used as a marker of breast cancer stem cells in murine tumours (Luo, Fan et al. 2009).

### 1.2.7 Treatment of breast cancer

The treatment of newly diagnosed breast cancer generally depends on the extent of the disease and usually involves surgery combined with post-operative radiotherapy. Adjuvant treatment with combination chemotherapy regimens such as CMF (Cyclophosphamide, Methotrexate, Fluorouracil) or FEC (Fluorouracil, Epirubicin, Cyclophosphamide) to reduce the risk of recurrence after surgery is also commonplace (reviewed in Lopez-Tarruella and Martin 2009). In spite of the advances in the treatment of newly diagnosed breast cancers, still about 30% of patients eventually develop metastatic disease that is generally incurable (reviewed in O'Shaughnessy 2005). The recent molecular characterisation and identification of distinct breast cancer subtypes has allowed the development of targeted therapies that are directed specifically towards certain biological features of individual tumours.

#### 1.2.7.1 *EGFR family receptor signalling: molecular targets for breast cancer treatment*

Currently, there are several fundamental molecular signalling pathways against which targeted therapies are being directed in breast cancer. Among these is the Epidermal Growth Factor Receptor (EGFR) family of tyrosine kinase receptors (for review, see Normanno, Bianco et al. 2003). The EGFR family consists of four different receptor tyrosine kinases: EGFR (ERBB1), ERBB2 (HER2), ERBB3 and ERBB4 (Ullrich, Coussens et al. 1984; Coussens, Yang-Feng et al. 1985; Kraus, Issing et al. 1989; Plowman, Culouscou et al. 1993). These receptors are composed of an extracellular ligand-binding domain, a transmembrane domain and a cytoplasmic tyrosine kinase-containing domain. The EGFR family of receptors are activated following ligand binding and subsequent homo- or hetero- dimerisation. Dimer formation results in kinase activation, which leads to auto- and trans-phosphorylation of tyrosine residues (King, Borrello et al. 1988; Stern and Kamps 1988; Carraway and Cantley 1994; Zhang, Gureasko et al. 2006; reviewed in Schlessinger 2000).

EGFR family receptors and their ligands are often over-expressed in breast cancer and frequently play an important role in the pathology of the disease. In particular, EGFR expression has been reported in 14-91% of human breast cancers and has been associated with an aggressive tumour phenotype and poor patient prognosis (Walker and Dearing 1999; Prenzel, Fischer et al. 2001). More recently, EGFR over-expression has been linked to the basal or triple-negative subtype of the disease

(Nielsen, Hsu et al. 2004; Reis-Filho and Tutt 2008). ERBB2 over-expression occurs in approximately 20% of human breast cancers and generally correlates with poor prognosis (Paik, Hazan et al. 1990). Furthermore, ERBB3 and ERBB4 over-expression have also been reported (Lemoine, Barnes et al. 1992; Srinivasan, Gillett et al. 2000; Suo, Risberg et al. 2002).

Following ligand binding, the EGFR family receptors undergo tyrosine phosphorylation, which enables them to interact with adapter proteins linking them to intracellular signalling pathways that are implicated in cancer initiation and progression (reviewed in Normanno 2009). The primary intracellular signalling cascades activated by the EGFR family receptors are the phosphatidylinositol 3-kinase/v-akt murine thymoma viral oncogene homologue 1 (PI3K/AKT) pathway, of which mTOR (mammalian target of rapamycin) and NF- $\kappa$ B are key targets, and the Ras/Raf/mitogen-activated protein kinase kinase (MEK)/mitogen-activated protein kinase (MAPK) pathway. Many drugs that specifically target different elements of these signalling pathways are under development or currently being used in the clinic (Figure 1.5).

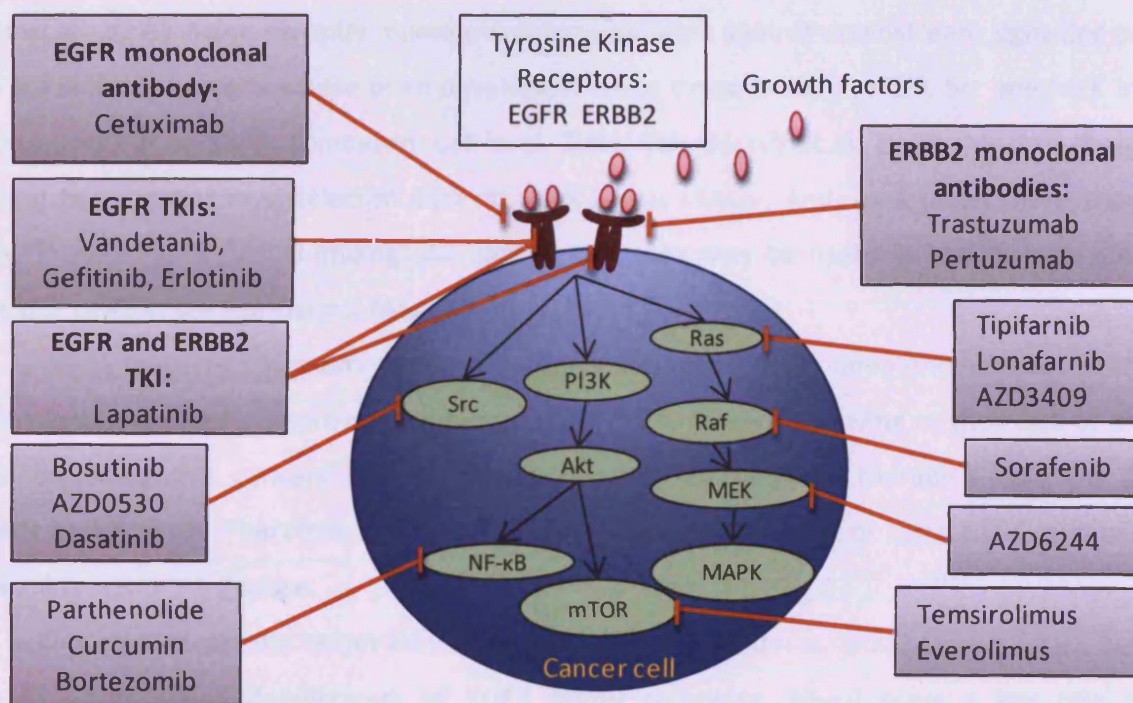


**Figure 1.5: EGFR and ERBB2-driven signalling pathways and target-based agents in development for breast cancer treatment**

Growth factors produced either by tumour cells or by surrounding stromal cells bind to and activate growth factor receptors, including EGFR and ERBB2, that are over-expressed on tumour cells. The growth factor receptors activate downstream signalling pathways that regulate different processes involved in the pathogenesis of breast cancer including cell proliferation, survival and invasion. Many agents that specifically target different aspects of these signalling pathways are in clinical development. TKI, Tyrosine kinase inhibitor (figure adapted from Normanno, Morabito et al. 2009).

### 1.2.7.2 *Target-based agents in breast cancer*

Target-based therapies can be divided into three broad categories: agents directed against specific subtypes of the disease, inhibitors of specific signalling pathways, and drugs targeted towards aspects of the tumour microenvironment such as angiogenesis. The first target-based therapeutic strategy for breast cancer came in the form of endocrine treatment for ER+ subtypes of the disease, firstly with tamoxifen (reviewed in Jordan 2006) and later on with the aromatase inhibitors (Nabholtz, Buzdar et al. 2000) and fulvestrant (Howell, Osborne et al. 2000). Since then, many agents that are active against the EGFR family receptors have been developed (for review, see Normanno, Morabito et al. 2009; Figure 1.5). These include monoclonal antibodies such as trastuzumab, which bind the extracellular domain of the receptor (Carter, Presta et al. 1992) and small-molecule tyrosine kinase inhibitors, such as lapatinib, which directly inhibit tyrosine kinase phosphorylation of the receptor (Rusnak, Affleck et al. 2001). When used in combination with chemotherapy, these agents have been shown to have considerable efficacy in treating subtypes of the disease that over-express certain EGFR family receptors (Geyer, Forster et al. 2006; Slamon, Layland-Jones et al. 2001; Gasparini, Gion et al. 2007; von Minckwitz, du Bois et al. 2009). More recently, numerous agents directed against downstream signalling pathways of the EGFR family receptors have been developed. These drugs include mTOR, Src and MEK inhibitors (Yu, Toral-Barza et al. 2001; Lombardo, Lee et al. 2004; Yeh, Marsh et al. 2007). Most of these agents have only been tested in unselected patients with breast cancer, and, as a result, have shown little efficacy. However, pre-clinical findings do suggest that they may be useful in specific subtypes of the disease (for review, see Normanno, Morabito et al. 2009).

While responses to many of these targeted treatments have been encouraging, resistance is still prevalent, and disease improvement can be short-lived. Moreover, owing to their lack of molecular targets, triple-negative cancers are completely resistant to targeted therapies that are currently approved in the clinic. Therefore, there is still a need to identify new or synergistic targets to treat various subtypes of the disease.

One such molecular target may be the NF- $\kappa$ B family of transcription factors which have been shown to be activated downstream of EGFR family receptors. NF- $\kappa$ B plays a key role in many physiological processes, such as innate and adaptive immune responses, inflammation and cell proliferation, death and motility. The potential of NF- $\kappa$ B as a therapeutic target in breast cancer has already been highlighted in a number of reports in the literature (Helbig, Christopherson et al. 2003; Aggarwal, Shishodia et al. 2005; Cao, Luo et al. 2007; Park, Zhang et al. 2007; Connelly, Barham et al. 2010; Liu, Sakamaki et al. 2010). This has led to a great deal of interest in the development of inhibitors of NF- $\kappa$ B signalling.

## 1.3 NF- $\kappa$ B

### 1.3.1 NF- $\kappa$ B family of transcription factors

Nuclear factor binding to the intronic kappa-light-chain enhancer element in B cells (NF- $\kappa$ B) was first identified in 1986 (Sen and Baltimore 1986). NF- $\kappa$ B is a family of transcription factors that can both induce and repress gene expression through binding to DNA sequences, known as  $\kappa$ B motifs, in promoters. The family is made up of five subunits — p65 (RelA), c-Rel, RelB, NF- $\kappa$ B1 (p105/p50) and NF- $\kappa$ B2 (p100/p52) — which all share a conserved REL Homology Domain (RHD) within their N-terminus that is required for dimerisation, DNA binding and interaction with inhibitors of NF- $\kappa$ B (I $\kappa$ B) (reviewed in Perkins 2007) (Figure 1.6).

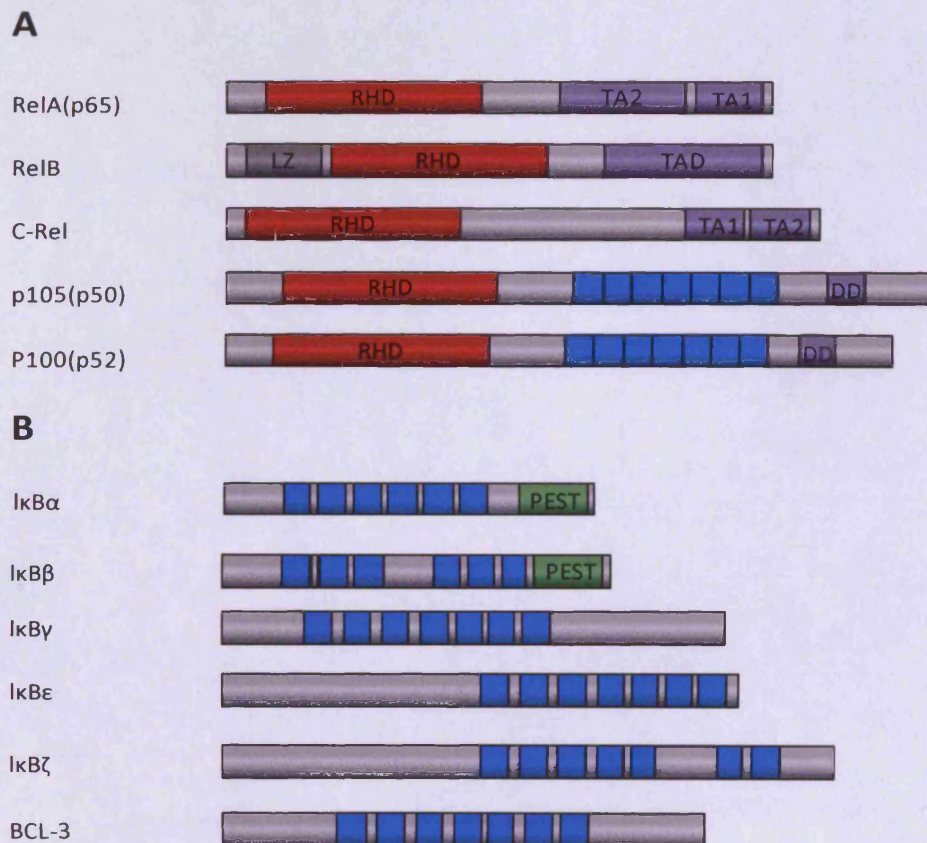


**Figure 1.6: Structural domains of the NF- $\kappa$ B and I $\kappa$ B family of proteins**

All NF- $\kappa$ B family members contain an N-terminal Rel-homology domain (RHD, red) that contains a nuclear localization domain and mediates DNA binding and dimerisation. The Rel sub-family contains transactivation domains (TAD, purple; TA1 and TA2 are sub-domains of the TAD). The inhibitor of  $\kappa$ B family consists of I $\kappa$ B $\alpha$ , I $\kappa$ B $\beta$ , I $\kappa$ B $\gamma$ , I $\kappa$ B $\epsilon$ , I $\kappa$ B $\zeta$  and BCL3. Like p100 and p105, they all contain ankyrin repeat domains (ARD, blue). DD, region with homology to a death domain; LZ, Leucine zipper-like motif; PEST, domain rich in proline (P), glutamate (E), serine (S) and threonine (T), (figure adapted from Perkins 2007).

The subunits can be split into two broad groups depending on their requirement for proteolytic cleavage. The first group consists of the REL subunits, p65 (RelA), c-Rel and RelB, which are synthesised in their mature forms. They contain a transactivation domain (TAD) within their C-terminus which is necessary for transcriptional activation (Kamens, Richardson et al. 1990; Ryseck, Bull et al. 1992; Schmitz and Baeuerle 1991) and has also been shown to interact with some transcription components such as the p300/cyclic-AMP-response element-binding protein (CBP) (Zhong, Voll et al. 1998), the TATA-binding protein (TBP) and the transcription factor IIB (TFIIB) (Xu, Prorock et al. 1993). The second group consists of NF- $\kappa$ B1 (p105) and NF- $\kappa$ B2 (p100), which are synthesised as large precursors to the mature DNA-binding proteins, p50 and p52. These active NF- $\kappa$ B subunits are produced upon proteolytic cleavage of the C-terminus (Palombella, Rando et al. 1994; Heusch, Lin et al. 1999). p50 and p52 subunits do not have a TAD and are therefore only able to activate transcription when bound to either other transcriptionally active NF- $\kappa$ B subunits or co-activating proteins (reviewed in Beinke and Ley 2004), such as BCL3 (see section 1.4).

### 1.3.2 NF- $\kappa$ B regulation and signalling pathways

In most unstimulated mammalian cells, the REL subunits, p65, c-Rel and RelB, are retained in an inactive state within the cytoplasm through interactions with I $\kappa$ B proteins. There are five principle I $\kappa$ B proteins, I $\kappa$ B $\alpha$ , I $\kappa$ B $\beta$ , I $\kappa$ B $\epsilon$ , I $\kappa$ B $\gamma$  and I $\kappa$ B $\zeta$  (Figure 1.6). These proteins are characterised by the presence of multiple ankyrin repeats in their C-terminus and function predominantly by masking a conserved nuclear localisation sequence that is found in the RHD of NF- $\kappa$ B subunits (reviewed in Hayden and Ghosh 2004; Huxford, Huang et al. 1998; Jacobs and Harrison 1998; Malek, Chen et al. 2001; Malek, Huang et al. 2003). p50 and p52 are also retained in an inactive state in the cytoplasm in the form of their larger precursors, p105 and p100. These I $\kappa$ B-like proteins contain ankyrin repeat domains in their C-terminus, which are similar to those found in traditional I $\kappa$ B proteins and, as a result, are also able to inhibit the activity of multiple NF- $\kappa$ B subunits by sequestering them to the cytoplasm (Mercurio, DiDonato et al. 1993; Sun, Ganchi et al. 1994; Rice, MacKichan et al. 1992). The processing of p105 and p100 is essential for p50 and p52 to function as nuclear transcription factors. Both p50 and p52 homodimers can interact with another I $\kappa$ B family member, BCL3 which contains the classical I $\kappa$ B ankyrin repeat motif in its C-terminus but, in contrast with other I $\kappa$ B proteins, can function as either a transcriptional activator or repressor of NF- $\kappa$ B activity (see section 1.4).

NF- $\kappa$ B subunits form a variety of different hetero- or homo-dimers, which can be activated by over 150 stimuli such as pro-inflammatory cytokines, bacterial products, viruses and growth factors (reviewed in Pahl 1999). NF- $\kappa$ B activation occurs via a number of distinct activation pathways. The two most commonly observed are the canonical (classical) and non-canonical (non-classical) pathways (Figure 1.7). Both of these key pathways are induced via activation of the I $\kappa$ B Kinase (IKK) complex, although IKK-

independent signalling pathways have also been identified (Schoonbroodt, Ferreira et al. 2000; Romieu-Mourez, Landesman-Bollag et al. 2002; Kato, Delhase et al. 2003). The IKK complex consists of two catalytic subunits, IKK $\alpha$  and IKK $\beta$  (also known as IKK1 and IKK2; Zandi, Rothwarf et al. 1997), and multiple copies of a regulatory subunit called the NF- $\kappa$ B essential modifier (NEMO, also known as IKK $\gamma$  Rothwarf, Zandi et al. 1998). Upon activation, the IKK complex acts to phosphorylate NF- $\kappa$ B-bound I $\kappa$ B proteins, which target them for ubiquitin-dependent degradation by the proteasome. This results in the release of NF- $\kappa$ B dimers, which are then free to translocate to the nucleus, where they can regulate transcription of a wide variety of genes.

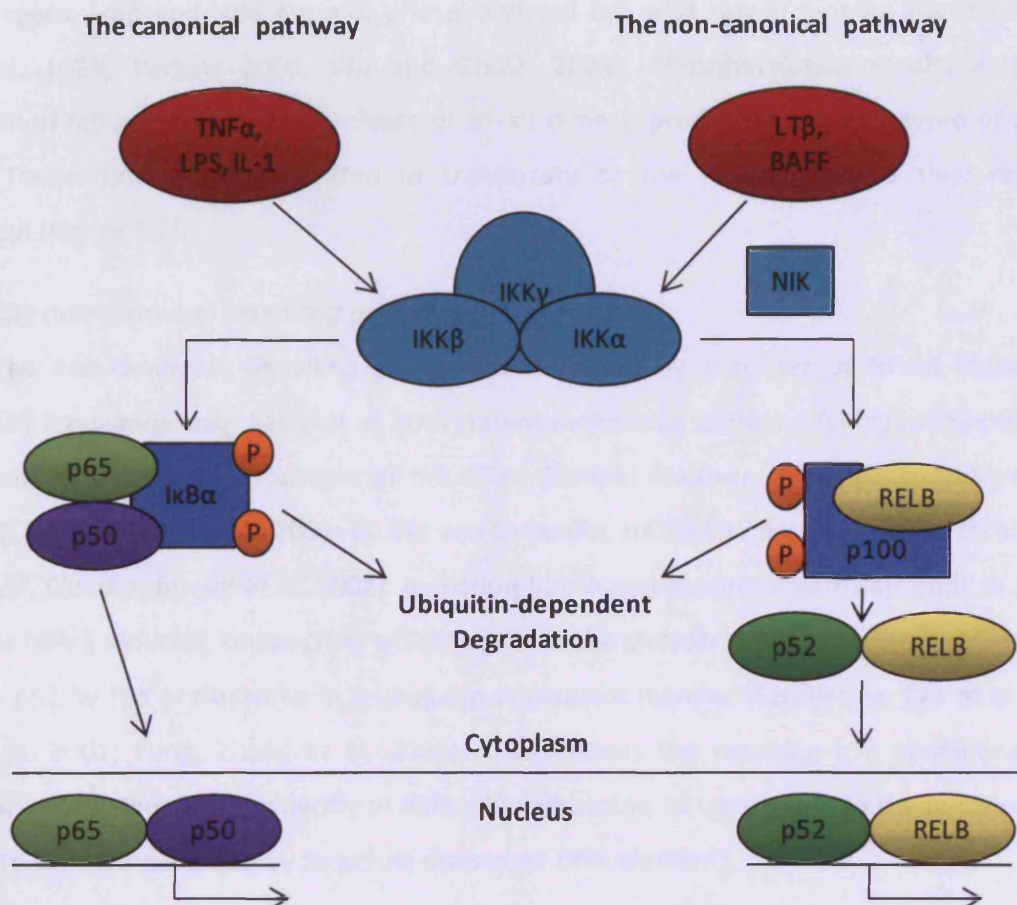


**Figure 1.7: Canonical and non-canonical NF- $\kappa$ B signalling pathways**

The inhibitor of  $\kappa$ B kinase (IKK) complex is composed of IKK $\alpha$ , IKK $\beta$  and IKK $\gamma$ . The IKK $\beta$  subunit of the canonical pathway is activated in response to a range of stimuli such as tumour-necrosis factor- $\alpha$  (TNF- $\alpha$ ), interleukin (IL-1) or lipopolysaccharide (LPS) and phosphorylates the NF- $\kappa$ B bound I $\kappa$ B proteins targeting them for ubiquitin-dependent degradation. This allows translocation of p65:p50 (or c-REL:p50) heterodimers to the nucleus where they can transcriptionally activate target genes. The IKK $\alpha$  subunit of the non-canonical pathway is activated by the NF- $\kappa$ B inducing kinase (NIK) in response to other stimuli such as the TNF family members, lymphotoxin  $\beta$  (LT $\beta$ ) and BAFF, resulting in the phosphorylation of p100. This triggers the ubiquitin-dependent degradation of the C-terminal half of p100, releasing the N-terminal half, p52. Dimers composed of p52 and another subunit (most commonly RELB) translocate to the nucleus and activate transcription (figure adapted from Cao and Karin 2003)

### 1.3.2.1 *The canonical signalling pathway*

The canonical signalling pathway is activated by a variety of stimuli including viral infections (Hammar-skjold and Simurda 1992; Mastronarde, He et al. 1996), exposure to bacterial products such as lipopolysaccharide (LPS) (Souvannavong, Saidji et al. 2007) and cytokines, such as tumour necrosis factor- $\alpha$  (TNF- $\alpha$ ) and interleukin-1 (IL-1) (Osborn, Kunkel et al. 1989). The predominant IKK subunit involved in canonical signalling is IKK $\beta$  (Li, Van Antwerp et al. 1999), although some IKK $\beta$ -independent mechanisms have also been reported (Cao, Bonizzi et al. 2001; Merkhofer, Cogswell et al. 2010). Upon activation of this pathway, I $\kappa$ B $\alpha$  is rapidly phosphorylated on serines 32 and 36 by IKK $\beta$  (Woronicz, Gao et al. 1997). In some cell types, I $\kappa$ B $\beta$  and I $\kappa$ B $\epsilon$  are also phosphorylated but with slower kinetics (reviewed in Fischer, Page et al. 1999; Perkins 2006; Wu and Ghosh 2003). Phosphorylation results in proteasomal degradation of I $\kappa$ B proteins and the release of NF- $\kappa$ B dimers, predominantly composed of p50 and p65 subunits. These dimers are then free to translocate to the nucleus, where they regulate gene transcription (Figure 1.7).

### 1.3.2.2 *The non-canonical signalling pathway*

The non-canonical signalling pathway is activated by a subset of NF- $\kappa$ B induction stimuli including LPS (Souvannavong, Saidji et al. 2007) latent membrane protein-1 (LMP1) of Epstein–Barr virus (Luftig, Yasui et al. 2004), stimulation of the CD40 (Coope, Atkinson et al. 2002) and lymphotoxin- $\beta$  receptors (Dejardin, Droin et al. 2002; Muller and Siebenlist 2003), and B-cell-activating factor of the TNF family (BAFF, Claudio, Brown et al. 2002). Induction of the non-canonical pathway leads to activation of IKK $\alpha$  by the NF- $\kappa$ B inducing kinase (NIK) which results in the phosphorylation and subsequent processing of p100 to p52 by the proteasome in a ubiquitin-dependent manner (Senftleben, Cao et al. 2001; Xiao, Harhaj et al. 2001; Fong, Zhang et al. 2002). This releases the resulting p52 containing hetero- or homodimers, consisting predominantly of RelB:p52 complexes, to translocate to the nucleus where they can regulate gene transcription by targeting distinct  $\kappa$ B DNA elements.

### 1.3.2.3 *Atypical NF- $\kappa$ B signalling pathway: processing of p105 to p50*

As well as the canonical and non-canonical signalling pathways, NF- $\kappa$ B activation can occur via a number of other IKK-dependent or independent mechanisms (reviewed in Perkins and Gilmore 2006; Schoonbroodt, Ferreira et al. 2000; Romieu-Mourez, Landesman-Bollag et al. 2002; Huang, Wuerzberger-Davis et al. 2003; Kato, Delhase et al. 2003). An important alternative signalling pathway results in the generation of p50 subunits from p105. Once generated, p50 can produce either hetero- or homo-dimers, which can translocate to the nucleus and modulate transcription.

In many cell types, high levels of p50 can be generated in the absence of a stimulus via either post-translational or co-translational mechanisms (reviewed in Beinke and Ley 2004; Pereira and Oakley

2008). Post-translational processing involves the constitutive proteolytic removal of the c-terminal half of p105 by the proteasome. p105 contains a glycine-rich region (GRR) between the RHD and ankyrin repeats, which is essential to this process (Lin and Ghosh 1996). The GRR functions as a processing stop signal, which prevents the RHD from entering into the proteasome (Orian, Schwartz et al. 1999). This ensures that only the C-terminus of p105 is degraded and p50 is released. In co-translational processing, p50 and p105 are generated from a single mRNA as a result of the proteolysis of incompletely synthesised p105 polypeptides by the 26S proteasome (Lin, DeMartino et al. 1998). In addition to these two constitutive mechanisms, some reports have demonstrated that p105 can also undergo inducible IKK $\beta$ -dependent processing, which results in either complete degradation or the production of p50 (reviewed in Orian, Gonen et al. 2000; Beinke and Ley 2004; Cohen, Achbert-Weiner et al. 2004).

#### 1.3.2.4 *Modulators of NF- $\kappa$ B activity*

There are a number of proteins and stimuli that do not directly induce the activation and nuclear translocation of NF- $\kappa$ B subunits, but are known to alter NF- $\kappa$ B in alternative ways. Modulators of NF- $\kappa$ B activity can mediate a number of post-translational modifications or can form co-operative interactions that result in the targeting of NF- $\kappa$ B subunits to specific promoters. Post-translational modifications can either promote or inactivate the transcriptional activity of NF- $\kappa$ B and in some cases can cause NF- $\kappa$ B subunits to become transcriptionally repressive (reviewed in Chen and Greene 2004).

A key post-translational modification is nuclear phosphorylation of NF- $\kappa$ B subunits by nuclear kinases. Phosphorylation of p65 has been particularly well studied and can result in either transcriptional activation or repression (reviewed in Viatour, Merville et al. 2005). For example, protein kinase A can phosphorylate p65 at Ser-276 (Zhong, SuYang et al. 1997). Phosphorylations at this site have been shown to stimulate p65 transcriptional activity by promoting its interaction with the cAMP response element-binding (CREB)-binding protein (CBP) and p300 co-activators (Zhong, Voll et al. 1998) and to displace p50-histone deacetylase (HDAC)-1 repressive complexes from DNA (Zhong, May et al. 2002). In contrast, p65 transactivation can be inhibited by the ARF tumour suppressor via the chk1-dependent phosphorylation of p65 at Thr-505 (Rocha, Garrett et al. 2005). p65 transcriptional activity can also be stimulated or inhibited by acetylation at lysine residues (reviewed in Campbell and Perkins 2004). Acetylation is induced, at least in part, by Histone acetyl transferases (HATs), such as p300 and PCAF, while HDACs such as HDAC3 and SIRT1 can promote their removal (Chen, Fischle et al. 2001; reviewed in Chen and Greene 2004).

The numerous post-translational modifications and protein interactions that can occur, allow tight control over the transcriptional activity and function of NF- $\kappa$ B subunits at specific promoters. They also highlight the complexity and context-specific differences of this signalling pathway, all of which must be considered when investigating NF- $\kappa$ B-mediated events.

### 1.3.3 Biological roles of NF- $\kappa$ B proteins

Once in the nucleus, NF- $\kappa$ B dimers can regulate gene transcription by binding to  $\kappa$ B sites consisting of 5'-GGGRNWYYCC-3' sequences (R=purine, W=adenine or thymine, Y=pyrimidine and N=any nucleic acid). Almost all combinations of NF- $\kappa$ B hetero- and homodimers can be formed. The composition of the dimer can vary dramatically depending on cell type and the nature of the stimulus. Furthermore, different NF- $\kappa$ B complexes bind to  $\kappa$ B sites with varying preferences and form different protein—protein interactions at promoter sites, resulting in the transcription of distinct gene subsets. Consequently, NF- $\kappa$ B transcription factors are able to tightly regulate a wide range of genes in a manner that is suitable for the context in which they are set (reviewed in Hoffmann, Natoli et al. 2006).

Genetically engineered NF- $\kappa$ B knock-out models of both individual and multiple NF- $\kappa$ B subunits have been generated in order to gain a greater understanding of their specific biological roles (Weih, Carrasco et al. 1995; Beg, Sha et al. 1995; Sha, Liou et al. 1995; Caamano, Rizzo et al. 1998; Franzoso, Carlson et al. 1998; Grumont, Rourke et al. 1998). These studies indicate that NF- $\kappa$ B subunits have distinct functions in innate and adaptive immune responses and also reveal an essential role for NF- $\kappa$ B in regulating apoptosis, particularly in the nervous and immune systems and liver (for review, see Gerondakis, Grumont et al. 2006).

NF- $\kappa$ B mediates the expression of over 150 genes, many of which are known to be involved in immunity and homeostasis, such as cytokines, immunoreceptors, acute phase proteins, enzymes, adhesion molecules and transcription factors (reviewed in Pahl 1999). In addition, NF- $\kappa$ B signalling can promote cell survival through the induction of either anti-apoptotic genes, such as *c-IAP1* and 2 (Wang, Mayo et al. 1998) and *BCL-XL* (Chen, Edelman et al. 2000), or growth-promoting genes such as *CYCLIN D1* (Guttridge, Albanese et al. 1999) and *IGFBP2* (Cazals, Nabeyrat et al. 1999). Conversely, in certain circumstances it can induce cell death through the regulation of pro-apoptotic genes such as the death receptors, *DR4-DR6* (Ravi, Bedi et al. 2001; Kasof, Lu et al. 2001), and the BCL2 family member, *BCL-XS* (Chen, Kandasamy et al. 2003; reviewed in Kucharczak, Simmons et al. 2003). The multitude of NF- $\kappa$ B gene targets renders this family of transcription factors essential mediators of normal tissue development and homeostasis within the body.

### 1.3.4 NF- $\kappa$ B in mammary gland development and breast cancer

#### 1.3.4.1 Normal mammary gland development

Although there is little evidence to suggest that NF- $\kappa$ B is involved in the early embryonic development of the mammary gland, this family of transcription factors have been shown to exhibit dynamic and tightly regulated expression patterns during the post-natal stages of development. p65, p50 and I $\kappa$ B $\alpha$  are expressed in the mammary epithelial cells of virgin, pregnant, lactating and involuting mice.

NF- $\kappa$ B DNA-binding activity peaks at day 16 of gestation in mice and decreases to undetectable levels during lactation before being re-activated during involution (Brantley, Yull et al. 2000). This well-regulated expression of NF- $\kappa$ B activity is essential for mammary gland development, as demonstrated by the fact that genetically modified mice harbouring altered NF- $\kappa$ B proteins show substantial defects at multiple stages of mammary gland development (Baxter, Came et al. 2006; Brantley, Chen et al. 2001; Cao, Bonizzi et al. 2001). For example, mammary epithelia with elevated NF- $\kappa$ B activity as a consequence of I $\kappa$ B $\alpha$  deficiency showed increased lateral ductal branching and hyperplasia when transplanted into wild-type mammary fat pads, indicating that it has an important role in maintaining normal epithelial architecture (Brantley, Chen et al. 2001). Moreover, during pregnancy, NF- $\kappa$ B activation has been shown to be essential for lobuloalveolar development. This was demonstrated by the use of IKK $\alpha$  knock-in mice, which display no IKK $\alpha$  kinase activity and, as a result, have severely impaired pregnancy-induced NF- $\kappa$ B activation. Knock-in IKK $\alpha$  mice showed reduced epithelial cell proliferation during pregnancy to such an extent that alveolar development at the end of gestation in mutant mice was comparable to that of mid-pregnant wild-type glands (Cao, Bonizzi et al. 2001). Furthermore, during involution, suppressed NF- $\kappa$ B activity brought about by the conditional deletion of the IKK $\beta$  gene was shown to result in delayed apoptosis and mammary gland remodelling (Baxter, Came et al. 2006). Collectively, these data demonstrate that NF- $\kappa$ B signalling is essential in the development of the normal mammary gland.

#### 1.3.4.2 *NF- $\kappa$ B in breast cancer*

As well as being an essential mediator of normal physiological processes, NF- $\kappa$ B signalling, when deregulated, has been implicated in the aetiology of a number of human autoimmune diseases such as multiple sclerosis, inflammatory bowel diseases, rheumatoid arthritis and psoriasis (reviewed in Kurylowicz and Nauman 2008). Furthermore, NF- $\kappa$ B transcription factors have been shown to regulate many genes implicated in malignant cell growth, such as those involved in cell proliferation and survival, angiogenesis, metastases and inflammation (Figure 1.8). There is now an increasing number of experimental and epidemiological studies to indicate that inappropriate activation of NF- $\kappa$ B by pathogens, carcinogens or inflammatory cytokines plays a direct or indirect role in the initiation and progression of many human cancers (reviewed in Baldwin 2001).

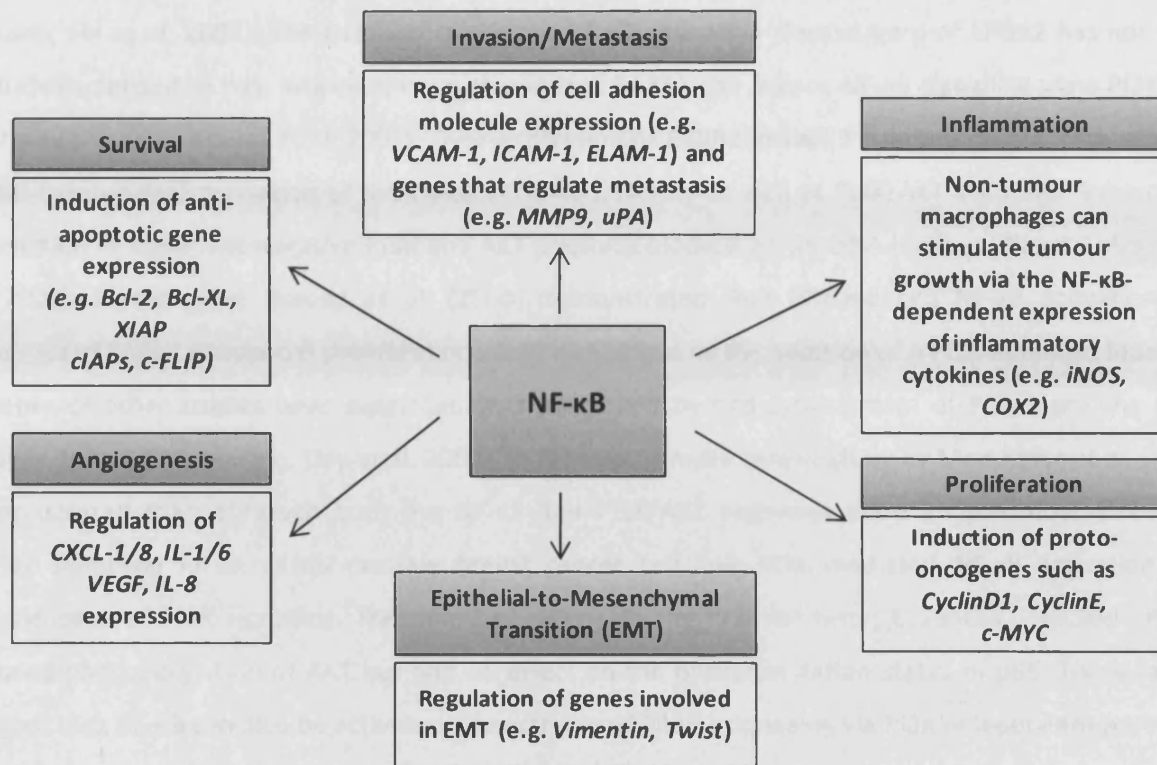


**Figure 1.8: NF-κB target genes involved in the pathogenesis of cancer**

De-regulated NF-κB signalling can promote carcinogenesis by regulating target genes involved in cell survival, proliferation, invasion, inflammation, epithelial-to-mesenchymal transition and angiogenesis.

The evidence to suggest that NF-κB signalling plays an important role in breast carcinogenesis is overwhelming. A number of studies have demonstrated elevated NF-κB activity in both breast cancer cell lines and tissues (Nakshatri, Bhat-Nakshatri et al. 1997; Sovak, Bellas et al. 1997; Cogswell, Guttridge et al. 2000; Biswas, Shi et al. 2004; Zhou, Eppenberger-Castori et al. 2005). Increased canonical signalling, as demonstrated by the presence of p50:p65 heterodimers, was reported in the majority of these studies. However, Cogswell et al. (2000) showed elevated DNA binding of the p50, p52 and c-Rel subunits in human tumour samples (Cogswell, Guttridge et al. 2000), suggesting that the non-canonical signalling pathway may also play a role in mammary tumourigenesis.

Mechanisms that lead to constitutive NF-κB activation are not absolutely clear. However, *in vitro* studies have demonstrated that NF-κB can be activated downstream of a number of known oncogenes such as EGFR (Biswas, Cruz et al. 2000) and Ha-Ras (Finco, Westwick et al. 1997). Interestingly, a positive correlation between over-expression of the ERBB2 oncogene and NF-κB activation has been observed in both human breast cancer cell lines and primary tumour samples (Biswas, Shi et al. 2004; Zhou, Eppenberger-Castori et al. 2005). Furthermore, in ERBB2-expressing cell lines, administration of the EGFR family ligand, heregulin, resulted in rapid activation of NF-κB, and,

conversely, treatment with the ERBB2 monoclonal antibody, trastuzumab, inhibited NF- $\kappa$ B activation (Biswas, Shi et al. 2004). The pathway leading to NF- $\kappa$ B activation downstream of ERBB2 has not been well characterised. It has, however, been shown that ERBB2 can induce NF- $\kappa$ B signalling via a PI3K/AKT pathway (Pianetti, Arsura et al. 2001). Over-expression of ERBB2 in Ba/F3 haematopoietic cells resulted in IKK-independent activation of the classical NF- $\kappa$ B pathway as well as PI3K/AKT activities. Subsequent expression of dominant-negative PI3K and AKT plasmids blocked NF- $\kappa$ B DNA binding (Pianetti, Arsura et al. 2001). Furthermore, Biswas et al. (2000) demonstrated that EGF-induced NF- $\kappa$ B activation and subsequent breast cancer cell proliferation could be blocked by the addition of a PI3K inhibitor. Indeed, a number of other studies have suggested that NF- $\kappa$ B is activated downstream of PI3K signalling (Dan, Cooper et al. 2008; Makino, Day et al. 2004). In contrast, a more recent study by Merkhofer et al. (2010) demonstrated that, although both the NF- $\kappa$ B and PI3K/AKT pathways were induced downstream of ERBB2 signalling in an ERBB2-positive breast cancer cell line, IKK $\alpha$ -mediated NF- $\kappa$ B activation was independent of PI3K signalling. Treatment of cells with the PI3K inhibitor, LY294002, blocked ERBB2-induced phosphorylation of AKT but had no effect on the phosphorylation status of p65. These results suggest that NF- $\kappa$ B can also be activated downstream of ERBB2 signalling via PI3K independent pathways that are yet to be elucidated.

Although one study showed that high NF- $\kappa$ B activity was able to identify a subset of aggressive hormone-dependent breast cancers (Zhou, Eppenberger-Castori et al. 2005), it appears that NF- $\kappa$ B over-expression or activation is predominantly found in ER-negative breast cancer cells and tissues (Nakshatri, Bhat-Nakshatri et al. 1997; Biswas, Shi et al. 2004). In addition, the correlation between ERBB2 and NF- $\kappa$ B signalling was also primarily found in ER-negative tumours (Biswas, Shi et al. 2004). It has been suggested that this effect may be due to the ability of the ER to exert a general inhibition of NF- $\kappa$ B transcriptional activity (Nakshatri, Bhat-Nakshatri et al. 1997). The constitutive activity of an NF- $\kappa$ B-dependent promoter was shown to be efficiently inhibited when ER-negative cells were transfected with ER. Alternatively, the effect may be due to the development of oestrogen independence as a result of NF- $\kappa$ B activation, as suggested by Pratt et al. (2003).

Many genes important for the metastatic process have been shown to be regulated by NF- $\kappa$ B. These include MMPs (which facilitate tissue penetration), chemokines (which induce cell migration) and vascular endothelial growth factor (VEGF) (which is essential for tumour angiogenesis; reviewed in Basseres and Baldwin 2006). Furthermore, a number of experimental studies have demonstrated a role for NF- $\kappa$ B in promoting metastases. For example, reduced lung metastases and suppression of MMP-9 was observed in a mouse xenograph model following the pharmacological inhibition of NF- $\kappa$ B in human breast cancer cells with curcumin (Aggarwal, Shishodia et al. 2005). Administration of a different pharmacological inhibitor of NF- $\kappa$ B, parthenolide, in combination with docetaxel also resulted in reduced

metastases in another breast cancer xenograph model (Sweeney, Mehrotra et al. 2005). Furthermore, inhibition of NF- $\kappa$ B in the Ha-Ras-transformed mammary epithelial cell line, EpRas, resulted in reduced lung lesions in an experimental tail vein metastases model (Huber, Azoitei et al. 2004). This was due to its effect on epithelial-to-mesenchymal transition. More recently, Connelly et al. (2010) demonstrated that conditional inhibition of NF- $\kappa$ B in the aggressive polyoma middle T oncogene (PyVT) breast cancer model resulted in a reduction in tumour burden and metastases in comparison with controls. Another recent study showed that inhibition of NF- $\kappa$ B, as a consequence of the stable expression of I $\kappa$ B $\alpha$  resulted in reduced tumour angiogenesis via the down-regulation of VEGF in an ERBB2-positive murine allograft breast cancer model (Liu, Ju et al. 2009).

#### 1.3.4.3 *Inhibition of NF- $\kappa$ B: a potential therapeutic target in breast cancer?*

It is clear from the extensive literature on the role of NF- $\kappa$ B in breast cancer that this pathway has great therapeutic potential as a target for inhibition in the disease. The obvious association between ERBB2 expression and NF- $\kappa$ B activation strongly suggests that ERBB2-positive tumours may preferentially benefit from NF- $\kappa$ B blockade. Furthermore, the identification of an inverse correlation between NF- $\kappa$ B activity and ER status may also be exploited in the therapy of human breast cancers. For example, combination treatment of ER-positive tumours with both an anti-oestrogen and an NF- $\kappa$ B inhibitor may prevent the development of resistance to hormonal therapy in some patients.

More than 750 compounds have been shown to have inhibitory effects on NF- $\kappa$ B signalling (reviewed in Gilmore and Herscovitch 2006). These agents can generally be classified into those that block activation of the IKK complex, those that prevent the phosphorylation or proteasomal degradation of I $\kappa$ B and those that inhibit the nuclear translocation and function of NF- $\kappa$ B subunits (Figure 1.9). A few of these agents, such as the proteasome inhibitor, bortezomib, have undergone clinical trials in breast cancer patients with some success (Orlowski and Dees 2003; Awada, Albanell et al. 2008; Schmid, Kuhnhardt et al. 2008; Irvin, Orlowski et al. 2010). However, a major caveat to global sustained inhibition of NF- $\kappa$ B signalling is that many of the functions regulated by this transcription factor that make it such a desirable drug target also play a major role in homeostasis within the body. Unselective disruption to this pathway during development or in adulthood will potentially lead to adverse effects such as immune suppression, which could be particularly harmful in cancer patients, who are likely to already be immunocompromised from other drug treatments. Moreover, as NF- $\kappa$ B has been shown to play an integral role in normal murine mammary gland development, therapeutic inhibition of this signalling pathway in breast cancer may have particularly pronounced and detrimental effects on the normal cells within the gland. Establishing a balance between treating the disease and unwanted side effects is the challenge faced when designing suitable therapeutics to target this pathway. An alternative approach to global inhibition of NF- $\kappa$ B is to target modifying co-factors such as the I $\kappa$ B-like protein, BCL3, which could

potentially provide a more selective inhibitory effect on cancer cells while having minimal effects on the normal surrounding tissue.

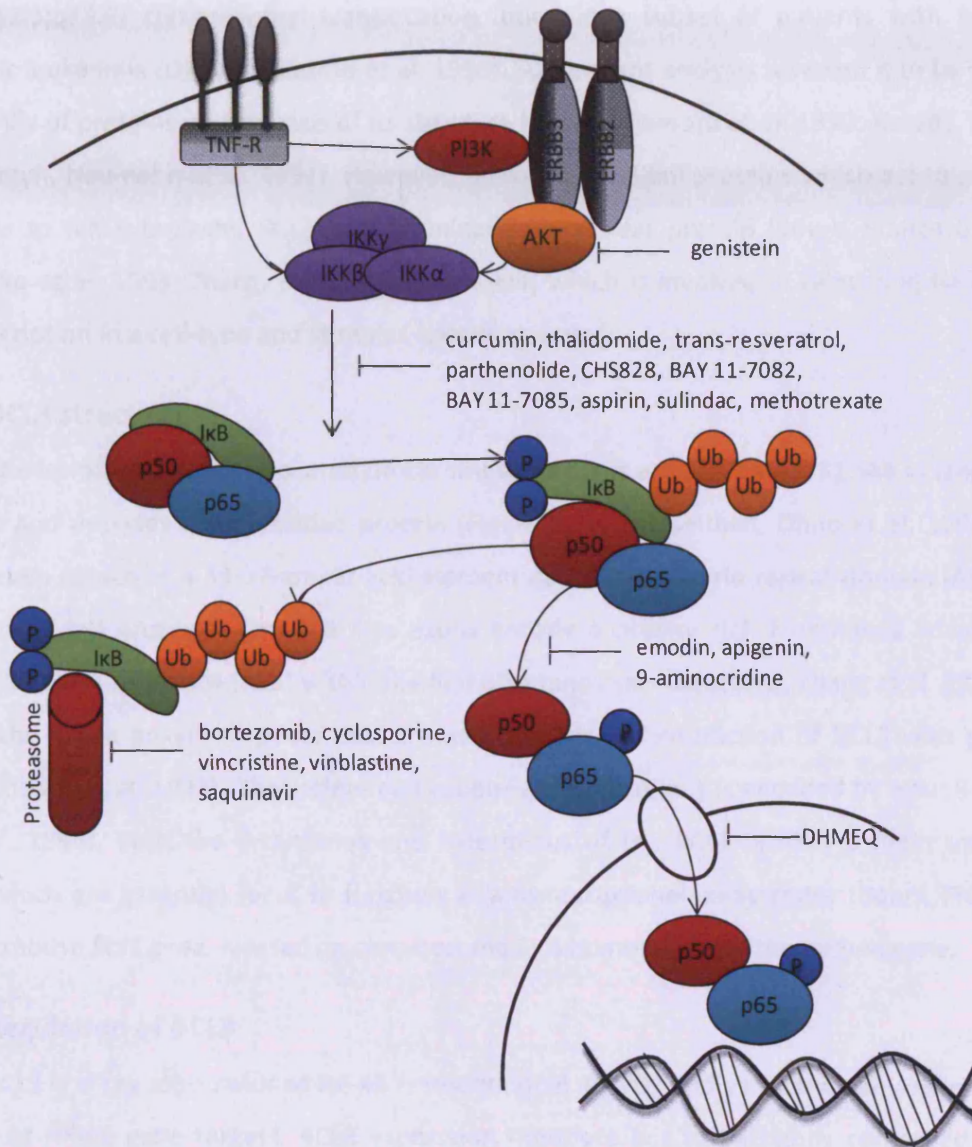


**Figure 1.9: Targets of NF-κB inhibitors**

AKT which links ERBB2 to NF-κB signalling, can be blocked by genistein. IKK and proteosomal inhibitors prevent the degradation of IκB that is required for the nuclear translocation of NF-κB dimers. emodin, apigenin and 9-aminocridine inhibit the phosphorylation of p65. DHMEQ (dehydroxymethylepoxyquinomicin) acts to block the nuclear translocation of the p50/p65 complex (figure adapted from Haffner, Berlato et al. 2006).

## 1.4 B-Cell Lymphoma 3

### 1.4.1 Introduction

B-Cell Lymphoma 3 (BCL3) was originally discovered through its involvement in the t(14;19)(q32.3;q13.2) chromosomal translocation found in a subset of patients with B-cell chronic lymphocytic leukaemia (Ohno, Takimoto et al. 1990). Subsequent analysis revealed it to be a member of the I $\kappa$ B family of proteins on the basis of its structure (Ohno, Takimoto et al. 1990; Hatada, Nieters et al. 1992; Wulczyn, Naumann et al. 1992). However, unlike classical I $\kappa$ B proteins which act to sequester NF- $\kappa$ B subunits to the cytoplasm, BCL3 is predominantly a nuclear protein (Bours, Franzoso et al. 1993; Nolan, Fujita et al. 1993; Zhang, Didonato et al. 1994) which is involved in regulating NF- $\kappa$ B-mediated gene transcription in a cell-type and stimulus-specific manner.

### 1.4.2 BCL3 structure

The human *BCL3* gene, located on chromosome 19, is approximately 11.5kb in length, contains nine exons and encodes a 446-residue protein (Figure 1.10) (McKeithan, Ohno et al. 1994). The gene encodes seven copies of a 33-37-amino acid element called the ankyrin repeat domain (ARD), which is common to all I $\kappa$ B proteins. The first two exons encode a proline rich N-terminus which contains a nuclear localisation sequence (NLS) within the first 30 amino acids (Keutgens, Zhang et al. 2010). Exons 3-8 encode the seven ankyrin repeats that are essential for the interaction of BCL3 with p50 and p52 (Bours, Franzoso et al. 1993). The serine- and proline-rich C-terminus is encoded by exon 9 (McKeithan, Ohno et al. 1994). Both the C-terminus and N-terminus of the BCL3 protein contain transactivation domains, which are essential for it to function as a transcriptional co-activator (Bours, Franzoso et al. 1993). The mouse *Bcl3* gene, located on chromosome 7, is homologous to the human gene.

### 1.4.3 Regulation of BCL3

BCL3 is a key modulator of NF- $\kappa$ B transcriptional activity and as such it can cause the aberrant expression of NF- $\kappa$ B gene targets. BCL3 expression therefore has to be tightly controlled at both the transcriptional and protein level.

#### 1.4.3.1 Transcriptional regulation

*BCL3* gene expression has been shown to be induced by a number of different factors including cytokines, hormones, endotoxins and viral oncogenic proteins (Table 1.2). The function of the resulting BCL3 protein can vary dramatically according to the stimulus that induced it and the cell type in which it was induced.

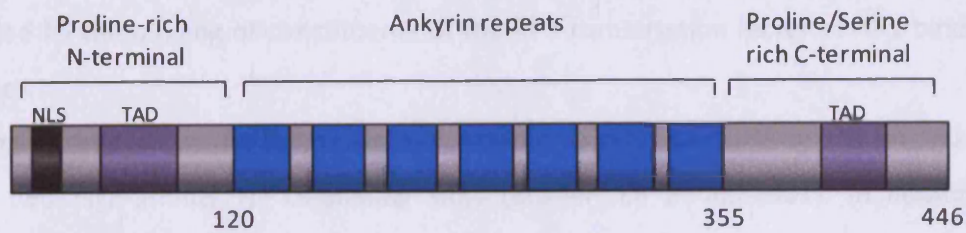


**Figure 1.10: Structure of the BCL3 protein**

BCL3 is a 446-residue protein consisting of a proline-rich N-terminal domain (first 120 amino acids), an ankyrin repeat domain (between amino acids 120 and 355) and a proline/serine-rich C-terminus (between amino acids 355 and 446). A nuclear localisation sequence (NLS, black) is contained within the first 30 amino acids of the N-terminus. Both the N- and C-termini contain transcriptional activation domains (TAD, purple; figure adapted from Michel, Soler-Lopez et al. 2001; Perkins 2007).

Inducer	Cell Type	Reference
Granulocyte-macrophage colony-stimulating factor (GM-CSF) Erythropoietin (Epo)	Human Erythroleukaemia Cells, Haematopoietic Progenitor Cells	(Zhang, Harhaj et al. 1998), (Crocker, Mielke et al. 2008)
Granulocyte colony-stimulating factor (G-CSF)	Mouse Myeloid Progenitors	(Kreisel, Sugimoto et al. 2011)
Interleukin-4 (IL-4)	Murine T-Helper Cells	(Rebollo, Dumoutier et al. 2000).
Interleukin-9 (IL-9)	Mouse T-Lymphocytes, Mast Cells	(Richard, Louahed et al. 1999)
Interleukin-6 (IL-6)	Human Multiple Myeloma Cells, Haematopoietic Progenitor Cells	(Brocke-Heidrich, Ge et al. 2006) (Brenne, Fagerli et al. 2009) (Crocker, Mielke et al. 2008)
Interleukin-10 (IL-10)	Mouse Macrophages	(Kuwata, Watanabe et al. 2003)
Interleukin (IL)-15,21, TNF $\alpha$ and Insulin-Like Growth Factor-1 (IGF-1)	Human Myeloma Cells	(Brenne, Fagerli et al. 2009)
Interleukin (IL)-4 and-13	Normal human primary epidermal keratinocytes	(Buchau, MacLeod et al. 2009)
TNF- $\alpha$	Human Hepatocellular Carcinoma Cells	(Brasier, Lu et al. 2001).
Adiponectin	Human Macrophages	(Folco, Rocha et al. 2009)
Epstein-Barr virus (EBV) latent membrane protein 1 (LMP1)	Cervical carcinoma cells	(Kung and Raab-Traub 2008)
Lipopolysaccharide (LPS)	Mouse primary T Cells	(Bassetti, White et al. 2009)

**Table 1.2: Examples of inducers of BCL3 expression**

Using various model systems it has been demonstrated that BCL3 expression is regulated at the transcriptional level by the inducible transcription factors, Activator Protein 1 (AP1), STAT3 and NF- $\kappa$ B itself. Analysis of the murine *Bcl3* promoter revealed two AP1-binding sites (Rebollo, Dumoutier et al. 2000). The same study showed that the induction of *Bcl3* expression by IL-4 in a murine T helper cell line

was controlled by the binding of constituents of the AP1 transcription factor at AP1-binding sites in the *Bcl3* promoter.

Further analysis of the *Bcl3* promoter identified one STAT3-binding site (Kung and Raab-Traub 2008), and two high-affinity NF- $\kappa$ B-binding sites (Brasier, Lu et al. 2001). In addition, two highly conserved enhancers for BCL3 transcription, HS3 and HS4, have been described (Ge, Li et al. 2003). The HS3 enhancer contains binding sites for NF- $\kappa$ B, STAT3, AP1, CRE and Ets, as well as two potential AP4-binding sites (Ge, Li et al. 2003). The HS4 enhancer contains three STAT3 binding sites (Brocke-Heidrich, Ge et al. 2006). The importance of STAT3 in the regulation of *BCL3* expression was demonstrated in a study investigating the effects of LMP1 on *BCL3* expression and EGFR induction. The results showed that, in LMP1-expressing cells, increased levels of phosphorylated STAT3 were detected at binding sites not only on the *BCL3* promoter but also on the HS3 and HS4 intronic enhancers (Kung and Raab-Traub 2008), resulting in induced *BCL3* expression.

The transcriptional regulation of *BCL3* is a tightly controlled process that is cell and stimulus specific. This is illustrated by the regulation of *BCL3* in response to IL-6. *BCL3* expression was shown to be induced by IL-6 in multiple myeloma cell lines via STAT3 binding to the HS4 intronic enhancer, resulting in *BCL3* negatively regulating its own transcription at NF- $\kappa$ B sites within its own promoter (Brocke-Heidrich, Ge et al. 2006). However, in the hepatocellular carcinoma cell line, HepG2, IL-6 was incapable of inducing *BCL3* expression even though STAT3 was also found to be bound to, and to activate, an HS4 reporter construct in response to the cytokine (Brocke-Heidrich, Ge et al. 2006). Interestingly, an earlier study showed that *BCL3* could be induced in this HepG2 cell line in response to a different stimulus, TNF- $\alpha$ , in an NF- $\kappa$ B-dependent rather than STAT3-dependent manner (Brasier, Lu et al. 2001). The authors suggested that *BCL3* transcription can be initiated by both NF- $\kappa$ B and STAT3, but only NF- $\kappa$ B can additionally stabilise the *BCL3* mRNA. Thus, in multiple myeloma cells that are known to have a sustained low level of NF- $\kappa$ B activation (Feinman, Koury et al. 1999), IL-6-induced *BCL3* mRNA may be stabilised by NF- $\kappa$ B. However, in HepG2 cells that lack background NF- $\kappa$ B activation, IL-6-induced *BCL3* mRNA is not stabilised and protein expression is not observed. This suggests that NF- $\kappa$ B is essential for *BCL3* expression. The exact mechanisms behind the co-ordinated actions of AP1, STAT3 and NF- $\kappa$ B on *BCL3* expression remain to be identified.

#### 1.4.3.2 Post-transcriptional regulation

After DNA is transcribed and mRNA is formed, the translation of transcripts is regulated by Micro-RNAs (MiRNAs) or RNA-binding proteins. There is evidence to suggest that BCL3 is regulated at the post-transcriptional level. For example, a recent study demonstrated that MiRNA-125 targets and down-regulates *BCL3* at the translational level in human ovarian cancer cells (Guan, Yao et al. 2010). In addition, it has been shown that, although *BCL3* mRNA is highly expressed in mouse splenocytes, it is not

detected at the protein level unless mice are treated with oestrogen, which induces strong nuclear BCL3 protein expression (Dai, Phillips et al. 2007). The mechanism behind this post-transcriptional modification was not explored, but the authors again suggest that MiRNAs may be involved.

#### 1.4.3.3 Degradation

Mechanisms underlying BCL3 degradation are generally still poorly defined. However, a few recent studies have given some insight into this process. An early study demonstrated that glycogen synthase kinase (GSK)-mediated phosphorylation of BCL3 resulted in its ubiquitination and degradation (Viatour, Dejardin et al. 2004). It has subsequently been shown that an interaction between the N-terminal domain of BCL3 and the proteasome subunit  $\beta$  type-1 (PSMB1), is essential for this degradation to occur (Keutgens, Zhang et al. 2010). BCL3 has also been shown to interact with the E3-ligase, transducin  $\beta$ -like 1X-related protein 1 (TBLR1), which promoted its polyubiquitination and subsequent degradation in a GSK3-independent manner (Keutgens, Shostak et al. 2010).

### 1.4.4 Molecular functions of BCL3

Unlike other I $\kappa$ B proteins, which act primarily to sequester NF- $\kappa$ B subunits in an inactive state in the cytoplasm, BCL3 most often binds to p50 and p52 NF- $\kappa$ B subunits, where it has been shown to modulate their cellular localisation and transcriptional activity in a variety of contrasting ways.

#### 1.4.4.1 Modulation of NF- $\kappa$ B p50 and p52 transcriptional activity

The very first reports on the function of BCL3 showed that its central ARD preferentially interacts with p50 and p52 homodimers to inhibit their binding to DNA (Hatada, Nieters et al. 1992; Kerr, Duckett et al. 1992; Wulczyn, Naumann et al. 1992; Franzoso, Bours et al. 1992; Franzoso, Bours et al. 1993; Inoue, Takahara et al. 1993; Naumann, Wulczyn et al. 1993; Nolan, Fujita et al. 1993). Some of these studies proposed that BCL3 could prevent both p50:p65 heterodimers and p50 homodimers from binding to  $\kappa$ B sites (Kerr, Duckett et al. 1992; Wulczyn, Naumann et al. 1992; Naumann, Wulczyn et al. 1993). This was subsequently disputed by other reports demonstrating that BCL3 could only inhibit the binding of p50 and p52 homodimers. The discrepancy between these observations was suggested to be due to the model systems used (Nolan, Fujita et al. 1993). Wulczyn et al. (1992) used a bacterially derived, truncated version of BCL3 that was unlikely to have undergone sufficient post-translational modifications. BCL3 phosphorylation was subsequently shown to be essential for the efficient inhibition of p50 and p52 DNA binding (Nolan, Fujita et al. 1993). Truncation and the resulting loss of phosphorylation may well have reduced BCL3 specificity towards p50 and p52 homodimers. In the case of Kerr et al. (1992), inhibition of p50:p65 only occurred at very high BCL3 concentrations, which may not have been physiologically relevant. Despite these discrepancies, all of the initial reports supported the proposal suggested by Franzoso et al. (1992 & 1993) that BCL3 can facilitate NF- $\kappa$ B transactivation of

target genes by binding to, and removing inhibitory p50 and p52 dimers from NF- $\kappa$ B DNA-binding sites, and thereby enhancing the binding of active NF- $\kappa$ B subunits.

In contrast with these early studies that were predominantly carried out using BCL3 derived from bacteria or insect cells, it was subsequently shown that, in mammalian-derived models, BCL3 does not necessarily inhibit the binding of NF- $\kappa$ B subunits to DNA, but it can instead function as a co-activator that can promote transcription in association with p50 and p52 homodimers (Fujita, Nolan et al. 1993; Bours, Franzoso et al. 1993). Analysis of the N-terminus and C-terminus of the BCL3 protein revealed that they both contain essential and co-operative transactivation domains (Fujita, Nolan et al. 1993), further supporting the notion that BCL3 can behave as a co-activator of transcription. Numerous subsequent studies have demonstrated the co-activating function of BCL3 (Hirano, Tanaka et al. 1998; Pan and McEver 1995; Na, Choi et al. 1999; Zhang, Warren et al. 2007).

More recent reports have shown that BCL3 can also indirectly repress NF- $\kappa$ B activation by facilitating the binding of inactive p50 homodimers to NF- $\kappa$ B-binding sites, thereby preventing the association of other transactivating dimers (Muhlbauer, Chilton et al. 2008; Kuwata, Watanabe et al. 2003; Caamano, Perez et al. 1996; Carmody, Ruan et al. 2007; Wessells, Baer et al. 2004). For example, Kuwata et al. (2003) demonstrated that BCL3 was able to suppress TNF- $\alpha$  expression in macrophages by driving inhibitory p50 homodimers onto the TNF- $\alpha$  promoter. It is possible that the BCL3-dependent increase in p50 homodimer binding is not due to an increase in the DNA-binding affinity of p50 homodimers, but is instead due to altered turnover of p50, resulting in an increase in the number of homodimers present in the nucleus. Indeed, it has been shown that BCL3 can delay the K<sup>48</sup>-ubiquitination and subsequent degradation of DNA-bound p50 homodimers, thereby promoting p50 DNA occupancy (Carmody, Ruan et al. 2007).

Overall, the literature suggests that BCL3 has two contrasting functions in the regulation of NF- $\kappa$ B-mediated transcription which are context and stimulus specific. In one role, it binds to p50 and p52 homodimers and acts as a co-activator of NF- $\kappa$ B target gene transcription. In the other role, it can delay the turnover of p50 and promote the stable occupancy of repressive p50 homodimers to DNA, thereby indirectly inhibiting the transcription of NF- $\kappa$ B target genes.

The precise mechanisms underlying these dual functions remain unclear. However, it is highly likely that post-translational modifications may be essential in determining the functional outcome of BCL3 expression. A number of reports have shown BCL3 to be heavily phosphorylated in its C-terminal domain in a variety of different cell types (reviewed in Viatour, Merville et al. 2004; Fujita, Nolan et al. 1993; Viatour, Dejardin et al. 2004; Bundy and McKeithan 1997; Nolan, Fujita et al. 1993; Caamano, Perez et al. 1996). The phosphorylation status of BCL3 has been found to have a pronounced effect on its interaction with p50 and p52 NF- $\kappa$ B subunits (Nolan, Fujita et al. 1993; Caamano, Perez et al. 1996;

Bundy and McKeithan 1997). Bundy et al. (1997) proposed that the ability of BCL3 to enhance or inhibit p52 DNA binding is heavily dependent on its concentration and phosphorylation status, which, as a result, is likely to affect NF- $\kappa$ B-dependent gene transcription. Later work by Viatour et al. (2004) demonstrated that GSK3 can mediate BCL3 phosphorylation at two C-terminal serine residues (Viatour, Dejardin et al. 2004). BCL3 phosphorylation at these sites modulated its association with HDACs-1, -3 and -6 and limited the expression of target genes such as *SLP1* and *CXCL1*. Interestingly, the binding of BCL3 to p50 and p52 NF- $\kappa$ B subunits was later shown to be required for its GSK3-dependent constitutive phosphorylation (Keutgens, Zhang et al. 2010). C-terminal phosphorylation of BCL3 also resulted in the ubiquitination of two lysine residues in the N-terminus of the protein, which lead to its subsequent degradation (Viatour, Dejardin et al. 2004). Interestingly, these N-terminal lysine residues are located in one of the transactivation domains of BCL3 (Bours, Franzoso et al. 1993). Previous studies have demonstrated that ubiquitination of DNA bound transcription factors within their transactivation domain is essential for their transcriptional activity (reviewed in Freiman and Tjian 2003; Conaway, Brower et al. 2002). This raises the possibility that the ubiquitination status of BCL3 may be important in determining its transcriptional activity. In addition, Lys<sup>63</sup>-polyubiquitination of BCL3 has been shown to be necessary for its nuclear translocation in keratinocytes and B-cells (Massoumi, Chmielarska et al. 2006; Hovelmeyer, Wunderlich et al. 2007). Deubiquitination of BCL3 was found to prevent its nuclear translocation and, as a result, inhibited p50:BCL3- or p52:BCL3-dependent transcription (Massoumi, Chmielarska et al. 2006; Hovelmeyer, Wunderlich et al. 2007; Massoumi, Kuphal et al. 2009). It is also possible that other post-translational modifications such as acetylation are responsible for regulating the transcriptional function of BCL3, although this is yet to be proven experimentally.

#### 1.4.4.2 Subcellular localisation of NF- $\kappa$ B subunits

BCL3 has also been shown to regulate NF- $\kappa$ B signalling by influencing the subcellular localisation of NF- $\kappa$ B transcription factors in a variety of contrasting ways (Naumann, Wulczyn et al. 1993; Zhang, Didonato et al. 1994; Watanabe, Iwamura et al. 1997). An early study demonstrated that BCL3 was generally confined to the cytoplasm in Cos7 cells and that it was able to promote the translocation of p50 from the nucleus into the cytoplasm (Naumann, Wulczyn et al. 1993). The BCL3 protein has subsequently been shown to contain a nuclear localisation sequence in its N-terminal domain (Keutgens, Zhang et al. 2010) and to predominantly reside in the nucleus (Bours, Franzoso et al. 1993; Nolan, Fujita et al. 1993; Zhang, Didonato et al. 1994; Keutgens, Zhang et al. 2010). Furthermore, BCL3 has now been demonstrated to successfully translocate p50 from the cytoplasm into the nucleus (Zhang, Didonato et al. 1994) and in another study, enhance the number of p50 homodimers in the nucleus by the apparent liberation of p50 from cytoplasmic p105:p50 complexes (Watanabe, Iwamura et al. 1997).

#### 1.4.4.3 Regulation of alternative transcription factor pathways

Although BCL3 primarily acts as a mediator of NF- $\kappa$ B transcription via interactions with p50 and p52 homodimers, it has also been shown to function independently of NF- $\kappa$ B subunits and regulate the transcriptional ability of other transcription factors (Na, Choi et al. 1998; Na, Choi et al. 1999; Jamaluddin, Choudhary et al. 2005). For example, specific associations between BCL3 and the general transcription factors, TFIIB, TBP, and TFIIA, have been demonstrated (Na, Choi et al. 1998). In addition, BCL3 has been shown to co-activate both the Retinoid X receptor (RXR) and the AP1 transcription factors (Na, Choi et al. 1998; Na, Choi et al. 1999) and in contrast, repress STAT1 transcriptional activity (Jamaluddin, Choudhary et al. 2005). These effects on other transcriptional pathways give increased insight into the functional diversity of BCL3.

#### 1.4.4.4 Formation of co-activating or co-repressing complexes

Co-activator and co-repressor complexes are composed of multiple proteins that bind to transcription factors and control chromatin modifications, thereby aiding in the regulation of transcription. BCL3 has been shown to form both co-activator and co-repressor complexes to facilitate transcriptional regulation (Na, Choi et al. 1998; Dechend, Hirano et al. 1999; Na, Choi et al. 1999; Kim, Kim et al. 2005; Zhao, Ramakrishnan et al. 2005; Kabuta, Hakuno et al. 2010; Hishiki, Ohshima et al. 2007; Jamaluddin, Choudhary et al. 2005; Yang, Williams et al. 2009; Keutgens, Shostak et al. 2010; Wessells, Baer et al. 2004). Dechend et al. (1999) demonstrated that the ankyrin repeat domain of BCL3 can physically interact with the nuclear proteins TIP60, BARD1, JAB1 and Pirin. TIP60 or BARD1 were able to form quaternary complexes with BCL3:p50 homodimers, JAB1 increased the DNA-binding ability of BCL3:p50 and Pirin had both of the above effects. The TIP60:BCL3:p50 interaction led to super-activation of an NF- $\kappa$ B target gene in *Drosophila* SL2 cells. Interestingly, all of these BCL3-interacting proteins are able to bind other transcription factors, suggesting that BCL3 can act to mediate cross talk between NF- $\kappa$ B and a variety of other transcriptional regulators (Dechend, Hirano et al. 1999). Additionally, BCL3 has been shown to interact with other co-activators of transcription such as SRC-1, CBP/300 and PPAR $\gamma$  co-activator 1 $\alpha$  (Na, Choi et al. 1999; Na, Choi et al. 1998; Yang, Williams et al. 2009). In contrast, it has also been shown that BCL3 can form complexes with transcriptional co-repressors such as HDACs to inhibit transcription (Wessells, Baer et al. 2004; Jamaluddin, Choudhary et al. 2005). A study by Wessells et al. (2004) demonstrated that LPS induced TNF- $\alpha$  production in macrophages could be attenuated by BCL3, p50 and HDAC1 complexes. In addition, BCL3 has been shown to recruit HDAC1 to the IL-8 promoter and repress NF- $\kappa$ B- and STAT1- mediated transcription (Jamaluddin, Choudhary et al. 2005). Interestingly, another report suggested that, rather than forming a co-repressor complex with HDACs, BCL3 could bind to, and remove, repressive HDACs from DNA in order to promote transcription (Viatour, Dejardin et al. 2004). More recently, interactions between BCL3 and

the co-repressor, CtBP, have been observed (Keutgens, Shostak et al. 2010). This association was identified to be crucial for both stabilising BCL3 and for its ability to repress gene transcription. The underlying mechanisms that determine how these complexes interact with BCL3 remain unclear. However, there is evidence to suggest that the specific sequence of the  $\kappa$ B DNA-binding site may dictate which co-regulatory complex is formed (Leung, Hoffmann et al. 2004).

#### 1.4.5 Physiological functions of BCL3

As a modifier of the NF- $\kappa$ B signalling pathway, BCL3 is involved in the regulation of a number of cellular processes. BCL3 knock-out mice have been generated in order to gain an understanding of the basic physiological roles of the gene (Franzoso, Carlson et al. 1997; Schwarz, Krimpenfort et al. 1997). These mice develop apparently normally, in that they display no alterations in their gross anatomy or behaviour. However, they have disorganised B and T cells in germinal centres and severe defects in the microarchitecture of the spleen and lymph nodes. This is accompanied by an inability to produce antigen-specific antibodies and a failure to resist infection by certain microbial pathogens such as *Toxoplasma gondii*, *Listeria monocytogenes*, and *Streptococcus pneumoniae* (Franzoso, Carlson et al. 1997; Schwarz, Krimpenfort et al. 1997; Riemann, Endres et al. 2005).

*Bcl3*- deficient and *nf- $\kappa$ b1* (*p105/p50*)- or *nf- $\kappa$ b2* (*p100/p52*)- deficient mice share similar phenotypes in many respects. For example, both *Bcl3*-deficient and *nf- $\kappa$ b2*-deficient mice have similar defects in lymphoid organogenesis (Caamano, Rizzo et al. 1998; Franzoso, Carlson et al. 1998). Moreover, the response to pathogenic challenge is remarkably similar in *nf- $\kappa$ b1*- and *Bcl3*- deficient mice (Sha, Liou et al. 1995). These similarities serve to confirm the biochemical co-operation between BCL3 and the p50 and p52 subunits for transcriptional regulation *in vivo*. However, although there is clear overlap in the phenotypes of these knock-out mice, several differences also exist, indicating that BCL3 is capable of functioning independently of p50 and p52 NF- $\kappa$ B subunits. Interestingly, mice lacking both BCL3 and p52 fail to survive beyond 4 weeks of age because of severe multi-organ inflammation, attributed to an enrichment of autoreactive T-cells (Zhang, Wang et al. 2007). This indicates that BCL3 has additional redundant roles in preventing the immune system from attacking its host that only become apparent in the absence of p52.

##### 1.4.5.1 BCL3 and immune responses

The immunological defects observed in *Bcl3*- deficient mice indicate a central role for BCL3 in the immune system. Subsequent studies have investigated this further and highlighted BCL3 to be essential for appropriate T-cell survival and immune responses. The inability of *Bcl3*<sup>-/-</sup> mice to resist certain microbial challenges was found to be due to an impaired protective T helper 1-like response (Franzoso, Carlson et al. 1997). Further analysis of T-cells from *Bcl3*-deficient mice revealed that they

displayed defects in T helper 2 (Th2) cell differentiation with impaired IL-4, IL-5 and IL-13 cytokine production (Corn, Hunter et al. 2005). This was attributed to a BCL3-dependent decrease in the expression of GATA-3, a transcription factor known to activate IL-4 expression, which in turn induces the differentiation of naive helper T-cells to Th2 cells (Zhu, Yamane et al. 2006). A number of studies have demonstrated that BCL3 is also able to prolong the survival of T-cells after activation with an immunological adjuvant, a material that improves the immune response of vaccines (Rebollo, Dumoutier et al. 2000; Mitchell, Hildeman et al. 2001; Mitchell, Teague et al. 2002; Mitchell, Thompson et al. 2002; Bauer, Villunger et al. 2006; Li, Eppolito et al. 2006; Rangelova, Kirschnek et al. 2008; Valenzuela, Hammerbeck et al. 2005; Bassetti, White et al. 2009). For example, *BCL3* expression was shown to be up-regulated in T-cells in response to IL-12 (Valenzuela, Hammerbeck et al. 2005; Li, Eppolito et al. 2006), a cytokine produced in antigen-presenting cells which are the direct targets of adjuvants (Trinchieri 2003). The downstream consequences of BCL3 induction in T-cells has been shown to involve the blockade of BIM activation to inhibit apoptosis (Bauer, Villunger et al. 2006). Interestingly, later studies suggest that, although BCL3 over-expression is able to mimic the effect of adjuvants, it is not absolutely essential for their action on T-cell survival (Bassetti, White et al. 2009; Chilton and Mitchell 2006). This was demonstrated by the fact that T-cells from *Bcl3*<sup>-/-</sup> mice exhibited long-term survival in response to adjuvants that was comparable to that in wild-type mice. The authors presented data to suggest that other IκB proteins, such as IκBβ or IκBε, could act in the absence of BCL3 to promote a survival advantage to T-cells activated in response to adjuvant stimulation (Chilton and Mitchell 2006). This study also proposed an essential role for BCL3 in the production of gamma interferon (INFγ) upon secondary stimulation of T-cells with antigens (Chilton and Mitchell 2006). INFγ is a cytokine that is critical for immunity against viral and intracellular bacterial infections. The link between INFγ and BCL3 provides further insight into how BCL3 functions as a mediator of microbial resistance. Evidence to support this association was provided in another study in which BCL3-deficient mice were shown to be highly susceptible to *L. monocytogenes* infection, in part due to diminished INFγ brought about by the increased expression of IL-10 in *Bcl3*<sup>-/-</sup> macrophages (Riemann, Endres et al. 2005). In addition, this increase in IL-10 and loss of INFγ was recapitulated in BCL3-deficient mice after lung challenge with *Klebsiella pneumoniae*, rendering them more susceptible to this pathogen than wild-type mice (Pene, Paun et al. 2011).

As well as playing an important role in supporting T-cell responses, BCL3 can also regulate the immunological functions of other cells. BCL3-deficient mice have been shown to be incapable of developing tolerance to repeated toll-like receptor (TLR) stimulation, which is important in preventing deleterious inflammatory responses (Carmody, Ruan et al. 2007). This defect was attributed to the hyper-responsiveness of BCL3-deficient macrophages, dendritic cells and B-cells to TLR signalling,

resulting in aberrant cytokine production. Another report showed that BCL3 can act as a transcriptional modulator of the cutaneous innate host immune response by regulating the expression of antimicrobial peptides and cytokines in keratinocytes (Buchau, MacLeod et al. 2009). Furthermore, BCL3 has been shown to play a critical role in limiting granulocyte proliferation and differentiation under emergency inflammatory conditions in the lung, resulting in the prevention of acute inflammatory tissue injury (Kreisel, Sugimoto et al. 2011).

Overall, BCL3 clearly plays a subtle but important role in the regulation and function of cells of the immune system. Consequently, when deregulated it has been shown to be implicated in the pathology of a number of human diseases of the immune system, such as autoimmune type 1 diabetes (Ruan, Zheng et al. 2010), atopic dermatitis (Massoumi 2009), crohn's disease (Fransen, Visschedijk et al. 2010) and lymphoid malignancies (see section 1.4.6).

#### *1.4.5.2 BCL3 and cell survival, proliferation and apoptosis*

A number of reports have shown that BCL3 expression can enhance the survival of a variety of different cell types by either promoting proliferation or preventing apoptosis. Studies relating to the role of BCL3 in the immune response clearly demonstrated that BCL3 can prolong the survival of T-cells by delaying their apoptosis (see section 1.4.5.1 above). To study this further, mice over-expressing BCL3 in T- and B-cells were generated. These transgenic animals developed a lymphoproliferative disorder involving splenomegaly and an accumulation of mature B-cells in the bone marrow, lymph nodes and peritoneal cavity (Ong, Hackbarth et al. 1998). B-cell expansion was found to be due to increased proliferation of the cells rather than as a result of a defect in apoptosis. Subsequently to this, numerous studies have demonstrated the ability of BCL3 to promote the proliferation of a variety of cell types (Zhang, Harhaj et al. 1998; Na, Choi et al. 1999; Viatour, Dejardin et al. 2004; Park, Chung et al. 2006; Zhang, Warren et al. 2007; Brenne, Fagerli et al. 2009; Zamora, Espinosa et al. 2010). For example, the expression of BCL3 in response to GM-CSF and Epo in an erythroleukaemia cell line was associated with increased proliferation, suggesting that BCL3 may participate in the regulation of NF- $\kappa$ B target genes involved in erythropoiesis (Zhang, Harhaj et al. 1998). Na et al. (1999) showed that microinjection of a BCL3 expression vector into Rat-1 fibroblast cells stimulated AP1 transactivation and enhanced the proliferation potential of the cells. This pro-proliferative effect has also been demonstrated in murine xenograft and allograft transplant models (Pratt, Bishop et al. 2003; Viatour, Dejardin et al. 2004). For example, over-expression of BCL3 in NIH3T3 fibroblast cells resulted in the formation of tumours when injected into the flanks of nude mice whereas injection of wild-type NIH3T3 cells did not. Interestingly, GSK-mediated phosphorylation of BCL3 attenuated this effect (Viatour, Dejardin et al. 2004).

Numerous studies have now demonstrated that BCL3-mediated increases in cell proliferation involve the transcriptional upregulation of CYCLIN D1, an important regulator of G1- to S-phase

transition (Westerheide, Mayo et al. 2001; Massoumi, Chmielarska et al. 2006; Park, Chung et al. 2006; Zhang, Warren et al. 2007; Wang, Shi et al. 2010). Over-expression of BCL3 in immortalized human breast epithelial cells resulted in a shortened G1 phase of the cell cycle and an increase in *CYCLIN D1* mRNA and protein expression. BCL3, in co-operation with p52 homodimers was found to directly transactivate the *CYCLIN D1* promoter via NF- $\kappa$ B-binding sites (Westerheide, Mayo et al. 2001). Subsequently, BCL3 has been shown to upregulate *CYCLIN D1* expression in a number of different cell types, such as mouse primary keratinocytes (Massoumi, Chmielarska et al. 2006), human bronchial epithelial cells (Wang, Shi et al. 2010) and human hepatocytes (Park, Chung et al. 2006).

Inhibition of BCL3 expression by the tumour suppressor, p53, can also alter cell survival. Over-expression of p53 in H1299 human non-small-cell-lung carcinoma cells reduced the levels of transcriptionally active BCL3:p52 complexes and concomitantly increased the levels of repressive HDAC1:p52 complexes, resulting in active repression of the *CYCLIN D1* promoter and subsequent cell cycle arrest (Rocha, Martin et al. 2003). Interestingly, BCL3 has also been shown to be capable of suppressing DNA damage-induced p53 activity by transcriptionally up-regulating its inhibitor, HDM2 (Kashatus, Cogswell et al. 2006). This suppression inhibited p53-induced apoptosis via reduced transcription of the pro-apoptotic genes, *p21* and *NOXA*. A number of other studies have also demonstrated that BCL3 is able to provide an overall survival advantage by inhibiting apoptosis rather than driving proliferation (Ahmed and Milner 2009; Kabuta, Hakuno et al. 2010).

A few studies have demonstrated that instead of promoting cell survival, BCL3 can have a pro-apoptotic effect in some contexts (Nishikori, Ohno et al. 2005; Brocke-Heidrich, Ge et al. 2006). Ectopic expression of BCL3 resulted in increased apoptosis in a myeloma cell line (Brocke-Heidrich, Ge et al. 2006) and induction of a hyperphosphorylated form of BCL3 by CD30 in anaplastic large cell lymphoma cell lines was associated with a concomitant increase in pro-apoptotic genes and subsequent cell death (Nishikori, Ohno et al. 2005). In spite of this, the overwhelming evidence suggests that a primary role of BCL3 is to enhance the overall survival of cells by either promoting cell proliferation or inhibiting apoptosis in response to a variety of stimuli. These functions provide insight into how de-regulated expression of BCL3 could potentially fulfil an oncogenic role.

#### 1.4.6 BCL3 and cancer

BCL3 was originally identified through its involvement in a recurring chromosomal translocation t(14;19)(q32;q13) found in some cases of B-cell chronic lymphocytic leukaemia (Ohno, Takimoto et al. 1990; Ueshima, Bird et al. 1985; McKeithan, Ohno et al. 1990; Yabumoto, Ohno et al. 1994). As a result of this translocation, BCL3 becomes juxtaposed to the immunoglobulin heavy chain gene locus, leading to the high expression of *BCL3* mRNA and protein (reviewed in Willis and Dyer 2000). Over-expression of BCL3 has now also often been observed in a number of other B-and T-cell

malignancies (Canoz, Rassidakis et al. 2004; Martin-Subero, Wlodarska et al. 2006; Martin-Subero, Ibbotson et al. 2007; Mathas, Johrens et al. 2005; Au, Horsman et al. 2002; McKeithan, Takimoto et al. 1997; Rassidakis, Oyarzo et al. 2003; Ohno, Nishikori et al. 2005; Soma, Gollin et al. 2006; Szymanowska, Klapper et al. 2008). The expression of BCL3 has been assessed in a large panel of lymphoid neoplasms by immunohistochemistry (Canoz, Rassidakis et al. 2004). This study revealed that BCL3 was over-expressed in 6% of B-cell malignancies, 23% of T-cell malignancies, and 41% of Hodgkin lymphomas. A subsequent study assessed BCL3 expression in 72 cases of chronic lymphocytic leukaemia and observed that 17% were positive for BCL3 expression (Schlette, Rassidakis et al. 2005). Interestingly, high expression of BCL3 correlated with trisomy 12 and genetic abnormalities on chromosome 19, but was not limited to cases with the t(14;19)(q32;q13) translocation, implying that these other chromosomal alterations may also lead to BCL3 expression. As well as B- and T-cell malignancies, BCL3 expression has recently been observed in myeloma cells from patients with multiple myeloma and was shown to be induced by a number of cytokines in myeloma cell lines, resulting in increased cell proliferation (Brenne, Fagerli et al. 2009). Notably, some studies suggest that high expression of BCL3 correlates with aggressive disease and poor patient outcome (Chapiro, Radford-Weiss et al. 2008; Martin-Subero, Ibbotson et al. 2007; Kelly, Wright et al. 2008; Brenne, Fagerli et al. 2009). Chapiro et al. (2008) proposed that chronic lymphocytic leukaemias with the t(14;19)(q32;q13) translocation and high BCL3 expression define a particularly aggressive subtype of the disease. In addition, high BCL3 expression in patients with multiple myeloma correlated with a shorter 5-year survival (Brenne, Fagerli et al. 2009). These studies indicate a potential role for BCL3 in promoting the progression of haematological malignancies.

Although BCL3 has primarily been investigated in lymphomas, it has also been shown to be highly expressed in a number of solid epithelial cell cancers (Thornburg, Pathmanathan et al. 2003; Cogswell, Guttridge et al. 2000; Mishra, Bharti et al. 2006; Pallares, Martinez-Guitarte et al. 2004; O'Neil, Buzkova et al. 2007). In nasopharyngeal cancers, BCL3:p50 homodimer complexes were shown to be specifically activated (Thornburg, Pathmanathan et al. 2003). Chromatin immunoprecipitation (ChIP) assays demonstrated that this complex was bound to  $\kappa$ B consensus sequences within the EGFR promoter. Similarly, in oral carcinoma, p50 was shown to be up-regulated and bound to DNA in conjunction with BCL3 (Mishra, Bharti et al. 2006). Interestingly, expression of p50 and BCL3 was shown to be higher in Human Papillomavirus (HPV)-positive oral cancers that have a good prognosis in comparison with those that were HPV-negative and generally have a worse prognosis. The authors suggested that HPV-driven NF- $\kappa$ B activation could promote the differentiation of oral carcinoma cells, leading to better patient prognosis (Mishra, Bharti et al. 2006).

Studies evaluating the expression of NF- $\kappa$ B subunits in hepatocellular and endometrial cancers revealed a very high percentage of BCL3-positive cells within tumours (Pallares, Martinez-Guitarte et al.

2004; O'Neil, Buzkova et al. 2007). In a study of 30 patients with hepatocellular carcinoma, BCL3 was found to be over-expressed in 90% of all hepatocellular tumour cell nuclei in comparison with 26% of adjacent non-neoplastic cells (O'Neil, Buzkova et al. 2007). p50 and p52, but not p65, were also commonly observed in the nuclei of tumour cells, suggesting that BCL3:p52 and BCL3:p50 interactions may be important in the pathogenesis of this disease. Likewise, evaluation of 84 cases of endometrial cancer revealed that all tumours displayed BCL3 positivity, with 60.7% of them showing nuclear immunostaining (Pallares, Martinez-Guitarte et al. 2004). BCL3 nuclear positivity correlated with p52 nuclear positivity, suggesting an involvement of BCL3:p52 complexes in this cancer type. Interestingly, in colon cancer, BCL3 expression was found to be the same in primary tumours and normal tissues in a study of 23 patients with metastatic disease (Puvvada, Funkhouser et al. 2010). However, nuclear BCL3 expression in primary tumours correlated negatively with patient survival, implying that BCL3 may play a role in, and be a good prognostic marker for, metastatic disease.

Cylindromas have also been shown to be associated with BCL3 (Ikeda and Dikic 2006; Massoumi, Chmielarska et al. 2006). Cylindromas are generally benign skin tumours caused by loss of function mutations in the tumour suppressor gene, *CYLD* (for review, see Massoumi and Paus 2007). *CYLD* can bind to and deubiquitinate BCL3 to prevent its nuclear translocation in some cell types (Massoumi, Chmielarska et al. 2006; Hovelmeyer, Wunderlich et al. 2007; Massoumi, Kuphal et al. 2009). Mice lacking *CYLD* are highly susceptible to chemically induced skin tumours because of the accumulation of nuclear BCL3 resulting in up-regulated *CYCLIN D1* expression (Massoumi, Chmielarska et al. 2006). A similar mechanistic observation has been made in melanoma cells. The transcription factor, *SNAIL*, was shown to inhibit *CYLD* expression, resulting in the nuclear translocation of BCL3. In these cells, nuclear BCL3 was shown to activate both the *CYCLIN D1* and *N-cadherin* promoters leading to increased proliferation and invasion, implicating it in the poor prognosis observed in patients with *CYLD*-negative myeloma (Massoumi, Kuphal et al. 2009).

#### 1.4.6.1 *BCL3 and breast cancer*

The role of BCL3 in breast cancer development has not been extensively investigated. There are, however, a small number of studies describing BCL3 expression and function in human breast tumour samples, normal mammary epithelial cells and breast cancer cell lines. Cogswell et al. (2000) was the first to analyse BCL3 expression in primary human breast tumours and human breast cancer cell lines. Although the nuclear extracts from the majority of breast cancer cell lines analysed expressed NF- $\kappa$ B subunits, BCL3 was found not to be expressed in any of them. However, analysis of samples from four breast cancer patients revealed that the protein levels of BCL3, along with p50, p52 and c-Rel, were increased in all tumour samples in comparison with normal adjacent tissue. This was found to be regulated at the RNA level in two further samples, which also showed increases in *CYCLIN D1* expression.

In support of these data, a more recent report found that 9 out of 12 human breast cancer tumours had higher BCL3 protein levels than their corresponding adjacent tissue (Choi, Lee et al. 2010). In contrast with the study by Cogswell et al. (2000), this report also showed that BCL3 protein levels were elevated in breast cancer cell lines in comparison with a normal breast cell line. The discrepancies are likely to be due either to the use of different cell lines (work from Cogswell and co-workers does not clearly state which cells were analysed) or the fact that the latter study did not specifically assess nuclear extracts. In addition to demonstrating BCL3 over-expression in breast tumours, the work by Choi et al. (2010) also established a mechanism underlying the potential pro-oncogenic function of BCL3 in breast cancer. BCL3 was shown to bind to and stabilize the transcriptional repressor, CtBP, by inhibiting its ubiquitination. This BCL3-mediated stabilisation resulted in the repression of CtBP-dependent pro-apoptotic genes, such as *p21* and *NOXA*, and consequently inhibited apoptosis. The interaction between BCL3 and CtBP was subsequently shown to be clinically relevant, as the over-expression of BCL3 protein levels in breast tumour samples correlated with the over-expression of CtBP in the same samples. In addition to this anti-apoptotic function, the well-established mechanism behind BCL3-induced proliferation involving transactivation of the *CYCLIN D1* promoter has also been demonstrated in mammary epithelial cells of human and rat origin (Westerheide, Mayo et al. 2001; Zhang, Warren et al. 2007).

As NF- $\kappa$ B activity has been associated with ER-negative breast cancer, the effect of NF- $\kappa$ B and BCL3 on the transition of breast cancer cells from oestrogen dependence to independence has also been investigated (Pratt, Bishop et al. 2003). It was established that the withdrawal of oestrogen from the oestrogen-dependent MCF7 breast cancer cell line resulted in up-regulated BCL3 expression, suggesting that it had a role to play in promoting the transition to oestrogen independence. Interestingly, transplantation of MCF7 cells ectopically expressing BCL3 into ovariectomised nude mice resulted in substantially augmented tumour establishment and growth but it was insufficient to maintain tumour growth, upon removal of an oestrogen pellet. Although these results demonstrate that BCL3 expression alone is unable to confer oestrogen independence, they do clearly demonstrate its oncogenic potential in breast cancer cells.

Collectively, the limited evidence in the literature would suggest that BCL3 can potentially fulfil an oncogenic function in the mammary gland. Further investigation into the role of BCL3 in specific subtypes of the disease and elucidation of the precise mechanisms determining its effects will help to establish its potential as a new therapeutic target in breast cancer.

## 1.5 Aims of this study

As described in the introduction, both STAT3 and NF- $\kappa$ B transcription factors play an important role in regulating mammary gland involution. As BCL3 is a known STAT3 transcriptional target and NF- $\kappa$ B co-factor that is up-regulated at the onset of involution, it is possible that it may also play a role in the regulation of involution. The first aim of this study was therefore to:

- Determine the effect of BCL3 deficiency on normal mammary gland development and progression through the pregnancy cycle with particular reference to involution.

NF- $\kappa$ B is known to be heavily involved in the pathogenesis of ERBB2-positive breast cancer which has resulted in much interest in the development of NF- $\kappa$ B inhibitors for treating the disease. However, as NF- $\kappa$ B is essential for a variety of normal physiological functions, sustained global inhibition of this transcription factor is likely to have many detrimental side effects. It was hypothesised that as a modulator of NF- $\kappa$ B activity, BCL3 may contribute to the initiation or progression of breast cancer, but that therapeutic inhibition of this co-factor may be less likely to have unfavourable side effects than universal inhibition of NF- $\kappa$ B. The rest of the thesis therefore aimed to:

- Establish the effect of BCL3 deficiency on ERBB2-driven breast cancer development and progression in mice.
- Investigate mechanisms behind BCL3-mediated effects on murine ERBB2-driven breast cancer *in vitro*.
- Determine whether any BCL3-mediated effects on murine ERBB2-positive breast carcinogenesis are also observed in human breast cancer cell lines representing both ERBB2-positive and negative sub-types of the disease.

# **Chapter 2:**

## **Materials and Methods**

## 2.1 Animal experiments

All procedures involving the use of animals were carried out in accordance with the institutional guidelines complying with the U.K. Home Office Regulations (Animals [Scientific Procedures] Act 1986).

### 2.1.1 Animals

The generation of *Bcl3*<sup>-/-</sup>, *MMTV/N<sub>2</sub>* and *MMTV/NK* mice has been described previously (Muller, Sinn et al. 1988; Guy, Webster et al. 1992; Schwarz, Krimpenfort et al. 1997). These animals were all obtained from Jax Mice and Services (Bar Harbor, Main, US) and in-bred on an FVB background. *MMTV/N<sub>2</sub>* or *MMTV/NK* mice were crossed with *Bcl3*<sup>-/-</sup> mice to create three further cohorts of transgenic mice, *Bcl3*<sup>-/-</sup>/*MMTV/N<sub>2</sub>* (or *NK*), *Bcl3*<sup>+/-</sup>/*MMTV/N<sub>2</sub>* (or *NK*) and *Bcl3*<sup>+/+</sup>/*MMTV/N<sub>2</sub>* (or *NK*).

The generation of mice with the mammary specific deletion of *Stat3* (*Blg/Cre/Stat3*<sup>fl<sup>ox</sup>/-</sup>) has been described previously (Chapman, Lourenco et al. 1999). Briefly, mice with one null *Stat3* allele and one floxed *Stat3* allele were crossed with mice expressing *Cre* under the control of the  $\beta$ -lactoglobulin milk gene (*Blg*) promoter (Selbert, Bentley et al. 1998). These animals were a gift from Professor Alan Clarke and maintained on a Black-6 background.

The above experimental mice received an RM3(E) expanded diet (Special Diets Service, UK) and tap water *ad Libitum* and were housed in colony specific cages (max 5/cage) with a 12hr day/night cycle. Animals were weaned and ear marked at approximately 4 weeks of age.

Six to eight week old Balbc/scid mice were obtained from Charles River Laboratories (Wilmington, US) and were housed in individually ventilated cages (Allentown Inc. New Jersey, US) with a 12hr day/night cycle. Mice received a Teklad global 19% protein extruded rodent diet (Harlan Laboratories, Indianapolis, US) and water *ad Libitum*. All food, water, saw dust and water bottles were autoclaved before use. All procedures were performed under a laminar flow hood (Allentown).

### 2.1.2 Genotyping

All mice were genotyped by polymerase chain reaction (PCR) at 6-8 weeks of age. DNA was extracted from tail or ear biopsies after weaning at 4 weeks of age.

#### 2.1.2.1 DNA extraction

A small section of the tail or ear was taken, placed in a 1.5ml eppendorf tube and stored at -20°C. DNA was then isolated by adding 500 $\mu$ l lysis buffer (100mM Tris-HCl; pH8.5 [Sigma], 5mM EDTA [Fisher Scientific], 0.2% w/v sodium dodecyl sulphate [SDS; Sigma], 200mM sodium chloride [Fisher Scientific]) and 5 $\mu$ l of proteinase K [Roche]) to the sample and incubated overnight at 55°C. Samples were mixed thoroughly and centrifuged at 13,000rpm for 10 minutes. The supernatant was transferred to a clean eppendorf tube and 500 $\mu$ l of isopropanol (Fisher Scientific) was added and left for 5 minutes

to precipitate out the DNA. Samples were centrifuged for 5 minutes to pellet the DNA. The pellet was washed in 70% ethanol (Fisher Scientific) and dried at 55°C before being dissolved in 100µl RNase and DNase free H<sub>2</sub>O at 55°C for 1 hour. This DNA solution was used for the PCR protocols outlined in Table 2.1-2.4.

#### 2.1.2.2 *Generic PCR protocol*

Primers were purchased from Sigma-Genosys and were either designed using primer 3 software (<http://frodo.wi.mit.edu/primer3/>) or using previously published sequences (Table 2.2). To check for mis-priming, all sequences were verified by performing in silico PCR <http://genome.csdb.cn/cgi-bin/hgPcr>.

Appropriate volumes (Table 2.3& 2.4) of DNA extract or DNase and RNase free water (Sigma) control were loaded into separate wells of 0.2ml strip tubes (StarLabs). A PCR mastermix containing all other reaction components was then prepared according to Table 2.3 or 2.4. Appropriate volumes of mastermix was added to each well and gently pipetted to ensure homogeneous mixing of DNA and reaction mix. Strip tubes were sealed with appropriate caps (StarLabs) and were then briefly spun in a Technico Mini Centrifuge (Technico). Reactions were then run on a iCycler PCR machine (BioRad) according to the cycling conditions detailed in Table 2.1.

#### 2.1.2.3 *Gel electrophoresis*

After the completion of PCR reactions, products were visualised by gel electrophoresis. An appropriate marker (e.g. EasyLadder 1 [Bioline]) and all samples were loaded onto 3% agarose gels (made by dissolving twelve 0.5g agarose tablets [Bioline] in 1 x Tris-Borate-EDTA [TBE] Buffer [Sigma] containing 0.006% [v/v] SafeView Nucleic Acid Stain [NBS Biologicals]). Gels were run in 1 x TBE buffer at 150V for 20-30minutes and products were visualised under UV light on a Geldoc (BioRad).

PCR Step	<i>Bcl3</i>			<i>N2/NK</i>			<i>Stat3 WT/Flox</i>			<i>Stat3 Null</i>			<i>Blg/Cre</i>		
	No. Cycles	Temp (°C)	Time	No. Cycles	Temp (°C)	Time	No. Cycles	Temp (°C)	Time	No. Cycles	Temp (°C)	Time	No. Cycles	Temp (°C)	Time
Initial Denaturation	1	94	3 min	1	94	2 min	1	95	3 min	1	95	3 min	1	94	3
Denature	35	94	30 sec	35	94	30 sec	35	95	30 sec	38	95	30 sec	30	95	30
Anneal		66	1 min		60	30 sec		67	1 min		55	1 min		55	30
Extension		72	1 min		72	1 min		72	1 min		72	1 min		72	1
Final Extension	1	72	2 min	1	72	5 min	1	72	5 min	1	72	10	1	72	5
Hold	1	4	∞	1	4	∞	1	4	∞	1	4	∞	1	4	∞

**Table 2.1: PCR cycling conditions**

Target	Forward Primer Sequence (5' to 3')	Reverse Primer Sequence (3' to 5')	Product Size
<i>Bcl3 WT</i>	AGG TGG CAG AAA TGT TCA C	CAC CAT GTT CAG GCT GTT GT	598bp
<i>Bcl3 null</i>	AAA AGT TCG ACA GCG TCT CCG ACC	TTG GCG ACC TCG TCT TGG GAA TCC	209bp
<i>N2/NK</i>	TTT CCT GCA GCA GCC TAC GC	CCG GAC TAC ACC CAA GGC	600bp
<i>Stat3 WT/Floxed</i>	CCT GAA GAC CAA GTT CAT CTG TGT GAC	CAC ACA AGC CAT CAA ACT CTG GTC TCC	WT 230bp Floxed 320bp
<i>Stat3 null</i>	AGC AGC TGA CAA CGC TGG CTG AGA AGC T	ATC GCC TTC TAT CGC CTT CTT GAC GAG	1000bp
<i>Blg/Cre</i>	TGA CCG TAC ACC AAA ATT TG	CTA TCA CTT TG T CCC CGT TA	1000bp

**Table 2.2: Genotyping primers and product sizes**

PCR Reaction Component	<i>N<sub>2</sub>/NK</i>	<i>Stat3 WT/Flox</i>	<i>Stat3 Null</i>	<i>Blg/Cre</i>
Crude DNA	1.5µl	2µl	2.4µl	2µl
PCR-grade Water (Sigma)	15.5µl	32.2µl	22µl	32.2µl
Go Taq PCR Buffer (Promega)	5µl	10µl	N/A	10µl
Magnesium Chloride (25mM; Promega)	2.5µl	5µl	N/A	5µl
Failsafe Buffer E (Epicentre Technologies)	N/A	N/A	25µl	N/A
dNTPs (25mM; dATP, dCTP, dGTP, dTTP; Promega)	0.2µl	0.4µl	N/A	0.4µl
Forward Primer (Sigma Genosys, 100µM)	0.1µl	0.1µl	0.1µl	0.1µl
Reverse Primer (Sigma Genosys, 100µM)	0.1µl	0.1µl	0.1µl	0.1µl
Go Taq DNA Polymerase (Promega)	0.1µl	0.2µl	N/A	0.2µl
Failsafe Taq (Epicentre Technologies)	N/A	N/A	0.4µl	N/A
Total Reaction Volume	25µl	50µl	50µl	50µl

**Table 2.3: PCR reaction components (*N<sub>2</sub>*, *NK*, *Stat3*, *Blg/Cre*)**

PCR Reaction Component	<i>Bcl3</i>
Crude DNA	1.2µl
PCR-grade Water (Sigma)	15.25µl
10xNH <sub>4</sub> Reaction Buffer (Bioline)	3µl
Magnesium Chloride (50mM; Bioline)	1.2µl
dNTPs (10mM; dATP, dCTP, dGTP, dTTP; romega)	0.6µl
Null Primer Mix (Sigma Genosys, 20µM) 20µM)	1.5µl
WT Primer Mix (Sigma Genosys, 20µM)	1.5µl
BIOTAQ Red DNA Polymerase (Bioline)	0.75µl
Total Reaction Volume	25µl

**Table 2.4: PCR reaction components (*Bcl3*)**

## 2.1.3 Experimental procedures

### 2.1.3.1 Tumour checking

Twice weekly, *Bcl3<sup>-/-</sup>/MMTV/N<sub>2</sub>* (or *NK*), *Bcl3<sup>+/-</sup>/MMTV/N<sub>2</sub>* (or *NK*) and *Bcl3<sup>+/+</sup>/MMTV/N<sub>2</sub>* (or *NK*) mice were inspected for tumours by palpation and existing tumours were measured with callipers. When tumours reached their size limit (either 500mm<sup>3</sup> or 4000mm<sup>3</sup>), animals were killed by cervical dislocation and tissues were either snap frozen in liquid nitrogen for protein or RNA analysis or fixed in formalin for histological analysis. Tumour volume was calculated using the following formula:

$$(\text{tumour width}^2) \times \text{tumour length} / 2.$$

### 2.1.3.2 Tail vein injections

Cells were transfected for 48 hours (see section 2.5.5). Cells were harvested using Trypsin/EDTA (0.25% w/v [Invitrogen]), washed, disaggregated into single cell suspensions and resuspended at  $4 \times 10^6$  cells/ml in serum free L-15 media (Invitrogen), maintained on ice and taken to the surgical room. Six-eight week old female virgin Balbc/scid mice were used for tail vein injections. When removed from their individually ventilated cages, animals were continually kept under a laminar flow hood and all procedures were carried out aseptically. The oxygen flowmeter for the induction chamber was set to 0.8L/min and animals were placed into the induction chamber, ensuring the lid was closed tightly. Anaesthesia was induced by turning the vaporiser to deliver 5% isoflurane (Abbot). When the animal was fully anaesthetised, as determined by a lack of movement and slow but steady breathing, it was transferred from the induction chamber to the maintenance anaesthetic mask and the vaporiser for the induction chamber was turned to 0. The oxygen flow meter for the mask was set to 0.8L/min and the anaesthetic vaporiser was set to 2.5% to adequately maintain anaesthesia. The animal was placed on its side and its tail was gently warmed by placing a bag of warm water over it. When the tail was warm enough for the tail vein to become clearly visible, 200 $\mu$ l of suspended cells were drawn into a 29G needle (BD Micro-Fine), ensuring all bubbles were removed. The tail was held straight and horizontally in the left hand and the needle was carefully inserted into the lateral tail vein with the right hand. The solution was injected slowly into the tail vein. A successful injection was characterised by the immediate clearing of the solution down the vein. The animal was then removed from the anaesthesia, placed into a recovery cage, kept warm and monitored frequently. Animals were left for 21 days before being culled by cervical dislocation. Lungs were dissected and fixed in 4% formalin before being processed for H&E staining (see sections 2.2.2-2.3.1). Metastases were measured and counted as outlined in section 2.3.2.2.

## 2.2 Tissue sampling and processing

### 2.2.1 Removal and fixation of tissues

All animals were culled by cervical dislocation prior to dissection.

#### 2.2.1.1 Tissues for involution studies

Mammary tissue was collected from animals at 10 days lactation and at 12, 18 and 24 hours after forced involution, initiated by the removal of pups. Fourth abdominal mammary glands were fixed in 4% formalin in Phosphate buffered saline (PBS, Gibco) at 4°C overnight after which they were transferred to 70% ethanol (in distilled H<sub>2</sub>O[dH<sub>2</sub>O]) and stored at 4°C until processed for histology. For protein or RNA extraction, lymph nodes were excised from whole mammary glands which were then removed and immediately snap frozen in liquid nitrogen before being stored at -80°C until required.

### 2.2.1.2 *Wholemouting*

Fourth abdominal mammary glands were carefully dissected. The gland was spread across a microscope slide (R.A. Lamb) ensuring that the structure and shape of the gland were preserved. The spread tissue was placed into a 50ml tube containing Carnoy's solution (60% v/v ethanol, 30% v/v chloroform [Fisher Scientific], 10% acetic acid [Fisher Scientific]) for 2-4 hours. The tissue was transferred into 70% ethanol for 15 minutes and washed under a slow running tap for 5 minutes before being transferred into a 50ml tube containing Carmine solution for staining (Carmine solution was prepared by mixing 1g Carmine (Sigma) with 2.5g aluminium potassium sulphate (Sigma) in 500ml dH<sub>2</sub>O. This was then boiled for 20 minutes and adjusted to a final volume of 500ml with dH<sub>2</sub>O. The solution was filter sterilised and a crystal of thymol [Alfa Aesar] was added as a preservative before it was stored at 4°C). The tissue was incubated in Carmine solution overnight at room temperature. The next day, the tissue was transferred into a coplin jar (R.A. Lamb) and rinsed with tap water until the water ran clear. The tissue was dehydrated by incubation in increasing concentrations of ethanol (10%, 50%, 70%, 90% and 100% ethanol for 10 minutes each). The tissue was then transferred to xylene (Fisher Scientific) for at least an hour. Slides were mounted for visualisation using DPX (R.A. Lamb).

### 2.2.1.3 *Tissues for tumour studies*

All mammary tumours were excised when they reached their size limit (either 500mm<sup>3</sup> or 4000mm<sup>3</sup>). Half of each tumour was fixed in 4% formalin for histology and the other half was immediately snap frozen in liquid nitrogen and stored at -80°C for future RNA or protein extraction. Any available tissue from either pre-neoplastic, non-tumour bearing mammary glands or from mammary tissue adjacent to tumours was also fixed and frozen in the same way. Lungs were also dissected and fixed in 4% formalin for histology.

## 2.2.2 **Tissue processing and sectioning for histology**

### 2.2.2.1 *Dehydration of tissue*

Tissue processing was performed by the Cardiff Biosciences Histology Unit using an automatic processor (Leica TP1050). Tissues were first dehydrated in increasing concentrations of ethanol followed by xylene and finally paraffin (70% ethanol for 1 hour, 95% ethanol for 1 hour, 2 x 100% ethanol for 1 hour 30 minutes, 100% ethanol for 2 hours, 2 x xylene for 1 hour, 2 x paraffin for 2 hours). Tissues were then embedded in paraffin wax. Paraffin tissue blocks were cut at a thickness of 5µm on a microtome cutter (Leica RM2135) Sections were then placed on poly-L-lysine (PLL) coated slides (polysine, Thermo Fisher) and heated at 58°C for 24 hours before being stained for histology or for use in immunohistochemistry.

## 2.3 Histological analysis of tissue sections

### 2.3.1 Haematoxylin and eosin (H&E) staining

H&E staining was performed by the Cardiff Biosciences Histology Unit. Tissue sections were firstly de-waxed and rehydrated (see section 2.4.1.1) before being incubated in Meyer's Haemalum (R.A. Lamb) for 5 minutes to stain all nuclei. The sections were then washed for 5 minutes in running tap water, counterstained in 1% aqueous Eosin (R.A. Lamb) for 5 minutes and then washed again (2x15 seconds) in tap water. Sections were then dehydrated, cleared and mounted as described in section 2.4.1.5.

### 2.3.2 Visualisation and quantification of H&E stained sections

Visualisation and quantification of all histological sections was carried out on an Olympus BX41 Light Microscope (Olympus). All digital photos of sections were taken on a Colorview III (5 megapixel, soft imaging systems) camera with aid of the Analysis Software Package (Version 3.2, Build 831, Soft Imaging Systems).

#### 2.3.2.1 *Analysis of apoptotic bodies in mammary involution samples*

Apoptotic bodies were identified on mammary involution H&E sections by their distinctive appearance and location within the secretory alveoli lumens. Two random 4 x magnification pictures were taken and apoptotic bodies were counted with the aid of Image J software (<http://rsbweb.nih.gov/ij/>). The average (mean) number of apoptotic bodies within these two fields was calculated and then the mean across all sections of the same genotypes was taken to generate an overall mean value. The standard error of the mean was calculated by standard methods and statistical analysis to identify any significant differences between genotypes was carried out using the Mann-Whitney U-test.

#### 2.3.2.2 *Analysis of lung metastases*

Photos of all visible lung metastases on H&E sections were taken and the area of each metastasis was measured using Image J software. The average (mean) area of an individual metastasis within each genotype was calculated and statistical analysis to identify significant differences between groups was carried out using the Mann-Whitney U-test.

## 2.4 Immunohistochemistry (IHC)

### 2.4.1 Generic IHC protocol

All IHC was carried out using the following generic protocol. Any modifications used for a specific target are outlined in Table 2.5.

#### 2.4.1.1 *De-waxing and rehydration*

Tissues were de-waxed by soaking slides in xylene (2x5 minutes) and then rehydrated by soaking in decreasing concentrations of ethanol (100% ethanol for 2x2 minutes, 95% ethanol for 2 minutes, 70% ethanol for 2 minutes) followed by a wash in dH<sub>2</sub>O.

#### 2.4.1.2 *Antigen retrieval and prevention of endogenous staining*

Antigen retrieval was performed either by heat treatment or by pressure treatment (see Table 2.5). For heat treatment, a 1 x citrate buffer solution (Thermo Scientific) was pre-heated to 99.9°C in a glass coplin jar (R.A.Lamb) in a waterbath after which slides were immersed into the solution and allowed to boil for 20 minutes. For pressure treatment, adequate citrate buffer was added to a pressure cooker and heated to boiling. Slides were then immersed in the solution and pressure cooked for 8 minutes. Following either treatment, slides were left to cool in the solution at room temperature for at least 30 minutes and then rinsed once in dH<sub>2</sub>O. To prevent endogenous peroxidase activity, the slides were treated with a 3% Hydrogen Peroxide solution (30% aqueous solution diluted 1:10 in dH<sub>2</sub>O; Sigma) for 20 minutes and then washed twice in dH<sub>2</sub>O for 5 minutes and once in PBS/T (PBS plus 0.1% TWEEN-20 [Sigma]) for 5 minutes. Non-specific binding of antibodies was blocked by the addition of serum from the host species of the secondary antibody (Vector Laboratories) or Bovine Serum Albumin (BSA; Sigma) diluted in PBS/T in a humidified chamber at room temperature for 20 minutes.

#### 2.4.1.3 *Incubation with primary and secondary antibodies*

Primary antibody was diluted according to Table 2.5 in 5% BSA in PBS/T and applied to the slides which were then incubated overnight at 4°C in a humidified chamber. The next morning primary antibody was removed and the slides were washed in PBS/T (3x5 minutes). Biotinylated secondary antibody (DAKO) was diluted 1:200 in 5% BSA in PBS/T and applied to the slides for 30 minutes at room temperature in a humidified chamber.

#### 2.4.1.4 *Signal amplification and visualisation of positivity using 3,3'-diaminobenzidine (DAB)*

Signal amplification was achieved by the formation of an Avidin-Biotin Complex (ABC) using the Vectastain ABC kit (Vector Labs). The ABC reagents were prepared 30 minutes before required by adding 1 drop of A and then 1 drop of B to 5mls of PBS/T and mixing well. Slides were washed in PBS/T (3x5 minutes) and the ABC mix was applied and left at room temperature for 30 minutes. After this, the slides

were washed in PBS/T (3x5 minutes). The colorimetric detection of signal was achieved by the DAB method. Immediately before use, the DAB reagents from the DAB+ kit (DAKO) were prepared by mixing 1 drop of chromagen per 1 ml of substrate buffer. This DAB solution was then applied to slides at room temperature and the development of colour was monitored for 5-10 minutes until brown staining was visualised. The slides were then washed once for 5 minutes in PBS/T and then 2x5 minutes in dH<sub>2</sub>O.

#### *2.4.1.5 Counterstaining, dehydration, clearing and mounting of slides*

Slides were counterstained by immersion in Meyer's Haematoxylin (R.A. Lamb) for 45 seconds. They were then thoroughly washed in tap water until it ran clear. The slides were dehydrated by soaking in increasing concentrations of ethanol (70% ethanol for 1x30 seconds, 95% ethanol for 1x30 seconds, 100% ethanol 2x30 seconds) and cleared by soaking in xylene (2x2 minutes). Slides were then mounted and coverslipped for viewing using DPX mounting solution.

Antigen	Ki67	Cleaved Caspase 3	p50	Phospho-p50 (Ser337)	p52	Phospho-p52 (Ser222)	Vimentin
Primary Antibody Source	Vector Labs	Cell signalling	Santa Cruz	Santa Cruz	Santa Cruz	Gift from Prof. Neil Perkins	Santa Cruz
Catalogue Number	VP-K452	9661	sc-114	sc-101744	sc-7386	N/A	sc-7557
Primary Antibody raised in	Mouse (mAb)	Rabbit (pAb)	Rabbit (pAb)	Rabbit (pAb)	Mouse (mAb)	Rabbit (mAb)	Goat (pAb)
Antigen Retrieval	Boiling water bath	Pressure Cooker	Boiling water bath	Pressure Cooker	Pressure Cooker	Pressure Cooker	Pressure Cooker
Serum Block	20% Normal Rabbit Serum	5% BSA	5% Normal Goat Serum	5% Normal Goat Serum	5% Normal Rabbit Serum	5% Normal Goat Serum	5% Normal Rabbit Serum
Primary Antibody Dilutions	1:20	1:200	1:5000	1:50	1:200	1:100	1:100
Secondary Antibody	Biotinylated Rabbit anti-Mouse (Dako)	Biotinylated Goat anti-Rabbit (Dako)	Biotinylated Goat anti-Rabbit (Dako)	Biotinylated Goat anti-Rabbit (Dako)	Biotinylated Rabbit anti-Mouse (Dako)	Biotinylated Goat anti-Rabbit (Dako)	Biotinylated Rabbit anti-Goat (Dako)
Secondary Antibody Dilutions	1:200	1:200	1:200	1:200	1:200	1:200	1:200

**Table 2.5: Immunohistochemistry antibodies and conditions**

## 2.5 Cell culture maintenance and procedures

### 2.5.1 Experimental cell lines

The human breast cancer cell lines, MDA-MB-231 and SKBR3, used in this investigation were a gift from Dr. Julia Gee (Department of Pharmacy, Cardiff University). The HCC1954 human breast cancer cell line was a gift from Dr. Mohamed Bentires-Alj (Friedrich Miescher Institute for Biomedical Research, Switzerland) and the ZR-75-1 human breast cancer cell line was a gift from Prof. Wen Jiang (Wales College of Medicine, Cardiff University). The MG1361 murine mammary tumour cell line and the EPH4 normal murine mammary epithelial cell line were gifts from Dr. Christine Watson (Department of Pathology, Cambridge University). The N202A and N202E murine mammary tumour cell lines were gifts from Dr. Pier-Luigi Lollini (Sezione di Cancerologia, Italy) and the 4T1 murine mammary tumour cell line was a gift from Dr. Robin Anderson (Department of Pathology, University of Melbourne). Descriptions of the main cell lines used in this thesis are outlined below:

#### 2.5.1.1 MDA-MB-231

MDA-MB-231 is a highly metastatic human basal epithelial cell line isolated from the pleural effusion of an adenocarcinoma. The cells are 'triple negative' as they lack oestrogen, progesterone and ERBB2 receptors (Neve, Chin et al. 2006; Chapter 6, section 6.2.1). They strongly over-express EGFR (see Chapter 6, section 6.2.1).

#### 2.5.1.2 ZR-75-1

The ZR-75-1 cell line is a moderately metastatic human luminal epithelial cell line derived from a malignant ascitic effusion with infiltrating ductal carcinoma. ZR-75-1 cells are oestrogen receptor positive and progesterone receptor negative (Neve, Chin et al. 2006). They express very low levels of the ERBB2 receptor and over-express EGFR (see Chapter 6, section 6.2.1).

#### 2.5.1.3 HCC1954

HCC1954 is a moderately metastatic human basal epithelial cell line derived from a primary grade 3 invasive ductal carcinoma. HCC1954 cells are oestrogen and progesterone receptor negative (Neve, Chin et al. 2006). They over-express both the ERBB2 receptor and EGFR (see Chapter 6, section 6.2.1).

#### 2.5.1.4 SKBR3

The SKBR3 cell line is a poorly metastatic human luminal epithelial cell line derived from a pleural effusion. SKBR3 cells are oestrogen and progesterone receptor negative (Neve, Chin et al. 2006). They over-express the ERBB2 receptor and have very low levels of the EGFR receptor (see Chapter 6, section 6.2.1).

### 2.5.1.5 MG1361

The MG1361 cell line was established from a mammary adenocarcinoma that had arisen in a *MMTV/NK* (activated *Neu*) transgenic CD-1 mouse (Sacco, Gribaldo et al. 1998). This cell line shows an epithelial-like morphology and maintains a high level of NEU expression *in vitro*. The cells are oestrogen and progesterone receptor positive (Sacco, Gribaldo et al. 1998).

### 2.5.2 Maintenance of cell lines

All human cell lines and murine Eph4 cells were maintained in Dulbecco's modified Eagle's medium (DMEM) supplemented with 10% v/v foetal bovine serum (FBS, Sigma), penicillin (50units/ml Invitrogen) streptomycin (50units/ml, Invitrogen) and L-glutamine (2mM, Invitrogen). The N202A and N202E cell lines were maintained in the same media as above but supplemented with 15% v/v FBS. The MG1361 cell line was maintained in Williams Media E (Invitrogen) supplemented with L-glutamine (2mM), penicillin (50units/ml), streptomycin (50µg/ml), 15% v/v FBS and 5ml non-essential amino acids (Sigma). The 4T1 cell line was maintained in RPMI (Invitrogen) supplemented with 10% v/v FBS, penicillin (50units/ml Invitrogen) streptomycin (50units/ml, Invitrogen) and L-glutamine (2mM, Invitrogen).

All cell lines were incubated at 37°C and 5% CO<sub>2</sub> in T25 tissue culture flasks (Nunc) and were routinely passaged every 3 – 8 days at a split ratio of 1:4 -1:12, when they became 80-90% confluent. Growth media was completely aspirated and the cells were washed with PBS to remove any remaining serum. The wash was removed and 2mls of 0.25% Trypsin/EDTA was added to the flask followed by incubation at 37°C. When the cells were detached, a known volume of growth medium was added to the cells which were then split at an appropriate ratio by the removal excess cell suspension into waste. The remaining volume of cell suspension was made up to 6mls with complete growth media.

### 2.5.3 Cell counting

Cells were trypsinised using 0.25% Trypsin/EDTA. Once detached, cells were resuspended in 10mls of growth medium, transferred to a 15ml falcon tube (BD Biosciences) and centrifuged at 1100rpm for 5 minutes at room temperature. The supernatant was removed and the cells were resuspended in a known volume of growth media. Cells were counted in four 1mm<sup>2</sup> fields using an Improved Neubauer Counting Chamber (Hawksley, Lancing, UK). The number of cells per ml of suspension was determined by calculating the average count per square and multiplying it by  $1 \times 10^4$ .

### 2.5.4 Frozen storage of cells

A confluent T75 flask of cells were trypsinised, resuspended in 10mls of growth medium, transferred to a 15ml falcon tube and centrifuged at 1100rpm for 5 minutes at room temperature. The supernatant was removed and cells were resuspended in 6mls of complete media containing 10% (v/v) dimethyl sulfoxide (DMSO, Sigma) before being aliquoted into 1ml cryo tube vials (Nunc) and stored in

liquid nitrogen. When necessary, frozen stocks were retrieved from the liquid nitrogen stores and defrosted quickly to 37°C in a waterbath before being transferred to 10mls of complete medium in a 15 ml falcon tube. Cells were centrifuged at 1100rpm at room temperature for 5 minutes, and the pellet was resuspended in 7mls of complete growth media and transferred to a T25 flask.

### 2.5.5 Transient SiRNA transfection

ON-TARGET plus SMARTpool small interfering RNA (SiRNA) targeting an irrelevant control RNA, mouse *Bcl3* or human *BCL3* were purchased from Dharmacon (Table 2.6). The SMARTpool SiRNA contains a mixture of four SiRNAs that target the same gene to increase the efficiency of gene silencing. The negative control SiRNA was designed to have minimal targeting of known genes in human or mouse. Cells were transfected with SiRNA using lipofectamine RNAiMAX (Invitrogen) according to the manufacturers protocols to give a final SiRNA concentration of 10nM. Volumes and concentrations of reagents used in different tissue culture plates are outlined in Table 2.7. The appropriate volume of SiRNA was diluted in serum-free Opti-MEM 1 (Invitrogen) in the well of a tissue culture plate and mixed gently. Lipofectamine RNAiMAX was mixed before use and the appropriate volume was added to each well containing the SiRNA. This was mixed and incubated for 20 minutes at room temperature to allow the SiRNA-Lipofectamine complexes to form. Meanwhile, cells were diluted in complete growth medium without antibiotics to a concentration that would give 30-50% confluency 24 hours after seeding (see Table 2.8). Cells were then carefully and evenly added to each well containing SiRNA-lipofectamine complexes to give a final concentration of 10nM. Cells were incubated at 37°C in 5% CO<sub>2</sub>. Transfection times for each cell line were optimised (see Chapter 5 and Chapter 6).

SIRNA	Target Sequences (5'-3')	Final SiRNA Concentration	Source	Catalogue Number
<b>Human <i>Bcl3</i> ON-TARGETplus SMART pool</b>	AGACACGCCUCUCCAUAUU	10nM	Dharmacon (Thermo Scientific)	L-003874-00-0005
	GGCCGGAGGCGCUUUACUA			
	GCGCAA AUGUACUCCGGCA			
	GCCGGGAGCUCGACAUCUA			
<b>Mouse <i>Bcl3</i> ON-TARGETplus SMART pool</b>	GCUUGGGAGCCGCGAAGUA	10nM	Dharmacon (Thermo Scientific)	L-045102-01-0005
	GCGCAAACGUGAACGCUCA			
	GCGCGGACAUCGAUGCAGU			
	CCUGGAGGUUCGCAAUUAU			
<b>Human/Mouse Control ON-TARGETplus SMART pool</b>	UGGUUUACAUGUCGACUAA	10nM	Dharmacon (Thermo Scientific)	D-001810-10
	UGGUUUACAUGUUGUGUGA			
	UGGUUUACAUGUUUUCUGA			
	UGGUUUACAUGUUUCCUA			

**Table 2.6: SiRNA reagents and concentrations**

Tissue Culture Vessel	Relative Surface Area	Volume of cell plating medium	Volume of OptiMEM 1 dilution medium	SIRNA (pmol)	Final SIRNA concentration (nM)	Lipofectamine RNAiMAX
96-well	0.2	100µl	20µl	1.2	10	0.2
48-well	0.4	200µl	40µl	2.4	10	0.4
24-well	1	500µl	100µl	6	10	1
6-well	5	2.5ml	500µl	30	10	5

**Table 2.7: Volumes and concentrations used for SiRNA transfections**

Tissue Culture Vessel	No. cells plated for SiRNA transfection or CellTitre Blue Assays (96-well plate only)				
	MDA-MB-231	ZR-75-1	HCC1954	SKBR3	MG1361
96-well	$6 \times 10^3$	$6 \times 10^3$	$8 \times 10^3$	$8 \times 10^3$	$8 \times 10^3$
48-well	$1.2 \times 10^4$	$1.2 \times 10^4$	$1.6 \times 10^4$	$1.6 \times 10^4$	$1.6 \times 10^4$
24-well	$3 \times 10^4$	$3 \times 10^4$	$4 \times 10^4$	$4 \times 10^4$	$4 \times 10^4$
6-well	$1.5 \times 10^5$	$1.5 \times 10^5$	$2 \times 10^5$	$2 \times 10^5$	$2 \times 10^5$

**Table 2.8: Seeding densities for SiRNA transfections and CellTitre Blue assays**

### 2.5.6 CellTitre-blue cell viability assays

The CellTitre-Blue assay (Promega) provides a homogeneous, fluorometric method for estimating the number of viable cells present. It measures the metabolic capacity of the cells using an indicator dye, resazurin. Viable cells are able to reduce resazurin to the highly fluorescent product, resorufin. Any non-viable cells present lose their metabolic capacity, fail to convert the resazurin and do not produce a fluorescent signal.

The CellTitre-Blue reagent was thawed to room temperature. Cells were plated at low confluency (see Table 2.8) into 96 well plates in 100µl complete growth medium to allow exponential growth. Triplicate control wells, containing only media were also plated. Cells were incubated at 37°C in 5% CO<sub>2</sub> for the desired test exposure period (see individual experiments). Assay plates were removed from the incubator and 20µl CellTitre-Blue reagent was added to each well. The cells were incubated for a further hour at 37°C in 5% CO<sub>2</sub>. Fluorescence was then recorded at 560/590nm on a FLUOstar Optima plate reader (BMG Labtech, Offenburg, Germany).

### 2.5.7 Trypan blue dye exclusion cell viability counts

The number of viable cells present in a culture was also determined using Trypan Blue dye exclusion cell viability counts. Cells were removed from the plate using 0.25% w/v Trypsin/EDTA and resuspended in a known volume of media. 10µl of the cell suspension was mixed with 10µl Trypan Blue (Sigma) and placed on an Improved Neubauer Counting Chamber and only viable cells excluding the blue

dye were counted. The average number of cells per  $1\text{mm}^2$  was multiplied by  $2 \times 10^4$  to determine the number of viable cells per ml of suspension.

### 2.5.8 Boyden chamber assays

The Boyden chamber assay is a method used to analyse the migratory or invasive capacity of cells. This assay utilises a Boyden chamber containing two medium filled compartments separated by a porous membrane for motility assays or a porous membrane coated with Matrigel basement membrane matrix for invasion assays. Cells are placed into the upper chamber containing a low concentration of serum and allowed migrate or invade through the membrane into the lower compartment containing media with a high serum concentration. The membranes can then be fixed and stained and the number of cells that have migrated or invaded to the lower side of the membrane can be counted.

Transfected cells were removed from tissue culture plates using 0.25% w/v Trypsin/EDTA and centrifuged at 1100rpm for 5 minutes. Cells were washed twice in serum free media by resuspension and centrifugation. The appropriate number of cells ( $2 \times 10^5$  cells/ml for ZR-75-1 and MDA-MB-231 cells, and  $4 \times 10^5$  cells/ml for HCC1954, SKBR3 and MG1361 cells) were resuspended in their normal growth media containing only 0.2% FBS. Complete growth media (750 $\mu$ l containing a standard amount of BSA [10-15% - see section 2.5.2) was placed into each well of a 24 well cell culture insert companion plate (BD Biosciences) to be used. A cell culture insert (BD Biosciences) was then carefully placed into each well of the insert companion plate using tweezers. For motility assays, a cell culture insert composed of an 8 $\mu$ m pore, transparent polyethylene terephthalate (PET) membrane (BD Biosciences) was used and for invasion assays, BD BioCoat™ Growth Factor Reduced Matrigel Invasion chamber (BD Biosciences) was used. 350 $\mu$ l of the cell suspension was added to the appropriate upper chambers and plates were incubated for 24-48 hours at 37°C and 5% CO<sub>2</sub> (see individual results for incubation periods).

#### 2.5.8.1 Cell fixing and staining

After incubation, all media was carefully aspirated from top and bottom wells and replaced with 70% ice cold ethanol to fix the cells. Plates were incubated at -20°C for at least 1 hour. After this time, ethanol was aspirated from the inserts and replaced with tap water. Each insert was picked up individually using tweezers and immersed in a beaker of tap water to ensure all ethanol was removed. A moisten cotton wool bud was then used to mechanically remove all cells fixed on the upper side of the membranes. Following this, cells were stained by individually immersing the inserts into filtered Harris' Haematoxylin (Sigma) for 1 minute. Inserts were then washed in a beaker of tap water to remove the dye before being immersed in 0.5% filtered Eosin (Sigma) for 2 minutes. The inserts were washed in a beaker of tap water and placed back into the companion plates to await mounting.

### 2.5.8.2 Mounting of membranes

Glycerol Gelatin (Sigma) was heated in a beaker of boiling water and once liquefied, a drop was placed onto an appropriately labelled microscope slide (R.A.Lamb). Using a sharp blade, the membrane was cut out of the insert and placed onto the corresponding slide with tweezers. Another drop of Glycerol Gelatin was added to the top of the membrane and a coverslip was placed on the slide under firm pressure. Mounted slides were left to air dry before being counted as described in individual results sections.

### 2.5.9 Flow cytometry

Transfected cells were removed from tissue culture plates using 1mM EDTA (Sigma) and centrifuged at 1100rpm for 5 minutes. The pellet was washed twice in Fluorescence activated cell sorting (FACS) buffer (PBS supplemented with 2% v/v FBS). Cells were resuspended at a density of  $4 \times 10^6$  cells /ml and 100 $\mu$ l of this suspension was aliquoted into the appropriate wells of a 96 well plate before being centrifuged on a plate spinner at 1100rpm for 5 minutes. The supernatant was removed and the pellet was resuspended in 100 $\mu$ l of the appropriate fluorescently conjugated primary antibody (FITC-conjugated anti-CD24 [BD Pharmingen, Cat no. 553261], PE-conjugated anti-Sca1 [BD Pharmingen, Cat no. 553336]) and left on ice for 30 minutes in the dark. Cells were then centrifuged on a plate spinner and the antibody was removed. The pellet was washed twice in FACS buffer before being filtered through a 40 $\mu$ m cell strainer (BD Biosciences) into a FACS collection tube (BD Biosciences) to ensure a single cell suspension. FACS was performed on a FACSAria Flow Cytometer (BD Biosciences) and analysis of results was undertaken using a FlowJo software package. Gates were set to exclude >99% of cells labelled with isoform-matched control antibodies conjugated with the corresponding fluorochromes. If sorting was performed, cells were collected in an appropriate volume of FACS buffer.

#### 2.5.9.1 Aldefluor assay

The aldefluor assay (Stemcell Technologies, Grenoble, France) is a method to identify stem cells on the basis of their high aldehyde dehydrogenase (ALDH) activity. A fluorescent aldefluor reagent diffuses into cells and is a substrate for ALDH. The amount of fluorescent ALDH reaction product is directly proportional to the ALDH activity in cells. Cells with high expression of ALDH are recognised by comparing the fluorescence of test cells with that of a control sample containing the specific ALDH inhibitor, diethylaminobenzaldehyde (DEAB).

Aldefluor reagents were prepared according to manufacturer's instructions. Transfected cells were removed from tissue culture plates using 1mM EDTA and centrifuged at 1100rpm for 5 minutes. The cells were washed twice in FACS buffer by resuspension and centrifugation. Cells were suspended in 1ml of aldefluor assay buffer and counted. The samples were adjusted to a concentration of  $1 \times 10^6$

cells/ml with aldefluor assay buffer. A 'control' and a 'test' tube were prepared for each sample to be tested and 1ml of the adjusted cell suspension was placed into each 'test' tube. 5µl of DEAB reagent was added to the control tube and recapped immediately before 5µl of activated aldefluor substrate was added per ml of test suspension in the 'test' tube. The suspension was mixed and 0.5ml was immediately transferred to the 'control' tube containing the DEAB substrate. The 'test' and 'control' tubes were incubated for 45 minutes at 37°C. The tubes were then centrifuged at 1100rpm for 5 minutes and the pellets were resuspended in aldefluor buffer. Samples were placed on ice. The fluorescence of cells was measured in the green fluorescence channel of a FACSAria flow cytometer (BD Biosciences). Analysis was performed using FlowJo software. Gates were set to exclude >99% of control cells incubated with DEAB.

### 2.5.10 Mammosphere assays

Mammosphere assays can be used for the *in vitro* propagation of mammary epithelial cells in an undifferentiated state in non-adherent cell culture conditions. The resulting mammosphere colonies are enriched for mammary stem/early progenitor cells that are able to undergo self-renewal and form new colonies upon disaggregation and re-seeding (see Chapter 1: General Introduction, section 1.2.6). This assay is therefore suitable for the functional identification of this cell population.

Cells were removed from tissue culture plates using 0.25% w/v Trypsin/EDTA and centrifuged at 1100rpm for 5 minutes. Cells were then resuspended in mammosphere culture medium (serum-free epithelial growth medium [MEBM, Lonza], supplemented with B27 [invitrogen], 20ng/ml Epidermal Growth Factor [EGF, Sigma], 5mg/ml Insulin [Sigma], 0.0008% v/v β-mercaptoethanol [Sigma] and 1mg/ml hydrocortisone [Sigma]) and disaggregated into single cell suspensions by mechanical agitation. Cells were counted and seeded into ultra-low attachment plates (Corning) at density of 4000 cells/ml (unless otherwise stated) before being incubated for 7 days at 37°C and 5% CO<sub>2</sub> to allow the formation of mammosphere colonies. After this incubation period, the number of mammosphere per well were counted. In order to determine the self-renewal capacity of cells, mammospheres were collected by gentle centrifugation at 1100rpm and mechanically and enzymatically dissociated into single cells in 0.25% w/v Trypsin/EDTA at 37°C. Cells were centrifuged at 1100rpm before being counted and re-seeded into ultra-low attachment plates at a density of 4000 cells/ml. Cells were then incubated for 7 days at 37°C and 5% CO<sub>2</sub> after which time the number of mammospheres per well was counted.

## 2.6 Protein analysis by western blotting

### 2.6.1 Protein extraction from cells

#### 2.6.1.1 Preparation of whole cell protein extracts

Media was completely aspirated from cell culture flasks and the cells were washed twice in ice cold PBS. A further 12ml of PBS was added to the flask and cells were scraped using a cell scraper (Nunc) and transferred into 15ml falcon tubes. The cells were centrifuged at 1100rpm for 5 minutes and the supernatant was removed. Cell pellets were either stored at -80°C until required or immediately lysed by the addition of 100-300µl of RIPA buffer (150mM sodium chloride [Fisher Scientific], 1% v/v Nonidet-P40 [Roche], 0.5% w/v sodium deoxycholate [Sigma], 0.1% w/v sodium dodecyl sulphate [SDS; Sigma], 50mM Tris [Sigma], pH8) containing protease (Complete mini protease inhibitor tablets [Roche]) and phosphatase inhibitors (1mM sodium orthovanadate [Sigma], 10mM sodium fluoride [Fluka Biochemika], 10mM sodium pyrophosphate [Sigma]). The cell pellet was passed through a 23G needle 10 times to ensure complete cell lysis and incubated on ice for 30 minutes. Lysates were centrifuged at 10,000rpm for 15 minutes at 4°C to pellet cell debris and the supernatant was aliquoted into fresh tubes and snap frozen in liquid nitrogen before being stored at -80°C until required.

### 2.6.2 Protein extraction from tissues

#### 2.6.2.1 Preparation of whole tissues

Whole tissue samples were removed from the -80 freezer and 100mg was cut on dry ice and placed into a spinLyse tube (Lysing Matrix D; MP Biomedicals) containing 500µl of RIPA buffer (for composition of RIPA buffer see section 2.6.1.1) and homogenized twice at 6500rpm for 45 seconds on Precellys 24 lysis and homogenization machine (Bertin Technologies). Samples were transferred to a fresh tube and passed through a 23G needle 8 times before being placed on ice for 30 minutes. Samples were then centrifuged at 10,000rpm for 10 minutes at 4°C. The supernatant was carefully transferred to a fresh tube using a 23G needle and 1ml syringe to avoid the top layer of milk. This was then centrifuged at 10,000rpm for 10 minutes at 4°C and the supernatant was removed, aliquoted and snap frozen in liquid nitrogen before being stored at -80°C until required.

#### 2.6.2.2 Preparation of cytoplasmic and nuclear protein fractions from tissues

Whole tissue samples were removed from the -80 freezer and 50mg was cut on dry ice and placed into a spinLyse tube containing 1ml of filtered NEBA+ (filtered NEBA [10mM HEPES pH7.9, 10mM potassium chloride, 0.1mM EDTA pH8.0, 0.1mM EGTA pH8], 1mM 1,4 Dithiothreitol [Fluka Biochemika], 50mM sodium chloride, 1mM sodium orthovanadate, 1mM sodium pyrophosphate and one complete mini protease inhibitor tablet) and homogenized twice at 6500rpm for 45 seconds on Precellys 24 lysis

and homogenization machine. Samples were centrifuged at 3000rpm for 2 minutes at 4°C and the supernatant was transferred to a new tube, and placed on ice for 10 minutes. 50µl of 10% NP40-alternative (Calbiochem) was added to each sample and homogenised twice at 6500rpm for 45 seconds before being transferred to a new tube and centrifuged at 13,000rpm for 30 seconds at 4°C. The supernatant (cytoplasmic fraction) was removed, aliquoted and flash frozen in liquid nitrogen before being stored at -80 for later use. The pellet was resuspended in 100µl NEBC+ (filtered NEBC [10% v/v glycerol, 20mM Hepes pH7.0, 0.4M sodium chloride, 1mM EDTA pH8.0, 1mM EGTA pH8.0] 1mM 1,4 Dithiothreitol, 50mM sodium fluoride, 1mM sodium orthovanadate, 1mM sodium pyrophosphate and one complete mini protease inhibitor tablet) and placed on ice for 30 minutes before being centrifuged for 10 minutes at 4°C. The supernatant (nuclear fraction) was removed, aliquoted and snap frozen in liquid nitrogen before being stored at -80°C until required.

### 2.6.3 Determination of protein concentrations

Protein concentrations were analysed using the BCA protein Assay kit (Pierce) according to manufacturer's instructions. Protein samples were first diluted by 1:5 and 1:10 in RIPA Buffer (see section 2.6.1.1 for composition) and 12.5µl of each diluted sample was added to a 96 well round bottomed plate (Nunc) in duplicate. BCA protein assay reagent A was added to BCA protein assay reagent B in a ratio of 50:1 and 100µl of this mix was added to each sample. A standard curve was also generated by diluting 2mg/ml BSA in PBS to produce 4 known protein concentrations (2mg/ml, 1mg/ml, 0.5mg/ml, 0.25mg/ml) to which 100µl of BCA reagent mix was added. Samples were mixed well and incubated at 37°C for 30 minutes to allow the purple colour to develop. Colour intensity of each sample was measured on a nanodrop spectrophotometer (ND-1000; Labtech International) at 562nm. The relative concentration of protein in each sample was extrapolated from the standard curve.

### 2.6.4 Western analysis

#### 2.6.4.1 Preparation of protein samples

After protein concentrations were determined, 20µg (tissue samples) or 70µg (cell samples) of protein were diluted in RIPA buffer (see section 2.6.1.1 for composition) to produce a final volume of 10µl and 2.5µl of 5X laemmli buffer (0.125M Tris-HCL pH6.8, 4% w/v SDS, 40% v/v glycerol, 0.1% w/v bromophenol blue [Sigma], 6% v/v beta-mercaptoethanol [Sigma] in ddH<sub>2</sub>O) was added to each sample. Just before loading, the samples were heated to 95°C for 5 minutes to denature the proteins.

#### 2.6.4.2 Casting of polyacrylamide gels

All Mini western SDS-PAGE gels were set in Mini-Protean III (Bio-Rad) gel casting apparatus. Resolving gel mixtures composed of varying concentrations of Acrylamide/Bis (depending on target

protein size) were prepared (Table 2.9), poured and left to set for 30 minutes. Once set, the 4% stacking gel mixture was prepared and poured over the resolving gel (Table 2.9). A clean 10 or 15-well comb was inserted immediately into the apparatus and the gel was left to set for 30 minutes. Once set, the combs were removed and the wells were rinsed with ddH<sub>2</sub>O.

Component	8% Resolving Gel (x2)	10% Resolving Gel (x2)	12% Resolving Gel (x2)	4% Stacking Gel (x2)
Molecular Weight of Protein	40-150kDa	25-100kDa	15-75kDa	
ddH <sub>2</sub> O	4.7ml	4.1ml	3.4ml	6.1ml
30% Acrylamide/Bis (Sigma)	2.7ml	3.3ml	4.0ml	1.3ml
1.5M Tris-HCl, pH8.8	2.5ml	2.5ml	2.5ml	
0.5M Tris-HCl, pH6.8				2.5ml
10% w/v SDS	100µl	100µl	100µl	100µl
10% Ammonium Persulphate (Sigma)	50µl	50µl	50µl	50µl
TEMED	5µl	5µl	5µl	10µl

**Table 2.9: Composition of polyacrylamide gels**

#### 2.6.4.3 Gel electrophoresis

Gels were placed in the Mini-Protean III (Bio-Rad) electrophoresis tank and immersed in 1 x Tris-Glycine running buffer (Table 2.10). Protein molecular weight marker (PageRuler Plus; Fermentas) was loaded into the first lane of each gel and prepared protein samples were loaded into the appropriate remaining wells. The samples were resolved down SDS-PAGE gels for approximately 45-60 minutes at 150V until the dye front reached the bottom of the gel.

#### 2.6.4.4 Transfer of proteins to PVDF membranes

After separation of protein, gels were carefully removed from glass plates and soaked in 1 x Tris-Glycine transfer buffer (Table 2.10) for 10 minutes. Immobilon-P, Polyvinylidene difluoride (PVDF; Millipore) membrane was cut to size, pre-soaked in methanol (Fisher Scientific) for 10 seconds and washed in ddH<sub>2</sub>O. The stacking gel was then cut away and discarded and the resolving gel was placed onto the membrane in a standard wet electroblotting system (BioRad). Air bubbles were carefully rolled out after the addition of each layer. An ice block was inserted into the transfer apparatus and proteins were transferred by electroblotting in 1 x Tris-Glycine transfer buffer (Table 2.10) at 100V for 1 hour. Blotting apparatus was then dismantled and membranes were washed for 5 minutes in PBS/T.

#### 2.6.4.5 *Probing of membranes*

Following transfer, membranes were blocked in milk blocking solution (Table 2.10) under agitation for 1 hour at room temperature and then incubated in 5mls of primary antibody (Table 2.11 & 2.12) at 4°C on a roller mixer (Stuart, Merton, UK) overnight. The following morning the membrane was washed (3x5 minutes) in PBS/T before being incubated in 5mls of the appropriate horseradish-peroxidase (HRP)-conjugated secondary antibody (Table 2.11 & 2.12) for 1 hour at room temperature on a roller mixer. Following this incubation, membranes were washed 3x5 minutes in PBS/T prior to protein detection by enhanced chemiluminescence.

#### 2.6.4.6 *Visualisation of protein bands*

The appropriate ECL reagent kit (GE Healthcare; Table 2.11 & 2.12) was used to visualise the immobilised protein bands conjugated to HRP-labelled secondary antibodies according to manufacturer's instructions. ECL solutions were mixed well and 2mls were immediately distributed evenly across the membrane and incubated in the dark for 1 minute (ECL) or 5 minutes (ECL plus). After removal of excess reagent, the membrane was placed in a light-proof cassette and exposed to light sensitive films (Amersham Hyperfilm ECL; GE Healthcare) under safelight conditions for varying lengths of time to give a range of exposure intensities. All films were developed on an automatic film processor (Xograph Compact X4 automatic X-ray film processor). Processed films were then realigned with the original membrane and the target protein was identified by comparison to the molecular weight marker.

#### 2.6.4.7 *Stripping and re-probing of membranes*

In order to study more than one protein band from the same set of samples, membranes were stripped of their original antibodies and re-probed with a new one. The membrane was washed in PBS/T (3 x 5 minutes) and incubated in stripping buffer (Table 2.10) at 55°C for 30 minutes with gentle agitation. The stripping buffer was removed and the membrane was rinsed 5 times in dH<sub>2</sub>O before being incubated in PBS/T for 30 minutes at room temperature. After incubation for a further hour in milk blocking solution, the membrane was re-probed with the appropriate primary and secondary antibodies and protein bands were visualised using ECL or ECL plus reagents as described in section 2.6.4.6.

<b>Solution</b>	<b>Composition</b>
10 x Electrophoresis Buffer	30.3g Tris base (Sigma), 144.4g Glycine (Sigma), Upto 1L dH <sub>2</sub> O
1 x Tris-Glycine SDS-PAGE Running Buffer (1L)	890ml dH <sub>2</sub> O, 100ml 10 x Electrophoresis Buffer, 10ml 10% w/v SDS
1 x Tris-Glycine Transfer Buffer	700ml dH <sub>2</sub> O, 100ml 10 x Electrophoresis Buffer, 200ml Methanol
Milk Blocking Solution	5% w/v non-fat milk powder (Marvel) in PBS/T
Stripping Buffer	62.5mM Tris-Hcl (pH6.8), 2% w/v SDS, 100mM 2-beta-mercaptoethanol

**Table 2.10: Composition of solutions used in western analysis**

#### 2.6.4.8 Quantification of protein bands

In some cases protein bands were semi-quantified. The intensity of protein bands was measured using a GelDoc (BioRad) and normalised to the band intensity of their corresponding loading control. The average normalised intensity of all samples from one genotype was calculated to allow comparisons between genotypes to be made.

Target	EGFR(Total)	ERBB2 (NEU) (Total)	p50	p52	AKT(Total)	Phospho-AKT (Ser473)	ERK (Total)	Phospho-ERK (Thr202/Tyr204)	Caveolin-1
Primary Antibody Source	CST	Abcam	Santa Cruz	Santa Cruz	CST	CST	BD Transduction Laboratories	CST	CST
Catalogue Number	2232	Ab2428	sc-114	sc-7386	9272	9271	610123	20G11	3238
Primary Antibody Raised in	Rabbit (pAb)	Rabbit (pAb)	Rabbit (pAb)	Mouse (mAb)	Rabbit (pAb)	Rabbit (pAb)	Mouse (mAb)	Rabbit (mAb)	Rabbit (pAb)
Primary Antibody Dilution	1:1000 in 5% w/v BSA*	1:200 in 5% w/v BSA*	1:200 in 5% w/v BSA*	1:500 in 5% w/v BSA*	1:500 in 5% w/v BSA*	1:1000 in 5% w/v BSA*	1:5000 in 5% w/v BSA*	1:1000 in 5% w/v BSA*	1:1000 in 5% w/v BSA*
Secondary Antibody	HRP-conjugated anti-Rabbit (Dako)	HRP-conjugated anti-Rabbit (Dako)	HRP-conjugated anti-Rabbit (Dako)	HRP-cojugated anti-Mouse (Dako)	HRP-conjugated anti-Rabbit (Dako)	HRP-conjugated anti-Rabbit (Dako)	HRP-conjugated anti-Mouse (Dako)	HRP-conjugated anti-Rabbit (Dako)	HRP-conjugated anti-Rabbit (Dako)
Secondary Antibody Conditions	1:2000 in 5% w/v BSA*	1:2000 in 5% w/v BSA*	1:2000 in 5% w/v BSA*	1:2000 in 5% w/v BSA*	1:2000 in 5% w/v BSA*	1:2000 in 5% w/v BSA*	1:2000 in 5% w/v BSA*	1:2000 in 5% w/v BSA*	1:2000 in 5% w/v BSA*
Detection Reagents	ECL	ECL	ECL	ECL	ECL	ECL+	ECL	ECL	ECL
Target Protein Size	175kda	185kda	50/105kda	52/100kda	60kda	60kda	42-85kda	42, 44 kda	21kda

**Table 2.11: Western antibodies and conditions**

CST = Cell Signalling Technologies; pAb = polyclonal antibody; mAb monoclonal antibody; \*BSA or milk diluted in PBS/T

Target	STAT3 (Total)	Phospho-STAT3 (Tyr705)	E-Cadherin	Vimentin	Snail	BCL3	Tubulin	$\beta$ -Actin	Lamin A/C
Primary Antibody Source	CST	CST	Upstate	Santa Cruz	Santa Cruz	Santa Cruz	Abcam	Abcam	CST
Catalogue Number	9132	9131	07-697	sc-7557	sc-10433	sc-185x	Ab6160	Ab8227	2032
Primary Antibody Raised in	Rabbit (pAb)	Rabbit (pAb)	Rabbit (pAb)	Goat (pAb)	Goat (pAb)	Rabbit (pAb)	Rat (mAb)	Rabbit (pAb)	Rabbit (pAb)
Primary Antibody Dilution	1:1000 in 5% w/v BSA*	1:1000 in 5% w/v BSA*	1:500 in 5% w/v milk*	1:200 in 5% w/v BSA*	1:500 in 5% w/v milk*	1:200 in 5% w/v milk*	1:10000 in 5% w/v BSA*	1:5000 in 5% w/v BSA*	1:1000 in 5% w/v BSA*
Secondary Antibody	HRP-conjugated anti-Rabbit (Dako)	HRP-conjugated anti-Rabbit (Dako)	HRP-conjugated anti-Rabbit (Dako)	HRP-conjugated anti-Goat (Dako)	HRP-conjugated anti-Goat (Dako)	HRP-conjugated anti-Rabbit (Dako)	HRP-conjugated anti-Rat (Dako)	HRP-conjugated anti-Rabbit (Dako)	HRP-conjugated anti-Rabbit (Dako)
Secondary Antibody Conditions	1:2000 in 5% w/v BSA*	1:2000 in 5% w/v BSA*	1:2000 in 5% w/v BSA*	1:2000 in 5% w/v BSA*	1:2000 in 5% w/v BSA*	1:2000 in 5% w/v BSA*	1:2000 in 5% w/v BSA*	1:2000 in 5% w/v BSA*	1:2000 in 5% w/v BSA*
Detection Reagents	ECL	ECL	ECL	ECL+	ECL	ECL+	ECL	ECL	ECL
Target Protein Size	86kda	86kda	106kda	57kda	29kda	60kda	50kda	48kda	70kda

**Table 2.12: Western antibodies and conditions continued**

CST = Cell Signalling Technologies; pAb = polyclonal antibody; mAb monoclonal antibody; \*BSA or milk diluted in PBS/T

## 2.7 Caspase assays

Caspase-Glo 3/7, 8 and 9 assays (Promega) are luminescent assays that measure the activity of individual caspases. The assays provide luminogenic substrates for individual caspases. Addition of the Caspase-Glo reagent to the sample results in cell lysis followed by caspase cleavage of the substrate and a resulting luminescent signal which is proportional to the amount of caspase activity present in the sample.

### 2.7.1 Determination of caspase activity in mammary tissues

Whole mammary tissue samples were removed from the -80 freezer and approximately 100mg was cut on dry ice and placed in spinLyse tubes containing 1ml of lysis buffer (Promega) and 2µg/ml of aprotinin (Sigma). Samples were spin lysed twice for 45 seconds on Precellys 24 lysis and homogenization machine. The supernatant was transferred to a fresh tube and passed through a blue 23G needle seven times before being rested on ice for 10 minutes. Samples were centrifuged at 13,000rpm at 4°C for 15 minutes. Protein concentrations were determined as per section 2.6.3. Samples were normalised and stored at -80°C until required for the Caspase-Glo assay.

Caspase-Glo 3/7, 8 or 9 reagents were prepared according to manufacturer's instructions and 50µl of each normalised protein sample was pipetted into a well of a 96 well plate black walled plate (Corning). An equal amount of Caspase-Glo reagent was added to each sample and to one empty well to serve as a 'blank' control. The plate was placed on a plate shaker and agitated at 300-500rpm for 30 seconds before being incubated at room temperature for 1 hour. The luminescence of each sample was read on a FLUOstar Optima plate reader and the 'blank' control value was subtracted from all other values.

### 2.7.2 Determination of caspase activity in cells

Transfected cells were removed from tissue culture plates using 0.25% w/v Trypsin/EDTA and centrifuged at 1100rpm for 5 minutes before being resuspended in complete growth medium. Cells were counted and resuspended at a density of  $2 \times 10^5$  cells/ml and 100µl of this suspension was plated into appropriate wells of a black-walled 96-well plate. At the same time, 100µl of complete media alone was plated into triplicate wells to serve as a 'blank' control. The plate was incubated at 37°C and 5% CO<sub>2</sub> for an appropriate amount of time (as indicated in the results sections). After incubation, Caspase-Glo reagents were prepared according to manufacturer's instructions, and plates were removed from the incubator and allowed to equilibrate to room temperature. To each well containing cells or 'blank' controls, 100µl of Caspase-Glo reagent was added. The plate was then gently agitated on a plate shaker at 300-500rpm for 30 seconds before being incubated at room temperature 1 hour. The luminescence of

each sample was then measured on a FLUOstar Optima plate reader and the 'blank' control value was subtracted from all other values.

## 2.8 RNA analysis

### 2.8.1 Isolation of RNA

All bench work surfaces and equipment were treated with RNaseZAP (Ambion) before use and RNase free H<sub>2</sub>O (Sigma) was used throughout.

#### 2.8.1.1 *Extraction and purification of RNA from tissues*

Frozen tissue (50mg) was cut on a petri dish on dry ice and placed in a spinLyse tube containing 1ml of Trizol (Invitrogen) reagent. Tissues were spinLysed twice at 6500rpm for 45 seconds on Precellys 24 lysis and homogenization machine and were then centrifuged at 8000 x g for 10 minutes at 4°C. The supernatant was transferred to a new RNase free tube and 200µl of chloroform was added to each sample and shaken vigorously by hand for 30 seconds. Samples were left for 3 minutes at room temperature and then centrifuged again at 8000 x g for 15 minutes at 4°C. The aqueous phase was removed and placed into a fresh RNase free tube containing 400µl of isopropanol and mixed gently to precipitate out the RNA before being purified using an RNeasy Mini Kit (Qiagen) according to manufacturer's instructions. Concentration and quality of RNA was quantified on a NanoDrop spectrophotometer (ND-1000; Labtech International).

#### 2.8.1.2 *Purification of RNA from cells*

Purification of RNA from cells was achieved using the RNeasy Mini Kit according to manufacturer's instructions. Concentration and quality of RNA was quantified on a NanoDrop spectrophotometer.

### 2.8.2 Reverse transcription

Reverse transcription was performed using RevertAID Premium Reverse Transcriptase (Fermentas). cDNA was synthesised from 500 – 1000ng RNA samples diluted in 12.5µl of RNase free H<sub>2</sub>O. A master reaction mix containing Random Primers and dNTPs (Table 2.13) was prepared in a nuclease free tube on ice and 2µl was added to each sample to make a total volume of 14.5µl. Samples were then mixed gently, centrifuged and heated to 65°C for 5 minutes before being returned immediately to ice. A second reaction mix containing the reverse transcriptase (Table 2.13) was prepared and 5.5µl was added to each sample to make a final volume of 20µl. Samples were then incubated for 10 minutes at 25°C, 30 minutes at 50°C and 5 minutes at 85°C before being returned to ice. For each experiment, controls were prepared in exactly the same way but with reaction mixes lacking the reverse transcriptase enzyme. Samples were either used immediately or stored -70°C until required.

Reaction Mix 1 Component	Volume Per Reaction
dNTPs (10mM; dATP, dCTP, dGTP, dTTP; Promega)	1 $\mu$ l
Random Primers (500ug/ml [Promega])	1ul
Reaction Mix 2 Component	Volume Per Reaction
5xRT Buffer (Fermentas)	4 $\mu$ l
RNasin Plus (40u/ $\mu$ l; Promega)	0.5 $\mu$ l
RevertAID Premium Reverse Transcriptase (200u/ $\mu$ l; Fermentas)	1 $\mu$ l

**Table 2.13: Reaction mix components for reverse transcription**

### 2.8.3 Quantitative real-time polymerase chain reaction (QRT-PCR) & semi-quantitative PCR

#### 2.8.3.1 Primer design

All primer sets were designed across exon boundaries using the Primer3 web-based program <http://frodo.wi.mit.edu/primer3/>. To check for mis-priming, all sequences were verified by performing in silico PCR (<http://genome.csdb.cn/cgi-bin/hgPcr>). All primers were purchased from Sigma-Genosys and sequences can be found in Table 2.15.

#### 2.8.3.2 QRT-PCR

QRT-PCR was performed using Step One Plus Realtime PCR System (Applied Biosystems), in conjunction with StepOne (v2.1; Applied Biosystems) software. Each reaction was performed in triplicate and a minimum of 3 separate biological samples were analysed. One housekeeping gene (*Cyclophilin B* or *Beta-Actin*) was always run as a reference.

An arbitrary standard curve was generated by pooling 5 $\mu$ l of cDNA from each sample to make a neat cDNA control which was then diluted 1:5 and 1:25 with PCR-grade water to make three cDNA standards. Appropriate volumes (Table 2.14) of cDNA test samples, cDNA standards or PCR-grade H<sub>2</sub>O (Sigma) control were loaded into separate wells of a 96 well reaction plate (MicroAmp Fast Optical 0.1ml; Applied Biosystems).

A PCR mastermix containing all other reaction components was then prepared according to Table 2.14. Mastermix (22.5 $\mu$ l) was added to each well and gently pipetted to ensure homogeneous mixing of cDNA and reaction mix. The PCR plate was then sealed with appropriate caps (MicroAmp Optical 8-capstrip; Applied Biosystems) before being loaded into the Realtime PCR machine.

All reactions were run under the same cycling conditions of initial denaturation at 95°C for 10 minutes followed by 45 cycles of 95°C for 15 seconds and 60°C for 1 minute (with a plate read after each cycle). A melting curve (95°C for 15 seconds, 60°C for 1 minute [optics off], 60°C to 95°C at 0.2°C increments every 15 seconds [optics on]) was constructed at the end of the experiment and data was collected with Step one plus software.

### 2.8.3.3 Analysis of QRT-PCR data

Data was initially examined using Step One Plus software. Melting curves were analysed to ensure that only one peak at the expected melting temperature was observed and that the H<sub>2</sub>O control samples produced no product.

Ct values for standards were plotted against relative amounts (neat cDNA = 1, 1:5 dilution = 0.2, 1:25 dilution = 0.04) to generate a standard curve for each primer set. Relative mRNA expression in each sample was extrapolated by plotting Ct values on the standard curve. The differences between the amounts amplified in samples for a target gene and corresponding samples amplifying a reference gene was then calculated to get a normalised relative expression value. Generally, an average expression value across all biological replicates was taken and values were normalised back to the control samples.

### 2.8.3.4 Semi-quantitative PCR

When only semi-quantitative PCR analysis was required, PCR reactions were set up, run and visualised as described in sections 2.1.2.2 and 2.1.2.3, using master mixes detailed in Table 2.14 and cycling conditions detailed in section 2.8.3.2.

Reaction Component	QRT-PCR	Semi-quantitative PCR
cDNA Template	2.5µl	2.5µl
PCR grade Water	12.65µl	13.9µl
Go Taq PCR Buffer	5µl	5µl
Magnesium Chloride (25mM)	2.5µl	2.5µl
dNTPs (10mM; dATP, dCTP, dGTP, dTTP)	0.5µl	0.5µl
Forward Primer (10µM)	0.25µl	0.25µl
Reverse Primer (10µM)	0.25µl	0.25µl
Go Taq DNA Polymerase	0.1µl	0.1µl
Sybr Green (Invitrogen)	1.25µl	N/A
Total Reaction Volume	25µl	25µl

**Table 2.14: QRT-PCR and semi-quantitative PCR reaction components**

Target	Species	Forward Primer Sequence (5' to 3')	Reverse Primer Sequence (5' to 3')	Product Size
<i>Bcl3</i>	Mouse	AGC CTG AAC ATG GTG CAA CT	CCA CCA TGA GAG GTG TGT CA	184bp
<i>FasR</i>	Mouse	TCG GAG ATG CTA TTA GTA CCT TG	GAT CTG GGC TGT CCT GCC T	78bp
<i>FasL</i>	Mouse	TTC ATG GTT CTG GTG GCT CTG GT	CTG GGG TTG GCT ATT TGC TTT TCA	143bp
<i>DR 5</i>	Mouse	ATA AAA AGA GGC TGT GAA CGG G	GGT CCA AGA GAG ACG A	64bp
<i>TNFR 1</i>	Mouse	GAC CGG GAG AAG AGG GAT AG	GTT CCT TTG TGG CAC TTG GT	92bp
<i>TNFR 2</i>	Mouse	GAC CTG AGT TGG ATC CCT GA	TGT GCA CAT ATG CAG AAG CA	98bp
<i>Trail</i>	Mouse	ATA AAA AGA GGC TGT GAA CGG G	GGT CCA AGA GAG ACG A	64bp
<i>Faim</i>	Mouse	CGG GCG AGT TTG TCG ATG AT	AGC TCT GGG ATT TCC CTG TT	142bp
<i>c-flip</i>	Mouse	TGC TGA TGG AGA TTG GTG AG	CCT TGG CTA TCT TGC CTC TG	96bp
<i>Cyclin D1</i>	Mouse	AGT GCG TGC AGA AGG AGA TT	CTC TTC GCA CTT CTG CTC CT	89bp
<i>Cyclophilin B</i>	Mouse	CCA TCG TGT CAT CAA GGA CTT CAT	TTG CCA TCC AGC CAG GAG GTC T	216bp
<i>Nme1</i>	Mouse	AGA TCA TCA AGC GGT TCG AG	CAC CAG GCC AGT AAA GAA GG	128bp
<i>Nme2</i>	Mouse	GCG AGA TCA TCA AAC GGT TC	CGA TGT AAT GCT GCT TCA GG	96bp
<i>Nme3</i>	Mouse	CGC GAG AAA CCC TTC TAC AG	AAG CAT GCA CGA CAT CCA G	94bp
<i>Nme4</i>	Mouse	TAC ATG AGC TCT GGG CCT GT	TCT GTT GAG TCG GTG TGT CC	95bp
<i>Timp1</i>	Mouse	ATC AGT GCC TGC AGC TTC TT	TCA CTC TCC AGT TTG CAA GG	140bp
<i>Timp2</i>	Mouse	AAG CAG TGA GCG AGA AGG AG	GGG GGC CGT GTA GAT AAA CT	137bp
<i>Tgfβ</i>	Mouse	TGC GCT TGC AGA GAT TAA AA	CGT CAA AAG ACA GCC ACT CA	135bp
<i>Cav1</i>	Mouse	GCA CAC CAA GGA GAT TGA CC	TCC CTT CTG GTT CTG CAA TC	101bp
<i>Igf1r</i>	Mouse	CCT CGG TGA TGA AGG AGT TC	TCA CCG CGT GTC ATT AGT TC	106bp
<i>Rab21</i>	Mouse	GGT GGA AAA AGA GTA AAC CTT GC	CTC CGT TCG AAT CTC GGT AG	94bp
<i>Gab1</i>	Mouse	GGA CCT TTC CGA GCG ATA G	CTC TTC ACC CGA GAC ACC TC	98bp
<i>Sphk2</i>	Mouse	GGC ATT GTC ACT GTG TCT GG	GAT CCA CAG GGG AGG ACA C	116bp
<i>Tcfap2c</i>	Mouse	GAC CTG CTG CTG CCT CAC	TGC GAA TGA CAG TCT GAT CG	142bp
<i>Arhgdib</i>	Mouse	ATC TCG AGG CCC TCA AAA AG	CCA GTC CGG TAT GTG TGT TG	130bp
<i>BCL3</i>	Human	TAT TGC TGT GGT GCA GGG TA	GGT GTC TGC CGT AGG TTG TT	105bp
<i>B-ACTIN</i>	Human	ACA TCT GCT GGA AGG TGG AC	CCC AGC ACA ATG AAG ATC AA	103bp
<i>CYCLIN D1</i>	Human	CAA ATG TGT GCA GAA GGA GGT	CTC CTC GCA CTT CTG TTC CT	91bp
<i>NME1</i>	Human	ACC TTC ATT GCG ATC AAA CC	AAC AAG GCG GAA TCC TTT CT	90bp
<i>NME2</i>	Human	GCT TCG AGC AGA AGG GAT TC	ATG GTC GGT CTT TCA GGT CA	99bp
<i>NME4</i>	Human	GTG ATC CAG CGC TTT GAG AG	AGC TCA TGT AGC GGA TGA GG	139bp
<i>TIMP1</i>	Human	GGG CTT CAC CAA GAC CTA CA	GAC TGG AAG CCC TTT TCA GA	141bp
<i>TIMP2</i>	Human	AAG CGG TCA GTG AGA AGG AA	GGG GGC CGT GTA GAT AAA CT	137bp
<i>CAV1</i>	Human	GAG CTG AGC GAG AAG CAA GT	TCC CTT CTG GTT CTG CAA TC	130bp
<i>RAB21</i>	Human	TGC ATT GGG TCC AAT TTA CT	CAT TTC CCA ACA TTT TCC GTA	125bp
<i>GAB1</i>	Human	ATT CCA CGA GCA TTT CCA AG	GGT GAA TTG GGA TTC ATT GG	143bp
<i>SPHK2</i>	Human	GAG CCT GAG TGA GTG GGA TG	CAG TCA GGG CGA TCT AGG AG	90bp
<i>ARHGDI B</i>	Human	GCC CTC AAA AAG GAA ACC AT	TCC TGT AGG TGT GCT GAA CG	118bp

Table 2.15: QRT-PCR primer sequences

## 2.9 Microarray analysis

RNA was extracted according to section 2.8.1 and in order to remove any contaminating genomic DNA, RNA samples were treated with Deoxyribonuclease I, Amplification Grade (Invitrogen) according to manufacturer's instructions. Quality control, RNA labelling, hybridisation and bioinformatics were all performed by the Cambridge Genomic Service (Department of Pathology, University of Cambridge, Tennis court Road, Cambridge [[www.cgs.path.cam.ac.uk](http://www.cgs.path.cam.ac.uk)]). Microarray analysis was performed using an Illumina MouseRef-8 version 2 BeadChip which targets >25000 transcripts and enables the evaluation of eight samples in parallel. The content of this BeadChip is derived from the National Centre for Biotechnology Information Reference Sequence (NCBI RefSeq) database (Build 36, Release 22), supplemented with probes derived from the Mouse Exonic Evidence Based Oligonucleotide (MEEBO) set. Comparisons between datasets were performed by the Cambridge Genomic Service using the R-package Limma (Smyth 2004). Samples were ranked according to adjusted p-values obtained from T-tests corrected for multiple testing. Normalised data was returned in Excel format.

## 2.10 Statistical analysis

### 2.10.1.1 Kaplan-Meier survival analysis

All tumour-free survival curves and statistical analysis of tumour-free survival times were performed using the Kaplan-Meier method with the aid of MedCalc statistical analysis software (Version 11.4.3.0, [www.medcalc.org/](http://www.medcalc.org/)).

### 2.10.1.2 Kolmogorov-Smirnov analysis

Differences in the distribution of data to determine whether data was parametric or non-parametric were tested for using the Kolmogorov-Smirnov test. This test was performed using the Minitab statistics package (Version 14.20).

### 2.10.1.3 Mann-Whitney U-test

The Mann-Whitney U-test was used to determine statistical differences between non-parametric data sets. This was performed using the Minitab statistics package (Version 14.20).

### 2.10.1.4 Student's t-test

The Student's T-test was used to determine statistical differences between normally distributed data sets and between data sets with sample sizes of  $n=3$ . This test was performed using Excel 2007 software.

### 2.10.1.5 Chi-Squared test

The Chi-Squared test was used to determine statistical differences between observed frequencies and expected frequencies of data.

**Chapter 3:**  
**Analysis of BCL3 Deficiency in the**  
**Murine Mammary Gland**

### 3.1 Introduction

The mammary gland is a highly complex and specialised tissue which is able to undergo multiple cycles of proliferation, differentiation, secretion, and apoptosis. During pregnancy there is a huge expansion in the number of luminal epithelial cells which, at birth, become the milk secreting cells of the gland. After weaning, these cells become obsolete and are removed in a well co-ordinated event called involution, which involves extensive apoptosis, collapse of alveolar structures and tissue remodelling back to a pre-pregnant state. The process of involution is an extraordinary example of developmental apoptosis in mammals and can be studied not only to aid in the understanding of normal mammary gland development but also to identify key mediators of mammary epithelial cell death, which, when deregulated, could be involved in the pathology of diseases such as cancer.

Leukaemia inhibitory factor (LIF)-activated STAT3 has previously been identified as one of the key initiators of apoptosis in mammary gland involution (Chapman, Lourenco et al. 1999; Humphreys, Bierie et al. 2002; Kritikou, Sharkey et al. 2003; Schere-Levy, Buggiano et al. 2003). Although STAT3 activation is essential, it alone is not sufficient to induce apoptosis as it can be suppressed in the presence of constitutively active AKT (Schwertfeger, Richert et al. 2001), and as such, additional signalling pathways that synergise to mediate efficient cell death during involution must be involved. One such pathway is mediated by the NF- $\kappa$ B family of transcription factors which have previously been shown to be up-regulated at the immediate onset of involution (Clarkson, Heeley et al. 2000). Deletion of the NF- $\kappa$ B upstream regulator, IKK $\beta$ , resulted in delayed involution via a reduction in the transcription of death receptors and ligands (Baxter, Came et al. 2006) suggesting that, in addition to STAT3, this signalling pathway is also vitally important in the initiation of involution.

Currently there is little evidence for an interaction between the STATs and NF- $\kappa$ B in mammary epithelial cells. However, the two transcription factors have been shown to form a complex to activate the serum amyloid A gene (Hagihara, Nishikawa et al. 2005) which is upregulated during involution. A previous study of STAT3 and STAT5 transcriptional targets in mammary epithelial cells *in vitro* showed that while no NF- $\kappa$ B genes were significantly regulated by STATs, the NF- $\kappa$ B co-factor gene, *Bcl3*, was found to be a principal transcriptional target of STAT3 (Clarkson, Boland et al. 2006). This association has previously been observed in myeloma cells (Brocke-Heidrich, Ge et al. 2006) and reflects a possible mechanism by which the two pathways may undergo cross-talk to regulate involution.

The role of BCL3 in regulating mammary epithelial cell fate in the pregnancy cycle has not previously been investigated. However, large scale microarray analysis of the murine pregnancy cycle revealed that *Bcl3*, along with a group of other STAT3 or NF- $\kappa$ B transcriptional target genes, is up-regulated in the first 12 hours of involution with a subsequent decline by 24 hours (Clarkson, Wayland et

al. 2004). This is an indication that it might be involved in regulating the initial apoptotic signals that are transduced very early on in the involution process.

The overall aim of this chapter was to investigate the effect of BCL3 deletion on mammary gland development during the murine pregnancy cycle. Initially, the gross morphology of the mammary gland in the absence of BCL3 was assessed. As *Bcl3* has previously been shown to be a downstream target of STAT3 and to be transiently up-regulated in early involution, the rest of the chapter focussed on determining whether it contributes to the pro-apoptotic effects of STAT3 specifically at this stage of the cycle.

## 3.2 Results

### 3.2.1 Gross mammary epithelial morphology is unaffected by the absence of BCL3 in virgin glands and during pregnancy and lactation

As part of a previously performed large scale microarray analysis of transcriptional changes in the mouse pregnancy cycle, *Bcl3* mRNA levels were assessed. This study revealed that *Bcl3* expression remained at consistently low levels in the virgin gland and throughout the gestation and lactation stages of the cycle (Clarkson, Wayland et al. 2004).

In order to determine whether loss of BCL3 affected the gross mammary epithelial morphology during these stages of the pregnancy cycle, the fourth abdominal mammary glands from 3 *Bcl3*<sup>-/-</sup> and 3 *Bcl3*<sup>+/+</sup> post-pubescent virgin, pregnant and lactating mice were harvested before being fixed for subsequent H&E staining and analysis.

In virgin mice, the majority of the mammary glands were composed of adipocytes, with infrequent epithelial ducts present. No phenotypic differences were observed between the *Bcl3*<sup>+/+</sup> and *Bcl3*<sup>-/-</sup> mammary glands (Figure 3.1). At 15 days gestation, extensive expansion of the epithelial compartment that is classically associated with this stage of the cycle was evident. However, loss of BCL3 had no effect on the histology of the gland in comparison to wild-type controls at this time point (Figure 3.1). At 10 days lactation, glands were predominantly composed of alveoli lined by secretory epithelial cells. Again, loss of BCL3 did not result in any phenotypic differences in comparison to controls (Figure 3.1). Furthermore, no differences were observed in the ability of *Bcl3*<sup>-/-</sup> mothers to feed and maintain their litters in comparison to *Bcl3*<sup>+/+</sup> mothers.

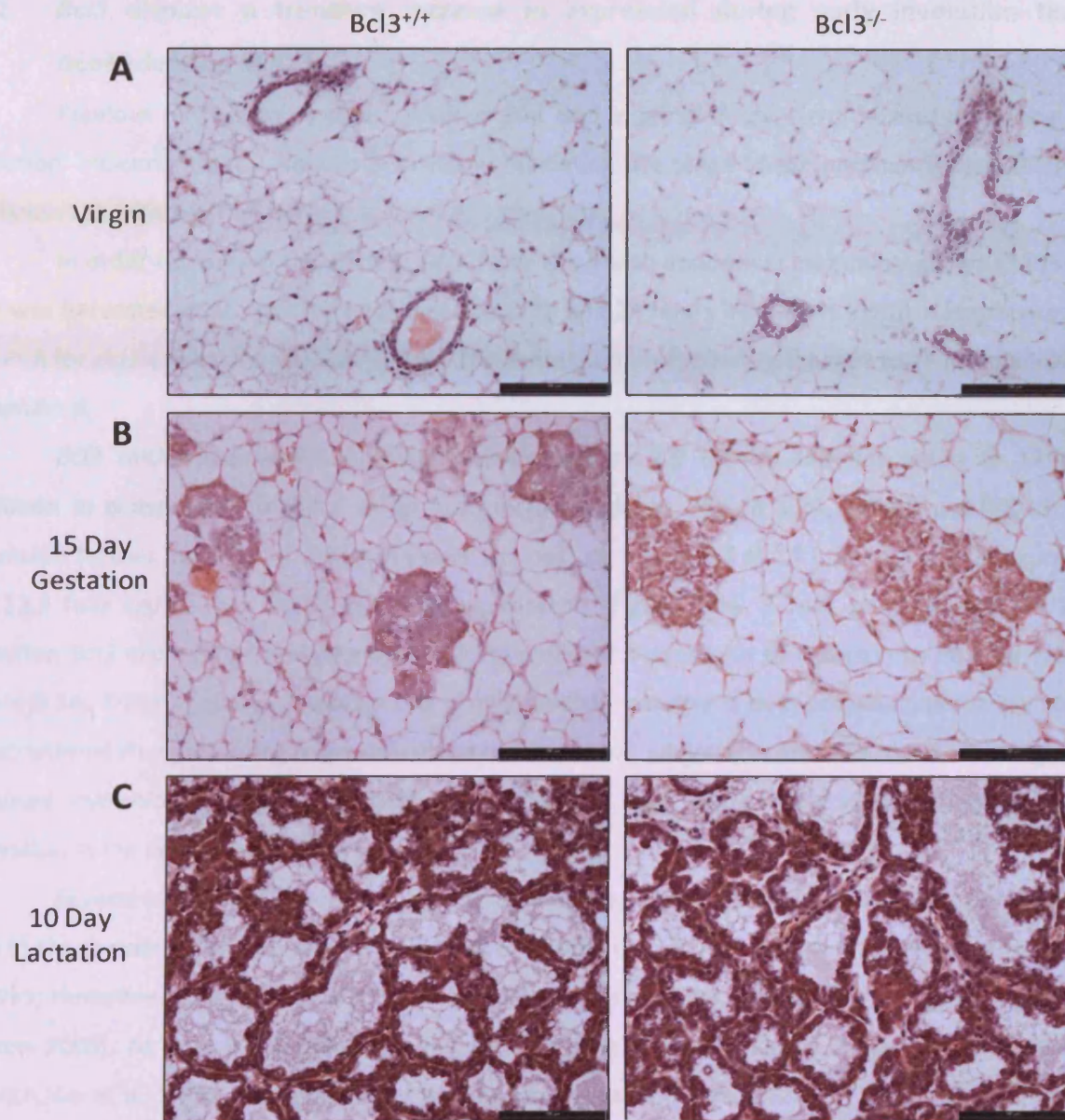


**Figure 3.1: Loss of BCL3 has no effect on the gross morphology of the mammary gland**

Fourth abdominal mammary glands from 3  $Bcl3^{+/+}$  and 3  $Bcl3^{-/-}$  mice were harvested at different stages of the pregnancy cycle (virgin, 15 day gestation and 10 day lactation). No gross histological differences were observed at any time point analysed. Representative images are shown. Scale bars indicate 100 $\mu$ m.

### 3.2.2 *Bcl3* displays a transient increase in expression during early involution that is dependent on STAT3

Previous microarray analysis revealed that *Bcl3* expression transiently increases during early involution, indicating that it may be involved in mediating this stage of the pregnancy cycle (Clarkson, Wayland et al. 2004).

In order to confirm this finding, RNA from the fourth abdominal mammary glands of four FVB mice was harvested at 10 days lactation and at 12, 18 and 24 hours involution. cDNA was prepared and QRT-PCR for *Bcl3* expression was performed. The expression profile was compared to an internal control, *cyclophilin B*.

*Bcl3* mRNA expression increased significantly by 2.5 fold in samples taken at 12 hours involution in comparison to those taken from lactating glands (Figure 3.2A, T-Test,  $p=0.00028$ ). *Bcl3* expression further increased dramatically over the next six hours and at 18 hours involution expression was 12.9 fold higher than in 10 day lactating controls (Figure 3.2A, T-Test,  $p=0.0001$ ). At 24 hours involution *Bcl3* expression showed a small but insignificant decrease in comparison to 18 hour samples (Figure 3.2A, T-Test,  $p>0.05$ ). Although this is only partially consistent with previous microarray data of transcriptional changes during mammary gland development, whereby expression levels were highest at 12 hours involution (Clarkson, Wayland et al. 2004), it does confirm a transient increase in *Bcl3* expression in the early stages of the process.

Several transcription factors, including LIF-activated STAT3 have been shown to play important roles in the regulation of apoptosis at the onset of murine mammary involution (Chapman, Lourenco et al. 1999; Humphreys, Bierie et al. 2002; Kritikou, Sharkey et al. 2003; Schere-Levy, Buggiano et al. 2003; Watson 2006). As *Bcl3* has previously been shown to be a transcriptional target of STAT3 (Brocke-Heidrich, Ge et al. 2006), the question of whether its expression is regulated by STAT3 during the early stages of mammary gland involution was addressed.

For this study, mammary specific *Stat3* knock-out mice, in which expression of Cre recombinase is directed specifically to mammary epithelial cells by the promoter of the beta-lactoglobulin (*Blg*) gene were utilised (Selbert, Bentley et al. 1998; Chapman, Lourenco et al. 1999). Fourth abdominal mammary glands of mice expressing *Blg/Cre* and either one floxed *Stat3* and one wild-type *Stat3* allele (*Blg/Cre/Stat3<sup>flox/+</sup>*) or one floxed *Stat3* and one null *Stat3* allele (*Blg/Cre/Stat3<sup>flox/-</sup>*) were harvested at 18 hours involution. RNA from these frozen glands ( $n=3$ ) was subsequently extracted and analysed for *Bcl3* expression by QRT-PCR.

Glands with the mammary epithelial specific loss of *Stat3* (*Blg/Cre/Stat3<sup>flox/-</sup>*) had 77% less *Bcl3* mRNA expression at 18 hours involution in comparison to *Stat3* expressing (*Blg/Cre/Stat3<sup>flox/+</sup>*) control

glands (Figure 3.2B, T-Test,  $p=0.034$ ). This indicated that elevated *Bcl3* expression during early murine mammary involution is dependent on STAT3 signalling.

Taken together, these results suggest that *Bcl3* expression is up-regulated between 12 and 24 hours involution, in response to STAT3.

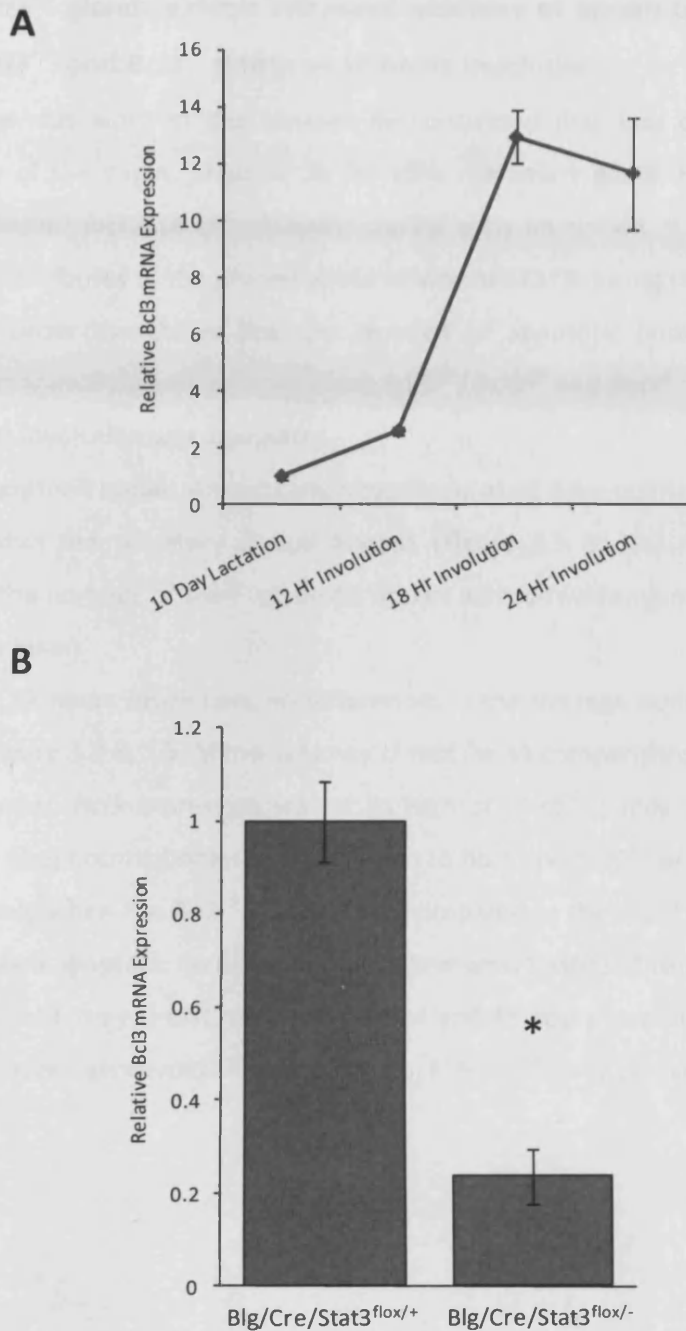


**Figure 3.2: *Bcl3* expression transiently increases in response to *STAT3* signalling at 18 hours involution**

RNA was harvested from the fourth abdominal mammary glands of FVB mice at 10 days lactation and at 12, 18 and 24 hours involution (n=4 at each time point). Subsequent QRT-PCR analysis revealed that *Bcl3* expression transiently increased to a maximum at 18 hours involution with a subsequent small decline at 24 hours involution. Error bars represent  $\pm$  standard error of the mean (SEM) (A). RNA was harvested from the fourth abdominal mammary glands of 3 *Blg/Cre/Stat3*<sup>flox/+</sup> and 3 *Blg/Cre/Stat3*<sup>flox/-</sup> mice. QRT-PCR analysis showed that *Bcl3* expression was significantly lower in the absence of *STAT3* at 18 hours involution (B, \*=T-test, p=0.0304). Data is represented as *Bcl3* mRNA levels relative to *cyclophilin B* mRNA levels. Error bars represent  $\pm$  SEM.

### 3.2.3 *Bcl3*<sup>+/-</sup> glands exhibit increased numbers of apoptotic bodies in comparison to both *Bcl3*<sup>+/+</sup> and *Bcl3*<sup>-/-</sup> glands at 18 hours involution

Previous work in this chapter demonstrated that loss of BCL3 does not affect the gross morphology of the virgin, pregnant or lactating mammary gland. However, as *Bcl3* showed a striking STAT3-dependent increase in expression during early involution, it was of interest to closely examine whether it contributes to the pro-apoptotic effects of STAT3 during this stage of the pregnancy cycle.

In order to achieve this, the number of apoptotic bodies present in H&E stained fourth abdominal mammary gland sections from *Bcl3*<sup>+/+</sup>, *Bcl3*<sup>+/-</sup> and *Bcl3*<sup>-/-</sup> ( $n \geq 4$ ) mice harvested at 12, 18, 24 and 48 hours involution was analysed.

Apoptotic bodies were clearly identifiable at all time-points by their distinctive appearance and location within the secretory alveoli lumens (Figure 3.3 & 3.4). To quantify any changes between genotypes, the number of shed apoptotic bodies across two random fields of view was counted and an average was taken.

At 12 hours involution, no differences in the average number of shed apoptotic bodies were observed (Figure 3.3 & 3.5, Mann-Whitney U-test for all comparisons,  $p > 0.05$ ). Interestingly, at 18 hours involution, when *Bcl3* expression was at its highest, *Bcl3*<sup>+/-</sup> glands displayed a marked increase in the appearance of apoptotic bodies in comparison to both the *Bcl3*<sup>+/+</sup> or *Bcl3*<sup>-/-</sup> glands. This was found to be significant only when the *Bcl3*<sup>+/-</sup> glands were compared to the *Bcl3*<sup>-/-</sup> glands (Figure 3.3-3.5), mean $\pm$ SEM number of shed apoptotic bodies per field of view was: 1036 $\pm$ 151 for *Bcl3*<sup>+/-</sup> glands and 586 $\pm$ 93 for *Bcl3*<sup>-/-</sup> glands, Mann-Whitney U-test,  $p = 0.0104$ ). At 24 and 48 hours involution, no significant differences were observed between genotypes (Figure 3.3 & 3.5, Mann-Whitney U-test for all comparison,  $p > 0.05$ ).

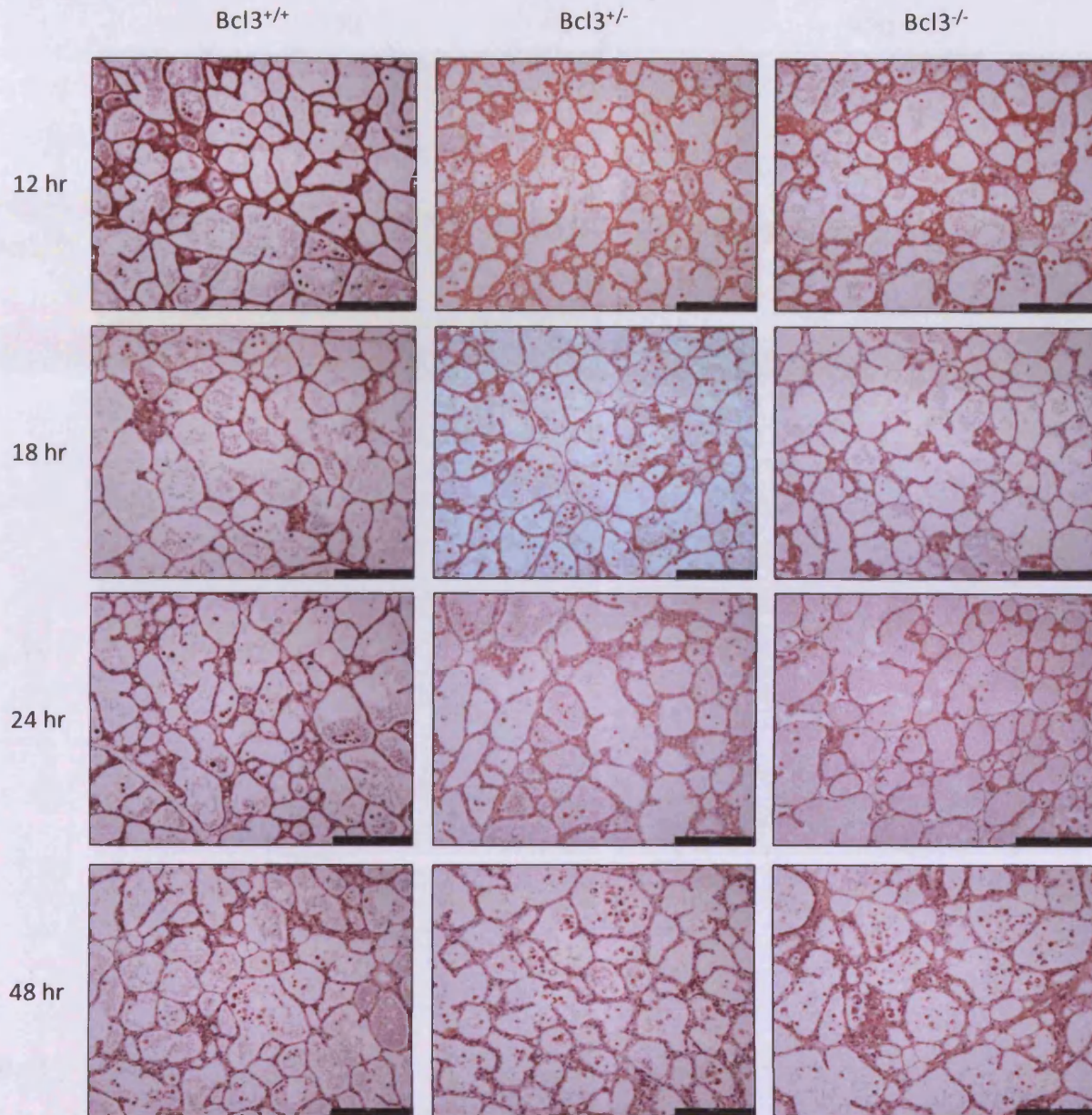


**Figure 3.3: Histological analysis of  $Bcl3^{+/+}$ ,  $Bcl3^{+/-}$  and  $Bcl3^{-/-}$  glands at 12, 18, 24 and 48 hours involution**  
 H&E stained sections ( $n \geq 4$ ) of fourth abdominal mammary glands from  $Bcl3^{+/+}$ ,  $Bcl3^{+/-}$  and  $Bcl3^{-/-}$  mice taken at 12, 18, 24 and 48 hours involution were analysed. No gross histological differences were observed at 12, 24 or 48 hours involution. At 18 hours involution increased numbers of apoptotic bodies were observed in  $Bcl3^{+/-}$  glands in comparison to  $Bcl3^{+/+}$  and  $Bcl3^{-/-}$  glands. Representative images are shown. Scale bars indicate 200 $\mu$ m. See figure 3.4 for higher magnification images and figure 3.5 for quantification of the number of shed apoptotic bodies present.

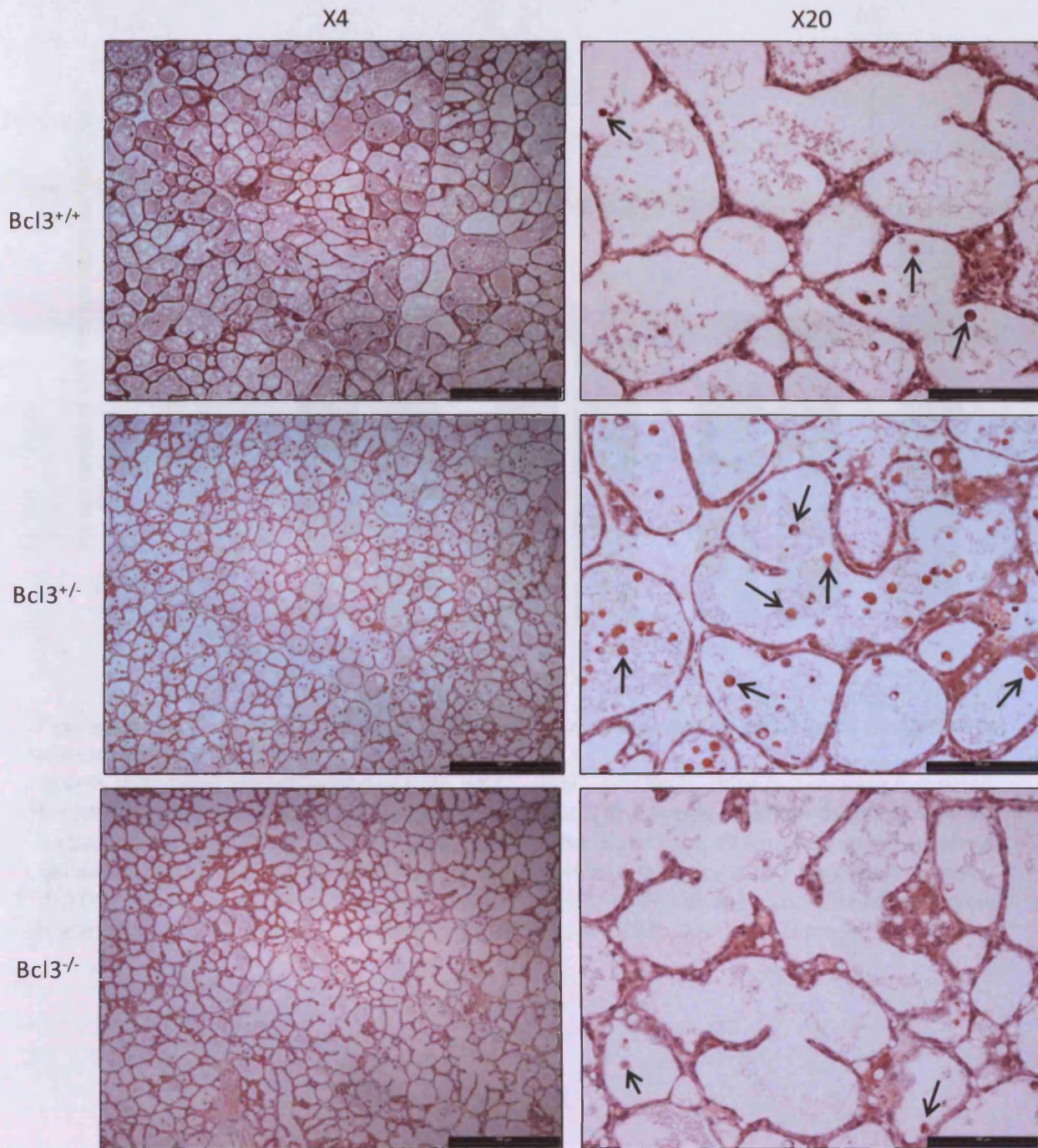


**Figure 3.4:  $Bcl3^{+/-}$  glands display increased apoptotic bodies in comparison to  $Bcl3^{+/+}$  and  $Bcl3^{-/-}$  glands at 18 hours involution**

Representative images of H&E stained sections from fourth abdominal mammary glands from  $Bcl3^{+/+}$ ,  $Bcl3^{+/-}$  and  $Bcl3^{-/-}$  mice at 18 hours involution.  $Bcl3^{+/-}$  glands display more apoptotic bodies than  $Bcl3^{+/+}$  or  $Bcl3^{-/-}$  glands. Representative apoptotic bodies are highlighted with arrows. Scale bars indicate: Left panel 500 $\mu$ m, Right panel 100 $\mu$ m.

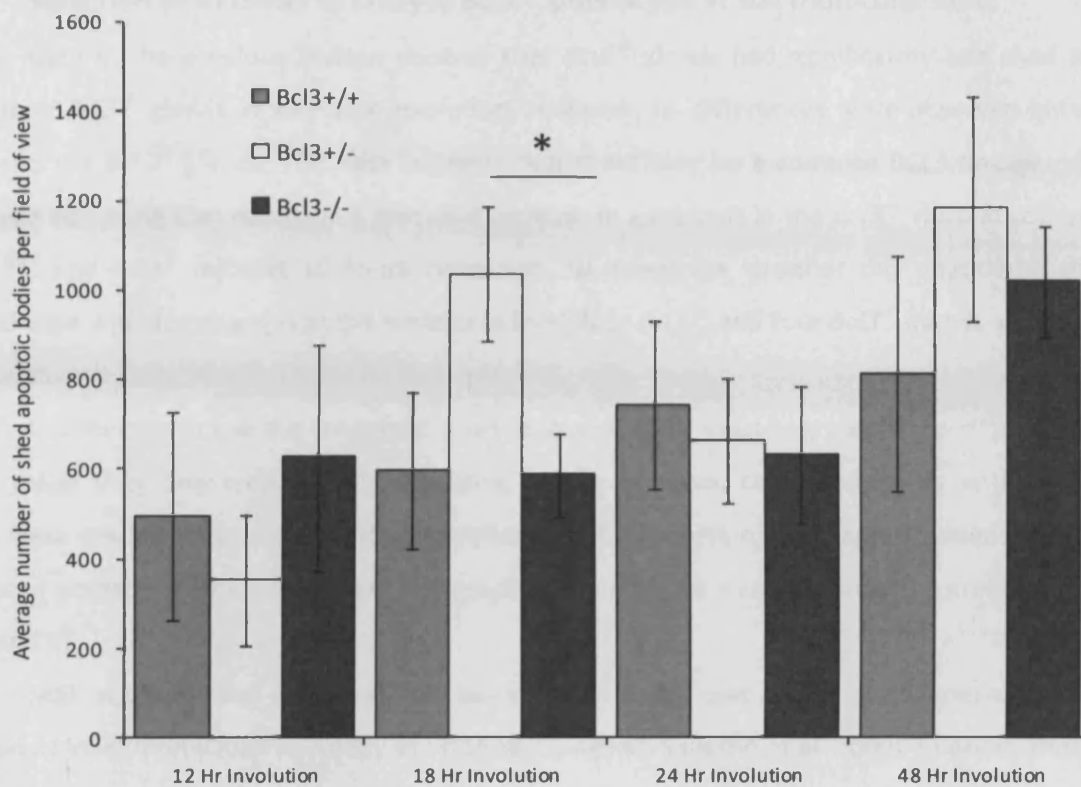


**Figure 3.5:  $Bcl3^{+/-}$  glands exhibit significantly more apoptotic bodies at 18 hours involution in comparison to  $Bcl3^{-/-}$  glands**

Fourth abdominal mammary glands from  $Bcl3^{+/+}$ ,  $Bcl3^{+/-}$  and  $Bcl3^{-/-}$  mice ( $n \geq 4$ ) were harvested for H&E sectioning and subsequent histological analysis. The average number of shed apoptotic bodies across two fields of view were counted. No significant differences were observed between genotypes at 12, 24 or 48 hours involution (Mann-Whitney U-test for all comparisons,  $p > 0.05$ ). At 18 hours involution,  $Bcl3^{+/-}$  glands displayed significantly more shed apoptotic bodies than  $Bcl3^{-/-}$  glands (\* = Mann-Whitney U-test,  $p = 0.0104$ ). Error bars represent  $\pm$  SEM.

### 3.2.4 Selection of a cohort to analyse *Bcl3*<sup>+/-</sup> phenotype at the molecular level

Data in the previous section showed that *Bcl3*<sup>-/-</sup> glands had significantly less shed apoptotic bodies than *Bcl3*<sup>+/-</sup> glands at 18 hours involution. However, no differences were observed between the *Bcl3*<sup>+/+</sup> and the *Bcl3*<sup>+/-</sup> glands. This data suggests that there may be a complex BCL3 dosage-dependent phenotype occurring that results in a transient increase in apoptosis in the *Bcl3*<sup>+/-</sup> mice in comparison to the *Bcl3*<sup>+/+</sup> and *Bcl3*<sup>-/-</sup> mice at 18 hours involution. To determine whether this phenotypic difference corresponded with any changes at the molecular level, four *Bcl3*<sup>+/-</sup> and four *Bcl3*<sup>-/-</sup> glands at 12, 18 and 24 hours involution were selected to be further analysed.

In order to choose the cohorts to analyse, glands were visually graded according to the degree of milk stasis they displayed. Glands displaying high milk stasis, characterised by entirely milk-filled lumens were graded 1 while glands that exhibited a high proportion of collapsed lumens with low milk stasis were graded 4. Glands displaying intermediate phenotypes were designated a grade of either 2 or 3 (Figure 3.6).

Milk accumulation and stasis has been shown to be one of the major mechanisms for the induction of involution (Quarrie, Addey et al. 1996; Quaglino, Salierno et al. 2009). In order, therefore, to use this physiological process as a selection criterion for a cohort to analyse, it was important to ensure that BCL3 had no effect on this parameter. To achieve this, the percentage of glands displaying high stasis was analysed in *Bcl3*<sup>+/-</sup> and *Bcl3*<sup>-/-</sup> mice and revealed no statistical differences in this parameter between cohorts at any involution time point (Table 3.1, Chi-Squared test  $p > 0.05$ ). Therefore, four animals with glands exhibiting high milk stasis (grades 1 or 2) were randomly chosen for each cohort. This exclusion criterion not only allowed the selection of a reasonable size cohort to work with but also removed additional biological variation between glands. The chosen cohort displayed a similar distribution of apoptotic bodies to the original full cohort with *Bcl3*<sup>+/-</sup> glands exhibiting significantly less apoptotic bodies than *Bcl3*<sup>+/-</sup> glands at 18 hours involution (Figure 3.7, Mean $\pm$ SEM number of shed apoptotic bodies per field of view was: 1105 $\pm$ 173 for *Bcl3*<sup>+/-</sup> glands and 530 $\pm$ 91 for *Bcl3*<sup>-/-</sup> glands, Mann-Whitney U-test,  $p = 0.0304$ ) indicating that the selection criteria did not artificially skew the data. These cohorts were used in all subsequent experiments to determine whether the observed change in apoptotic bodies also correlated with changes at the molecular level.

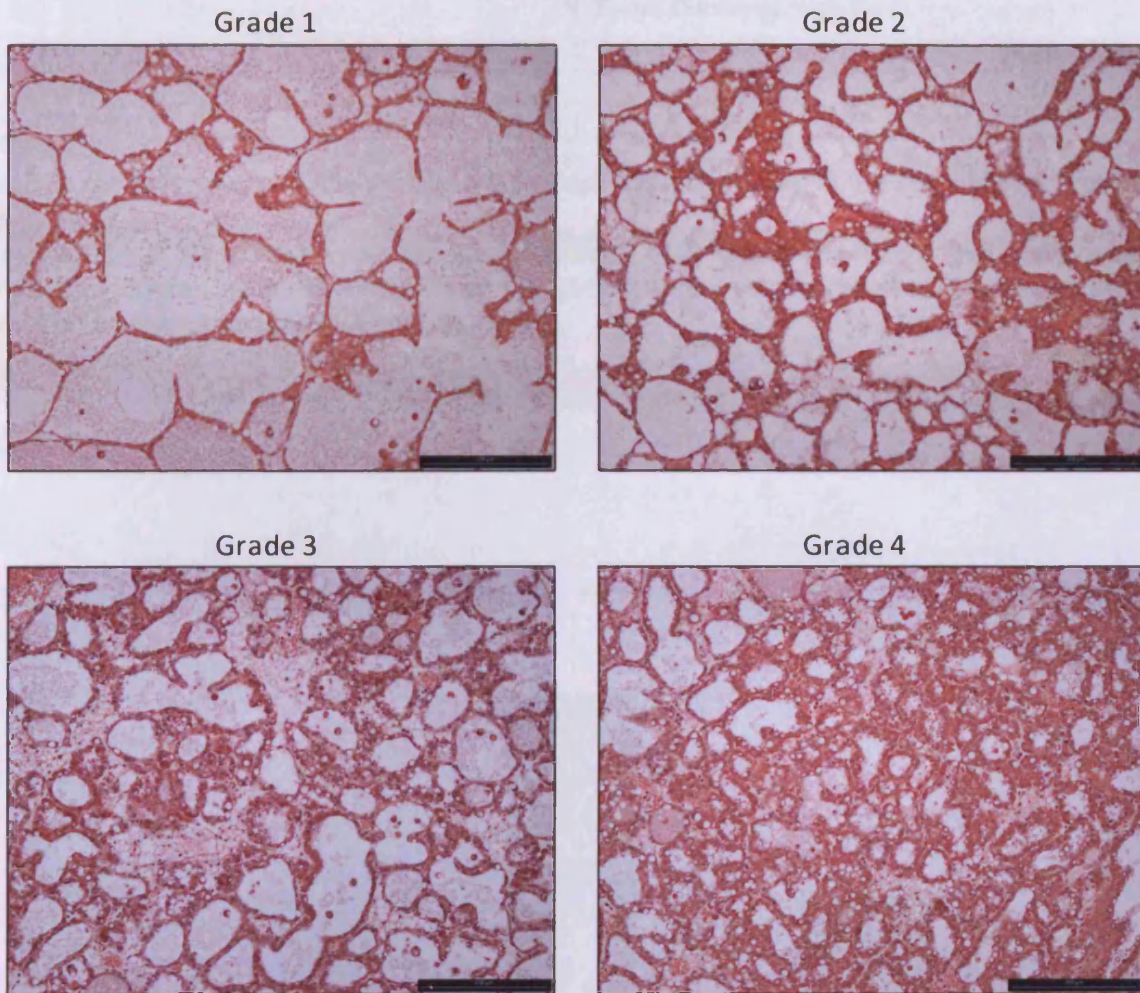


**Figure 3.6: Milk stasis grading scale**

Involuting mammary glands were graded visually according to the degree of milk stasis they displayed. Representative images of H&E sections at 18 hours involution indicating the milk stasis grading scale are shown. Grade 1 glands display a very high degree of stasis with entirely milk-filled lumens. Grade 4 glands have a large number of collapsed lumens with low levels of milk stasis. Grade 2 and 3 glands have intermediate levels of milk stasis. Scale bars indicate 200µm.

Genotype	% Glands Displaying High Stasis		
	12 Hrs Involution	18 Hrs Involution	24 Hrs Involution
<i>Bcl3</i> <sup>+/-</sup>	80%	66.6%	62.5%
<i>Bcl3</i> <sup>-/-</sup>	71.4%	80%	71.4%

**Table 3.1: The percentage of glands displaying a high degree of stasis is the same in *Bcl3*<sup>+/-</sup> and *Bcl3*<sup>-/-</sup> mice**

The percentage of glands displaying high stasis (grades 1 or 2) in *Bcl3*<sup>+/-</sup> and *Bcl3*<sup>-/-</sup> mice was calculated. No statistical differences in the frequency of high stasis glands was observed between genotypes at 12, 18 or 24 hours involution (Chi-Squared test  $p > 0.05$ ).

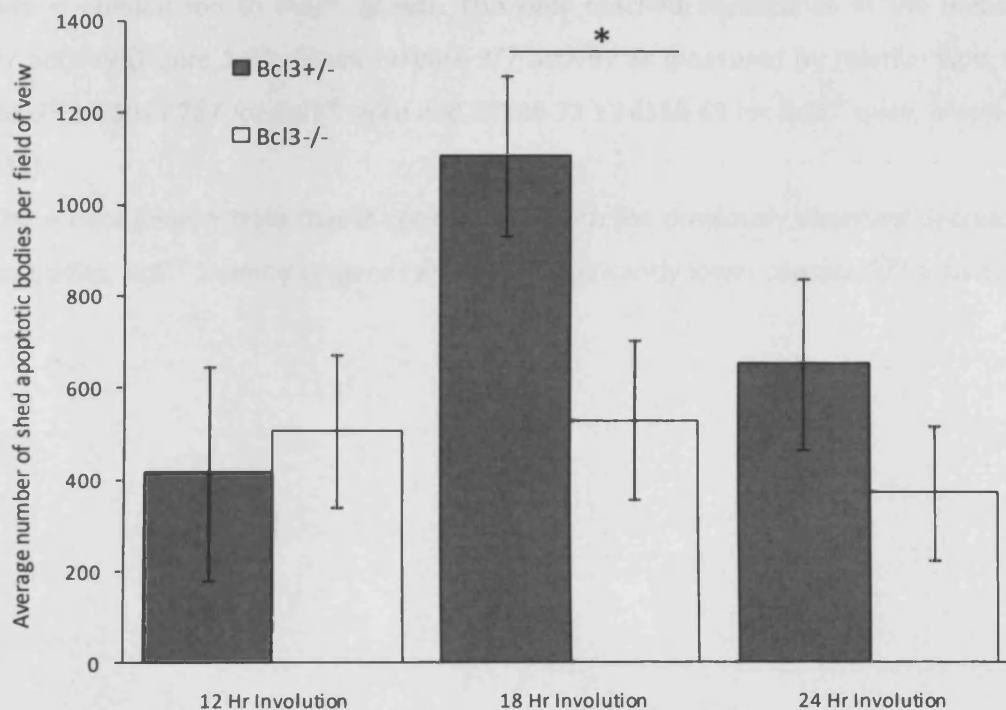


**Figure 3.7: *Bcl3*<sup>-/-</sup> glands have significantly less shed apoptotic bodies at 18 hours involution than *Bcl3*<sup>+/-</sup> glands from the chosen cohort**

H&E sections of mammary glands from *Bcl3*<sup>+/-</sup> and *Bcl3*<sup>-/-</sup> mice (n=4) in the chosen cohort were analysed for the average number of shed apoptotic bodies across two fields of view at 12, 18 and 24 hours involution. No significant differences were observed at 12 or 24 hours involution (Mann-Whitney U-test for both comparisons,  $p > 0.05$ ). At 18 hours involution, *Bcl3*<sup>+/-</sup> glands had significantly more shed apoptotic bodies than *Bcl3*<sup>-/-</sup> glands (\*=Mann-Whitney U-test,  $p = 0.0304$ ). Error bars represent  $\pm$  SEM.

### 3.2.5 *Bcl3*<sup>-/-</sup> glands display significantly less caspase 3/7 activity at 18 hours involution than *Bcl3*<sup>+/-</sup> glands

Having selected a final cohort and shown that *Bcl3*<sup>-/-</sup> mice had significantly less shed apoptotic bodies than *Bcl3*<sup>+/-</sup> mice at 18 hours involution, it of was interest to see if this difference corresponded to changes in caspase activity within the gland. Caspase 3/7, 8 and 9 assays (see Chapter 2: Materials and Methods, section 2.7) were performed on whole protein extracts from the fourth abdominal mammary glands of the four *Bcl3*<sup>+/-</sup> and four *Bcl3*<sup>-/-</sup> mice at 12, 18 and 24 hours involution.

At 12 and 24 hours involution, no significant differences in caspase 3/7, 8 or 9 activity were observed between the *Bcl3*<sup>+/-</sup> and *Bcl3*<sup>-/-</sup> mammary glands (Figure 3.8A-C, Mann-Whitney U-test for all comparisons,  $p > 0.05$ ). However, at 18 hours involution, the activity of all three caspases was lower in the *Bcl3*<sup>-/-</sup> glands in comparison to *Bcl3*<sup>+/-</sup> glands. This only reached significance in the measurement of caspase 3/7 activity (Figure 3.8A, Mean caspase 3/7 activity as measured by relative light units  $\pm$  SEM was:  $154158.75 \pm 16035.787$  for *Bcl3*<sup>+/-</sup> mice and  $60588.33 \pm 18350.63$  for *Bcl3*<sup>-/-</sup> mice; Mann-Whitney U-test,  $p = 0.034$ ).

These data demonstrate that in concordance with the previously observed decreased number of apoptotic bodies, *Bcl3*<sup>-/-</sup> mammary glands also have significantly lower capsase 3/7 activity than *Bcl3*<sup>+/-</sup> glands.

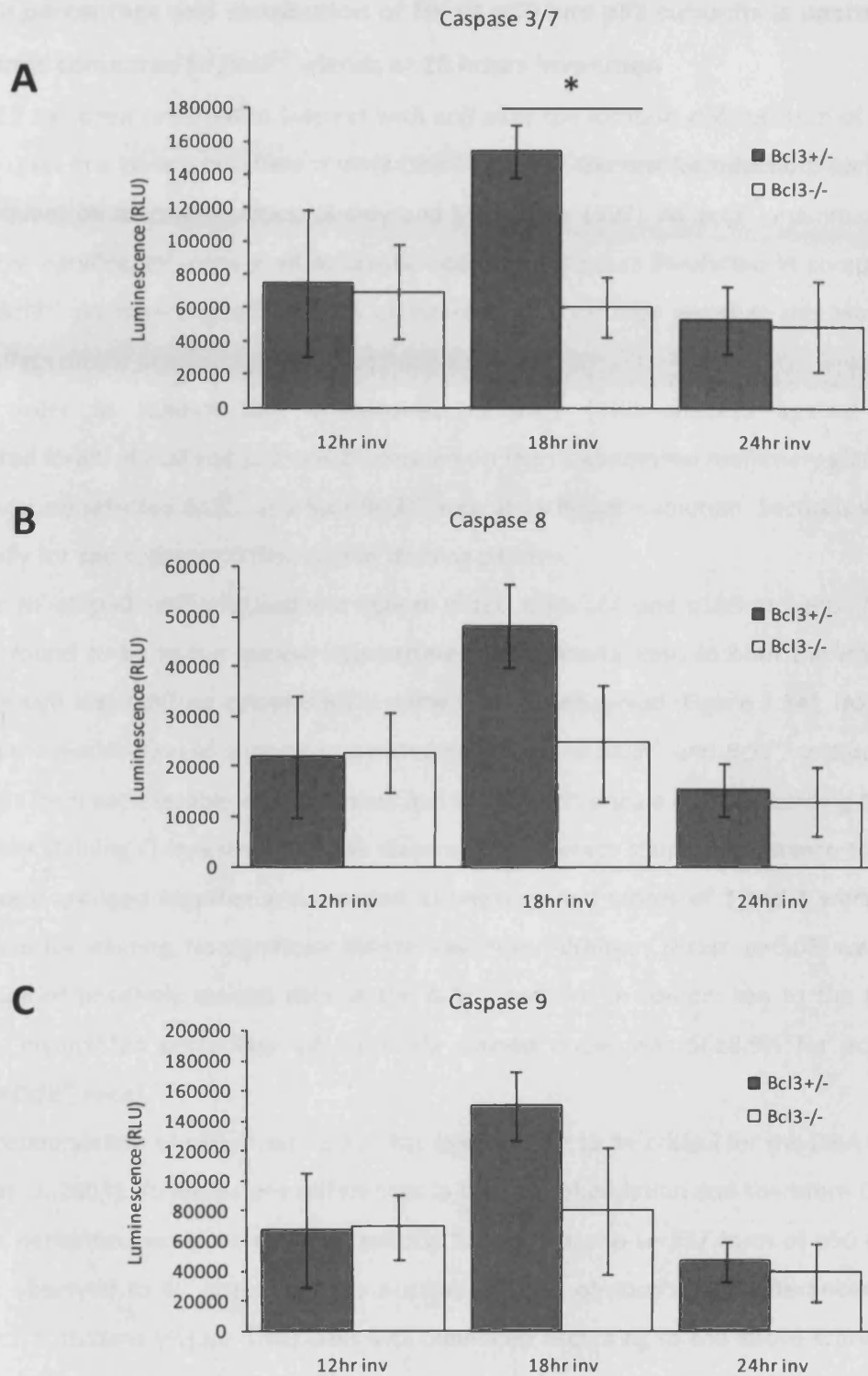


**Figure 3.8: *Bcl3*<sup>-/-</sup> mammary glands have significantly less caspase 3/7 activity than *Bcl3*<sup>+/-</sup> glands**  
 Whole protein extracts from *Bcl3*<sup>+/-</sup> and *Bcl3*<sup>-/-</sup> fourth abdominal mammary glands at 12, 18 and 24 hours involution (n=4) were prepared. Caspase 3/7, 8 and 9 assays were performed on all samples. No significant differences were observed in caspase 8 or 9 activity at any time point (Mann-Whitney U-test for all comparisons,  $p > 0.05$ ). *Bcl3*<sup>-/-</sup> mammary glands had significantly less caspase 3/7 activity than *Bcl3*<sup>+/-</sup> mammary glands at 18 hours involution (\*= Mann-Whitney U-test,  $p = 0.034$ ). No significant differences in caspase 3/7 activity were observed at 12 or 24 hours involution (Mann-Whitney U-test for all comparisons,  $p > 0.05$ ). Error bars represent  $\pm$  SEM.

### 3.2.6 The percentage and distribution of NF- $\kappa$ B p50 and p52 subunits is unaltered in *Bcl3*<sup>-/-</sup> glands compared to *Bcl3*<sup>+/-</sup> glands at 18 hours involution

BCL3 has been reported to interact with and alter the location and function of the NF- $\kappa$ B p50 and p52 sub-units in a variety of different ways (see Chapter 1: General Introduction, section 1.4.4) that can be dependent on its concentration (Bundy and McKeithan 1997). As *Bcl3*<sup>-/-</sup> mammary glands were shown to have significantly more shed apoptotic bodies at 18 hours involution in comparison to both *Bcl3*<sup>+/+</sup> and *Bcl3*<sup>+/-</sup> mammary glands, it was of interest to determine whether this was a BCL3-dose dependent effect on the distribution of p50 and p52 subunits.

In order to achieve this, Immunohistochemistry (IHC) directed against the total or phosphorylated forms of p50 and p52 was performed on fourth abdominal mammary glands taken from the four previously selected *Bcl3*<sup>+/-</sup> and four *Bcl3*<sup>-/-</sup> mice at 18 hours involution. Sections were examined microscopically for any apparent differences in staining pattern.

The NF- $\kappa$ B p50 antibody used was able to detect both p50 and p105 proteins. The majority of staining was found to be in the nuclear compartment of epithelial cells in both the *Bcl3*<sup>+/-</sup> and *Bcl3*<sup>-/-</sup> sections, although some diffuse cytoplasmic staining was also observed (Figure 3.9A). No obvious visual difference in the distribution of staining was noted between the *Bcl3*<sup>+/-</sup> and *Bcl3*<sup>-/-</sup> sections. To quantify this, 1000 cells from each sample were assessed and counted on a scale of 1-4 according to the intensity of their nuclear staining (1=negative, 2=weak staining, 3=moderate staining, 4=intense staining). Scores of 1 and 2 were grouped together and counted as negative and scores of 3 and 4 were grouped and counted as positive staining. No significant differences (Mann-Whitney U-test,  $p > 0.05$ ) were observed in the percentage of positively stained cells in the *Bcl3*<sup>+/-</sup> sections in comparison to the *Bcl3*<sup>-/-</sup> sections (Figure 3.9A, mean $\pm$ SEM percentage of positively stained nuclei was 56 $\pm$ 8.9% for *Bcl3*<sup>+/-</sup> mice and 55 $\pm$ 5.99% for *Bcl3*<sup>-/-</sup> mice).

Phosphorylation of p50 at serine 337 has been shown to be critical for the DNA binding of p50 (Hou, Guan et al. 2003). To assess any differences in the phosphorylation and therefore DNA binding of p50, IHC was performed using an antibody specific to the phospho-ser337 form of p50 (p-p50ser337). Staining was observed to be predominantly nuclear with no obvious visual differences between the *Bcl3*<sup>+/-</sup> and *Bcl3*<sup>-/-</sup> sections (Figure 3.9B). This was quantified according to the above scoring system and from this quantification no significant differences (Mann-Whitney U-test,  $p > 0.05$ ) in the percentage of positively stained cells between the *Bcl3*<sup>+/-</sup> and *Bcl3*<sup>-/-</sup> mammary glands were found (Figure 3.9B, mean $\pm$ SEM percentage of positively stained nuclei was 65.6 $\pm$ 7.699% for *Bcl3*<sup>+/-</sup> mice and 59.2 $\pm$ 19.9% for *Bcl3*<sup>-/-</sup> mice).

The NF- $\kappa$ B p52 antibody used detected both p52 and p100 proteins. The vast majority of staining observed with this antibody was found in the nuclear compartment of epithelial cells (Figure

3.10A) and no visual differences were observed between the *Bcl3*<sup>+/-</sup> and *Bcl3*<sup>-/-</sup> sections. Nuclear staining was quantified and this confirmed that there was no significant difference (Mann-Whitney U-test,  $p>0.05$ ) in the percentage of positively stained nuclei between the two cohorts (Figure 3.10A), mean $\pm$ SEM percentage of positively stained nuclei was 72.1 $\pm$ 15.7% for *Bcl3*<sup>+/-</sup> mice and 81.6 $\pm$ 5.63% for *Bcl3*<sup>-/-</sup> mice).

Phosphorylation of p52 at serine 222 has been shown to disrupt transcriptionally active p52 homodimer/BCL3 complexes and instead promote the formation of transcriptionally repressive p52/C-REL/HDAC1 complexes (Barre and Perkins 2010). IHC directed against serine 222 phosphorylated p52 was performed to determine whether there were any BCL3-dependent changes in this transcriptionally repressive form of p52. As with the pan-p52 antibody, the majority of staining was observed to be in the nucleus of the epithelial cells (Figure 3.10B) and no visual differences in the intensity or distribution of p-p52ser222 was observed between the *Bcl3*<sup>+/-</sup> and *Bcl3*<sup>-/-</sup> glands. Nuclear staining was quantified and this confirmed that there were no significant differences (Mann-Whitney U-test,  $p>0.05$ ) in the percentage of positively stained nuclei between the two cohorts (Figure 3.10B, mean $\pm$ SEM percentage of positively stained nuclei was 79.4 $\pm$ 21.2% for *Bcl3*<sup>+/-</sup> mice and 66.6 $\pm$ 13.95% for *Bcl3*<sup>+/-</sup> mice).

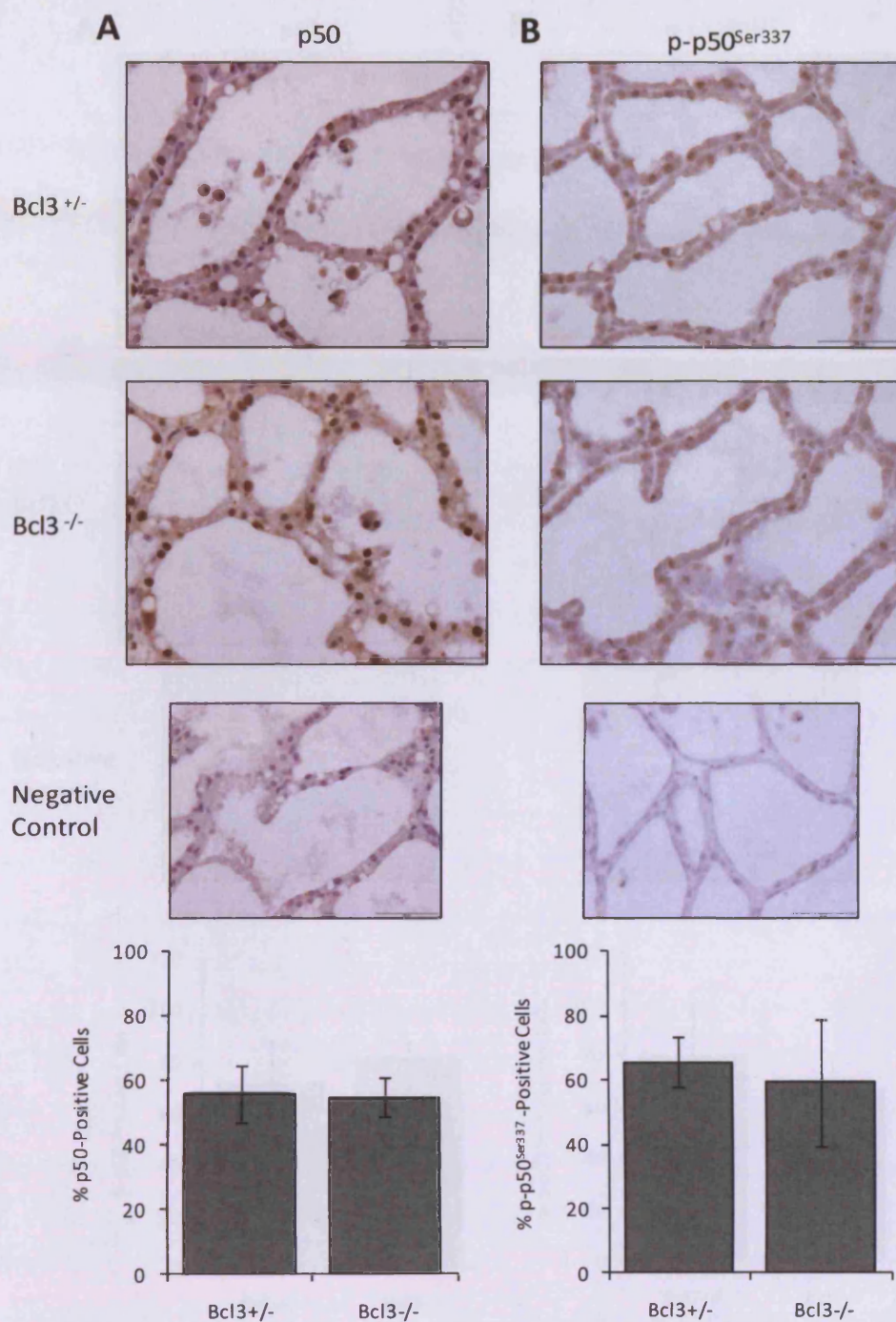


**Figure 3.9: The distribution and percentage of p50 and p-p50<sup>ser337</sup> positively stained epithelial cells is unchanged in Bcl3<sup>-/-</sup> glands compared to Bcl3<sup>+/-</sup> glands**

Fourth abdominal mammary glands from the 4 previously chosen Bcl3<sup>+/-</sup> and Bcl3<sup>-/-</sup> glands were harvested and subjected to p50 and p-p50<sup>ser337</sup> IHC. Representative images of p50 (A) and p-p50<sup>ser337</sup> (B) stained glands are shown along with negative controls. Scale bars indicate 50µm. p50 (A) and p-p50<sup>ser337</sup> (B) staining was predominately located in the nuclei but some diffuse cytoplasmic staining was also observed. No significant differences in the percentage of p50 (A) or p-p50<sup>ser337</sup> (B) positively stained nuclei were observed (Mann-Whitney U-test for both comparisons, p>0.05). Error bars represent ± SEM.

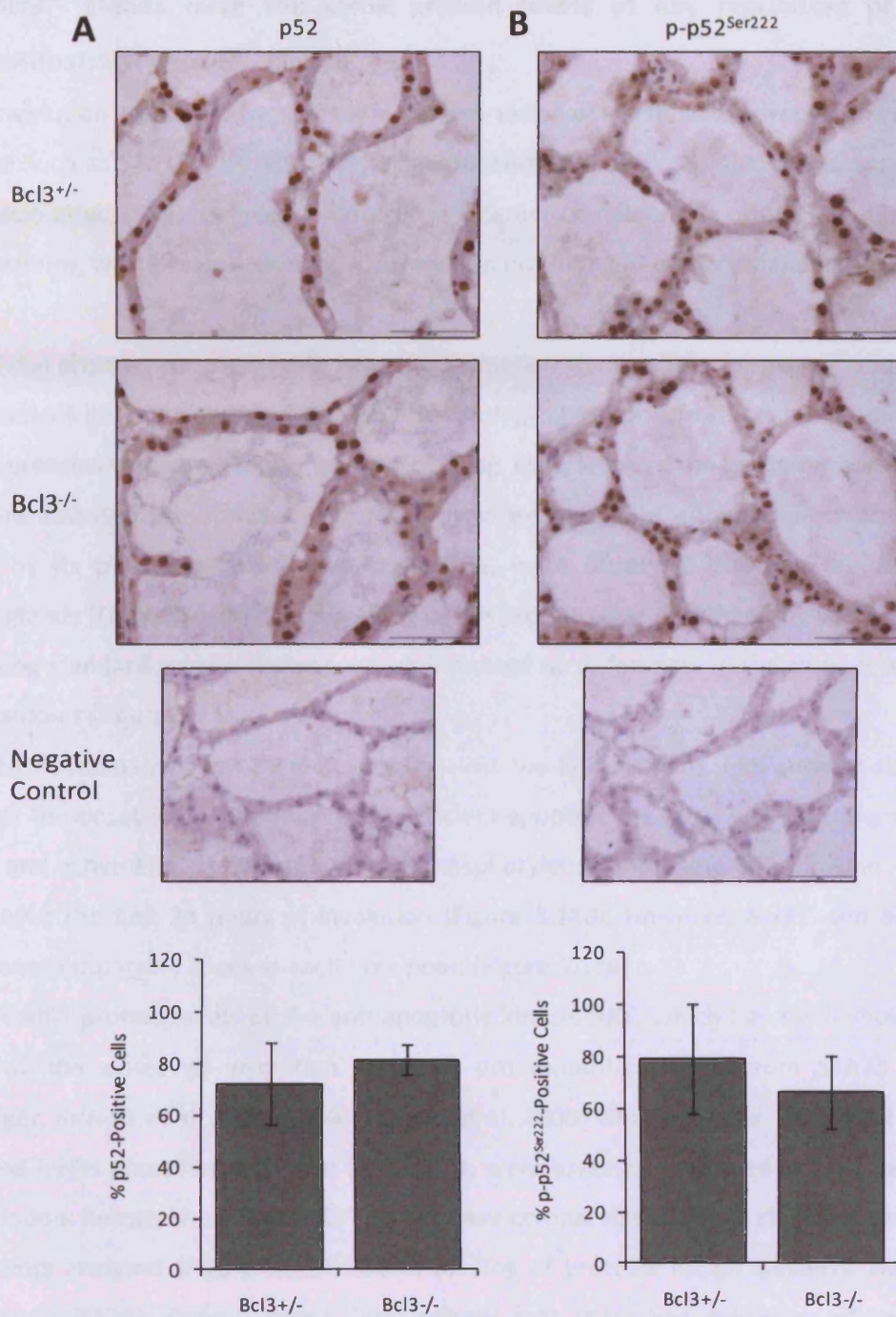


**Figure 3.10** The distribution and percentage of p52 and p-p52<sup>Ser222</sup> positively stained epithelial cells is unchanged in Bcl3<sup>-/-</sup> glands compared to Bcl3<sup>+/-</sup> glands

Fourth abdominal mammary glands from the 4 previously chosen Bcl3<sup>+/-</sup> and Bcl3<sup>-/-</sup> glands were harvested and subjected to p52 and p-p52<sup>Ser222</sup> IHC. Representative images of p52 (A) and p-p52<sup>Ser222</sup> (B) stained glands along with negative controls are shown. Scale bars indicate 50 $\mu$ m. p52 (A) and p-p52<sup>Ser222</sup> (B) staining was predominately located in the nuclei but some diffuse cytoplasmic staining was also observed. No significant differences in the percentage of p52 (A) or p-p52<sup>Ser222</sup> (B) positively stained nuclei were observed (Mann-Whitney U-test for both comparisons,  $p > 0.05$ ). Error bars represent  $\pm$  SEM.

### 3.2.7 *Bcl3*<sup>-/-</sup> glands have the same protein levels of key regulators of involution in comparison to *Bcl3*<sup>+/-</sup> glands

Involution is initiated by changes in the expression of key molecular regulators of apoptosis and cell survival such as STAT3, ERK and AKT (Chapman, Lourenco et al. 1999; Kritikou, Sharkey et al. 2003; Abell, Bilancio et al. 2005). In order to determine whether complete loss of BCL3 altered the expression of these proteins, western analysis was performed on involuting mammary glands from *Bcl3*<sup>+/-</sup> and *Bcl3*<sup>-/-</sup> mice.

Total proteins were extracted from the mammary glands of the four *Bcl3*<sup>+/-</sup> and four *Bcl3*<sup>-/-</sup> mice at 12, 18 and 24 hours involution. The individual biological samples from each time point were pooled and target proteins were analysed by western blotting. First, levels of the key initiator of early involution, STAT3, were assessed. No differences in the protein expression of either total or activated STAT3, as measured by its phosphorylation on tyrosine 705, were observed between the *Bcl3*<sup>+/-</sup> and *Bcl3*<sup>-/-</sup> mammary glands (Figure 3.11A). Equal loading of the proteins was confirmed by visualising levels of the housekeeping standard protein, Tubulin, which indicated no differences in the amount of protein loaded between samples (Figure 3.11A).

Western analysis was then directed against the ERK proteins. ERK survival signals are down-regulated at the onset of involution to allow efficient apoptosis to occur (Kritikou, Sharkey et al. 2003). Both total and active ERK, as measured by its phosphorylation threonine 202/tyrosine 204 were down-regulated over the first 24 hours of involution (Figure 3.11B). However, *Bcl3*<sup>+/-</sup> and *Bcl3*<sup>-/-</sup> mice were found to have comparable levels at each time point (Figure 3.11B).

Finally, protein levels of the anti-apoptotic kinase, AKT, which has been shown to be down-regulated at the onset of involution to allow pro-apoptotic signals from STAT3 to take effect (Schwertfeger, Richert et al. 2001; Abell, Bilancio et al. 2005) were analysed. Both total and active AKT, as measured by its phosphorylation on serine 473, were assessed in pooled samples at 12, 18 and 24 hours involution. Results show that *Bcl3*<sup>-/-</sup> glands have comparable AKT protein levels to *Bcl3*<sup>+/-</sup> glands at all time points analysed (Figure 3.11B). Equal loading of proteins for all westerns was confirmed by Tubulin (Figure 3.11B). Overall, these data indicate that these key mediators of involution remain unaltered in *Bcl3*<sup>-/-</sup> glands in comparison to *Bcl3*<sup>+/-</sup> glands.

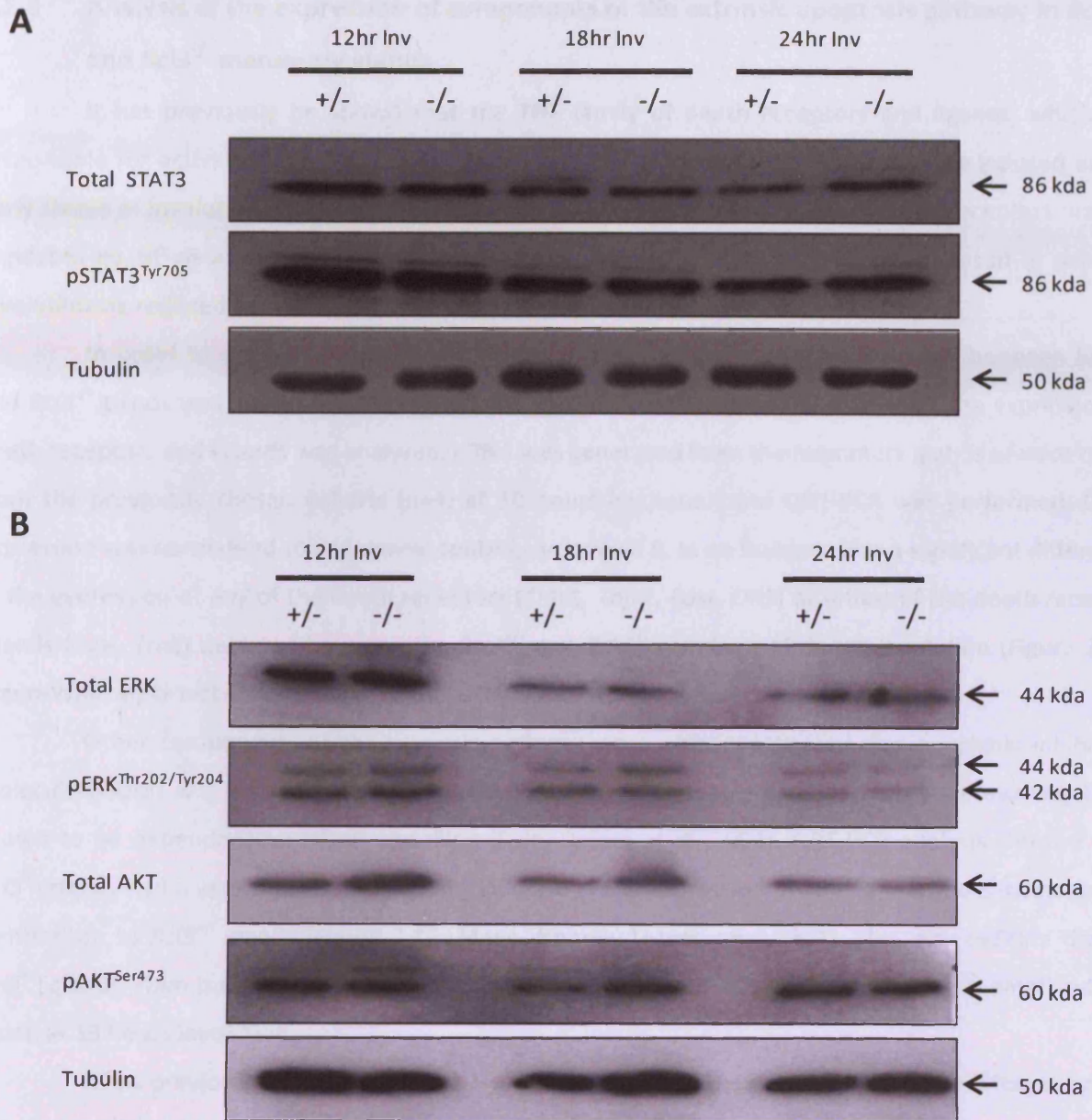


**Figure 3.11: *Bcl3*<sup>-/-</sup> glands exhibit comparable protein levels of key initiators of involution to *Bcl3*<sup>+/-</sup> glands**

Total protein extracts from four *Bcl3*<sup>+/-</sup> and four *Bcl3*<sup>-/-</sup> mammary glands at 12, 18 and 24 hours involution were pooled together and subjected to western analysis. No differences in total or phosphorylated STAT3 (A), ERK or AKT (B) protein levels were observed at any time-point analysed. Equal loading was confirmed by visualising levels of Tubulin.

### 3.2.8 Analysis of the expression of components of the extrinsic apoptosis pathway in *Bcl3<sup>+/-</sup>* and *Bcl3<sup>-/-</sup>* mammary glands

It has previously been shown that the TNF family of death receptors and ligands, which are responsible for activating the 5 principle mammalian extrinsic apoptosis pathways, are induced in the early stages of involution (Clarkson, Wayland et al. 2004). Furthermore, some of these receptors may be regulated by NF- $\kappa$ B as the absence of its up-stream regulator, IKK $\beta$ , was shown to result in delayed involution via reduced expression of death ligands (Baxter, Came et al. 2006).

In order to establish whether differences in the levels of apoptosis observed between *Bcl3<sup>+/-</sup>* and *Bcl3<sup>-/-</sup>* glands was due to BCL3-mediated changes in extrinsic apoptosis pathways, the expression of death receptors and ligands was analysed. cDNA was generated from the mammary glands of mice taken from the previously chosen cohorts (n=4) at 18 hours involution and QRT-PCR was performed. Gene expression was normalised to an internal control, *cyclophilin B*. In no instance was a significant difference in the expression of any of the death receptors (*Tnfr1*, *Tnfr2*, *Fasr*, *DR5*) or either of the death receptor ligands (*Fasl*, *Trail*) detected between the *Bcl3<sup>+/-</sup>* and *Bcl3<sup>-/-</sup>* glands at 18 hours involution (Figure 3.12, Mann-Whitney U-test for all comparisons,  $p > 0.05$ ).

Other components of the extrinsic pathway were also investigated. Fas apoptotic inhibitory molecule (FAIM) is a highly conserved antagonist of the FAS death receptor and has previously been shown to be dependent on NF- $\kappa$ B signalling (Sole, Dolcet et al. 2004). QRT-PCR analysis showed that *Bcl3<sup>-/-</sup>* glands had a very small but significant increase in the expression of *Faim* at 18 hours involution in comparison to *Bcl3<sup>+/-</sup>* glands (Figure 3.12, Mann-Whitney U-test,  $p = 0.0304$ ). This may indicate that in *Bcl3<sup>+/-</sup>* glands, *Faim* is down-regulated which allows for increased FAS signalling resulting in amplified cell death at 18 hours involution.

It has previously been shown that FAIM modulates FAS mediated apoptosis by influencing the expression of another antagonist of FAS signalling, C-FLIP, and in turn regulating the binding of caspase 8 to FAS (Huo, Xu et al. 2009). The expression of *c-flip* was therefore investigated in the presence or absence of BCL3 at 18 hours involution. No changes, however, were observed between the genotypes (Figure 3.12, Mann-Whitney U-test,  $p > 0.05$ ).

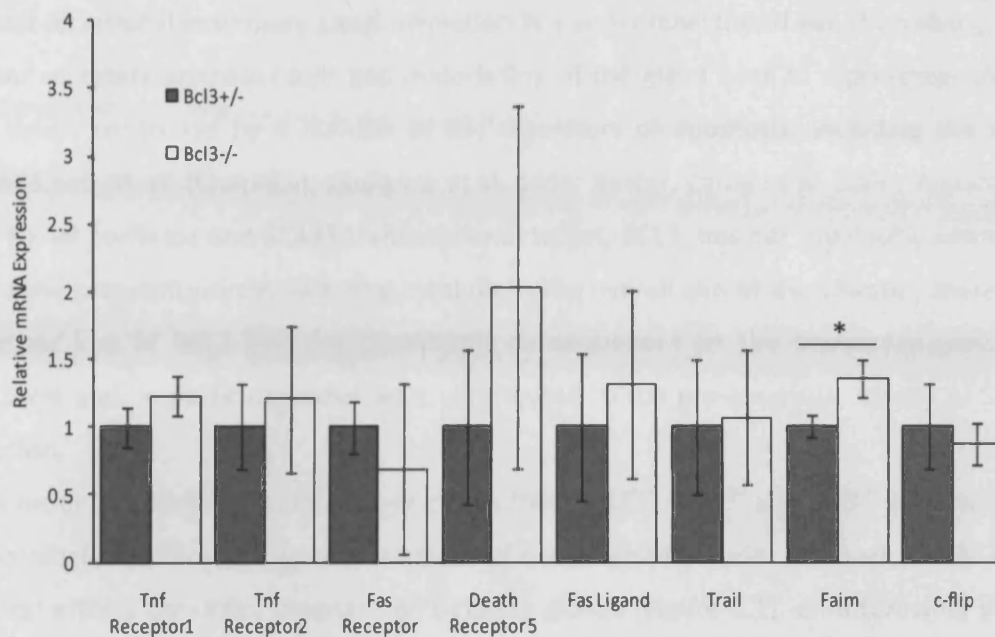


**Figure 3.12: *Bcl3*<sup>-/-</sup> mammary glands have significantly increased *Faim* expression in comparison to *Bcl3*<sup>+/-</sup> glands**

RNA was harvested from four *Bcl3*<sup>+/-</sup> and four *Bcl3*<sup>-/-</sup> mammary glands at 18 hours involution and subjected to QRT-PCR analysis directed against different components of the extrinsic apoptosis pathway. No significant differences were observed in any of the death receptors or ligands analysed (Mann-Whitney U-test for all comparisons,  $p > 0.05$ ). *c-flip* expression also remained unaltered (Mann-Whitney U-test,  $p > 0.05$ ). *Bcl3*<sup>-/-</sup> glands had significantly more *Faim* mRNA than *Bcl3*<sup>+/-</sup> glands (\* = Mann-Whitney U-test,  $p = 0.0304$ ). Data is represented as target gene mRNA expression relative to *cyclophilin B* mRNA expression. Error bars represent  $\pm$  SEM.

### 3.3 Discussion

Post-lactational mammary gland involution is a well orchestrated event involving the removal of redundant secretory epithelial cells and remodelling of the gland back to a pre-pregnant state. This process is tightly controlled by a number of key regulators of apoptosis, including the transcription factors, STAT3 and NF- $\kappa$ B (Chapman, Lourenco et al. 1999; Baxter, Came et al. 2006; Watson 2006). The role of the NF- $\kappa$ B co-factor and STAT3 transcriptional target, BCL3, has not previously been analysed at any stage of the pregnancy cycle, including involution. The overall aim of this chapter, therefore, was to assess whether loss of BCL3 had any phenotypic consequences on the mammary gland during the pregnancy cycle and, in particular, whether it contributed to the pro-apoptotic effects of STAT3 during early involution.

In order to address this, mammary glands from *Bcl3*<sup>+/+</sup>, *Bcl3*<sup>+/-</sup> and *Bcl3*<sup>-/-</sup> mice were examined for gross histological differences at various stages of the pregnancy cycle. Although loss of BCL3 had no morphological effects on virgin, pregnant or lactating glands (Figure 3.1), an interesting phenotype in which *Bcl3*<sup>+/-</sup> glands exhibited increased shed apoptotic bodies in comparison to both *Bcl3*<sup>-/-</sup> and *Bcl3*<sup>+/+</sup> glands at 18 hours involution was observed (Figure 3.3-3.5). To see a phenotype at this stage of the pregnancy cycle was not surprising as both this and a previous study have shown *Bcl3* to be transcriptionally up-regulated in early involution (Figure 3.2; Clarkson, Wayland et al. 2004). What was surprising, however, was to observe no difference between the *Bcl3*<sup>+/+</sup> and *Bcl3*<sup>-/-</sup> glands but to specifically identify a *Bcl3*<sup>+/-</sup> phenotype. One explanation for this could be that BCL3 is able to exert a very specific doseage-dependent effect on NF- $\kappa$ B subunit transcriptional activity. Indeed, previous studies have observed that BCL3 concentration can have a profound effect on the distribution and function of certain NF- $\kappa$ B complexes. For example, Bundy et al. (1997) demonstrated that the ratio of BCL3 to p52 was fundamental in determining the binding of p52 homodimers to DNA. More recently, down-regulation of BCL3 in H1299 human lung carcinoma cells was shown to result in a shift from p52 homodimer/BCL3 transactivating complexes to p52 homodimer/HDAC1 repressive complexes (Rocha, Martin et al. 2003). It is possible, therefore, that intermediate concentrations of BCL3, as a result of heterozygosity, could subtly alter the ratio of transactivating to inhibitory NF- $\kappa$ B complexes in such a way as to transiently promote apoptosis to an extent that isn't observed in glands that are either completely devoid of BCL3 or wild-type for BCL3.

Having identified this phenotype, it was of interest to establish whether it correlated with any BCL3-dependent changes at the molecular level. Firstly, in order to identify any changes in the distribution or phosphorylation of p50 and p52, IHC using antibodies directed against these NF- $\kappa$ B subunits was performed in *Bcl3*<sup>+/-</sup> and *Bcl3*<sup>-/-</sup> glands at 18 hours involution. No differences in the cellular distribution or phosphorylation status of either subunit were observed (Figure 3.9-10). IHC is, at best,

only a semi-quantitative method to analyse protein expression and so very subtle changes in the quantity of protein present are unlikely to be identified. Furthermore, BCL3 primarily acts to alter the transcriptional function of p50 and p52 homodimers. While the use of antibodies targeting phosphorylated forms of proteins can potentially identify the DNA binding ability of the subunits, they cannot determine which complexes are being formed and whether they are transactivating or inhibitory. To address this in the future, more precise experiments such as Co-IP and ChIP would need to be performed.

The increase in apoptotic bodies observed in *Bcl3*<sup>+/-</sup> glands at 18 hours involution correlated with a significant increase in caspase 3/7 activity and a trend towards an increase in caspase 8 and caspase 9 activity (Figure 3.8). Caspases have previously been shown to be involved in mediating epithelial cell apoptosis during mammary gland involution (Marti, Ritter et al. 2001) although a recent study suggests that this may be a redundant mechanism (Kreuzaler, Staniszewska et al. 2011). Activation of the caspase cascade occurs via either the intrinsic or extrinsic pathway. Caspase 3/7 is an effector caspase that conducts the overall execution of apoptosis via cleavage of a wide range of substrates, whereas caspase 8 and caspase 9 are upstream mediators of the extrinsic or intrinsic pathway respectively (reviewed in Jin and El-Deiry 2005). The observed increase in caspase 3/7 activity in the *Bcl3*<sup>+/-</sup> glands is not surprising as an increase in apoptotic bodies had already been identified in glands from the same mice. Therefore, rather than identifying a direct mechanism by which *Bcl3*<sup>+/-</sup> glands displayed enhanced apoptosis, the correlation in these results serves to confirm that the shed epithelial cells are, in fact, apoptotic.

Both the intrinsic and extrinsic apoptosis pathways have been implicated in mammary involution (Schorr, Li et al. 1999; Walton, Wagner et al. 2001; Baxter, Came et al. 2006). As NF- $\kappa$ B has specifically been shown to promote mammary epithelial cell apoptosis via death receptor signalling involving the extrinsic pathway (Baxter, Came et al. 2006), it was of interest to determine whether the increased apoptosis observed in *Bcl3*<sup>+/-</sup> glands, was also due to alterations in this pathway. However, as results from caspase 8 and 9 assays did not reach significance (Figure 3.8B&C), it is difficult to determine which apoptosis pathway was being up-regulated. Nevertheless, an insignificant trend towards an increase in the activity of both caspases was observed, suggesting that both pathways are up-regulated to induce apoptosis in the *Bcl3*<sup>+/-</sup> glands. Larger cohorts would be required to make a more definite conclusion on this.

*Bcl3*<sup>+/-</sup> and *Bcl3*<sup>-/-</sup> glands had similar total and phosphorylated protein levels of the key regulators of mammary gland involution, AKT, STAT3 and ERK, suggesting that these pathways are unaffected by the different concentrations of BCL3. Furthermore, even though NF- $\kappa$ B has previously been shown to promote apoptosis via increased death receptor signalling (Baxter, Came et al. 2006), no

differences in the expression of these receptors or their ligands were identified. However, *Bcl3*<sup>+/-</sup> glands did express significantly lower levels of *Faim* mRNA than *Bcl3*<sup>-/-</sup> glands at 18 hours involution (Figure 3.12). FAIM is known to antagonise FAS signalling in a variety of tissues (Sole, Dolcet et al. 2004; Choi, Reimers et al. 2007) and has been implicated in mediating resistance to FAS-induced cell death (reviewed in Rothstein 2000). Previous studies have shown that FAS signalling is fundamental in early involution as mice lacking FAS or FAS ligand display delayed involution (Song, Sapi et al. 2000). Increased FAS signalling mediated by the down-regulation of *Faim* may reflect a mechanism by which *Bcl3*<sup>+/-</sup> glands display a transient increase in apoptosis at 18 hours involution. This conclusion, however, must be viewed with some caution as the observed increase in *Faim* expression was very subtle.

### 3.3.1 Summary

Overall, the data from this chapter identified a heterozygous phenotype whereby *Bcl3*<sup>+/-</sup> glands display a transient increase in apoptotic bodies at 18 hours involution in comparison to both *Bcl3*<sup>+/+</sup> and *Bcl3*<sup>-/-</sup> glands. However, this did not correlate with any outstanding differences at the molecular level which may indicate that the molecular mechanism responsible for this phenotype has not been identified. However, it could also bring into question whether the observed phenotype is real or in fact due to small cohort numbers and large biological variation. This may need to be addressed in the future with larger cohorts of animals.

BCL3 was originally identified as a proto-oncogene in B-cell chronic lymphocytic leukaemia (Ohno, Takimoto et al. 1990) and has since been implicated in a number of other malignancies including breast cancer (Cogswell, Guttridge et al. 2000; Thornburg, Pathmanathan et al. 2003; Mathas, Johrens et al. 2005; Mishra, Bharti et al. 2006). The observation that loss of BCL3 had no gross effects at any stage of the pregnancy cycle is on one level disappointing. Nevertheless, it does indicate that it may potentially be an excellent therapeutic target in breast cancer as inhibition should have no detrimental side-effects on normal mammary tissue, which is a primary aim in cancer therapy. However, in order to establish whether this NF- $\kappa$ B co-factor is a *bone fide* therapeutic target in breast cancer, its function and mechanism of action in the disease must be investigated to beyond what is already known in the literature. This will therefore be the primary focus of the following three chapters of this thesis.

**Chapter 4:**  
**Analysis of BCL3 Deficiency in Two *Neu***  
**Transgenic Mouse Models**

## 4.1 Introduction

The NF- $\kappa$ B family of transcription factors has previously been shown to be elevated in many malignant diseases including breast cancer (Bargou, Emmerich et al. 1997; Cogswell, Guttridge et al. 2000; Sovak, Bellas et al. 1997; Suh, Payvandi et al. 2002; Nair, Venkatraman et al. 2003; Abdel-Latif, O'Riordan et al. 2004; Kojima, Morisaki et al. 2004). NF- $\kappa$ B activation is strongly associated with signalling downstream of the EGF family of receptors (EGFR), in both aggressive EGFR-positive, ER-negative (Biswas, Cruz et al. 2000) and ERBB2-positive, ER-negative breast cancer subtypes (Biswas, Shi et al. 2004).

ERBB2 is over-expressed in approximately 20% of breast cancers (Paik, Hazan et al. 1990). These tumours are a clinically aggressive subtype of breast cancer resulting in poor prognosis and an increased incidence of metastases. Current therapy for ERBB2-positive breast cancer involves the use of receptor-targeted drugs such as the humanised monoclonal antibody, trastuzumab (Herceptin), which, in combination with chemotherapy, can delay disease progression in patients with metastatic disease (Slamon, Leyland-Jones et al. 2001; Viani, Afonso et al. 2007). However, owing to prevalent *de novo* and acquired resistance mechanisms, relapse is common (Cobleigh, Vogel et al. 1999; Vogel, Cobleigh et al. 2002; reviewed in Nahta and Esteva 2006). Therefore, there is still a clinical need to identify new or synergistic therapeutic molecular targets for ERBB2-positive breast cancer and to identify mechanisms for suppressing disease progression in this patient group with poor prognosis.

The potential for NF- $\kappa$ B as a new therapeutic target in these aggressive forms of breast cancer has been highlighted by a number of studies in the literature (Helbig, Christopherson et al. 2003; Aggarwal, Shishodia et al. 2005; Cao, Luo et al. 2007; Park, Zhang et al. 2007). For example, inhibition of NF- $\kappa$ B by genetic modification of IKK $\alpha$ , a common upstream regulator of NF- $\kappa$ B activity, resulted in reduced tumourigenesis in an *in vivo* mouse model of ERBB2-positive breast cancer (Cao, Luo et al. 2007). Furthermore, numerous reports implicating NF- $\kappa$ B in the aetiology of metastasis in a variety of cancer cell types have been published (Rehman and Wang 2009; Fritz and Radziwill 2010; Gavert, Ben-Shmuel et al. 2010; Hernandez, Hsu et al. 2010; Yan, Xu et al. 2010; Li, Li et al. 2009). In breast cancer, NF- $\kappa$ B regulates pro-metastatic genes (Helbig, Christopherson et al. 2003; Park, Zhang et al. 2007), and it has also been shown to have a direct effect on metastasis in *in vivo* mouse models (Aggarwal, Shishodia et al. 2005; Aggarwal, Ichikawa et al. 2006; Park, Zhang et al. 2007).

Although this has led to much interest in the use of NF- $\kappa$ B inhibitors to suppress tumour progression in cancer patients (reviewed in Haffner, Berlato et al. 2006; Shen and Tergaonkar 2009) there are significant risks associated with sustained global inhibition of NF- $\kappa$ B signalling, as this would have profound effects on normal tissues, particularly on cells of the immune system. An alternative

strategy might therefore be to target modifying NF- $\kappa$ B co-factors, such as BCL3 that could potentially be more selective in their inhibitory actions.

BCL3 has previously been shown to be a proto-oncogene, originally identified on the basis of its high transcript expression in some patients with B-cell chronic lymphocytic leukaemia (Ohno, Takimoto et al. 1990). It has since been implicated in a number of other human malignancies including breast cancer (Cogswell, Guttridge et al. 2000; Thornburg, Pathmanathan et al. 2003; Mathas, Johrens et al. 2005; Mishra, Bharti et al. 2006). Interestingly, results from chapter 3 demonstrated that loss of BCL3 has no marked physiological effects on murine mammary gland development or progression through the pregnancy cycle, even in the early stages of involution when it is highly expressed; suggesting that therapeutic modulation of this NF- $\kappa$ B co-factor would not be detrimental to normal mammary tissues.

To date, no *in vivo* studies aimed at specifically assessing the effects of BCL3 modulation on ERBB2-driven tumourigenesis exist. In view of this, the overall aim of this chapter was to assess the potential role of BCL3 in two transgenic ERBB2-positive mouse models of breast cancer. The effects of BCL3 deletion on both tumour initiation and progression will be characterised.

## 4.2 Results

### 4.2.1 BCL3 deficiency significantly delays the onset of *MMTV/N<sub>2</sub>* but not *MMTV/NK* mammary adenocarcinomas

In order to establish the effects of BCL3 deficiency in the context of susceptibility to ERBB2-positive mammary tumours, BCL3-deficient mice (Schwarz, Krimpenfort et al. 1997) were crossed with mice over-expressing either the wild-type (*MMTV/N<sub>2</sub>*) (Guy, Webster et al. 1992) or the activated (*MMTV/NK*) (Muller, Sinn et al. 1988) rat *Neu* transgene to generate cohorts of female littermates of all genotype combinations. Mice were routinely taken through one pregnancy at 6-8 weeks of age to ensure high expression of the *MMTV* promoter. Cohorts were monitored for changes in mammary epithelial morphology and were inspected for the occurrence of palpable mammary tumours twice weekly. Kaplan-Meier analysis was performed to determine tumour-free survival times.

Initially, the effect of BCL3 deficiency on the formation of *MMTV/NK* adenocarcinomas was assessed. Mice from all three cohorts developed multifocal solid adenocarcinomas involving the majority of the mammary gland that were histologically identical to each other (Figure 3.4B). Analysis of tumour-free survival times showed that BCL3 deficiency had no significant effect on tumour latency in this mouse model (Figure 4.1A). *Bcl3<sup>+/+</sup>/MMTV/NK* and *Bcl3<sup>-/-</sup>/MMTV/NK* mice acquired mammary tumours with mean onset ages (T50) of 165 and 163 days, respectively, while *Bcl3<sup>-/-</sup>/MMTV/NK* mice had a small but insignificantly reduced rate of tumourigenesis (T50=179 days, Kaplan-Meier analysis, *Bcl3<sup>+/+</sup>/MMTV/NK* vs *Bcl3<sup>-/-</sup>/MMTV/NK*:  $p=0.3453$ ,  $\chi^2=0.8905$ , DF=1). As expected, *Bcl3<sup>-/-</sup>* mice lacking the *MMTV/NK* transgene did not acquire tumours.

It is well established that the activated NEU protein can act as an extremely potent oncogene in the mammary gland. However, no equivalent activating mutations in primary human ERBB2-positive breast cancer have been discovered (Lemoine, Staddon et al. 1990). It was therefore of interest to analyse BCL3 deficiency in the more clinically relevant, wild-type *Neu* over-expressing, *MMTV/N<sub>2</sub>* model. Results show that *Bcl3<sup>-/-</sup>/MMTV/N<sub>2</sub>* mice developed unifocal, solid adenocarcinomas that were histologically identical to those formed in *Bcl3<sup>+/+</sup>/MMTV/N<sub>2</sub>* and *Bcl3<sup>+/-</sup>/MMTV/N<sub>2</sub>* mice (Figure 4.2B). However, unlike in the *MMTV/NK* model, analysis of tumour-free survival times revealed that deletion of each *Bcl3* allele caused incremental delays in the formation of spontaneous tumours (Figure 4.2A). Mice expressing both alleles of *Bcl3* on the *MMTV/N<sub>2</sub>* background (*Bcl3<sup>+/+</sup>/MMTV/N<sub>2</sub>*) acquired mammary tumours with a mean onset age (T50) of 176 days. Deletion of a single *Bcl3* allele (*Bcl3<sup>+/-</sup>/MMTV/N<sub>2</sub>*) significantly reduced the rate of tumourigenesis to T50=214 days (Kaplan-Meier analysis,  $p=0.033$ ,  $\chi^2=4.53$ , DF=1), while deletion of both alleles (*Bcl3<sup>-/-</sup>/MMTV/N<sub>2</sub>*) further delayed the formation of neoplasias to T50=255 days (Kaplan-Meier analysis,  $p=0.0001$ ,  $\chi^2=15.22$ , DF=1).

These data indicate that depletion of BCL3 is able to suppress tumourigenesis in the clinically relevant wild-type *Neu* over-expressing (*MMTV/N<sub>2</sub>*) model, whereas it has no effect on the latency of tumours driven by the activated *Neu* (*MMTV/NK*) transgene.

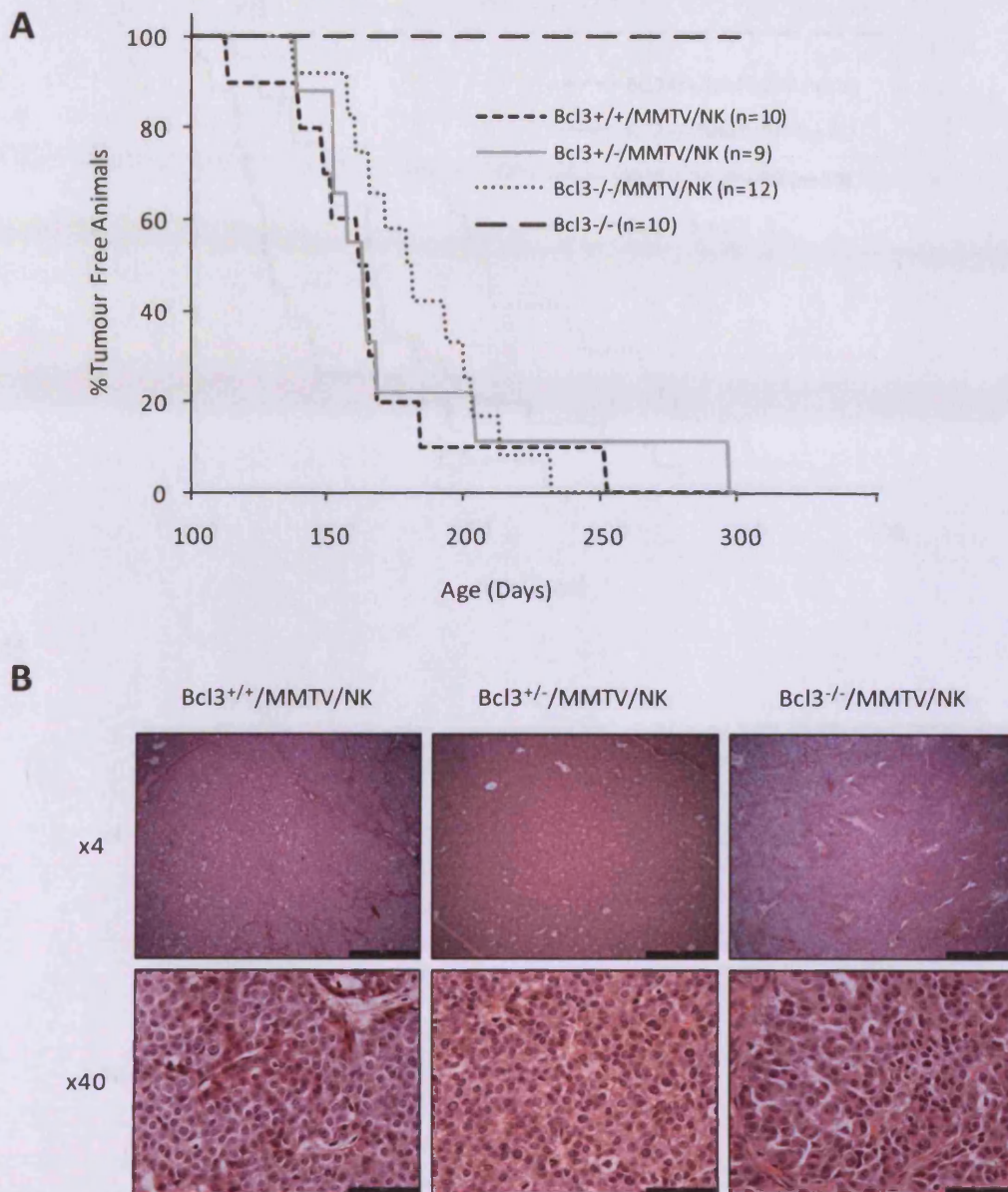


**Figure 4.1: Loss of BCL3 has no effect on the latency or histology of MMTV/NK induced mammary adenocarcinomas**

Mice from all cohorts were inspected twice weekly for the formation of mammary adenocarcinomas. No statistically significant differences were observed between any cohorts bearing the *MMTV/NK* transgene (A, Kaplan-Meier analysis for all comparisons,  $p > 0.05$ ). H&E sections revealed that mice from all three cohorts developed solid adenocarcinomas that were histologically similar to each other (B). Scale bars: top row=500 $\mu$ m, bottom row=50 $\mu$ m.

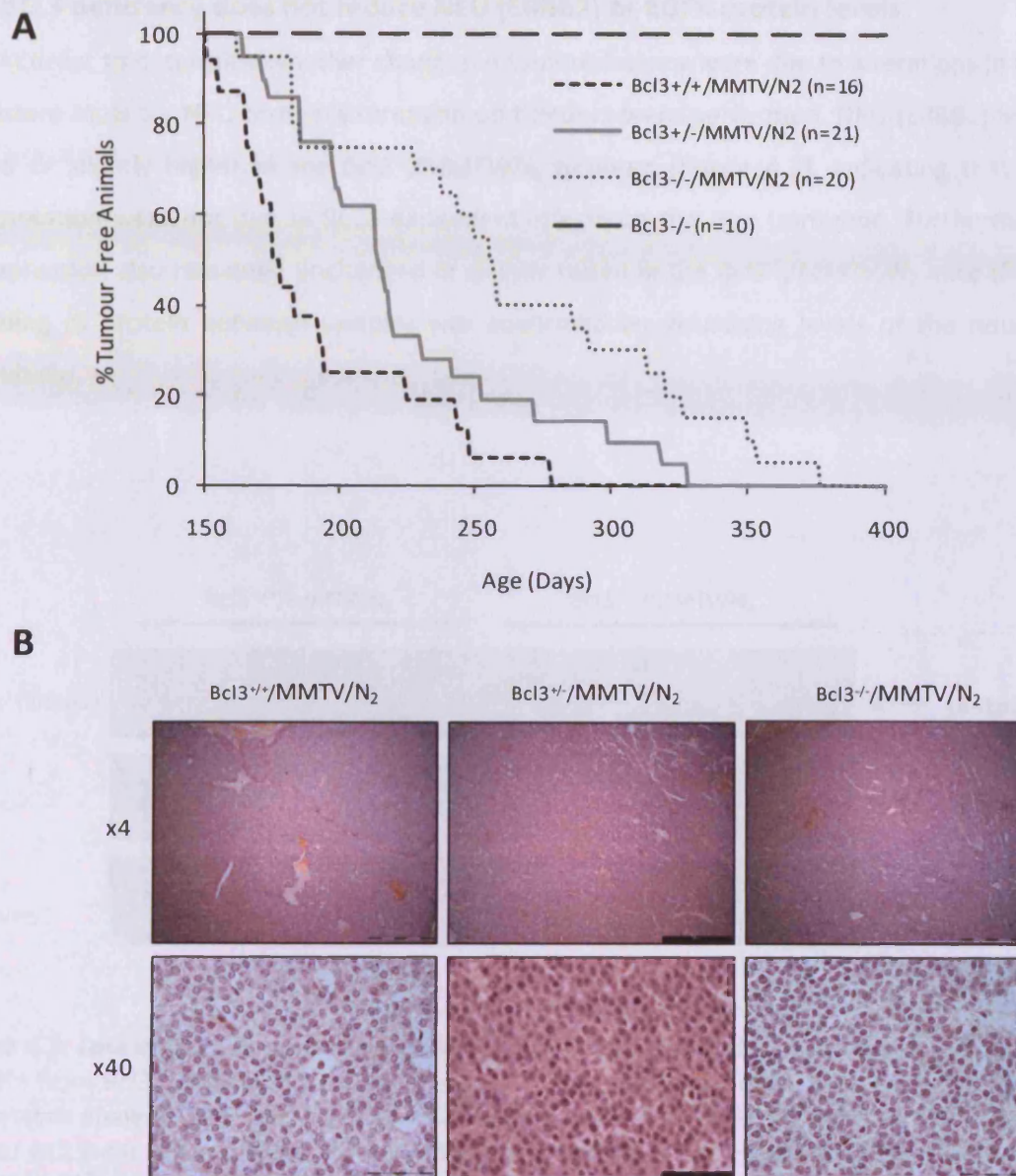


**Figure 4.2: Loss of BCL3 results in the delayed onset of MMTV/N<sub>2</sub> mammary adenocarcinomas**

Mice from all cohorts were inspected twice weekly for the formation of mammary adenocarcinomas. Deletion of each *Bcl3* allele resulted in incremental delays in tumour formation (A, Kaplan-Meier analysis *Bcl3*<sup>+/-</sup>/MMTV/N<sub>2</sub> vs *Bcl3*<sup>+/+</sup>/MMTV/N<sub>2</sub>,  $p=0.033$  and *Bcl3*<sup>-/-</sup>/MMTV/N<sub>2</sub> vs *Bcl3*<sup>+/+</sup>/MMTV/N<sub>2</sub>,  $p=0.0001$ ). H&E sections revealed that mice from all three cohorts developed solid adenocarcinomas that were histologically similar to each other (B). Scale bars: top row=500 $\mu$ m, bottom row=50 $\mu$ m.

#### 4.2.2 BCL3 deficiency does not reduce NEU (ERBB2) or EGFR protein levels

In order to determine whether changes in tumour latency were due to alterations in transgene levels, western blots for NEU protein expression on tumours were performed. NEU (ERBB2) levels were unchanged or slightly higher in the *Bcl3*<sup>-/-</sup>/MMTV/N<sub>2</sub> tumours (Figure 4.3), indicating that delays in tumour formation were not due to BCL3-dependent effects on the *Neu* transgene. Furthermore, EGFR protein expression also remained unchanged or slightly raised in the *Bcl3*<sup>-/-</sup>/MMTV/N<sub>2</sub> mice (Figure 4.3). Equal loading of protein between samples was confirmed by visualising levels of the housekeeping protein, Tubulin.

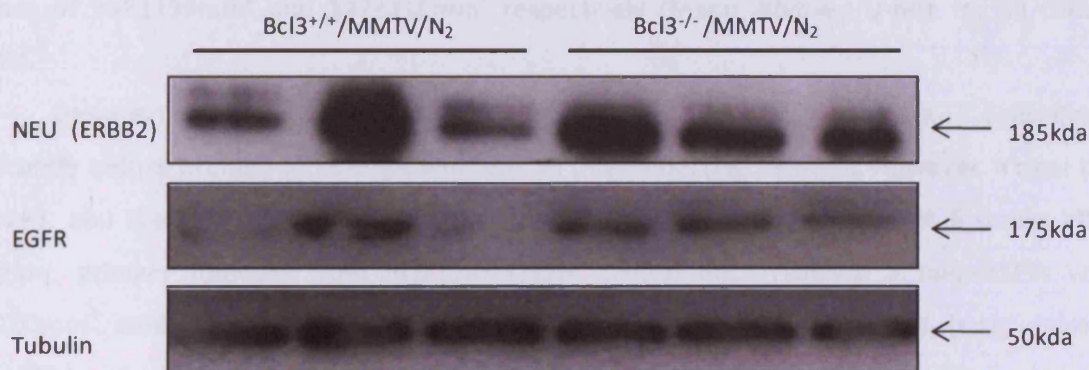


**Figure 4.3: Loss of BCL3 does not reduce NEU or EGFR protein levels**

Protein from *Bcl3*<sup>+/+</sup>/MMTV/N<sub>2</sub> and *Bcl3*<sup>-/-</sup>/MMTV/N<sub>2</sub> tumours was extracted and subjected to western analysis. NEU and EGFR protein expression was variable between tumours but loss of BCL3 did not correlate with a reduction in the levels of either of these proteins. Equal loading was confirmed by Tubulin.

### 4.2.3 BCL3 depletion has no effect on tumour growth rates in *MMTV/N<sub>2</sub>* or *MMTV/NK* mice

To directly assess the effects of BCL3 deletion on the growth rates of mammary tumours in *MMTV/N<sub>2</sub>* and *MMTV/NK* mice, tumours were measured twice weekly as described in Materials and Methods. Mean primary tumour volumes within each cohort were plotted against time to generate growth curves representing the mean primary tumour growth rate. Graphs represent growth curves up to the point when the first animals within any cohort had to be culled because of licensing tumour size restrictions.

In the *MMTV/NK* mice, no significant differences in primary tumour growth rates were detected between genotypes at any time-point (Figure 4.4A). At 4 weeks after initial detection, primary tumours from *Bcl3<sup>-/-</sup>/MMTV/NK* (n=13) mice reached a mean±SEM tumour volume of 390±133 mm<sup>3</sup>, while tumours from *Bcl3<sup>+/-</sup>/MMTV/NK* (n=10) and *Bcl3<sup>+/+</sup>/MMTV/NK* (n=8) mice reached mean±SEM volumes of 398±159mm<sup>3</sup> and 347±110mm<sup>3</sup> respectively (Mann-Whitney U-test for all comparisons, p>0.05).

Despite the striking effect on tumour latency in the *MMTV/N<sub>2</sub>* mice, BCL3 deficiency did not significantly reduce primary tumour growth rates in this model (Figure 4.4B). However, a clear trend was observed, and the lack of significance was due to large biological variation. At 6 weeks after initial detection, primary tumours from *Bcl3<sup>-/-</sup>/MMTV/N<sub>2</sub>* (n=20) mice reached a mean±SEM volume of 266±100mm<sup>3</sup>, while tumours from *Bcl3<sup>+/-</sup>/MMTV/N<sub>2</sub>* (n=21) and *Bcl3<sup>+/+</sup>/MMTV/N<sub>2</sub>* (n=16) mice reached mean±SEM volumes of 479±110mm<sup>3</sup> and 454±116mm<sup>3</sup>, respectively (Mann-Whitney U-test for all comparisons, p>0.05).

Taken together with previous results, these data suggest that BCL3 deficiency primarily affects tumour initiation rather than growth rates of established lesions.

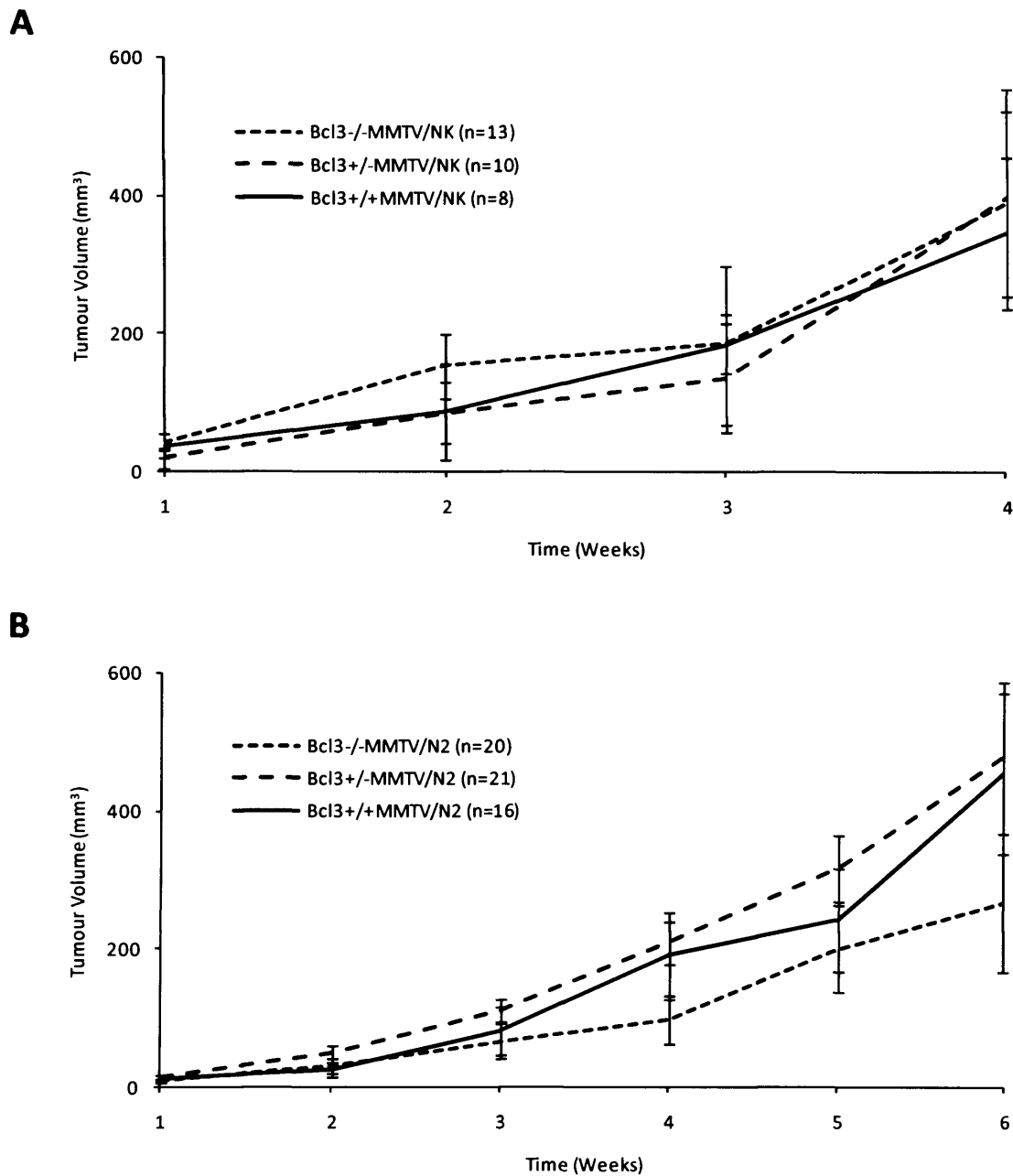


**Figure 4.4: Loss of BCL3 has no effect on the growth rates of MMTV/N<sub>2</sub> or MMTV/NK mammary adenocarcinomas**

Tumour growth was assessed by measuring tumours twice weekly. No significant differences in tumour volume were observed between cohorts carrying the MMTV/NK (A) or MMTV/N<sub>2</sub> (B) transgene at any time point (Mann-Whitney U-test for all comparisons,  $p > 0.05$ ). Error bars represent  $\pm$  SEM.

#### 4.2.4 BCL3 deficiency does not reduce tumour burden in *MMTV/N<sub>2</sub>* or *MMTV/NK* mice

At dissection (performed when primary tumours reached a size of  $500 \pm 13.5 \text{mm}^3$ ) all mammary glands from all experimental and control mice were carefully inspected macroscopically for the presence of tumours, and the mean number of tumours per mouse was calculated. Tumours were defined as any lesion greater than  $13.5 \text{mm}^3$ .

As expected, the tumour burden of mice expressing the *MMTV/NK* transgene was higher than those expressing the *MMTV/N<sub>2</sub>* transgene (Figure 4.5A compared to Figure 4.5C). In the *MMTV/NK* model, no significant differences in tumour burden were identified between cohorts (Figure 4.5A, mean  $\pm$  SEM number of tumours per animal was  $3.5 \pm 0.6$  for *Bcl3<sup>+/+</sup>/MMTV/NK* animals (n=12),  $4.6 \pm 1.3$  for *Bcl3<sup>+/-</sup>/MMTV/NK* animals (n=5), and  $4.5 \pm 2.5$  for *Bcl3<sup>-/-</sup>/MMTV/NK* animals (n=8); Mann-Whitney U-test for all comparison,  $p > 0.05$ ). BCL3 deficiency also did not result in a reduction in the percentage of mice with unifocal tumours (Figure 4.5B, percentage of mice with unifocal tumours was 12.5% for *Bcl3<sup>+/+</sup>/MMTV/NK* animals [n=12], 20% for *Bcl3<sup>+/-</sup>/MMTV/NK* animals [n=5], and 21.43% for *Bcl3<sup>-/-</sup>/MMTV/NK* animals [n=8]).

Similarly, despite the previously observed effect on primary tumour initiation in the *MMTV/N<sub>2</sub>* mice, BCL3 deficiency had no significant effect on overall tumour burden in this model (Figure 4.5C, mean  $\pm$  SEM number of tumours per animal was  $2.2 \pm 0.65$  for *Bcl3<sup>+/+</sup>/MMTV/N<sub>2</sub>* animals [n=5],  $1.8 \pm 0.37$  for *Bcl3<sup>+/-</sup>/MMTV/N<sub>2</sub>* animals [n=13], and  $1.78 \pm 0.24$  for *Bcl3<sup>-/-</sup>/MMTV/N<sub>2</sub>* animals [n=9]; Mann-Whitney U-test for all comparisons,  $p > 0.05$ ). As expected, the percentage of mice with unifocal tumours was higher in the *MMTV/N<sub>2</sub>*-expressing animals than those expressing the *MMTV/NK* transgene (Figure 4.5D compared with Figure 4.5B). However, BCL3 deficiency did not affect this, with *Bcl3<sup>+/+</sup>/MMTV/N<sub>2</sub>* animals having 40% unifocal tumours and *Bcl3<sup>+/-</sup>/MMTV/N<sub>2</sub>* and *Bcl3<sup>-/-</sup>/MMTV/N<sub>2</sub>* having 53.8% and 33.33%, respectively (Figure 4.5D).

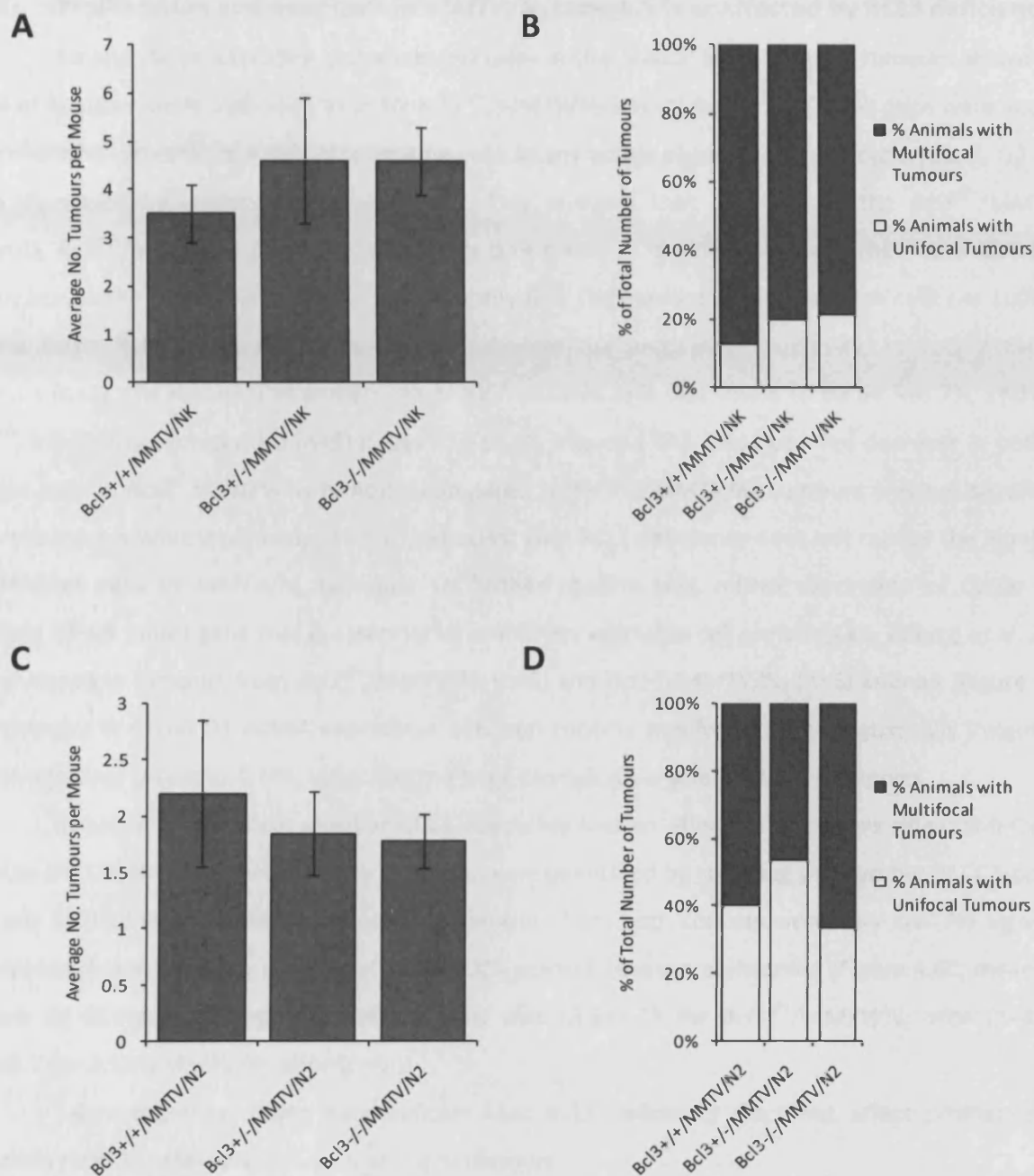


**Figure 4.5: BCL3 deficiency has no effect on the tumour burden of MMTV/NK or MMTV/N<sub>2</sub> mice**  
 The average number of tumours per mouse at sacrifice was assessed. BCL3 deficiency had no effect on the overall tumour burden in either the MMTV/NK (A) or MMTV/N<sub>2</sub> (C) mice (Mann-Whitney U-test for all comparisons,  $p > 0.05$ ). MMTV/N<sub>2</sub> mice had a higher proportion of unifocal tumours than MMTV/NK mice (B vs D). BCL3 deficiency had no clear effects on the percentage of animals with unifocal tumours in either the MMTV/NK (B) or MMTV/N<sub>2</sub> (D) models. Error bars represent  $\pm$  SEM.

#### 4.2.5 Proliferation and apoptosis in *MMTV/N<sub>2</sub>* tumours is unaffected by BCL3 deficiency

To analyse proliferation and apoptosis rates at the cellular level, primary tumours, dissected at a size of approximately 500 mm<sup>3</sup>, from six *Bcl3<sup>+/+</sup>/MMTV/N<sub>2</sub>* and six *Bcl3<sup>-/-</sup>/MMTV/N<sub>2</sub>* mice were analysed by immunohistochemistry (IHC). Proliferating cells at any active phase of the cell cycle (G1, S, G2 or M) were visualised by performing anti-Ki67 IHC. This revealed that, similarly to the *Bcl3<sup>+/+</sup>/MMTV/N<sub>2</sub>* controls, *Bcl3<sup>-/-</sup>/MMTV/N<sub>2</sub>* tumours had a high proportion of proliferating cells that were distributed evenly across the tumour (Figure 4.6A). To quantify this, the number of Ki67-positive cells per 1000 cells (across three fields of view) was scored to calculate the percentage positivity. In *Bcl3<sup>-/-</sup>/MMTV/N<sub>2</sub>* tumours (n=6), the mean±SEM percentage of Ki67-positive cells was found to be 55.5±6.7%, and in the *Bcl3<sup>+/+</sup>/MMTV/N<sub>2</sub>* control mice (n=6) it was 62.6±5.7% (Figure 4.6A). This observed decrease in positively stained cells in *Bcl3<sup>-/-</sup>/MMTV/N<sub>2</sub>* tumours compared to *Bcl3<sup>+/+</sup>/MMTV/N<sub>2</sub>* tumours was not significantly different (Mann-Whitney U-test, p>0.05), indicating that BCL3 deficiency does not reduce the number of proliferative cells in *MMTV/N<sub>2</sub>* tumours. To further confirm this, mRNA expression of *Cyclin D1*, a principle NF-κB target gene that is essential for mammary epithelial cell growth (Cao, Bonizzi et al. 2001), was analysed in tumours from *Bcl3<sup>+/+</sup>/MMTV/N<sub>2</sub>* (n=6) and *Bcl3<sup>-/-</sup>/MMTV/N<sub>2</sub>* (n=6) animals (Figure 4.6B). Any changes in *Cyclin D1* mRNA expression between cohorts was found to be statistically insignificant (Mann-Whitney U-test, p>0.05), reflecting the large biological variation between samples.

In order to establish whether BCL3 deficiency had an effect on apoptosis rates, anti-Cleaved Caspase 3 (CC3) IHC was performed, and results were quantified by counting the number of CC3-positive cells per field of view. Levels of apoptosis in tumours from both cohorts were very low. No significant differences (Mann-Whitney U-test, p>0.05) in CC3-positive cells were observed (Figure 4.6C, mean±SEM number of CC3-positive cells per field of view was 13.8±5.18 for *Bcl3<sup>+/+</sup>/MMTV/N<sub>2</sub>* mice [n=6] and 13.6±2.7 for *Bcl3<sup>-/-</sup>/MMTV/N<sub>2</sub>* mice [n=6]).

Taken together, these data indicate that BCL3 deficiency does not affect proliferation or apoptosis rates in *MMTV/N<sub>2</sub>*-driven mammary tumours.

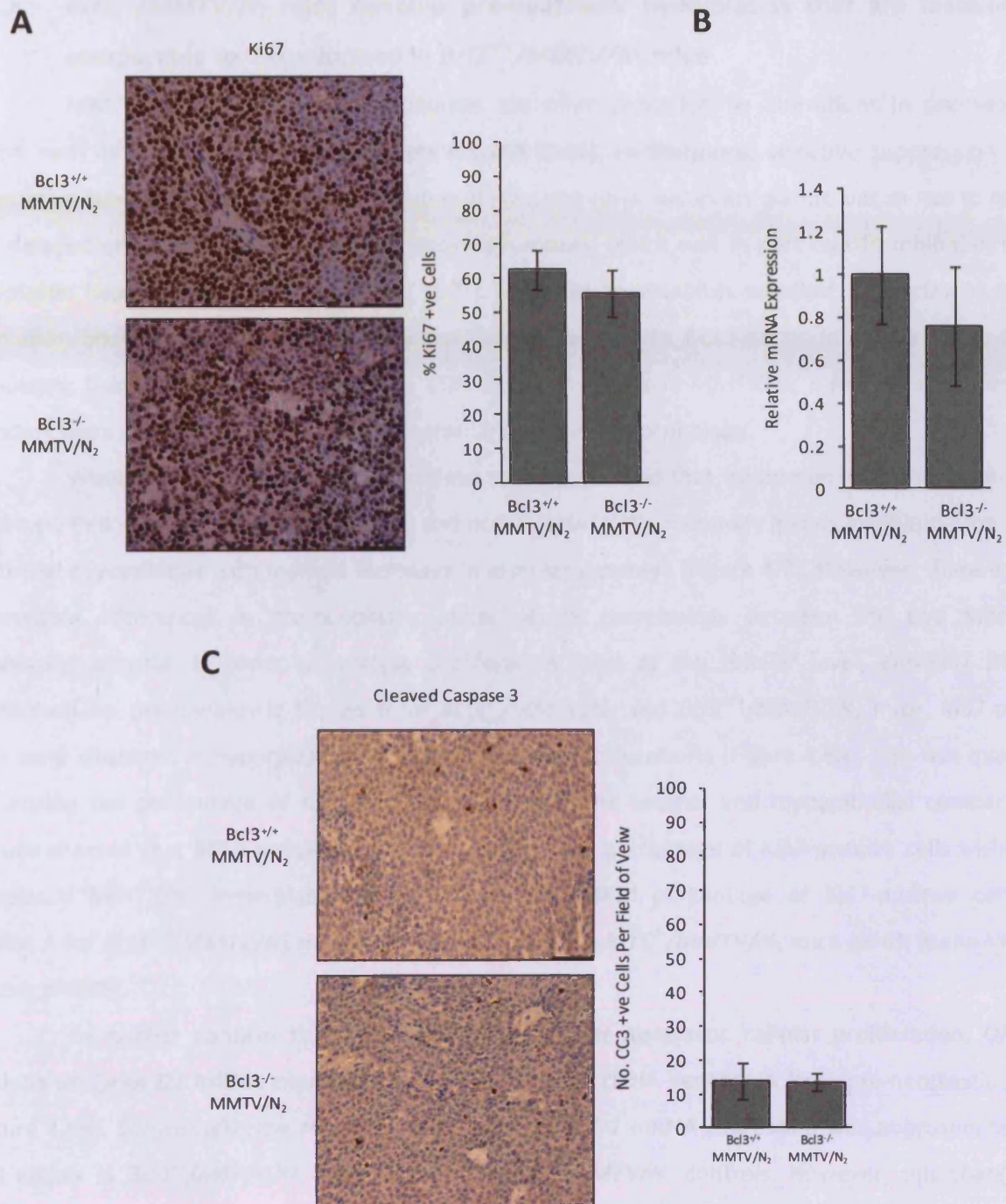


**Figure 4.6: Proliferation and apoptosis is unaffected by BCL3 deficiency in MMTV/N<sub>2</sub> tumours**

Sections from Bcl3<sup>+/+</sup>/MMTV/N<sub>2</sub> and Bcl3<sup>-/-</sup>/MMTV/N<sub>2</sub> tumours were generated and subjected to IHC analysis to assess levels of proliferation and apoptosis. No significant differences were observed in either Ki67 (A) or Cleaved Caspase-3 (C) staining (Mann-Whitney U-test for all comparisons,  $p > 0.05$ ). mRNA expression of *Cyclin D1* in the same cohorts was also assessed and revealed no significant differences (B, Mann-Whitney U-test,  $p > 0.05$ ). Scale bars indicate 100 $\mu$ m. Error bars represent  $\pm$  SEM.

#### 4.2.6 *Bcl3*<sup>-/-</sup>/*MMTV*/*N*<sub>2</sub> mice develop pre-neoplastic hyperplasias that are histologically comparable to those formed in *Bcl3*<sup>+/+</sup>/*MMTV*/*N*<sub>2</sub> mice

MMTV-induced mammary carcinomas are often preceded by alterations in pre-neoplastic tissue such as hyperplastic epithelial ducts (Cardiff 1984). Furthermore, selective suppression of the alternative NF-κB pathway by genetic deletion of IKKα in mouse mammary glands was shown to result in the delayed onset and growth of ERBB2-positive tumours, which was in part due to inhibition of pre-neoplastic hyperplasias (Cao, Luo et al. 2007). In order to establish whether the delay in tumour formation observed in the *MMTV*/*N*<sub>2</sub> mouse model was due to BCL3-dependent differences in pre-neoplastic tissue, mammary glands from 150-day-old nulliparous *MMTV*/*N*<sub>2</sub> mice without detectable tumours were analysed for alterations in mammary epithelial morphology.

Wholemount analysis and H&E-stained sections showed that, compared with oncogene-devoid wild-type FVB mice, both *Bcl3*<sup>-/-</sup>/*MMTV*/*N*<sub>2</sub> and *Bcl3*<sup>+/+</sup>/*MMTV*/*N*<sub>2</sub> mammary glands exhibited pronounced epithelial hyperplasias with marked increases in alveolar numbers (Figure 4.7). However, there were no observable differences in pre-neoplastic epithelial cell morphology between the two *MMTV*/*N*<sub>2</sub>-expressing cohorts. In order to analyse proliferation rates at the cellular level, anti-Ki67 IHC was performed on pre-neoplastic tissues from *Bcl3*<sup>-/-</sup>/*MMTV*/*N*<sub>2</sub> and *Bcl3*<sup>+/+</sup>/*MMTV*/*N*<sub>2</sub> mice. Ki67-positive cells were observed in hyperplastic ducts in tissues from both cohorts (Figure 4.8A). This was quantified by scoring the percentage of Ki67-positive cells within the luminal and myoepithelial compartment. Results showed that BCL3 deficiency had no effect on the percentage of Ki67-positive cells within pre-neoplastic *MMTV*/*N*<sub>2</sub> hyperplasias (Figure 4.8A, mean±SEM percentage of Ki67-positive cells was 14.4±2.4 for *Bcl3*<sup>+/+</sup>/*MMTV*/*N*<sub>2</sub> mice (n=6) and 17.2±4.5 for *Bcl3*<sup>-/-</sup>/*MMTV*/*N*<sub>2</sub> mice (n=6); Mann-Whitney U-test, p>0.05).

To further confirm that BCL3 did not affect pre-neoplastic cellular proliferation, QRT-PCR analysis of *Cyclin D1* mRNA expression was performed on cDNA generated from pre-neoplastic tissues (Figure 4.8B). Surprisingly, the results showed that *Cyclin D1* mRNA expression was approximately 2.5-fold higher in *Bcl3*<sup>-/-</sup>/*MMTV*/*N*<sub>2</sub> tissues than in *Bcl3*<sup>+/+</sup>/*MMTV*/*N*<sub>2</sub> controls. However, this change was found to be statistically insignificant (Mann-Whitney U-test, p≥0.05).

These data indicate that the BCL3-mediated delay in tumour latency is not due to reduced proliferation and delayed formation of hyperplastic ducts in pre-neoplastic tissues.

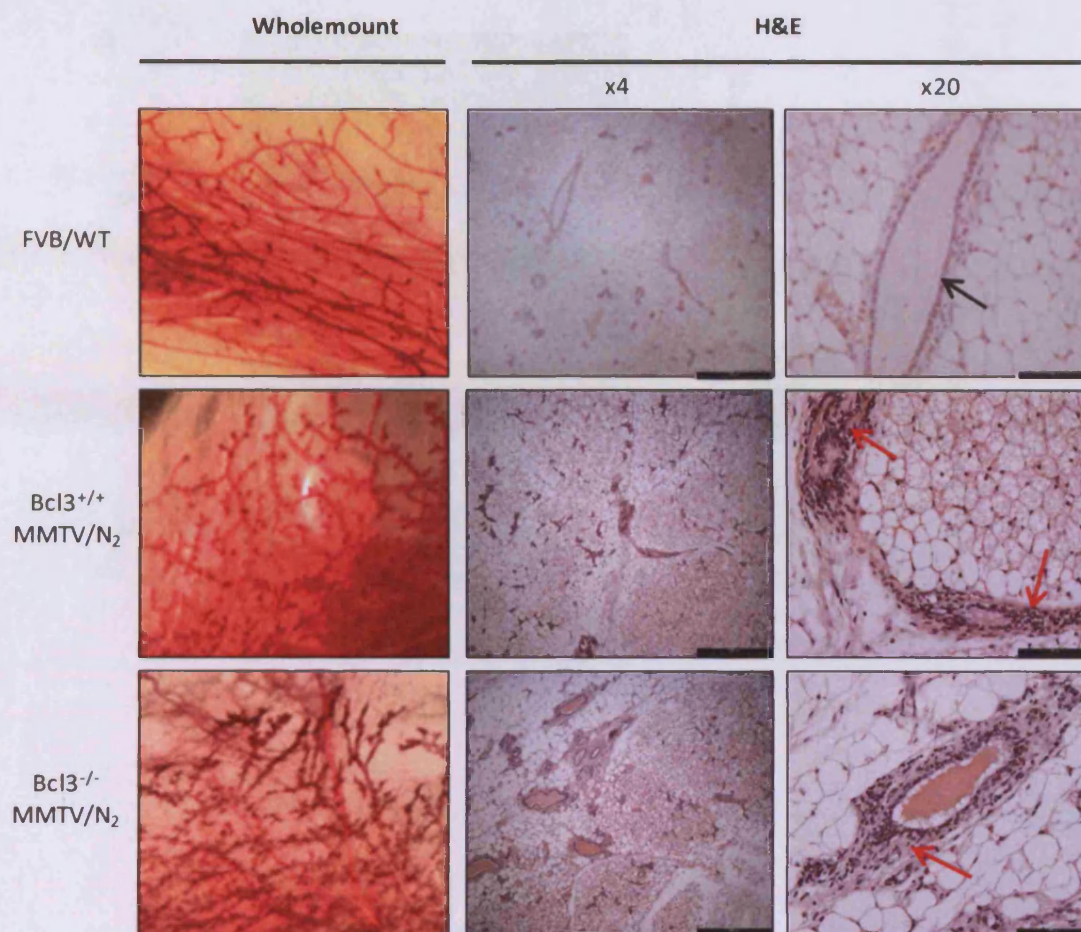


**Figure 4.7: Loss of BCL3 does not affect the formation of pre-neoplastic hyperplasias**

Wholemounts and H&E sections from pre-neoplastic tissues of FVB/WT,  $Bcl3^{+/+}$ /MMTV/ $N_2$  and  $Bcl3^{-/-}$ /MMTV/ $N_2$  animals ( $n \geq 3$ ) were analysed.  $Bcl3^{+/+}$ /MMTV/ $N_2$  (middle row) and  $Bcl3^{-/-}$ /MMTV/ $N_2$  (bottom row) tissues exhibited pronounced hyperplasias in comparison to FVB/WT (top row) glands (hyperplasias are highlighted by red arrows in  $Bcl3^{+/+}$ /MMTV/ $N_2$  and  $Bcl3^{-/-}$ /MMTV/ $N_2$  H&E sections whereas a normal epithelial duct is highlighted by a black arrow in the FVB/WT H&E section). Loss of BCL3 did not affect the formation of hyperplasias in MMTV/ $N_2$  expressing glands (middle row vs bottom row). Scale bars on H&E sections: middle panel=500 $\mu$ m, right panel=100 $\mu$ m. Representative images are shown.

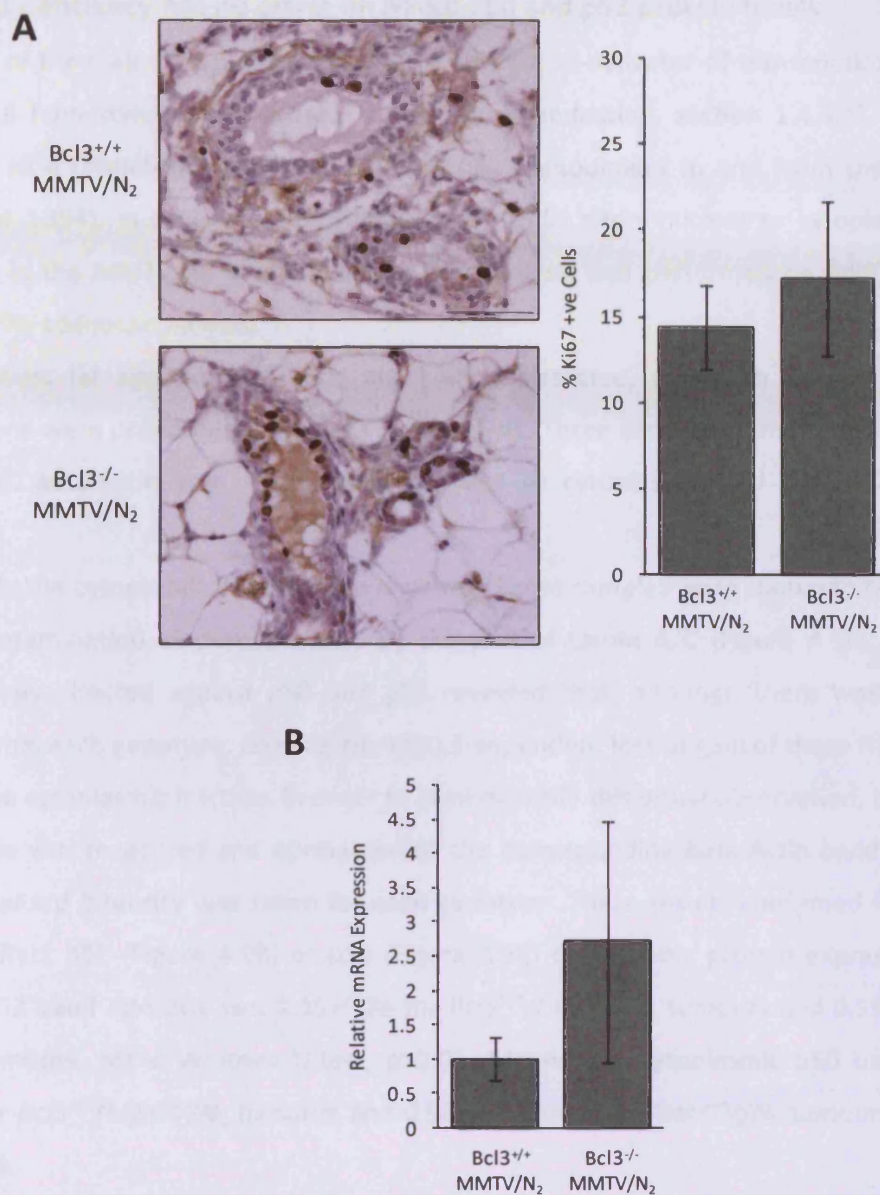


**Figure 4.8: Loss of BCL3 does not affect the proliferation of pre-neoplastic tissues**

Pre-neoplastic tissues from  $Bcl3^{+/+}$ /MMTV/ $N_2$  and  $Bcl3^{-/-}$ /MMTV/ $N_2$  animals were subjected to anti-Ki67 IHC. No differences in the percentage of Ki67 positive cells were observed (A, Mann-Whitney U-test,  $p=0.05$ ). QRT-PCR analysis in the same cohorts revealed no significant differences in *Cyclin D1* mRNA expression (B, Mann-Whitney U-test,  $p>0.05$ ). Scale bars indicate 50 $\mu$ m. Error bars represent  $\pm$  SEM.

#### 4.2.7 BCL3 deficiency has no effect on NF- $\kappa$ B p50 and p52 protein levels

One of the major functions of BCL3 is to act as a co-activator of transcriptionally inactive p50 and p52 NF- $\kappa$ B homodimers (see Chapter 1: General Introduction, section 1.4.4.1). It has also been shown to act as a chaperone to shuttle p50 and p52 homodimers to and from the nucleus (Zhang, Didonato et al. 1994). In order to determine whether BCL3 alters nuclear or cytoplasmic p50 or p52 protein levels in the *MMTV/N<sub>2</sub>* model, western blot analysis was performed on *Bcl3<sup>+/+</sup>/MMTV/N<sub>2</sub>* and *Bcl3<sup>-/-</sup>/MMTV/N<sub>2</sub>* adenocarcinomas.

Tumours (at approximately 500 mm<sup>3</sup>) were dissected, and both nuclear and cytoplasmic protein fractions were prepared for western blot analysis. Three separate tumours from each genotype were analysed. Beta-Actin and Lamin A/C were used as cytoplasmic and nuclear loading controls, respectively.

Firstly the cytoplasmic fraction was analysed. These samples were shown to be completely free of nuclear contamination as demonstrated by the lack of Lamin A/C (Figure 4.9A, Lamin A/C lane). Western analysis directed against p50 and p52 revealed that, although there was variable protein expression within each genotype, no consistent BCL3-dependent loss or gain of these NF- $\kappa$ B subunits was observed in the cytoplasmic fraction. In order to semi-quantify this visual observation, the band intensity of each sample was measured and normalised to the corresponding Beta-Actin band intensity and an average normalised intensity was taken for each genotype. These results confirmed that BCL3 did not significantly affect p52 (Figure 4.9B) or p50 (Figure 4.9C) cytoplasmic protein expression (mean $\pm$ SEM cytoplasmic p52 band intensity was 1.15 $\pm$ 0.28 for *Bcl3<sup>+/+</sup>/MMTV/N<sub>2</sub>* tumours and 0.99 $\pm$ 0.407 for *Bcl3<sup>-/-</sup>/MMTV/N<sub>2</sub>* tumours, Mann-Whitney U-test,  $p>0.05$ . Mean $\pm$ SEM cytoplasmic p50 band intensity was 1.35 $\pm$ 0.415 for *Bcl3<sup>+/+</sup>/MMTV/N<sub>2</sub>* tumours and 0.98 $\pm$ 0.12 for *Bcl3<sup>-/-</sup>/MMTV/N<sub>2</sub>* tumours, Mann-Whitney U-test,  $p>0.05$ ).

The nuclear fraction was then analysed. Although these samples were clearly enriched in nuclear protein as demonstrated by the expression of Lamin A/C, the crude nature of this extraction resulted in a high degree of cytoplasmic contamination, as indicated by the protein expression of Beta-Actin in these samples (Figure 4.9A). However, taking into account the fact that BCL3 did not affect the protein expression of p50 or p52 in the cytoplasmic fraction, it was concluded that any changes observed in these samples was likely to have occurred in the nuclear fraction. No obvious visual BCL3-dependent changes in p50 or p52 were observed in the nuclear fraction (Figure 4.9A). However, Lamin A/C protein expression showed that nuclear loading was not even. Therefore, in order to take this into account and to semi-quantify the results, the band intensity of each sample was normalised to the average band intensity of the corresponding two Lamin A/C bands and an average for each genotype was taken. This confirmed visual observations and showed that BCL3 did not significantly alter the expression of p52

(Figure 4.9D) or p50 (Figure 4.9E) in the nuclear fraction (mean $\pm$ SEM nuclear p52 band intensity was 1.12 $\pm$ 0.29 for *Bcl3*<sup>+/+</sup>/MMTV/*N*<sub>2</sub> tumours and 0.91 $\pm$ 0.15 for *Bcl3*<sup>-/-</sup>/MMTV/*N*<sub>2</sub> tumours, Mann-Whitney U-test, *p*>0.05. Mean $\pm$ SEM nuclear p50 band intensity was 0.418 $\pm$ 0.09 for *Bcl3*<sup>+/+</sup>/MMTV/*N*<sub>2</sub> tumours and 0.34 $\pm$ 0.06 for *Bcl3*<sup>-/-</sup>/MMTV/*N*<sub>2</sub> tumours, Mann-Whitney U-test, *p*>0.05).

A clear limitation in these results is that only a semi-quantitative analysis could be employed and that the nuclear fraction was not clear of cytoplasmic contamination. However, it can be cautiously concluded that depletion of BCL3 does not directly affect cytoplasmic or nuclear levels of p50 or p52 within tumours.

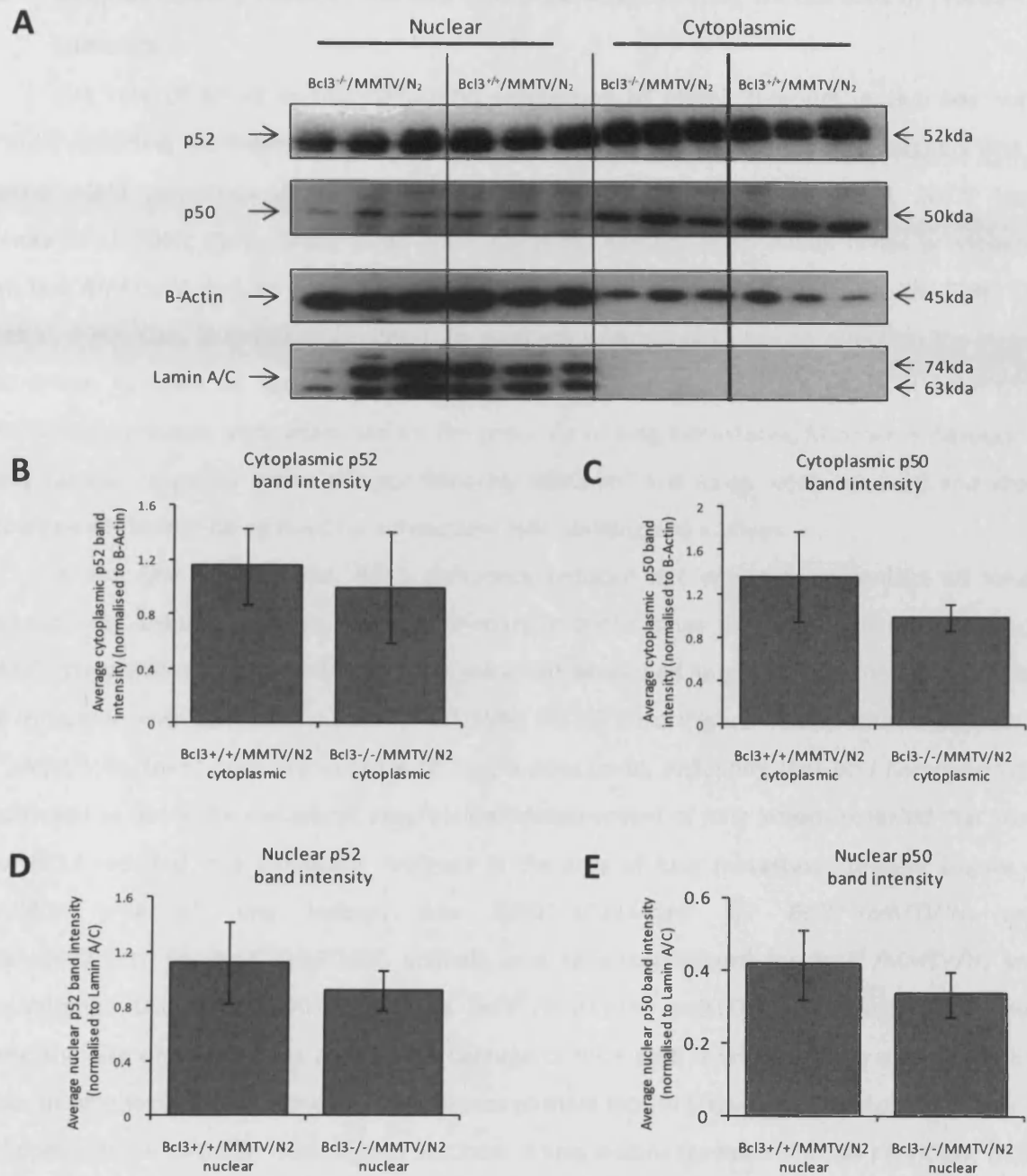


**Figure 4.9: Loss of BCL3 does not affect the expression of p50 or p52 in the nuclear or cytoplasmic fractions of MMTV/ $N_2$  tumours**

Nuclear and cytoplasmic protein fractions were extracted from three  $Bcl3^{+/+}/MMTV/N_2$  and three  $Bcl3^{-/-}/MMTV/N_2$  tumours and subjected to western analysis (A). Average p50 and p52 protein expression was normalised to Beta-Actin (cytoplasmic fraction, B&C) or Lamin A/C (nuclear fraction, D&E). No significant differences in p52 or p50 protein expression was observed in either the nuclear or cytoplasmic fractions (Mann-Whitney U-test for all comparisons,  $p > 0.05$ ). Error bars represent  $\pm$  SEM across the three samples from each genotype.

#### 4.2.8 BCL3 deficiency reduces the size and occurrence of lung metastases in ERBB2-driven tumours

The role of NF- $\kappa$ B in the metastatic progression of ERBB2 tumours *in vivo* has not been previously reported, yet there is a body of both *in vitro* and *in vivo* evidence that suggests that NF- $\kappa$ B signalling might contribute directly to this process (Helbig, Christopherson et al. 2003; Aggarwal, Shishodia et al. 2005; Park, Zhang et al. 2007; Connelly, Barham et al. 2010). It has previously been shown that *MMTV/N<sub>2</sub>* and, to a lesser extent, *MMTV/NK* mice develop metastases to the lungs (Muller, Sinn et al. 1988; Guy, Webster et al. 1992). To establish whether BCL3 has an effect on the invasion of ERBB2-driven tumours to secondary sites, experimental and control mice on both *MMTV/N<sub>2</sub>* and *MMTV/NK* backgrounds were examined for the presence of lung metastases. Mice were dissected when primary tumours reached a size of approximately 4000mm<sup>3</sup> and lungs were removed and visualised macroscopically before being fixed for subsequent H&E staining and analysis.

In the *MMTV/N<sub>2</sub>* model, BCL3 deficiency reduced not only the percentage of mice with metastatic lung lesions, but also the tumour mass in those lungs that exhibited metastases (Figure 4.10A&C). Only 50% of *Bcl3<sup>-/-</sup>/MMTV/N<sub>2</sub>* (n=8) mice had developed lung lesions at the experimental end-point compared with 82% of the *Bcl3<sup>+/+</sup>/MMTV/N<sub>2</sub>* (n=11) mice (Figure 4.10A). Interestingly, 100% of *Bcl3<sup>+/-</sup>/MMTV/N<sub>2</sub>* (n=8) mice presented with lung lesions (n=8), indicating that *Bcl3* heterozygosity was not sufficient to delay the metastatic progression. Measurement of lung lesions revealed that complete loss of BCL3 resulted in a significant decrease in the area of lung metastases present (Figure 4.10C, mean $\pm$ SEM area of lung lesions, was 195077 $\pm$ 62344 $\mu$ m<sup>2</sup> for *Bcl3<sup>+/+</sup>/MMTV/N<sub>2</sub>* animals, 135067 $\pm$ 36772 $\mu$ m<sup>2</sup> for *Bcl3<sup>+/-</sup>/MMTV/N<sub>2</sub>* animals, and 48555 $\pm$ 10083 $\mu$ m<sup>2</sup> for *Bcl3<sup>-/-</sup>/MMTV/N<sub>2</sub>* animals; Mann–Whitney U-test *Bcl3<sup>+/+</sup>/MMTV/N<sub>2</sub>* vs *Bcl3<sup>-/-</sup>/MMTV/N<sub>2</sub>* p=0.0051). Although BCL3 depletion reduced the size of lung lesions and the percentage of mice with them, it had no effect on the mean number of lung lesions developed per metastases-positive mouse (Figure 4.10B, Mann–Whitney U-test for all comparisons, p>0.05). H&E-stained sections of lung lesions revealed that, as previously described (Guy, Webster et al. 1992), the cellular morphology of lung metastases present in *Bcl3<sup>+/+</sup>/MMTV/N<sub>2</sub>* mice was identical to the primary tumour (Figure 4.11). This was also true of lesions arising in *Bcl3<sup>+/-</sup>/MMTV/N<sub>2</sub>* and *Bcl3<sup>-/-</sup>/MMTV/N<sub>2</sub>* mice, and no histological differences were observed between genotypes (Figure 4.11).

The frequency and size of metastatic lung lesions in the *MMTV/NK* model was also assessed. At the outset of this analysis, it should be noted that some cohort numbers for this experiment were low (*Bcl3<sup>+/+</sup>/MMTV/NK*, n=10; *Bcl3<sup>+/-</sup>/MMTV/NK*, n=5; *Bcl3<sup>-/-</sup>/MMTV/NK*, n=5). Complete loss of BCL3 resulted in a 20% reduction in the number of animals with evidence of lung metastases (Figure 4.12A, 60% *Bcl3<sup>+/+</sup>/MMTV/NK* metastases-positive animals in comparison with 40% *Bcl3<sup>-/-</sup>/MMTV/NK* metastases-

positive animals). As observed in the *MMTV/N<sub>2</sub>* model, 100% of *Bcl3<sup>+/-</sup>/MMTV/NK* mice developed metastatic lung lesions, again suggesting that *Bcl3* heterozygosity has no effect on the onset of metastatic lesions. Unlike in the *MMTV/N<sub>2</sub>* model, BCL3 deficiency did not result in a reduction in the area of lung metastases present (Figure 4.12C, mean±SEM area of lung lesions was 68236±8277µm<sup>2</sup> for *Bcl3<sup>+/-</sup>/MMTV/NK* animals, 174269±60695µm<sup>2</sup> for *Bcl3<sup>+/-</sup>/MMTV/NK* animals and 194194±169210µm<sup>2</sup> for *Bcl3<sup>-/-</sup>/MMTV/NK*; Mann–Whitney U-test for all comparisons p>0.05). However, a decrease in the mean number of lung lesions present per metastases-positive mouse was observed (Figure 4.12B, from 13.8±8.7 in the *Bcl3<sup>+/-</sup>/MMTV/NK* controls to 8.0±2.82 and 2.0±1.4 in the *Bcl3<sup>+/-</sup>/MMTV/NK* and *Bcl3<sup>-/-</sup>/MMTV/NK* animals, respectively). This was found to be insignificant because of very small cohort sizes (Figure 4.12B, Mann–Whitney U-test for all comparisons, p>0.05). All lung metastases were histologically identical to the primary tumours from which they originated, and, similarly to the *MMTV/N<sub>2</sub>* model, no morphological differences were observed between cohorts (Figure 4.13).

Overall, these data indicate that BCL3 delays the metastatic progression of mammary tumours driven by the *MMTV/N<sub>2</sub>* transgene. However, in the *MMTV/NK* model, BCL3-deficiency is unable to suppress the pro-metastatic effects of the highly aggressive, activated NEU protein.

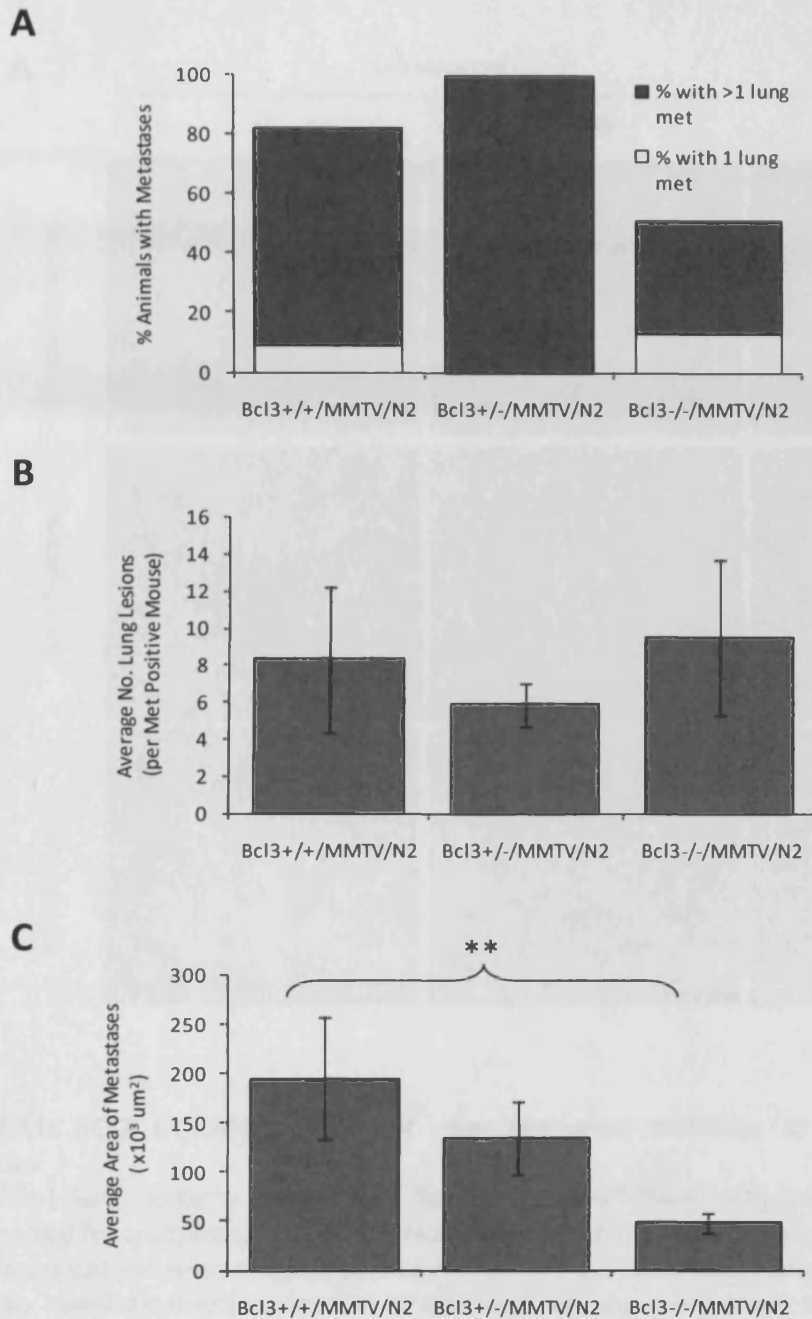


**Figure 4.10: BCL3 deficiency reduces the size and occurrence of lung metastases**

The percentage of mice harbouring lung metastases was reduced from 82% in *Bcl3*<sup>+/+</sup>/MMTV/N<sub>2</sub> mice (n=11) to only 50% in *Bcl3*<sup>-/-</sup>/MMTV/N<sub>2</sub> mice (n=8). 100% *Bcl3*<sup>+/-</sup>/MMTV/N<sub>2</sub> (n=8) mice exhibited lung metastases (A). The number of lung metastases per metastases positive mouse was unaffected by the absence of BCL3 (B, Mann-Whitney U-test, p>0.05). The average area of metastases in *Bcl3*<sup>-/-</sup>/MMTV/N<sub>2</sub> mice was significantly smaller than in *Bcl3*<sup>+/+</sup>/MMTV/N<sub>2</sub> mice (C, \*\*Mann-Whitney U-test, p=0.0051). Error bars represent ± SEM.

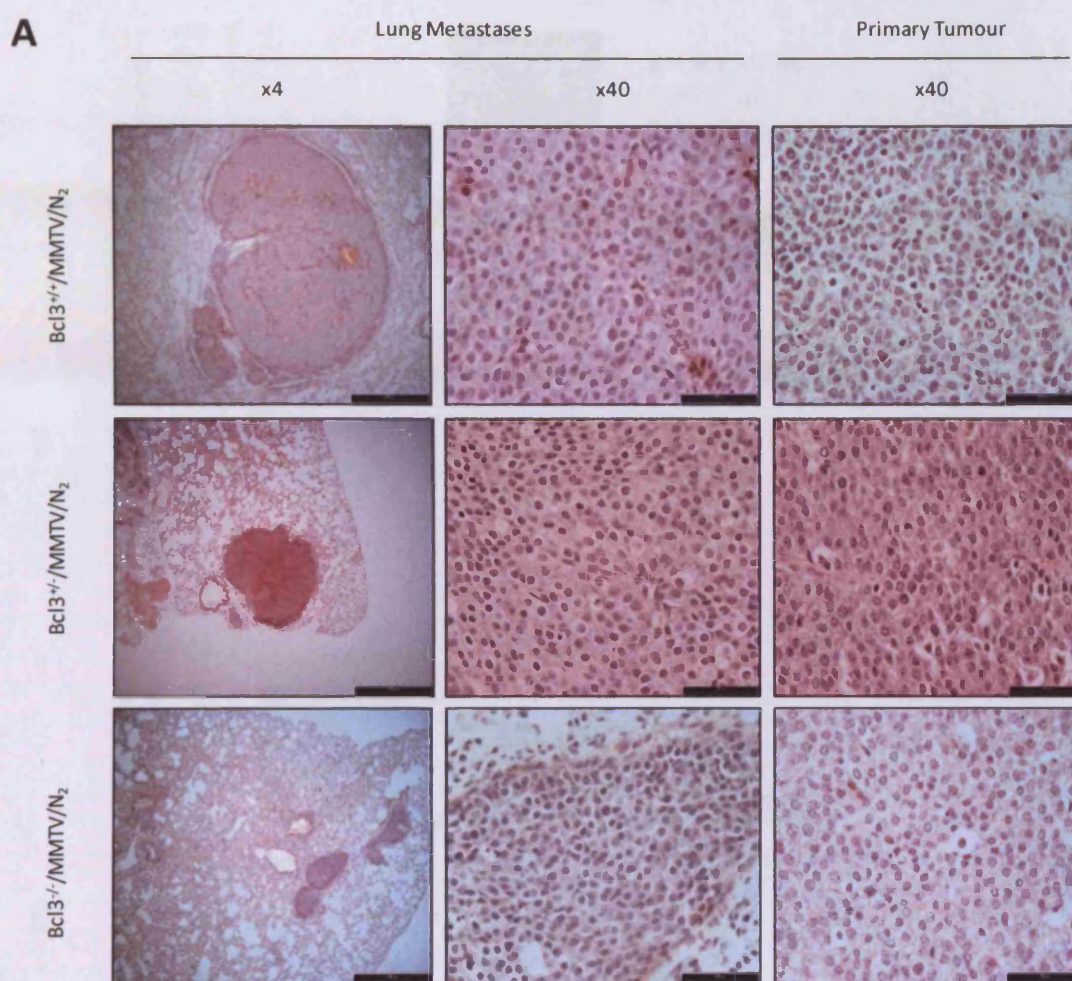


**Figure 4.11: BCL3 deficiency does not alter the gross histology of MMTV/ $N_2$  driven lung metastases**

H&E stained lung sections from  $Bcl3^{+/+}/MMTV/N_2$ ,  $Bcl3^{+/-}/MMTV/N_2$  and  $Bcl3^{-/-}/MMTV/N_2$  mice were analysed for histological changes. Mice from all three cohorts developed lung metastases that were histologically identical to the primary tumours from which they arose (middle panel vs right panel). No histological differences were observed in lung metastases between cohorts (middle panel). However, loss of BCL3 did result in an overall reduction in the size of lung metastases (left panel). Scale bars: Left panel=500 $\mu$ m, right and middle panels=50 $\mu$ m.

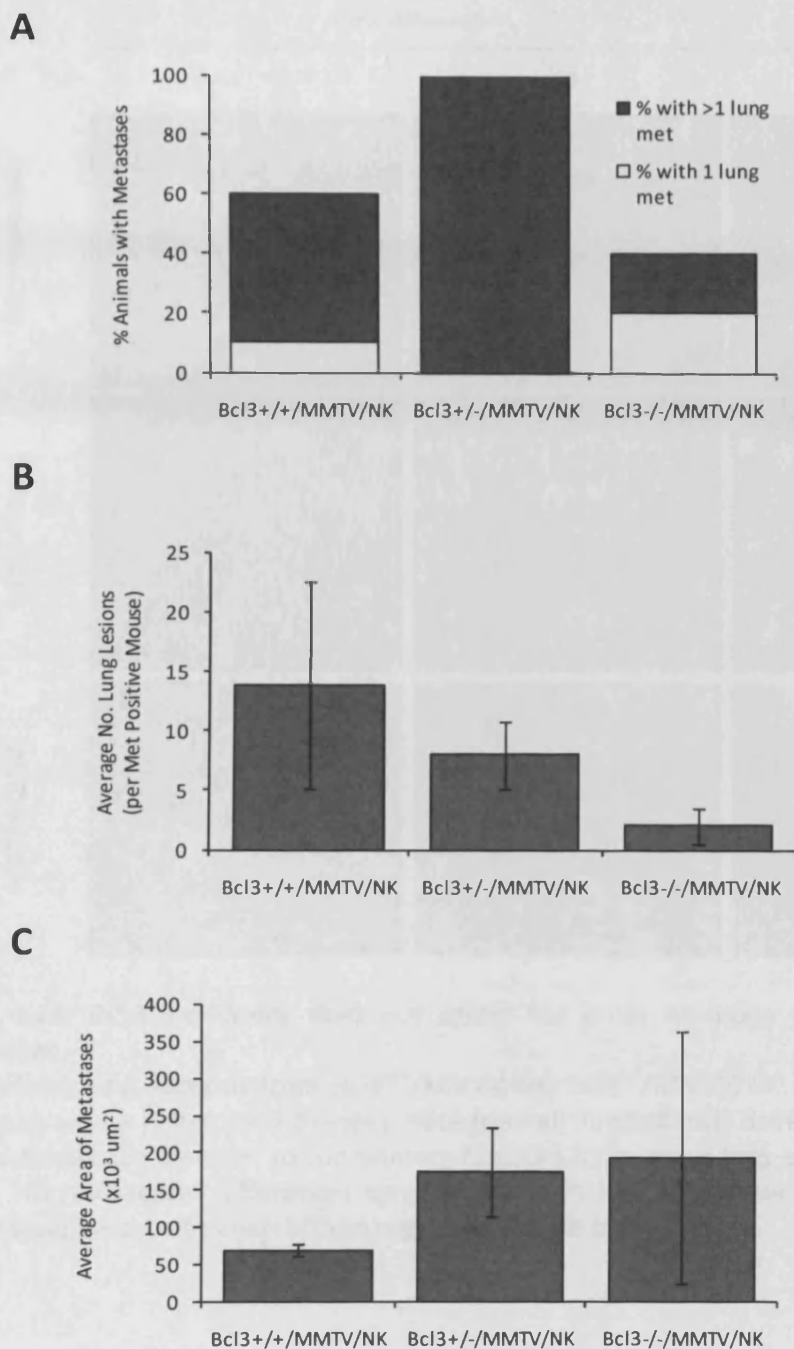


**Figure 4.12: BCL3 deficiency does not significantly reduce the size or number of MMTV/NK driven lung metastases**

The percentage of animals harbouring lung metastases was reduced from 60% in *Bcl3*<sup>+/+</sup>/MMTV/NK mice (n=10) to 40% in *Bcl3*<sup>-/-</sup>/MMTV/NK mice (n=5). 100% of *Bcl3*<sup>+/-</sup>/MMTV/NK mice (n=5) exhibited lung metastases (A). Loss BCL3 resulted in an insignificant decrease in the average number of lung lesions per metastases positive mouse (B, Mann-Whitney U-test,  $p > 0.05$ ). No significant differences were observed in the average area of metastases (C, Mann-Whitney U-test,  $p > 0.05$ ). Error bars represent  $\pm$  SEM.

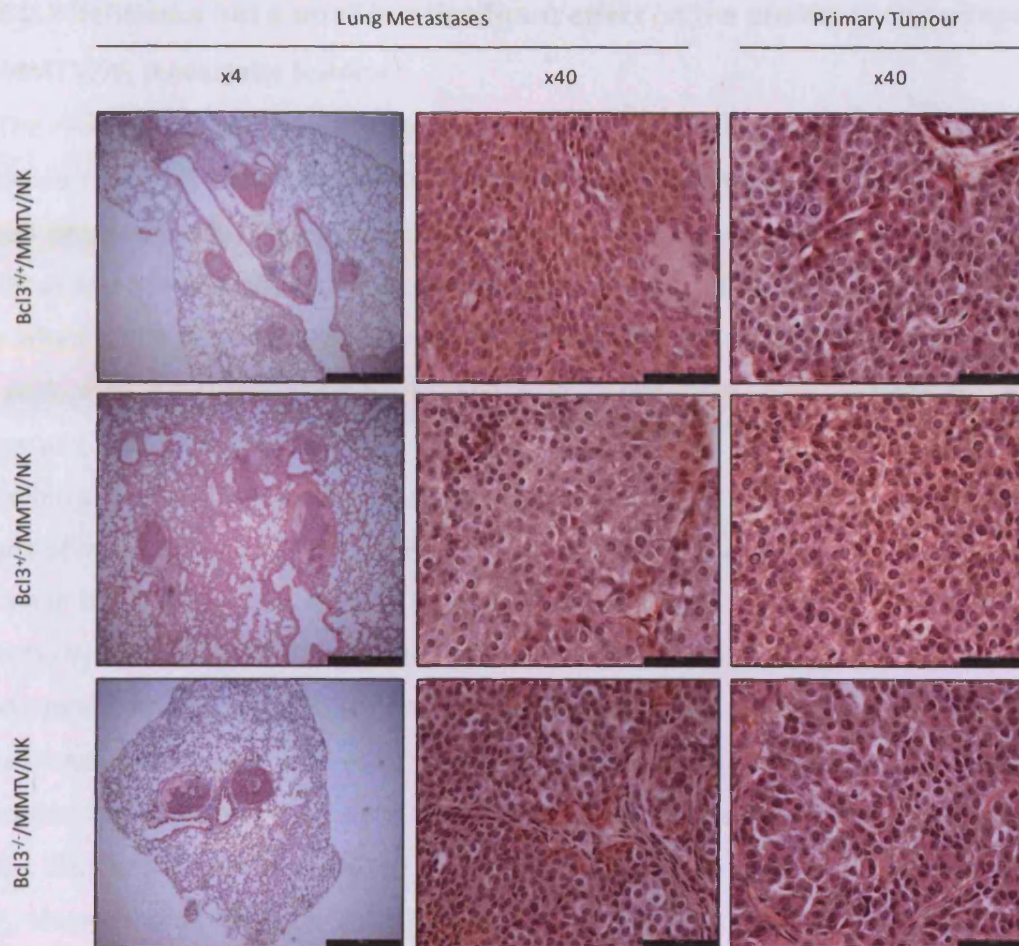


**Figure 4.13: *BCL3* deficiency does not affect the gross histology of MMTV/NK driven lung metastases**

H&E stained lung sections from *Bcl3*<sup>+/+</sup>/MMTV/NK, *Bcl3*<sup>+/-</sup>/MMTV/NK and *Bcl3*<sup>-/-</sup>/MMTV/NK mice were analysed for histological changes. Mice from all three cohorts developed lung metastases that were histologically identical to the primary tumours from which they arose (middle panel vs right panel). No histological differences were observed in lung metastases between cohorts (middle panel). Scale bars: Left panel=500µm, right and middle panels=50µm.

#### 4.2.9 BCL3 deficiency has a small but significant effect on the proliferation and apoptosis of MMTV/ $N_2$ metastatic lesions

The reduced size and occurrence of metastatic lesions within the lungs of  $Bcl3^{-/-}$ /MMTV/ $N_2$  mice suggested that BCL3 deficiency was able to delay the metastatic progression of ERBB2 tumours. This delayed progression could have been due either to later dissemination and seeding of primary tumour cells at secondary sites, or reduced tumour growth kinetics of the metastatic lesions. In order to determine whether the latter hypothesis could explain the observed phenotype, anti-Ki67 and anti-CC3 IHC was performed on 6  $Bcl3^{+/+}$ /MMTV/ $N_2$  and 6  $Bcl3^{-/-}$ /MMTV/ $N_2$  lung sections to visualise the proliferative and apoptotic nature of these secondary tumours. Ki67 staining revealed that there was a high proportion of actively proliferating cells distributed evenly across metastatic lesions in sections from both cohorts of mice (Figure 4.14A). Quantitative analysis of Ki67 staining (calculated as in section 4.2.5) showed a small but significant decrease in the percentage of Ki67-positive cells from  $52.4 \pm 4.12\%$  in the  $Bcl3^{+/+}$ /MMTV/ $N_2$  controls to  $37.95 \pm 4.19\%$  in the  $Bcl3^{-/-}$ /MMTV/ $N_2$  animals (Figure 4.14A, Mann-Whitney U-test,  $p=0.0294$ ). IHC directed against CC3 revealed very low levels of apoptosis within the secondary lesions of all mice. Quantitative analysis of this staining (calculated as in section 4.2.5) showed that loss of BCL3 resulted in a significant increase in the percentage of CC3-positive cells present (Figure 4.14B, % CC3-positive cells  $\pm$  SEM were:  $0.3567 \pm 0.11$  for  $Bcl3^{+/+}$ /MMTV/ $N_2$  mice and  $0.929 \pm 0.239$  for  $Bcl3^{-/-}$ /MMTV/ $N_2$ , Mann Whitney-U-test,  $p=0.0225$ ).

These data show that loss of BCL3 results in a small but significant reduction in the proliferation, and an increase in the apoptosis of cells seeded at secondary sites, indicating that the reduced size of metastatic lesions could be due BCL3 dependent effects on tumour growth kinetics.

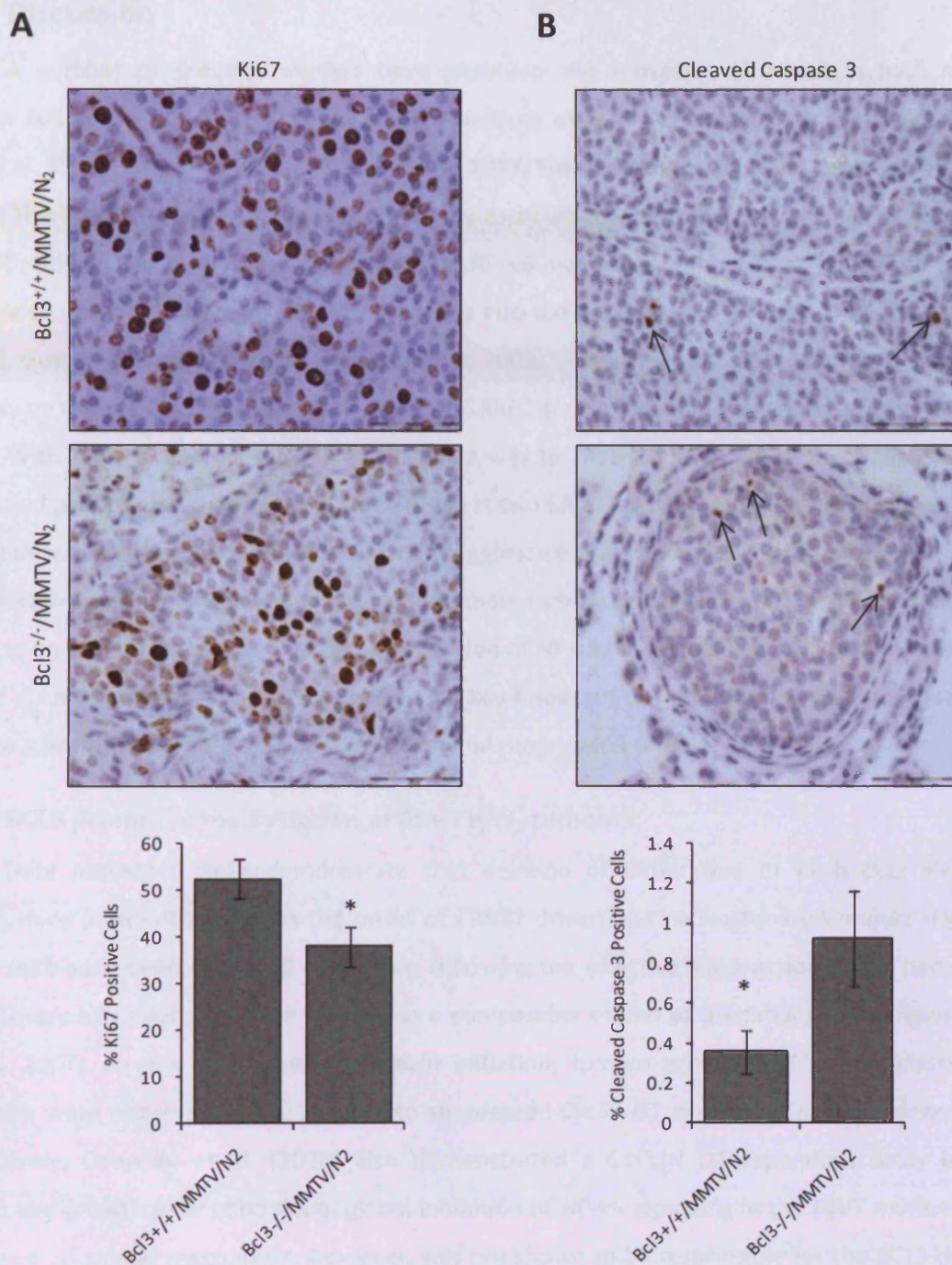


**Figure 4.14: Loss of BCL3 reduces the rates of proliferation and apoptosis in MMTV/N<sub>2</sub> metastatic lesions**

Sections from Bcl3<sup>+/+</sup>/MMTV/N<sub>2</sub> and Bcl3<sup>-/-</sup>/MMTV/N<sub>2</sub> lung lesions (n=6) were subjected to Ki67 and CC3 IHC. Depletion of BCL3 resulted in a significant decrease in the percentage of Ki67-positive cells (A, \* = Mann-Whitney U-test, p=0.0294) and a significant increase in the percentage of CC3 positive cells (B, \* = Mann-Whitney U-test, p=0.0255, CC3 positive cells highlighted by black arrows). Scale bar indicates 50µm. Error bars represent ± SEM.

### 4.3 Discussion

A number of previous studies have observed the activation of NF- $\kappa$ B in both mammary carcinoma cell lines and primary breast cancer samples of both human and rodent origin (Dejardin, Bonizzi et al. 1995; Nakshatri, Bhat-Nakshatri et al. 1997; Sovak, Bellas et al. 1997; Cogswell, Guttridge et al. 2000). This has been found to be predominantly associated with EGFR-family signalling (Biswas, Cruz et al. 2000; Biswas, Shi et al. 2004), indicating that NF- $\kappa$ B may have a primary function in this subtype of breast cancer. To date, however, only a few studies into the potential role of BCL3 in breast cancer exist (Cogswell, Guttridge et al. 2000; Pratt, Bishop et al. 2003; Choi, Lee et al. 2010), and none have focused specifically on the effects of this NF- $\kappa$ B co-factor in ERBB2-positive mammary carcinogenesis.

With this in mind, the aim of this chapter was to analyse the effect of BCL3 depletion on the initiation and progression of mammary carcinomas in two ERBB2-driven murine models of breast cancer. It was hypothesised that depletion of BCL3 in this aggressive subtype of the disease may modulate NF- $\kappa$ B activity in such a way as to selectively reduce mammary tumourigenesis without causing the detrimental side effects on mammary tissues that global inhibition of NF- $\kappa$ B has previously been shown to incur (Cao, Bonizzi et al. 2001; Baxter, Came et al. 2006). The key findings from this chapter were that loss of BCL3 resulted in a profound delay in both the initiation and progression of *MMTV/N<sub>2</sub>* tumours.

#### 4.3.1 BCL3 promotes the initiation of *MMTV/N<sub>2</sub>* tumours

Data presented here demonstrate that deletion of either one or both *Bcl3* alleles from *MMTV/N<sub>2</sub>* mice dramatically delays the onset of ERBB2-driven murine mammary tumours (Figure 4.2). Similar results have been observed previously, following the selective suppression of the non-canonical NF- $\kappa$ B pathway by genetic deletion of IKK $\alpha$  in a comparable model of mammary tumourigenesis (Cao, Luo et al. 2007). In this case, delayed tumour initiation, tumour growth and pre-neoplastic cellular proliferation were observed and attributed to suppressed *Cyclin D1* expression in the absence of IKK $\alpha$ . More recently, Connelly et al. (2010) also demonstrated a CYCLIN D1-dependent delay in tumour formation and growth after conditional global inhibition of NF- $\kappa$ B signalling in the PyVT murine model of breast cancer. A similar mechanism, however, was not shown to be responsible for the BCL3-dependent delays in tumour initiation observed in the present study, as *Cyclin D1* expression in both pre-neoplastic tissues and tumours was found to be unaltered in the absence of BCL3, and, furthermore, no effect on tumour growth (Figure 4.4 & 4.6) or pre-neoplastic cellular proliferation (Figure 4.8) was observed. Interestingly, in the less clinically relevant *MMTV/NK* model, tumour initiation was unaffected by BCL3 depletion (Figure 4.1). It is possible that the highly aggressive nature of the product of the activated *Neu* transgene may act to override any inhibitory effects that loss of BCL3 could incur. Alternatively, BCL3 inhibition may delay the kinase activation of the wild-type *MMTV/N<sub>2</sub>* transgene resulting in prolonged tumour latency in this model without having an effect on the latency of tumours driven by the already

kinase active *MMTV/NK* transgene (see Chapter 7: General Discussion, section 7.3.1, for further discussion on this).

#### 4.3.2 BCL3 promotes the metastatic progression of *MMTV/N<sub>2</sub>* tumours

Mortality in breast cancer is generally attributed to organ-specific metastasis rather than to the primary tumour. Therefore, one of the most interesting observations from this chapter was that BCL3-deficient *MMTV/N<sub>2</sub>* tumours exhibited an impaired capacity to metastasize to the lungs (Figure 4.10). Both the percentage of mice with lung lesions and the average tumour mass in those lungs that did exhibit metastases were reduced in *Bcl3<sup>-/-</sup>/MMTV/N<sub>2</sub>* mice. A similar result was not observed in the *MMTV/NK* model (Figure 4.12) which again may suggest that the potent oncogenic signal from the activated *Neu* transgene overrides any BCL3-mediated effects.

NF- $\kappa$ B-dependent changes in the metastatic potential of tumours driven by the PyVT oncogene have previously been observed (Connelly, Barham et al. 2010). However, a significant decrease in primary tumour burden was also detected in this model, and therefore whether the putative NF- $\kappa$ B-mediated effects were directly on metastases or as a result of reduced seeding from smaller primary tumours remained undetermined. Importantly, in the present study, loss of BCL3 resulted in no changes in overall tumour burden (Figure 4.5), and so it is highly unlikely that the observed reduction in lung metastases stems from anything but a direct BCL3-dependent metastatic phenotype.

A significant reduction in proliferation and increase in apoptosis, as measured by Ki67 and CC3 IHC, were observed in the metastatic lesions that formed in *Bcl3<sup>-/-</sup>/MMTV/N<sub>2</sub>* mice (Figure 4.14) in comparison to controls. On first consideration, this would suggest that loss of BCL3 reduces the capacity of cells to survive and proliferate at secondary sites. However, it must be noted that, because loss of BCL3 delayed the metastatic progression of *MMTV/N<sub>2</sub>* tumours, all of the *Bcl3<sup>-/-</sup>/MMTV/N<sub>2</sub>* lung lesions analysed were consistently smaller in size than controls. Therefore, the observed changes in growth kinetics could simply be due to the fact that smaller metastases at an earlier stage of seeding proliferate more slowly than well-established ones, regardless of BCL3 status. This hypothesis is somewhat supported by results from earlier experiments demonstrating that loss of BCL3 had no effect on the proliferation or apoptosis rates of comparably sized primary tumours (Figure 4.6). Therefore, whether this result reflects a genuine BCL3-mediated change in the growth kinetics of *MMTV/N<sub>2</sub>* lung metastases, or whether it is an experimental artefact remains unknown. Either way, the effect of BCL3 on the metastatic potential of *MMTV/N<sub>2</sub>* tumours is likely to extend further than simply affecting established secondary tumour growth. This is evident in the fact that a much higher percentage of *Bcl3<sup>-/-</sup>/MMTV/N<sub>2</sub>* mice displayed absolutely no evidence of lung metastases than controls, suggesting that there must be an additional anti-metastatic effect at an earlier stage of the process. This hypothesis will be explored further in the next chapter.

### **4.3.3 Summary**

In summary, work from this chapter has demonstrated for the first time that the NF- $\kappa$ B co-factor, BCL3, can have a profound effect on the initiation and metastatic progression of ERBB2-driven murine mammary tumours. Taken together with data from chapter 3 showing that loss of BCL3 has no detrimental effects on normal mammary tissues, these results indicate that BCL3 may represent an attractive new therapeutic target for this subtype of human breast cancer. Mechanisms involved in driving this BCL3-mediated oncogenic effect will be investigated further in chapter 5.

**Chapter 5:**  
**Investigation into the Cell Autonomous**  
**Effects of BCL3 on ERBB2-driven**  
**Carcinogenesis**

## 5.1 Introduction

Work in chapter 4 demonstrated that BCL3 deficiency delayed both the onset and progression of mammary carcinogenesis in a clinically relevant ERBB2-driven transgenic mouse model. This is the first time that BCL3 has been shown to have such an effect, although the NF- $\kappa$ B family of transcription factors have previously been implicated in this subtype of the disease.

Breast cancer development and progression is a multi-step process that involves primary tumour growth and local tissue invasion followed by dissemination and re-establishment at secondary sites. Multiple mechanisms, including individual cell autonomous alterations or more global changes in the tumour microenvironment, and large cell populations can influence this process. In order to further evaluate the potential of BCL3 as a new therapeutic target, it will be essential to elucidate the molecular mechanisms by which it exerts pro-oncogenic effects on breast cancer cells.

NF- $\kappa$ B has previously been implicated in a number of processes that contribute to mammary tumourigenesis. Firstly, it has been shown to directly regulate the transcription of cancer-related genes associated with proliferation, angiogenesis, metastases, inflammation and apoptosis suppression (reviewed in Basseres and Baldwin 2006). In addition to this, previous reports have also demonstrated its ability to influence genes that regulate the process of epithelial-to-mesenchymal transition (EMT) (Chua, Bhat-Nakshatri et al. 2007; Criswell and Arteaga 2007; Liu, Sakamaki et al. 2010), a type of cell plasticity whereby epithelial cells lose some of their epithelial characteristics and acquire properties that are typically associated with mesenchymal cells.

More recently, the incidence and metastatic properties of ERBB2-positive tumours have been attributed to the expansion of a tumour-initiating or cancer stem/progenitor cell population (Korkaya, Paulson et al. 2008). Canonical NF- $\kappa$ B signalling has been implicated in this process, as demonstrated by its elevation in luminal progenitor cell populations in a dimethylbenzanthracene (DMBA) murine mammary tumour model (Pratt, Tibbo et al. 2009) and more recently by loss of stem cell markers following its inhibition in a murine ERBB2 driven-tumour model (Liu, Sakamaki et al. 2010). Furthermore, NF- $\kappa$ B has been shown to promote the classic *in vitro* functional features of breast cancer stem cells, which include the capacity to invade the extracellular matrix and to grow as multicellular, spheroids, termed mammospheres (Zhou, Zhang et al. 2008; Wu, Deng et al. 2009; Storci, Sansone et al. 2010).

While the molecular mechanisms underlying the effect of NF- $\kappa$ B in cancer have been the subject of intensive study, the means by which BCL3 may promote carcinogenesis remain largely undetermined. Previous studies have, nevertheless, demonstrated it to be involved in the transcriptional regulation of cancer-related genes including those involved in proliferation (Westerheide, Mayo et al. 2001; Massoumi, Chmielarska et al. 2006; Park, Chung et al. 2006), apoptosis evasion (Kashatus,

Cogswell et al. 2006) and, more recently, cell motility and invasion (Massoumi, Kuphal et al. 2009; Miyazaki, Simizu et al. 2010) in a variety of cancer types.

The overall aim of this chapter was to more closely dissect mechanisms behind the BCL3-mediated effects on ERBB2-driven tumourigenesis identified in chapter 4. Firstly, in order to build upon previous *in vivo* results and to establish whether BCL3 deficiency directly influences tumour cell behaviour, a range of *in vitro* experiments utilising the MMTV/NK tumour-derived, MG1361 murine mammary cancer cell line were performed. Secondly, based on the previously identified involvement of NF- $\kappa$ B in the regulation of EMT and cancer stem/progenitor cell populations, the effect of BCL3 suppression on these cancer-associated processes was also evaluated. Finally, in an attempt to identify BCL3-regulated, cancer-associated genes, global gene expression analysis was performed on MG1361 cells subjected to BCL3 suppression.

## 5.2 Results

### 5.2.1 *Bcl3* is highly expressed in ERBB2-positive murine mammary cancer cell lines

Previous reports have demonstrated a strong association between ERBB2 receptor signalling and NF- $\kappa$ B activity in breast cancer (Biswas, Shi et al. 2004; Zhou, Eppenberger-Castori et al. 2005). In order to determine whether elevated *Bcl3* expression also correlates with ERBB2 status, *Bcl3* mRNA levels were analysed by QRT-PCR in two ERBB2-positive and three ERBB2-negative murine mammary cell lines (Figure 5.1). Four separate wells of each cell line were grown to 70% confluency and harvested for RNA isolation and subsequent cDNA preparation and QRT-PCR analysis. Gene expression was normalised to an internal control, *cyclophilin B*. Results show that the ERBB2-positive MG1361 and N202A cells, previously derived from *MMTV/NK* and *MMTV/N<sub>2</sub>* mammary tumour respectively (Sacco, Gribaldo et al. 1998; Nanni, Pupa et al. 2000), had significantly higher *Bcl3* expression than the N202E (ERBB2-negative) controls (N202E vs N202A, Mann–Whitney U-test,  $p=0.0304$ ; N202E vs MG1361, Mann–Whitney U-test,  $p=0.0304$ ). The other two ERBB2-negative cell lines (4T1 and Eph4) had comparable *Bcl3* mRNA expression to the N202E cells. These data suggest that, as with NF- $\kappa$ B subunits, high *Bcl3* expression correlates with ERBB2 positivity in murine mammary tumour cells.

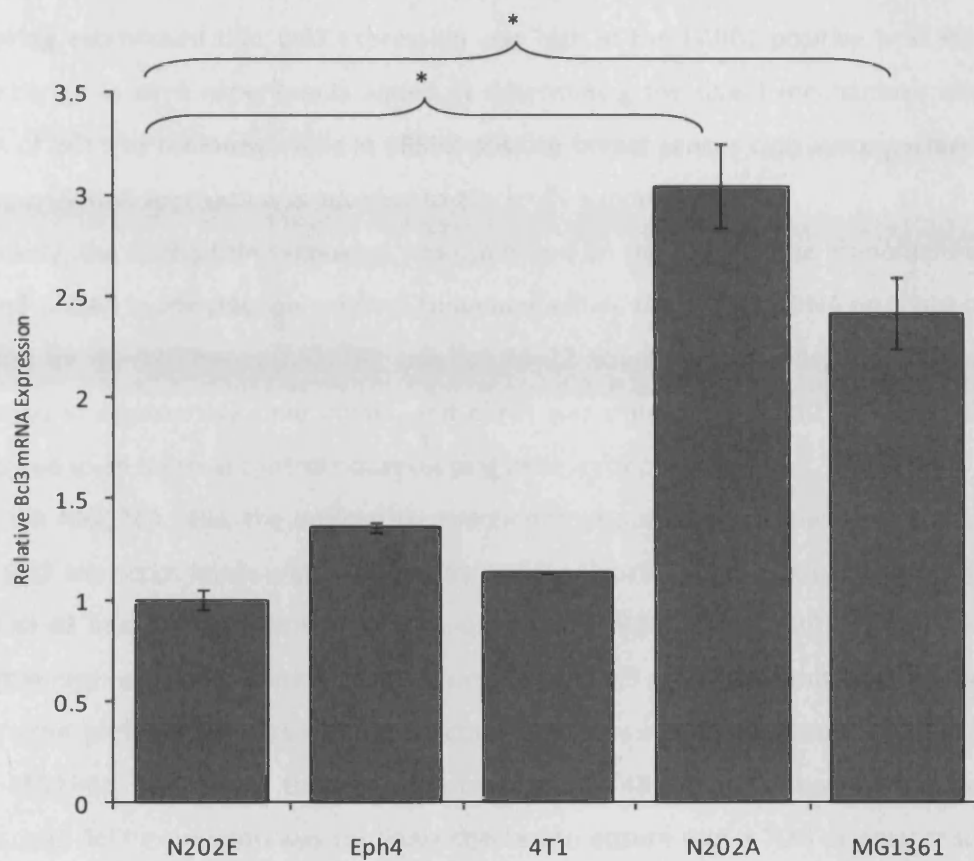


**Figure 5.1: Bcl3 expression is highest in ERBB2-positive murine mammary cancer cell line.**

QRT-PCR analysis of *Bcl3* mRNA expression in two ERBB2-positive and three ERBB2-negative murine cancer cell lines. *Bcl3* mRNA expression was significantly higher in the ERBB2-positive N202A and MG1361 cells in comparison to the ERBB2-negative N202E cells (\*=Mann-Whitney U-test,  $p=0.0304$ ). Four independent wells for each cell line were analysed. Error bars represent  $\pm$  SEM.

### 5.2.2 Optimisation of *Bcl3* SiRNA in MG1361 cells

Having established that *Bcl3* expression was high in the ERBB2-positive MG1361 and N202A cells, a number of *in vitro* experiments aimed at determining the direct mechanisms involved in the contribution of BCL3 to tumourigenesis in ERBB2-positive breast cancer cells were performed. In these experiments, an SiRNA approach was adopted to efficiently suppress *Bcl3*.

Initially, the *Bcl3* SiRNA technique was optimised on the basis of the manufacturer's protocol. The cells were plated in transfection medium containing either 10nM *Bcl3* SiRNA or 10nM control SiRNA and incubated for 48–120 hours (MG1361 cells) or 24–72 hours (N202A cells). Triplicate wells of cells were harvested at appropriate time points, and cDNA was prepared for QRT-PCR analysis. All results were normalised to an internal control housekeeping gene, *cyclophilin B*.

In the MG1361 cells, the optimal transfection time period was shown to be 48 hours, during which time *Bcl3* transcript levels were reduced by greater than 80% of constitutive levels (Figure 5.2A). Loss of *Bcl3* at 48 hours was confirmed by semi-quantitative PCR (Figure 5.2B). Transfection for longer periods of time also resulted in considerable suppression of *Bcl3* mRNA, but this was never equivalent to the 48 hour time period (72 hours = 60% reduction, 96 hours = 52% reduction, and 120 hours = 47% reduction). MG1361 cells were therefore transfected for 48 hours before all subsequent SiRNA experiments, and *Bcl3* expression was routinely checked to ensure that a 70% or greater suppression of transcript levels was achieved.

Optimisation of *Bcl3* knock-down was also attempted in N202A cells. However, these cells proved difficult to transfect, and at no time point were *Bcl3* transcript levels suppressed to below 50% of controls (Figure 5.2C, 24 hours = 44% reduction, 48 hours = 37% reduction, and 72 hours = 30% reduction). These cells were therefore not used for subsequent SiRNA experiments.

Three different BCL3 antibodies were used in an attempt to analyse BCL3 protein levels after transfection. However, after numerous attempts, none of the antibodies gave a clear band at the appropriate size for BCL3 and therefore knock-down at the protein level could not be confirmed in these murine cells.

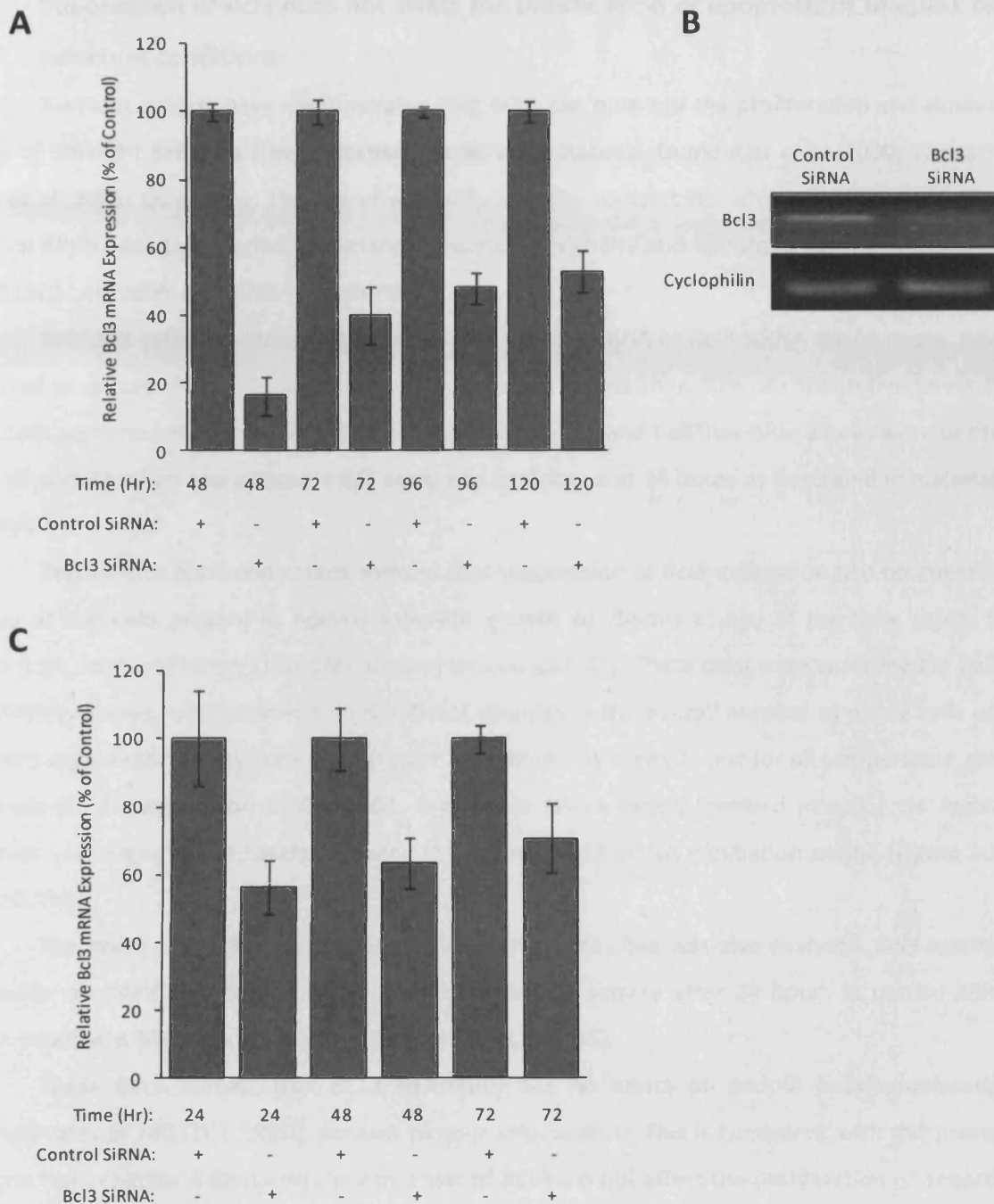


**Figure 5.2: Bcl3 SiRNA efficiently suppresses Bcl3 mRNA expression in MG1361 cells**

MG1361 cells were transfected for 48-120 hours with 10nM *Bcl3* or control SiRNA before being harvested for QRT-PCR analysis. *Bcl3* mRNA expression was most efficiently suppressed at 48 hours (A). Semi-quantitative PCR showing loss of *Bcl3* expression after SiRNA transfection for 48 hours (B). N202A cells were incubated for 24-72 hours with 10nM *Bcl3* or control SiRNA before being harvested for QRT-PCR analysis. *Bcl3* SiRNA did not suppress *Bcl3* mRNA expression to below 50% of constitutive levels at any time point analysed (C). Error bars represent  $\pm$  SEM.

### 5.2.3 Suppression of *Bcl3* does not affect the proliferation or apoptosis of MG1361 cells in adherent conditions

Previous reports have demonstrated that BCL3 can promote the proliferation and survival of a variety of different cell lines (Ong, Hackbarth et al. 1998; Rebollo, Dumoutier et al. 2000; Westerheide, Mayo et al. 2001; Dolgachev, Thomas et al. 2007). In order to establish whether BCL3 could have this effect on ERBB2-positive murine mammary tumour cells, viability and apoptosis assays were performed on MG1361 cells after *Bcl3* SiRNA transfection.

MG1361 cells were transfected with 10nM control SiRNA or *Bcl3* SiRNA for 48 hours. RNA was harvested to ensure that *Bcl3* expression was suppressed to less than 30% of constitutive levels and all other cells were reseeded into 96-well plates. Live cell counts and CellTiter-Blue assays were performed at 24, 48 and 72 hours and a caspase 3/7 assay was performed at 24 hours as described in materials and methods.

Trypan blue exclusion counts showed that suppression of *Bcl3* expression had no effect on the number of live cells present in normal adherent growth conditions at any of the time points tested (Figure 5.3A, Mann–Whitney U-test for all comparisons,  $p>0.05$ ). These data were confirmed in CellTiter-Blue viability assays, which showed no significant changes in the overall number of viable cells present after *Bcl3* suppression at any time point (Figure 5.3B, Mann–Whitney U-test for all comparisons,  $p>0.05$ ). Furthermore, the expression of *Cyclin D1*, a principle NF- $\kappa$ B target involved in cell cycle regulation, remained unchanged immediately following the 48 hour *Bcl3* SiRNA incubation period (Figure 5.3C, T-Test  $p>0.05$ ).

The ability of BCL3 to alter apoptosis rates in this cell line was also analysed. *Bcl3* suppression resulted in no significant differences in basal caspase 3/7 activity after 24 hours in normal adherent growth conditions (Figure 5.3D, Mann–Whitney U-test,  $p>0.05$ ).

These data suggest that BCL3 deficiency has no effect on overall basal proliferation or apoptosis rates in MG1361 ERBB2-positive tumour cells *in vitro*. This is consistent with the previous *in vivo* data from chapter 4 demonstrating that loss of BCL3 did not affect the proliferation or apoptosis of ERBB2-positive murine tumours.

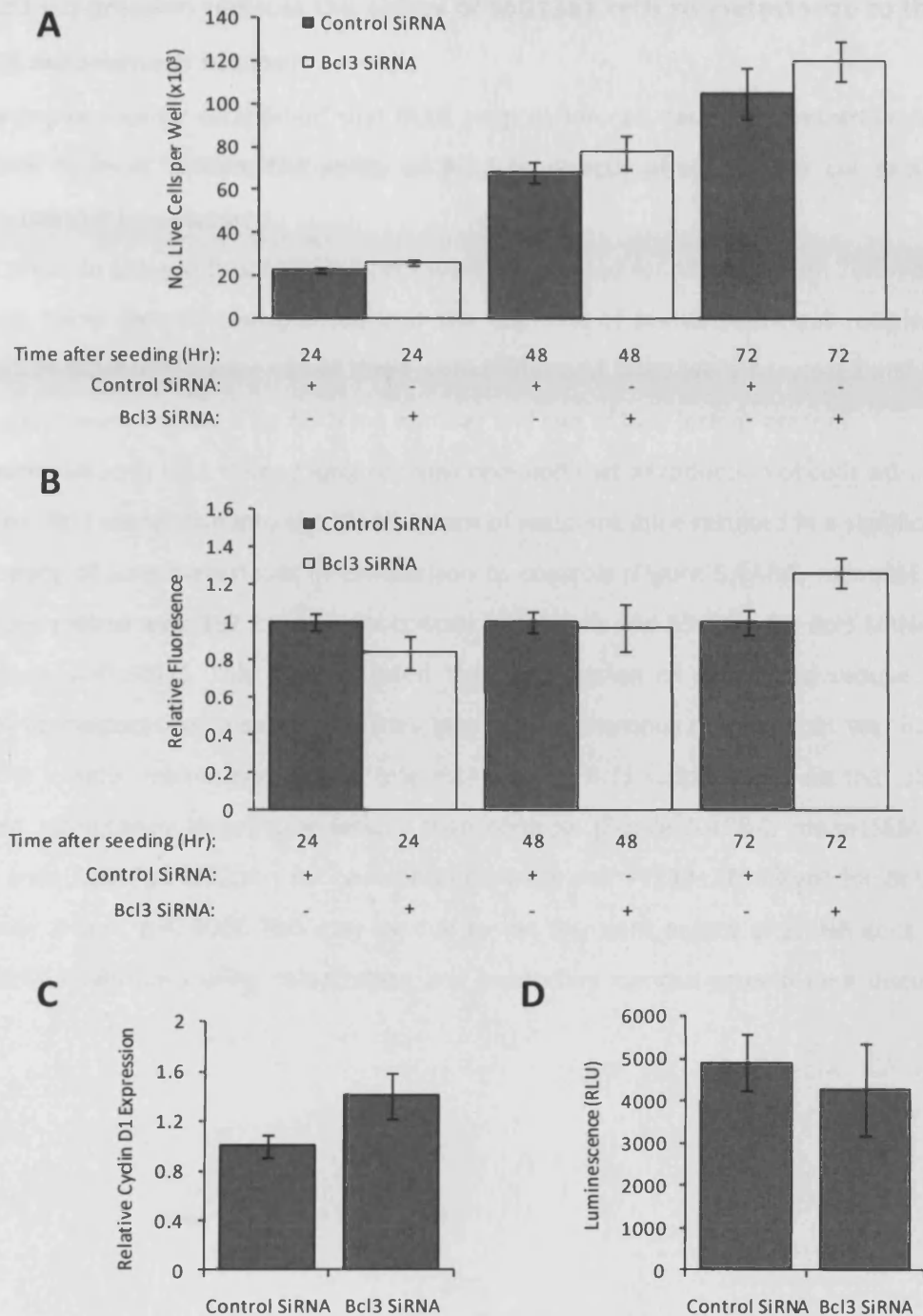


**Figure 5.3: Suppression of *Bcl3* does not affect the proliferation or apoptosis of murine MG1361 cancer cell lines in adherent growth conditions**

MG1361 cells were transfected with *Bcl3* or control SiRNA for 48 hours before being re-seeded into normal adherent growth conditions. Trypan blue exclusion counts (A) and CellTiter-Blue viability assays (B) were performed 24, 48 and 72 hours later. *Bcl3* suppression had no significant effects on the number of live cells per well (A) or on cell viability (B) at any time point tested (Mann-Whitney U-test for all comparisons,  $p > 0.05$ ). Error bars represent  $\pm$  SEM of 6 technical replicates. *Bcl3* suppression resulted in no significant differences in *Cyclin D1* mRNA expression (C, T-Test,  $p > 0.05$ ) or in basal caspase 3/7 activity after 24 hours in normal adherent growth conditions (D, Mann-Whitney U-test,  $p > 0.05$ ). Error bars represent  $\pm$  SEM of 3 technical replicates.

#### 5.2.4 *Bcl3* suppression reduces the ability of MG1361 cells to metastasize to the lungs in a cell autonomous manner

Having previously established that BCL3 suppression can delay the metastatic progression of ERBB2-positive tumours *in vivo*, the ability of BCL3 to directly affect tumour cell motility in a cell autonomous manner was assessed.

In order to achieve this, MG1361 cells were transfected for 48 hours with 10nM *Bcl3* or control SiRNA before being directly transplanted into the tail vein of immunodeficient recipient mice with normal levels of BCL3. Mice were culled three weeks later and lungs were harvested and fixed for H&E staining. Sections were analysed for both the number and size of lung lesions present.

Examination of H&E stained lung sections revealed that introduction of cells with less than 20% of constitutive *Bcl3* expression into the bloodstream of recipient mice resulted in a significant reduction in the frequency of lung metastases in comparison to controls (Figure 5.4A&C, mean $\pm$ SEM number of metastases per mouse was: 297.2 $\pm$ 140.3 for control SiRNA cells and 55 $\pm$ 29.3 for *Bcl3* SiRNA cells, Mann-Whitney U-test, p=0.0081). This demonstrated that suppression of *Bcl3* could reduce the ability of tumour cells to metastasize to secondary sites in a cell autonomous manner that was independent of effects on the tumour microenvironment. Interestingly, the *Bcl3* suppressed cells that did seed in the lungs formed significantly larger lung lesions than controls (Figure 5.4B&C, mean $\pm$ SEM area of lung metastases was: 40615 $\pm$ 19672 $\mu\text{m}^2$  for control SiRNA cells and 77233 $\pm$ 26538 $\mu\text{m}^2$  for *Bcl3* SiRNA cells, Mann-Whitney U-test, p=0.000). This may be due to the transient nature of SiRNA gene silencing and release of *Bcl3* inhibition during colonization and secondary tumour growth (see discussion section 5.3.1).

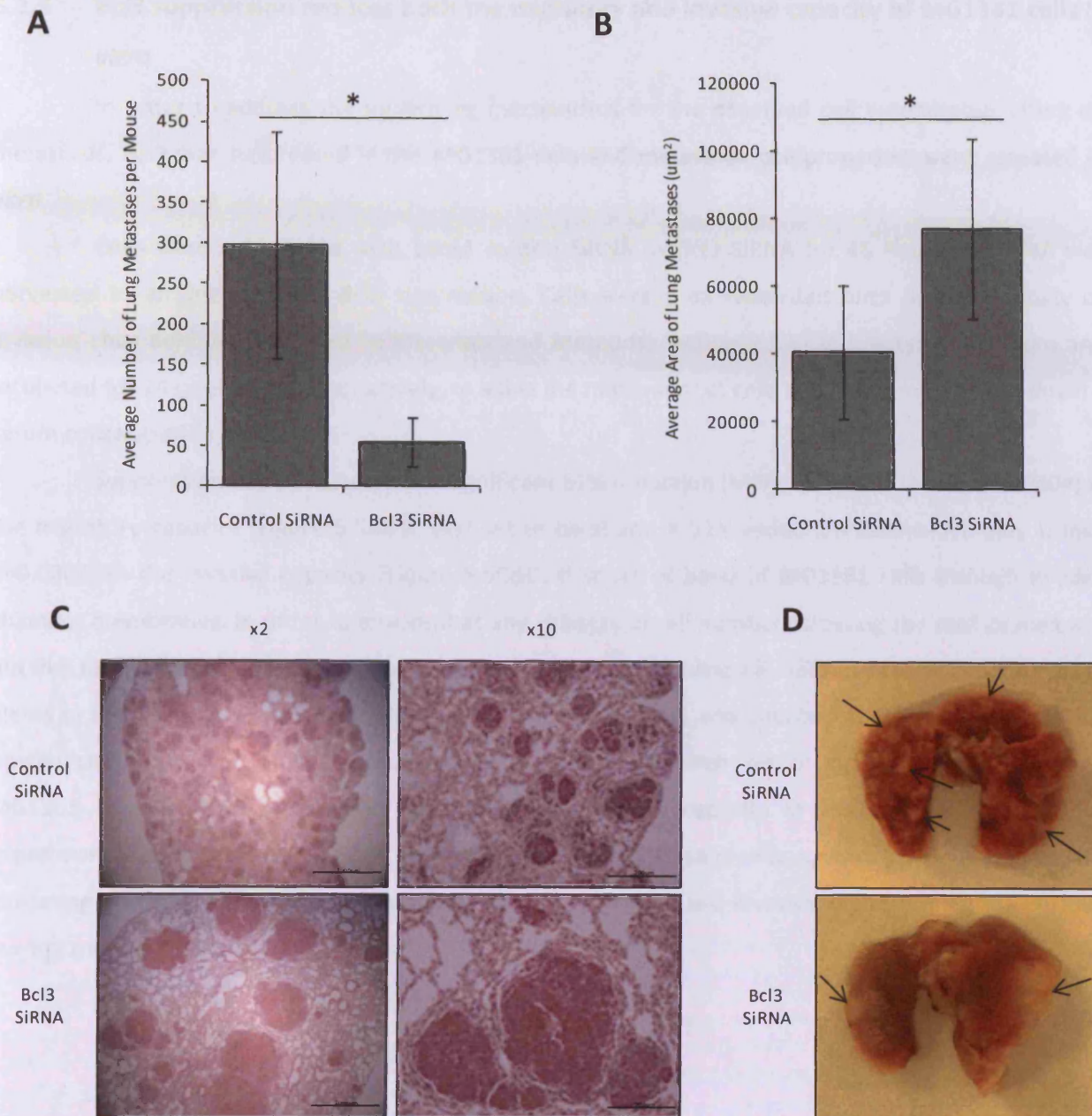


**Figure 5.4: *Bcl3* deficient cells are less able to seed in the lungs in an experimental metastases model**  
MG1361 cells were transfected with 10nM *Bcl3* or control SiRNA for 48 hours before being injected into the blood stream of immunodeficient mice (n=5) with normal BCL3 levels. Mice were culled three weeks later and lungs were harvested and fixed for H&E staining and analysis. *Bcl3* suppression significantly reduced the average number of metastases per mouse in comparison to controls (A, \*=Mann-Whitney U-test, p=0.0081). Lung metastases that did form from *Bcl3* suppressed cells were on average larger than controls (B, Mann-Whitney U-test, p=0.00). Error bars represent  $\pm$  SEM. Representative images of H&E stained lungs (C). Scale bars indicate: left panel 1000 $\mu$ m, right panel 200 $\mu$ m. Representative photographs of whole lungs immediately after dissection (D). Black arrows indicate visible lung metastases.

### 5.2.5 *Bcl3* suppression reduces both the migratory and invasive capacity of MG1361 cells *in vitro*

In order to address the underlying mechanisms for the observed cell autonomous effect on metastasis, *Bcl3* was suppressed in the MG1361 cells and metastatic cell properties were assessed *in vitro*.

Cells were transfected with 10nM control siRNA or *Bcl3* siRNA for 48 hours, and RNA was harvested to ensure sufficient *Bcl3* suppression. Cells were then re-seeded onto Boyden motility or invasion chambers (as described in Materials and Methods, section 2.5.8) in low-serum medium and incubated for 24 or 48 hours, respectively, to allow the movement of cells across the membranes down a serum concentration gradient.

Suppression of *Bcl3* resulted in a significant 61% reduction (Mann–Whitney U-test,  $p=0.0404$ ) in the migratory capacity (Figure 5.5A&B, first set of bars) and a 51% reduction (Mann–Whitney U-test,  $p=0.0205$ ) in the invasive capacity (Figure 5.5C&D, first set of bars) of MG1361 cells through Boyden chamber membranes. In order to ensure that any changes in cell numbers crossing the membranes was not due to reduced proliferation of the cells, parallel wells were plated in normal adherent tissue culture plates in low serum media for the duration of the experiments and counted at the same time as the Boyden chambers were fixed. Cell counts revealed that, as previously observed, depletion of *Bcl3* in the MG1361 cells did not significantly alter their proliferative capacity in the 24 hour or 48 hour experimental period (Figure 5.5B&D, second panel of bars). These results confirm previous *in vivo* data indicating that suppression of BCL3 reduces both the migratory and invasive capacity of ERBB2-positive murine tumour cells.

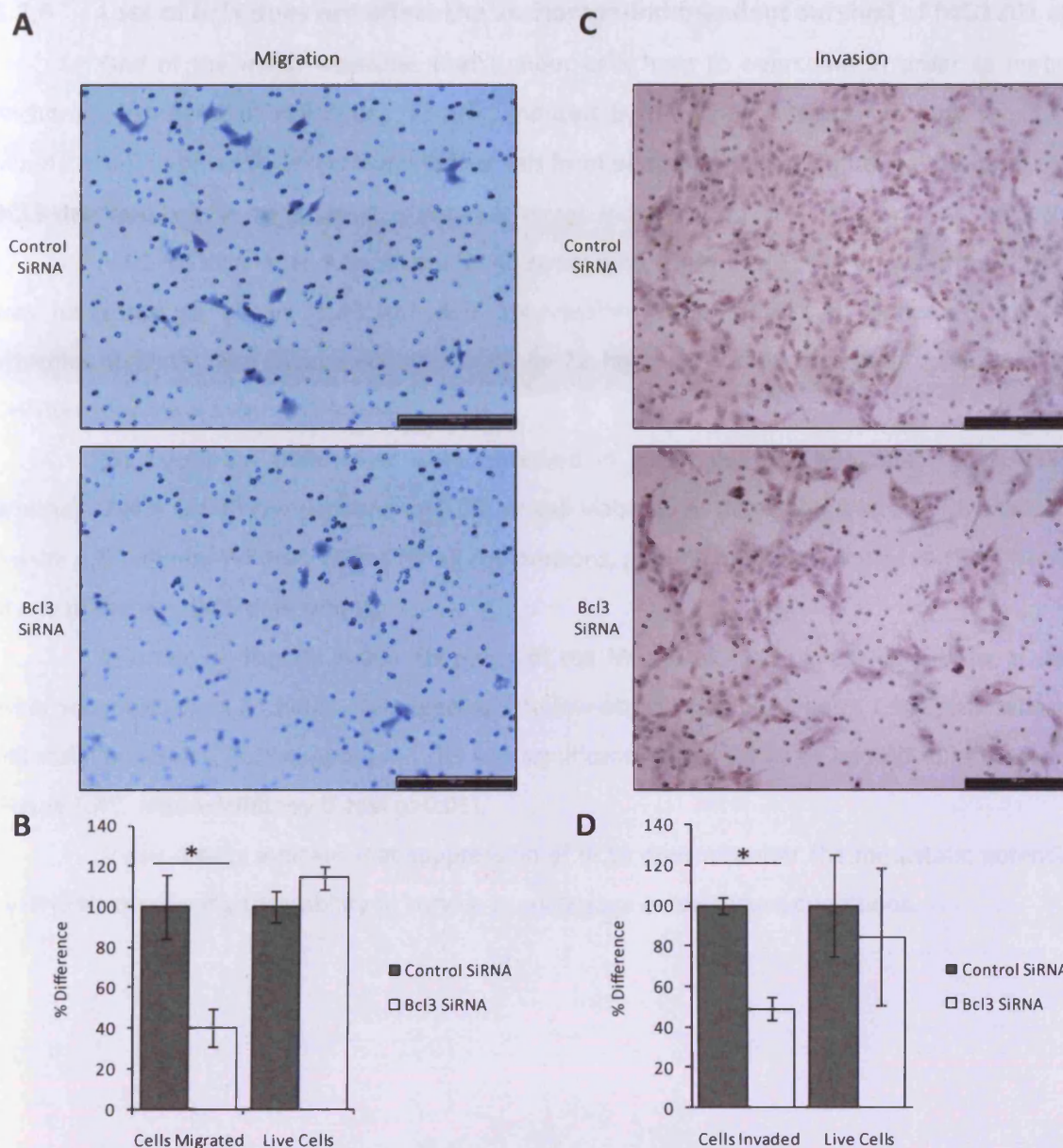


**Figure 5.5: *Bcl3* suppression reduces the migratory and invasive capacity of MG1361 murine mammary cancer cells**

MG1361 cells were transfected with *Bcl3* or control SiRNA for 48 hours before being plated onto Boyden motility or invasion chambers. Cells were left for 24 hours (for motility experiments) or 48 hours (for invasion experiments) before being fixed and stained on Boyden chamber membranes. Representative images of migrated cells (A) and invaded cells (C) fixed on Boyden chamber membranes are shown. Scale bars indicate 200 $\mu$ m. Migrated cells (B, first set of bars) or invaded cells (D, first set of bars) were counted from three fields of view of each of three replicate Boyden chambers and graphically represented as a percentage of the number of control cells counted (error bars represent  $\pm$  SEM of triplicate Boydens). Three parallel wells were plated for the duration of the experiments in normal adherent growth conditions in low serum media. Live cell counts were performed at the end of each experiment and represented as a percentage of the number of live control cells present (B&D, second set of bars, error bars represent  $\pm$  SEM of triplicate wells). *Bcl3* suppression resulted in a significant reduction in both the migratory capacity (B, \*=Mann-Whitney U-test,  $p=0.0404$ ) and the invasive capacity (D, \*=Mann-Whitney U-test,  $p=0.0205$ ) of MG1361 cells through Boyden chamber membranes. *Bcl3* suppression had no affect on the proliferation of cells in low serum media throughout the duration of the experiments (B&D, Mann-Whitney U-test,  $p>0.05$ ). 147

### 5.2.6 Loss of *Bcl3* does not affect the anchorage-independent survival of MG1361 cells

One of the major obstacles that tumour cells have to overcome in order to metastasise is anchorage-independent cell death (anoikis) induced by detachment from the bulk tumour into the bloodstream. In order to determine whether this form of apoptosis contributes to the reduced ability of BCL3-deprived cells to metastasise, *in vitro* anchorage-independent survival assays were performed.

MG1361 cells were transfected for 48 hours with 10nM *Bcl3* siRNA or a control siRNA, and RNA was harvested to ensure sufficient *Bcl3* suppression. Cells were then re-seeded into ultra-low-attachment plates and incubated for 24, 48 or 72 hours at which time-points live cell counts and CellTiter-Blue assays were performed.

No significant differences were observed in either live cell numbers (Figure 5.6A, Mann–Whitney U-test for all comparisons,  $p > 0.05$ ) or cell viability, as determined by the CellTiter-Blue assay; (Figure 5.6B, Mann–Whitney U-test for all comparisons,  $p > 0.05$ ) between control and *Bcl3*-depleted cells at any of the assessed time-points.

In order to directly assess apoptosis of the MG1361 cells in these conditions, a caspase 3/7 assay was performed 24 hours after seeding into low-attachment conditions. Consistent with the above cell viability results, *Bcl3* suppression did not significantly alter levels of apoptosis in these conditions (Figure 5.6C, Mann–Whitney U-test  $p > 0.05$ ).

These results indicate that suppression of BCL3 does not alter the metastatic potential of cells by directly decreasing their ability to survive in anchorage-independent conditions.

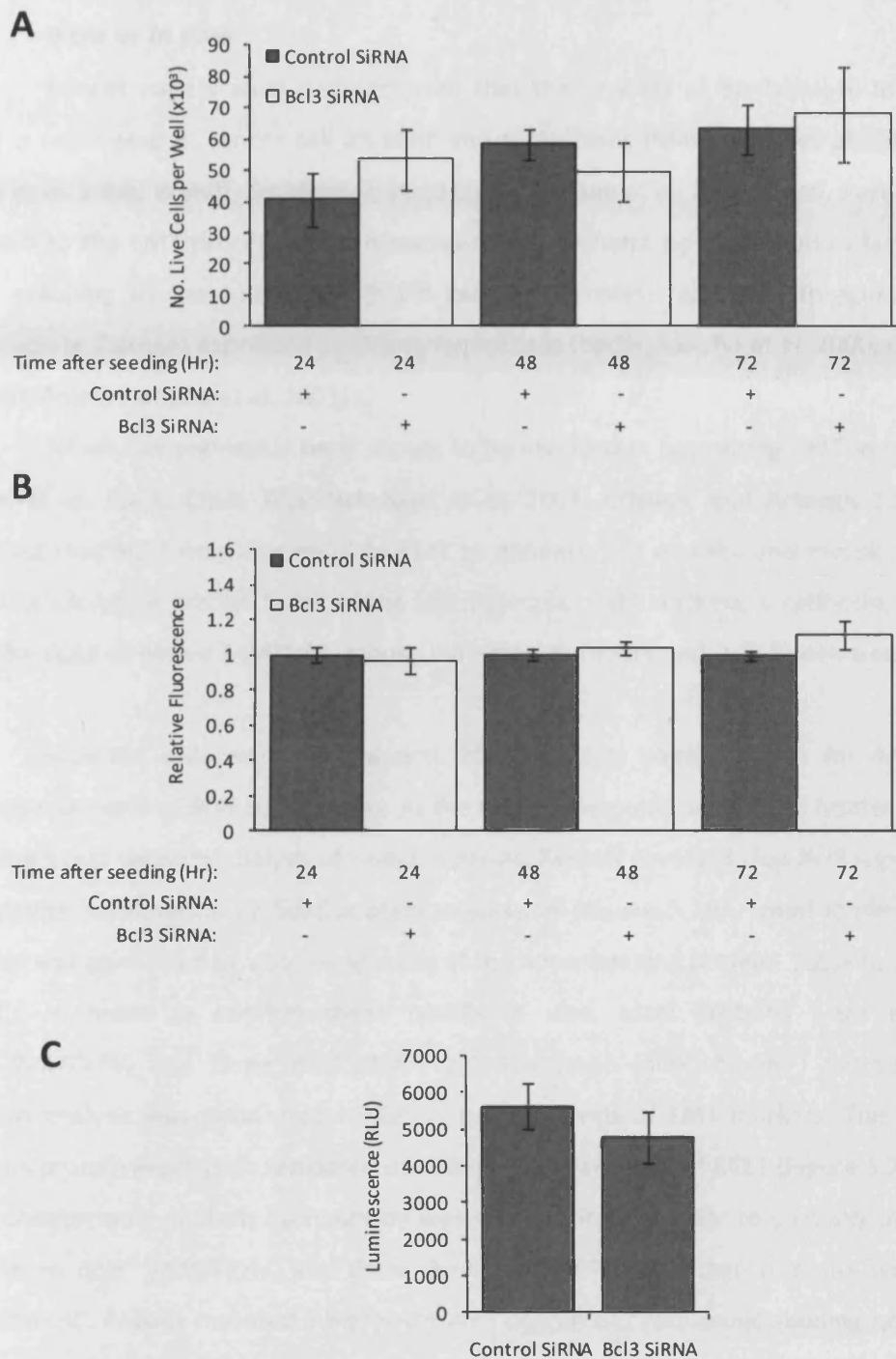


**Figure 5.6: *Bcl3* suppression does not affect the anchorage-independent survival of MG1361 murine mammary cancer cells**

MG1361 cells were transfected with *Bcl3* or control SiRNA for 48 hours before being re-plated into ultra-low attachment plates. Trypan blue exclusion counts (A) and CellTiter-Blue viability assays (B) were performed 24, 48 and 72 hours later. *Bcl3* suppression had no significant effect on the number of live cells per well (A) or on cell viability (B) at any time point tested (Mann-Whitney U-test for all comparisons,  $p > 0.05$ ). *Bcl3* suppression resulted in no significant differences in basal caspase 3/7 activity after 24 hours in anchorage-independent growth conditions (C, Mann-Whitney U-test,  $p > 0.05$ ). Error bars represent  $\pm$  SEM of 6 technical replicates.

### 5.2.7 Suppression of *Bcl3* does not alter epithelial-to-mesenchymal transition markers *in vitro* or *in vivo*

Recent papers have demonstrated that the process of epithelial-to-mesenchymal transition (EMT) is implicated in cancer cell invasion and metastases (Mani, Yang et al. 2007; Sarrío, Rodríguez-Pinilla et al. 2008; Wendt, Smith et al; 2010 Usami, Satake et al. 2008; Cano, Perez-Moreno et al. 2000). Essential to the EMT process is the repression of E-cadherin by transcription factors such as Snail and Slug resulting in the loss of epithelial cell–cell adhesion and the upregulation of Vimentin, an intermediate filament expressed in mesenchymal cells (Batlle, Sancho et al. 2000; Cano, Perez-Moreno et al. 2000; Bolos, Peinado et al. 2003).

NF- $\kappa$ B has previously been shown to be involved in promoting EMT in mammary cells (Huber, Azoitei et al. 2004; Chua, Bhat-Nakshatri et al. 2007; Criswell and Arteaga 2007). It was therefore proposed that BCL3 may also regulate EMT to enhance cell motility and invasion. This hypothesis was tested by analysing protein levels of the key molecular EMT markers, E-cadherin, Vimentin and Snail, in both the BCL3-depleted *MMTV/N<sub>2</sub>* mouse mammary tumours and *Bcl3* siRNA-treated mammary tumour cells.

MG1361 cells were treated with 10nM *Bcl3* or control siRNA for 48 hours and RNA was harvested to confirm *Bcl3* suppression. At the same time-point, whole cell lysates were extracted on ice for subsequent western analysis of target proteins. Results revealed that *Bcl3* suppression had no effect on E-cadherin, Vimentin or Snail protein expression (Figure 5.7A). Equal loading of protein between samples was confirmed by visualising levels of the housekeeping protein, Tubulin.

In order to confirm these results *in vivo*, total proteins were extracted from three *Bcl3<sup>+/+</sup>/MMTV/N<sub>2</sub>* and three *Bcl3<sup>-/-</sup>/MMTV/N<sub>2</sub>* late-stage (4000±50mm<sup>3</sup>) mouse mammary tumours. Western analysis was again used to detect protein levels of EMT markers. This demonstrated that E-cadherin protein expression remained unaltered in the absence of BCL3 (Figure 5.7B). Vimentin and Snail were undetectable in these tumours by western blotting. In order to partially overcome this, sections from three *Bcl3<sup>+/+</sup>/MMTV/N<sub>2</sub>* and three *Bcl3<sup>-/-</sup>/MMTV/N<sub>2</sub>* late-stage tumours were subjected to anti-Vimentin IHC. Results revealed a highly variable degree of cytoplasmic staining between samples within genotypes regardless of BCL3 status (Figure 5.7C), indicating that, within the samples analysed, BCL3 depletion did not correlate with loss of Vimentin in late-stage tumours.

Taken together these results suggest that BCL3 does not mediate a pro-metastatic phenotype by inducing EMT, as defined by these molecular markers of the process, in ERBB2-positive tumour cells either *in vitro* or *in vivo*.

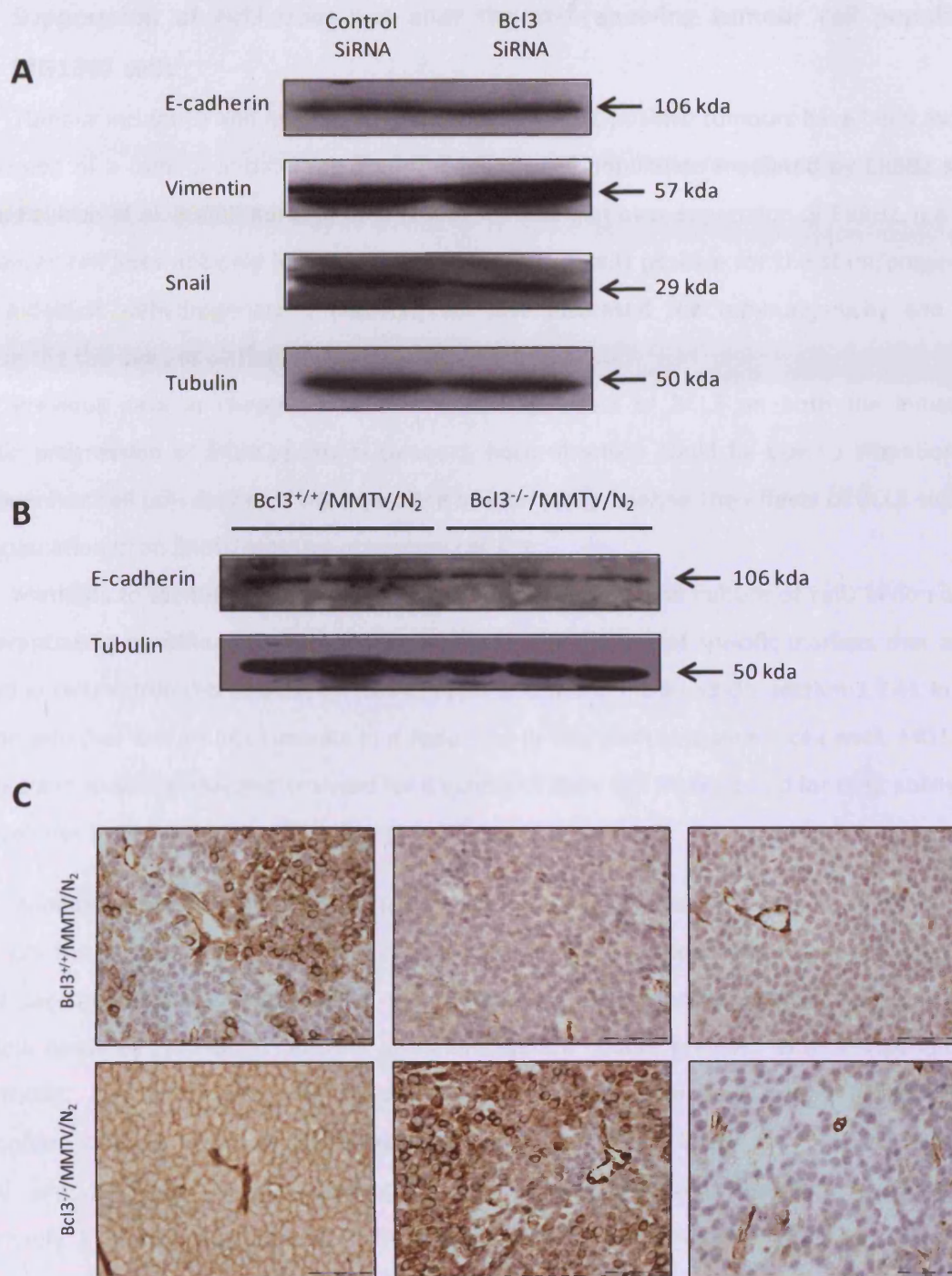


**Figure 5.7: Loss of *Bcl3* does not alter markers of EMT**

MG1361 cells were transfected with *Bcl3* or control SiRNA for 48 hours and protein was extracted and subjected to western analysis. Suppression of *Bcl3* had no effect on the protein expression of E-cadherin, Vimentin or Snail. Equal loading was confirmed by Tubulin (A). Protein from *Bcl3*<sup>+/+</sup>/MMTV/N<sub>2</sub> and *Bcl3*<sup>-/-</sup>/MMTV/N<sub>2</sub> tumours was extracted and subjected to western analysis. Loss of BCL3 had no effect on the expression of E-cadherin in MMTV/N<sub>2</sub> tumours. Equal loading was confirmed by Tubulin (B). Three *Bcl3*<sup>+/+</sup>/MMTV/N<sub>2</sub> and three *Bcl3*<sup>-/-</sup>/MMTV/N<sub>2</sub> tumours were subjected to anti-Vimentin IHC. Highly variable cytoplasmic staining was observed. This did not correlate with BCL3 status (C). Scale bars indicate 50µm.

### 5.2.8 Suppression of *Bcl3* does not alter the self-renewing tumour cell population in MG1361 cells

Tumour incidence and metastatic properties of ERBB2-positive tumours have been ascribed to the expansion of a tumour-initiating or stem/progenitor cell population mediated by ERBB2 signalling (Korkaya, Paulson et al. 2008). Korkaya et al (2008) showed that over-expression of ERBB2 in a panel of breast cancer cell lines not only increased the proportion of cells positive for the stem/progenitor cell marker, aldehyde dehydrogenase 1 (ALDH1), but also increased the tumourigenicity and invasive capacity of the this cell population.

Previous data in chapter 4 showed a striking effect of BCL3 on both the initiation and metastatic progression of ERBB2-positive tumours, both of which could be due to alterations in the stem/progenitor cell population. It was therefore of interest to analyse the effects of BCL3 suppression on this population in an ERBB2-positive mammary cell line.

Methods to identify stem/progenitor cell populations include culture of cells in non-adherent, non-differentiating conditions to form mammospheres and the use of specific markers that are highly expressed in cells within this population (see Chapter 1: General Introduction, section 1.2.4). In order to determine whether loss of BCL3 results in a reduction in the stem/progenitor cell pool, MG1361 cells were subjected to *Bcl3* SiRNA and analysed for a variety of stem cell markers and for their ability to form mammospheres in non-adherent cell culture conditions.

#### 5.2.8.1 *Analysing the effect of Bcl3 depletion on mammosphere formation*

On the basis of established cell culture conditions for tumour-initiating mammary cells, the ability of parental MG1361 cells to form mammospheres was assessed. Single cells were plated at various low densities (500–8000 cells/ml) in mammosphere culture medium as described in materials and methods. After incubation for 7 days, MG1361 cells generated clearly defined spherical mammosphere colonies at all seeding densities (Figure 5.8A). The number of mammospheres formed increased proportionally to the seeding density, with a mammosphere-forming frequency of approximately 1 in 100 (Figure 5.8B, light grey line), demonstrating that, at all seeding densities, mammospheres and not aggregates of bulk tumour cells were formed.

In order to show that the mammosphere structures formed contain cells that are capable of self-renewal, the sphere-initiating ability of passaged primary MG1361 mammospheres was analysed. Primary mammospheres were dissociated into single cells, re-plated at low densities (500–8000 cells/ml) and incubated for a further 7 days. The mammosphere-forming frequency increased from approximately 1 in 100 to between 2 and 5 in 100 (Figure 5.8B, passage 1 vs passage 2), demonstrating that the MG1361 mammospheres contain cells capable of self-renewal and secondary mammosphere formation.

Having established that MG1361 cells are able to form mammospheres containing cells with self-renewal capacity, the effect of *Bcl3* suppression on mammosphere formation was analysed. Cells were treated with 10nM *Bcl3* or control siRNA for 48 hours and RNA was harvested for subsequent QRT-PCR analysis to confirm *Bcl3* suppression. Single cells (4000 cells/ml) were re-seeded into ultra-low-attachment plates in mammosphere medium and incubated for 7 days. Figure 5.8C shows that initial *Bcl3* suppression did not result in a reduction in the percentage of mammosphere-forming units within the cell population (mean $\pm$ SEM % mammosphere-forming units was 2.32 $\pm$ 0.68% for control cells and 1.87 $\pm$ 0.53% for *Bcl3*-suppressed cells; T-test,  $p>0.05$ ). This indicates that BCL3 does not affect the size of the original stem/progenitor cell population in this cell line.

It has previously been reported that the number of mammospheres generated upon serial passage indirectly reflects the ability of the stem cells within them to self-renew and the size of the passaged mammospheres reflects progenitor cell proliferation capacity (Dontu, Abdallah et al. 2003). Also, primary mammary cells isolated from murine ERBB2-positive mammary tumours, harbouring a genetic alteration of IKK $\alpha$  to globally inhibit NF- $\kappa$ B signalling, were capable of forming primary mammospheres but could not form secondary mammospheres upon serial passage (Cao, Luo et al. 2007), indicating that inhibition of NF- $\kappa$ B impairs stem cell self-renewal ability. It was therefore of interest to passage on primary mammospheres into secondary culture to analyse the effect of BCL3 deficiency on their initial self-renewal capacity.

MG1361 cells were transfected with 10nM *Bcl3* or control siRNA for 48 hours. RNA was harvested to ensure sufficient *Bcl3* suppression and 4000 cells/ml were seeded into ultra-low-attachment plates in mammosphere medium and incubated for 7 days. Primary mammospheres were then enzymatically dissociated into single cells, re-plated at 4000 cells/ml into ultra-low-attachment plates, and incubated for a further 7 days to allow the formation of secondary mammospheres.

As previously demonstrated, *Bcl3* suppression did not significantly decrease the size or number of primary mammospheres (Figure 5.8D). Secondary passage of cells resulted in an increase in the percentage of mammosphere-forming units in both the control and *Bcl3*-suppressed cells (from 2.32% to 5.48% in control cells and from 1.87% to 4.72% in *Bcl3*-suppressed cells, Figure 5.8D), suggesting that both cell populations contain cells with self-renewal capacity. However, there was no significant difference in the size or number of secondary mammospheres formed between the *Bcl3*-suppressed and control cells (Figure 5.8D&E, mean $\pm$ SEM % secondary passage mammosphere-forming units was 5.48 $\pm$ 2% for control cells and 4.72 $\pm$ 1.57% for *Bcl3*-suppressed cells; T-test,  $p>0.05$ ).

These data suggest that early suppression of *Bcl3* does not alter the size or the self-renewal ability of the stem/progenitor cell populations within the MG1361 cell line. Clearly, a major limitation to this experiment is that suppression of *Bcl3* with siRNA is temporary. The assay therefore only evaluates

the effects of BCL3 on the initial anoikis-resistant cell population and the subsequent consequences that this early inhibition has on their self-renewal ability.

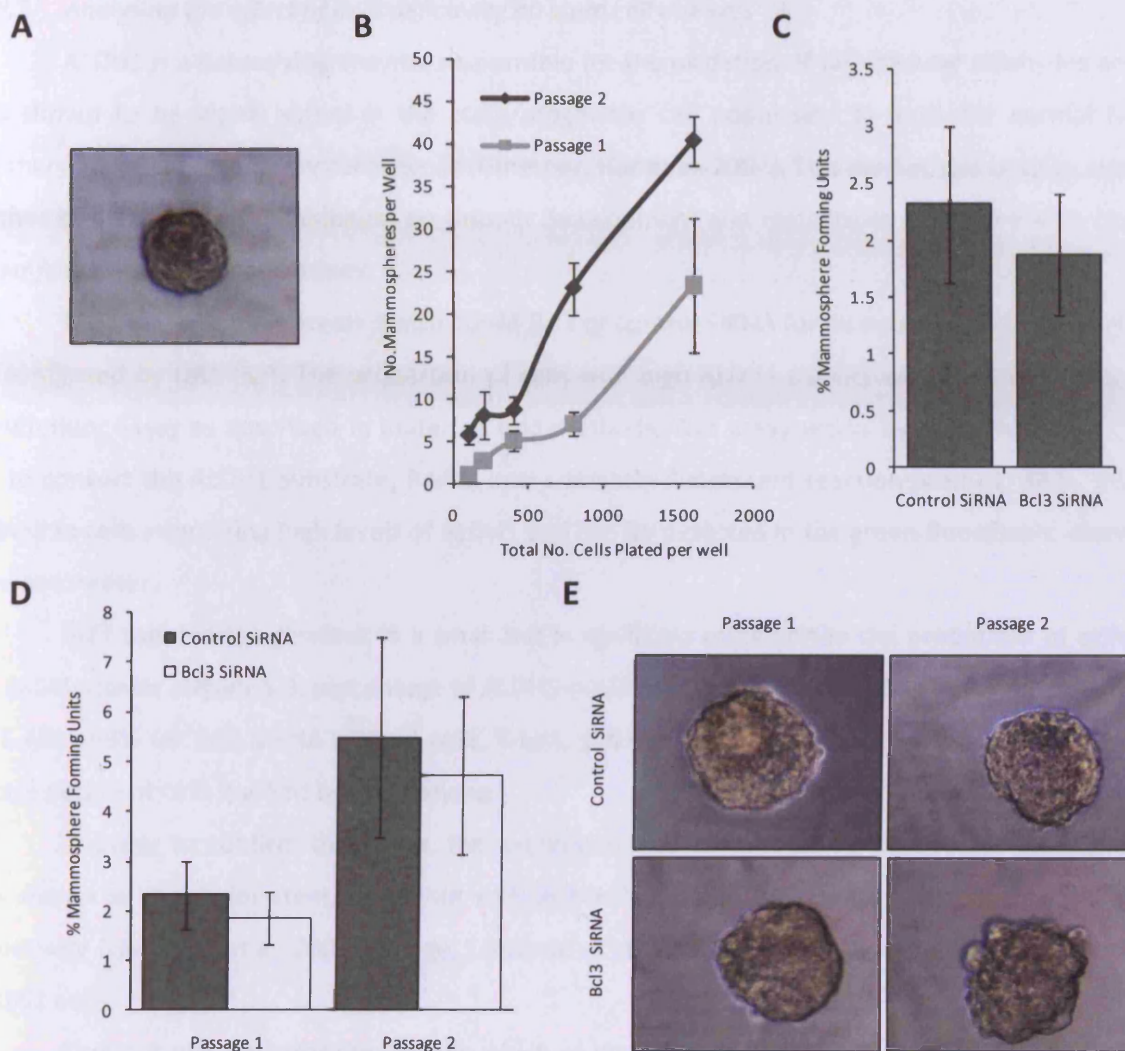


**Figure 5.8: *Bcl3* suppression has no effect on the formation of primary or secondary mammospheres**

MG1361 cells form spherical mammospheres in low attachment conditions (A). Mammospheres form at a range of seeding densities and are composed of cells that are able to self-renew as demonstrated by increased mammosphere numbers in secondary passages (B). MG1361 cells were transfected with *Bcl3* or control SiRNA for 48 hours and plated in mammosphere culture conditions for 7 days. *Bcl3* suppression had no significant effect on the formation of primary mammospheres (C, T-test,  $p > 0.05$ ). The percentage of mammosphere forming units increased upon secondary passaging but this was unaffected by *Bcl3* suppression (D, T-test,  $p > 0.05$ ). *Bcl3* suppression had no effect on the size of primary or secondary mammospheres (E). All data represent the mean of three independent transfection experiments and error bars represent  $\pm$  SEM.

### 5.2.8.2 Analysing the effect of *Bcl3* deficiency on stem cell markers

ALDH1 is a detoxifying enzyme responsible for the oxidation of intracellular aldehydes and has been shown to be highly active in the stem/progenitor cell population in both the normal human mammary gland and mammary carcinomas (Ginestier, Hur et al. 2007). This marker was used to establish whether the effect of BCL3 inhibition on tumour development and metastases correlated with changes in stem/progenitor cell populations.

MG1361 cells were treated with 10nM *Bcl3* or control siRNA for 48 hours, and *Bcl3* suppression was confirmed by QRT-PCR. The proportion of cells with high ALDH1 activity was then measured using the Aldefluor assay as described in materials and methods. This assay works by assessing the ability of cells to convert the ALDH1 substrate, BAAA, into a brightly fluorescent reaction product, BAA-, which is retained in cells expressing high levels of ALDH1 and can be detected in the green fluorescent channel of a flow cytometer.

*Bcl3* suppression resulted in a small but insignificant reduction in the proportion of cells with high ALDH activity (Figure 5.9, percentage of ALDH1-positive cells  $\pm$  SEM was  $8.01 \pm 1.24\%$  for control cells and  $6.83 \pm 1.98\%$  for *Bcl3* siRNA treated cells, T-test,  $p > 0.05$ ), indicating that it has little or no effect on the population of cells marked by this enzyme.

In order to confirm this result, the expression of CD24 and SCA1 which have independently been shown to enrich for stem/progenitor cells in *MMTV/N<sub>2</sub>* and *MMTV/NK* tumour cell populations, respectively (Liu, Deng et al. 2007; Grange, Lanzardo et al. 2008), were also assessed in *Bcl3* suppressed MG1361 cells.

Firstly, it was necessary to identify which of these markers enriched for tumour initiating cells in the MG1361 cell line. This was achieved by sorting the parental cells for CD24 and SCA1 expression and then plating cells from each quadrant under mammosphere growth conditions. When cells were plated at 2000 cells/ml, both of the CD24+ populations had a higher percentage of mammosphere forming units than the CD24- populations. This was significant in the CD24+/SCA1- population in comparison to all other quadrants and unsorted control cells (Figure 5.10, mean  $\pm$  SEM percentage of mammosphere forming units was  $3.2 \pm 0.52\%$  for CD24+/SCA1- cells in comparison to  $1.8 \pm 0.23\%$  in unsorted controls,  $0.75 \pm 0.27\%$  in SCA+/CD24- cells,  $1.16 \pm 0.23\%$  in SCA1-CD24- cells and  $1.75 \pm 0.37\%$  in SCA1+/CD24+ cells, T-test for percent of CD24+/SCA1- mammosphere forming units compared to cells from any other quadrant or unsorted controls,  $p < 0.05$ ). This indicated that in concordance with Liu et al. (2007), MG1361 tumour initiating cells, as defined by the mammosphere functional assay, were enriched in the CD24-positive population.

To assess whether loss of BCL3 resulted in a reduction in this CD24-positive population, MG1361 cells were treated with 10nM *Bcl3* or control siRNA for 48 hours and analysed on the basis of

CD24 or SCA1 expression. Interestingly, *Bcl3* depletion actually resulted in an increase in both of the CD24-positive populations (Figure 5.11). Loss of *Bcl3* significantly increased the percentage of CD24+/SCA1- cells from 19.8% to 26.9% (Figure 5.11B, far left graph, T-test,  $p=0.000023$ ) and the percentage of CD24+/SCA1+ cells from 13.72% to 16.8% (Figure 5.11B, far right graph, T-test,  $p=0.0048$ ) in comparison to controls.

These data show that, although the CD24-positive population enriches for mammospheres in the MG1361 cells, loss of BCL3 surprisingly does not deplete, but instead increases this population.

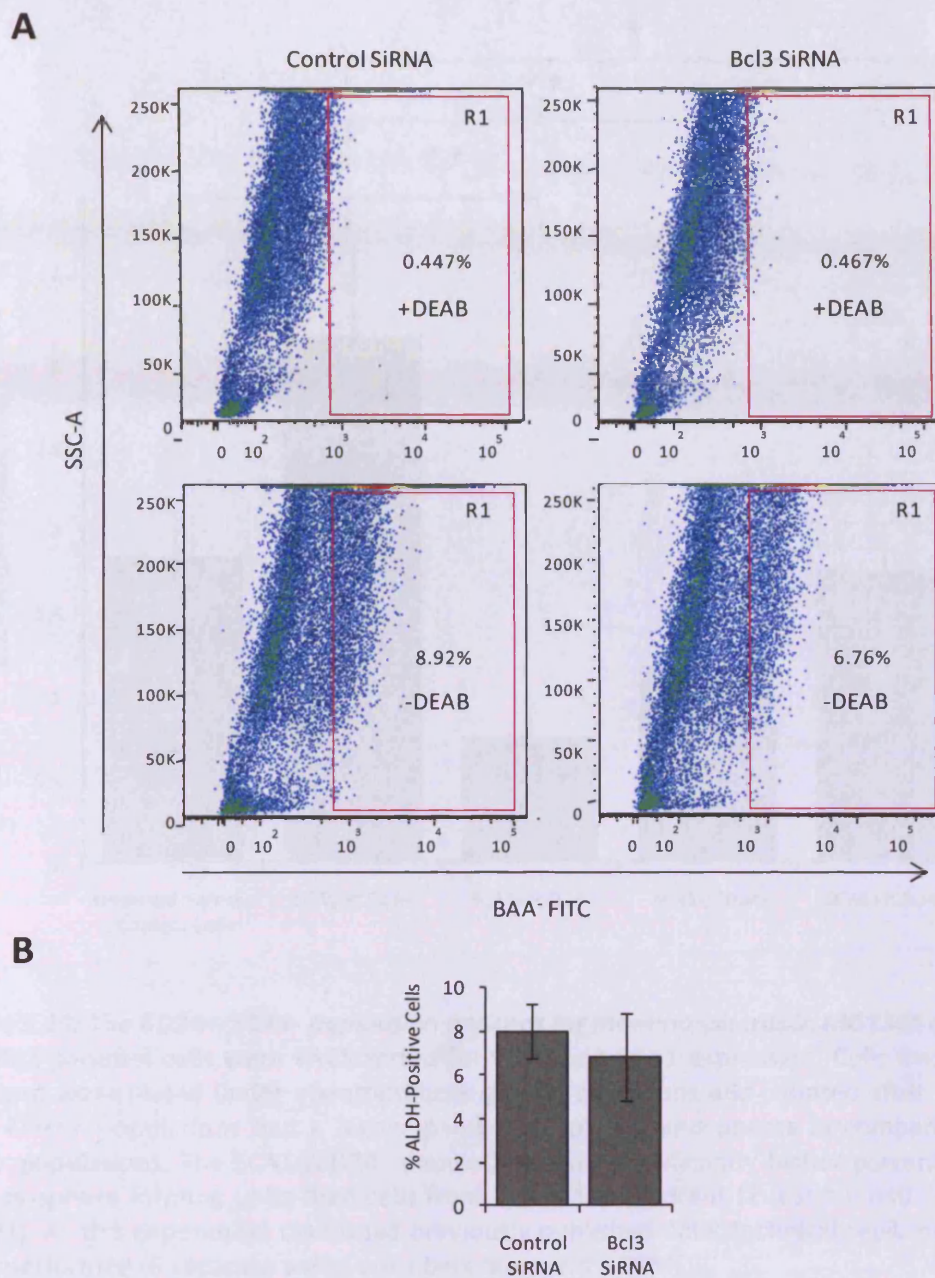


**Figure 5.9: Loss of *Bcl3* results in an insignificant reduction in the ALDH1-positive population in MG1361 murine mammary cancer cells**

MG1361 cells were transfected with *Bcl3* or control SiRNA for 48 hours before being subjected to the Aldeflour assay. Representative FACS plots of MG1361 cells (A). Cells incubated with the Aldeflour substrate (BAAA) and the specific inhibitor of ALDH, DEAB, were used as a control to establish the base-line fluorescence of the cells and to define the ALDH1 –positive region (R1) (top row, A). Incubation of cells with the Aldeflour substrate in the absence of DEAB induced a shift in BAAA fluorescence into the ALDH1-positive (R1) region in both control and *Bcl3* SiRNA treated cells (bottom row, A). Suppression of *Bcl3* resulted in an insignificant reduction in the percentage of ALDH1-positive cells (B, T-Test,  $p > 0.05$ ). Results are representative of three independent experiments and error bars represent  $\pm$  SEM.

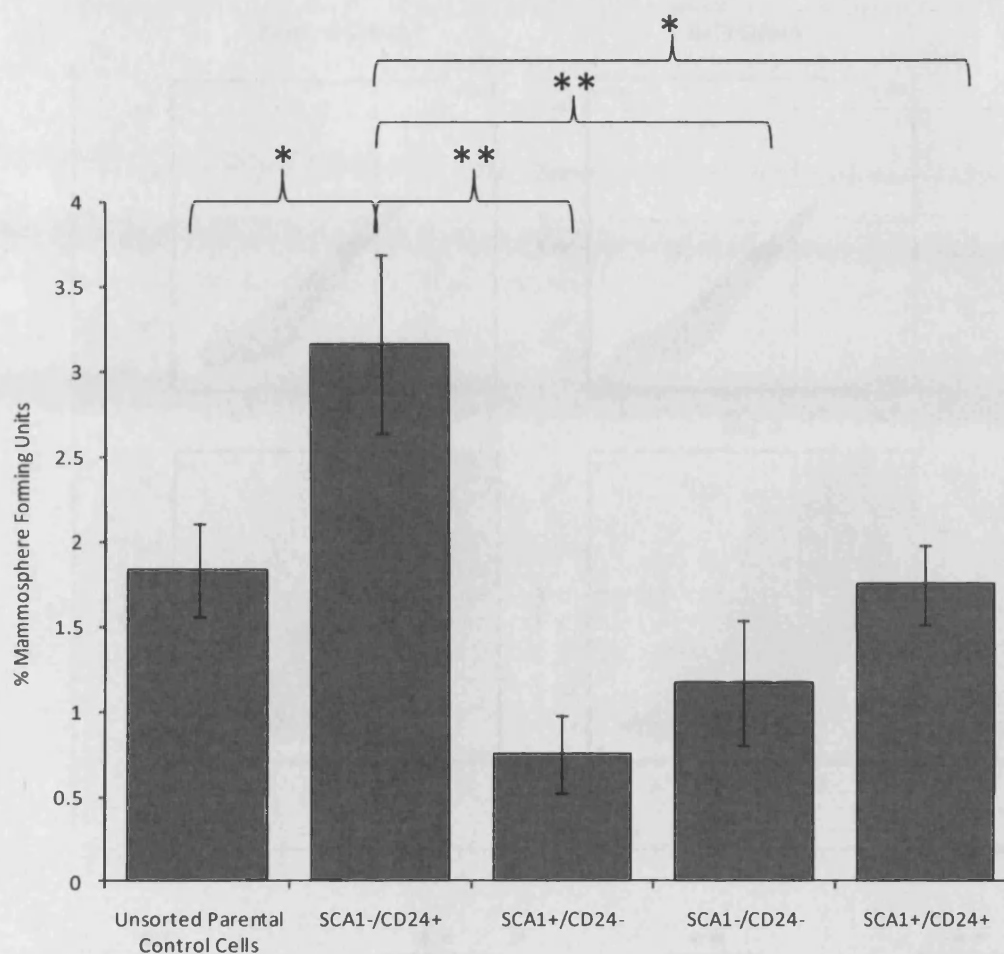


**Figure 5.10: The CD24+/SCA1- population enriches for mammospheres in MG1361 cells**

MG1361 parental cells were FACS sorted for CD24 and SCA1 expression. Cells from each quadrant were plated under mammosphere growth conditions and counted after 7 days. Both CD24+ populations had a higher percentage of mammospheres in comparison to CD24- populations. The SCA1-/CD24+ population had a significantly higher percentage of mammosphere forming units than cells from any other quadrant (T-test, \* =  $p < 0.05$ , \*\* =  $p < 0.01$ ). As this experiment confirmed previously published data, technical replicates only were performed (6 separate wells, error bars represent  $\pm$  SEM).

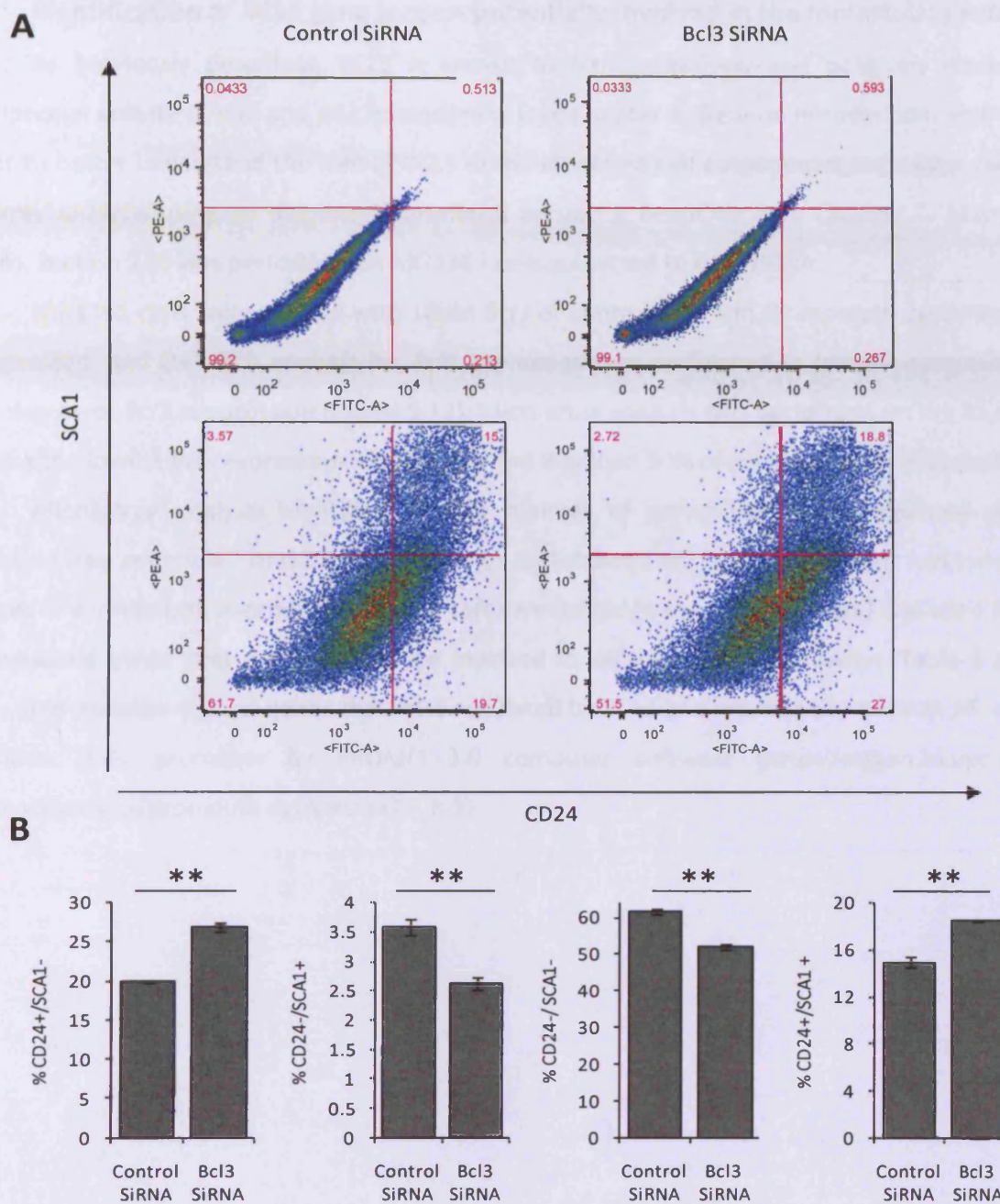


**Figure 5.11: *Bcl3* suppression increases the CD24<sup>+</sup> population in MG1361 cells**

MG1361 cells were transfected with *Bcl3* or control SiRNA for 48 hours before being analysed on the basis of CD24 and SCA1 expression. Representative FACS plots of MG1361 control (A, left panel) and *Bcl3* (A, right panel) SiRNA treated cells using CD24 and SCA1 cell surface markers are shown. Relevant isotype controls were used to establish the base-line fluorescence of the cells and to enable gates to be set (A, top row). The average percentage of cells in each quadrant was calculated and represented graphically (B). Suppression of *Bcl3* resulted in a significant increase in the percentage of CD24<sup>+</sup>/SCA1<sup>+</sup> and CD24<sup>+</sup>/SCA1<sup>-</sup> cells and a significant decrease in the percentage of CD24<sup>-</sup>/SCA1<sup>+</sup> and CD24<sup>-</sup>/SCA1<sup>-</sup> cells (B, T-test, \*\*= $p < 0.01$ ). Data is representative of three independent *Bcl3* SiRNA experiments performed on the same day and error bars represent  $\pm$  SEM. The experiment was also repeated on a different day and similar results were obtained (data not shown).

### 5.2.9 Identification of BCL3 gene targets potentially involved in the metastatic process

As previously described, BCL3 is known to both negatively and positively modulate the transcriptional activity of p50 and p52 homodimers (see Chapter 1: General Introduction, section 1.4.4). In order to better understand the role of BCL3 in the identified cell autonomous metastatic phenotype, microarray analysis using an Illumina MouseRef-8 version 2 BeadChip (see Chapter 2: Materials and Methods, section 2.9) was performed on MG1361 cells subjected to *Bcl3* SiRNA.

MG1361 cells were treated with 10nM *Bcl3* or control SiRNA in six separate experiments. RNA was harvested, and QRT-PCR analysis for *Bcl3* expression was performed to identify samples with the largest degree of *Bcl3* suppression (Figure 5.12). Microarray analysis was performed on the four samples displaying the lowest *Bcl3* expression, all of which had less than 30% of constitutive *Bcl3* transcript levels.

Microarray analysis identified a large number of genes that were regulated upon *Bcl3* suppression (see appendix 1 and 2 for lists of genes that showed the largest significant fold increases and decreases in expression). Ingenuity computer software (<http://www.ingenuity.com>) was used to identify BCL3-regulated genes that are known to be involved in cell motility and invasion. Table 5.1 lists the motility- and invasion-related genes that were regulated by BCL3 and predicted to have an NF- $\kappa$ B binding site within their promoter by PROMO 3.0 computer software ([http://algggen.lsi.upc.es/cgibin/promo\\_v3/promo/promoinit.cgi?dirDB=TF\\_8.3](http://algggen.lsi.upc.es/cgibin/promo_v3/promo/promoinit.cgi?dirDB=TF_8.3)).

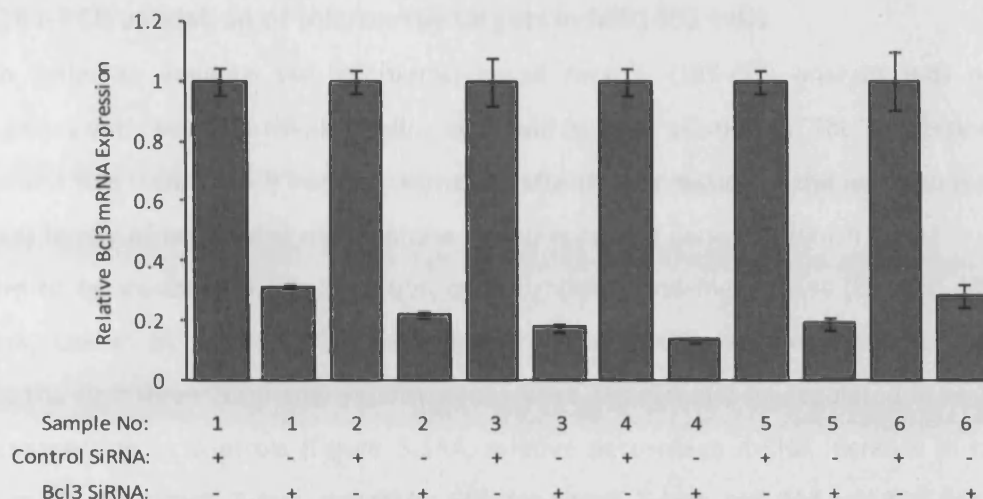


**Figure 5.12: Selection of MG1361 RNA samples for microarray analysis**

MG1361 cells were independently transfected with *Bcl3* or control SiRNA 6 times. RNA was harvested, cDNA was prepared and QRT-PCR analysis for *Bcl3* expression was performed to identify samples with the greatest *Bcl3* suppression. As a result of this analysis, samples 2, 3, 4 and 5 were sent for microarray analysis. Error bars represent  $\pm$  SEM of 3 technical replicates.

Accession Number	Definition	P-Value
NM_008704.2	Non-metastatic cells 1 (NM23A; (Nme1),	0.00092
NM_008705.4	Non-metastatic cells 2 (NM23B; Nme2)	0.00062
NM_019730.1	Non-metastatic cells 3 (Nme3)	0.00332
NM_019731.1	Non-metastatic cells 4 (Nme4)	0.000006
NM_011593.2	Tissue inhibitor of metalloproteinase 1 (Timp1)	0.00395
NM_011594.3	Tissue inhibitor of metalloproteinase 2 (Timp2)	0.00633
NM_011595.2	Tissue inhibitor of metalloproteinase 3 (Timp3)	0.00490
NM_007616.3	Caveolin 1 (Cav1)	0.00086
NM_007486.1	Rho, GDP dissociation inhibitor (GDI) beta (Arhgdib)	0.00121
NM_010288.2	Gap junction membrane channel protein alpha 1 (Gja1)	0.00412
NM_010688.2	LIM and SH3 protein 1 (Lasp1)	0.000979
NM_024454.1	Member RAS oncogene family (Rab21),	0.00081
NM_021356.2	Growth factor receptor bound protein 2-associated protein 1 (Gab1)	0.00980
NM_010513.2	Insulin-like growth factor I receptor (Igf1r)	0.001812
NM_020011.4	Sphingosine kinase 2 (Sphk2)	0.000183
NM_009335.1	Transcription factor AP-2, gamma (Tcfap2c)	0.002948
NM_011577.1	Transforming growth factor, beta 1 (Tgfb1)	0.003077

**Table 5.1: Motility and invasion related genes regulated by BCL3**

MG1361 cells were transfected with *Bcl3* or control SiRNA for 48 hours. Four independently transfected samples were analysed by microarray. BCL3-regulated invasion- and motility-related genes with putative NF- $\kappa$ B binding sites are listed.

### 5.2.10 QRT-PCR validation of microarray targets in MG1361 cells

In order to validate the microarray-based results, QRT-PCR analysis was performed on candidate genes with putative NF- $\kappa$ B binding sites within their promoters. The expression of all genes was normalised to a *cyclophilin B* internal control. Firstly, the expression of the first four members of the *Nme* (NM23) family of nucleoside diphosphate kinase encoding genes, of which *Nme1* in particular has been shown to be involved in the inhibition of cell motility and metastases (Boissan, Wendum et al. 2005; Horak, Lee et al. 2007; McDermott, Boissan et al. 2008) were verified. As observed in the microarray, the first three *Nme* anti-motility genes were significantly up-regulated in response to *Bcl3* SiRNA in comparison to controls (Figure 5.13A, relative percentage mRNA increase in comparison to controls was 57% for *Nme1*, T-test,  $p=0.0076$ ; 56% for *Nme2*, T-test,  $p=0.044$  and 36% for *Nme3*, T-test,  $p=0.038$ ). *Nme4* was also up-regulated but this was not found to be significant (54% upregulation, T-test,  $p>0.05$ ).

The microarray also identified that three of the tissue inhibitors of metalloproteinases (*Timps*) were regulated by BCL3. The products of these genes act to inhibit matrix metalloproteinases that can promote breast cancer invasion and metastases by breaking down the extracellular matrix of surrounding stromal tissue (Zhang, Cao et al. 2008; reviewed in Duffy, Maguire et al. 2000; Chakraborti, Mandal et al. 2003). The expression of *Timp1* and *Timp2* was verified by QRT-PCR, and, as observed in the microarray, mRNA expression of both genes was significantly up-regulated in response to *Bcl3* suppression (Figure 5.13B, relative percentage mRNA increase in comparison to controls was 36% for *Timp1*, T-test,  $p=0.00098$  and 50% for *Timp2*, T-test,  $p=0.029$ ).

The mRNA expression of several other putative NF- $\kappa$ B motility-related gene targets identified in the microarray was analysed. Of these targets, only three were confirmed to be significantly regulated by BCL3 when mRNA expression was assessed by QRT-PCR. Caveolin-1 (*Cav-1*) is a structural component of caveolae membrane domains in a variety of cells including mammary epithelia and has been shown to be a potent suppressor of mammary tumour growth and metastases *in vivo* (Williams, Medina et al. 2004). QRT-PCR analysis revealed that *Bcl3* suppression resulted in an 80% increase in the mRNA expression of this anti-invasive gene in comparison to controls (Figure 5.13C, T-test,  $p=0.00069$ ). Furthermore, *Arhgdib*, a Rho GDP dissociation inhibitor that has been shown to behave as a metastases suppressor (Gildea, Seraj et al. 2002), was significantly increased by 130% in response to *Bcl3* suppression (Figure 5.13C, T-test,  $p=0.00065$ ), and *Rab21*, a small GTPase that has been shown to enhance cell adhesion and migration of breast and prostate cells (Pellinen, Arjonen et al. 2006), was significantly decreased by 24% in *Bcl3*-depleted cells (Figure 5.13C, T-test,  $p=0.038$ ).

These data indicate that BCL3 regulates the transcription of a variety of motility- and invasion-related genes to mediate a pro-migratory and pro-invasive phenotype.

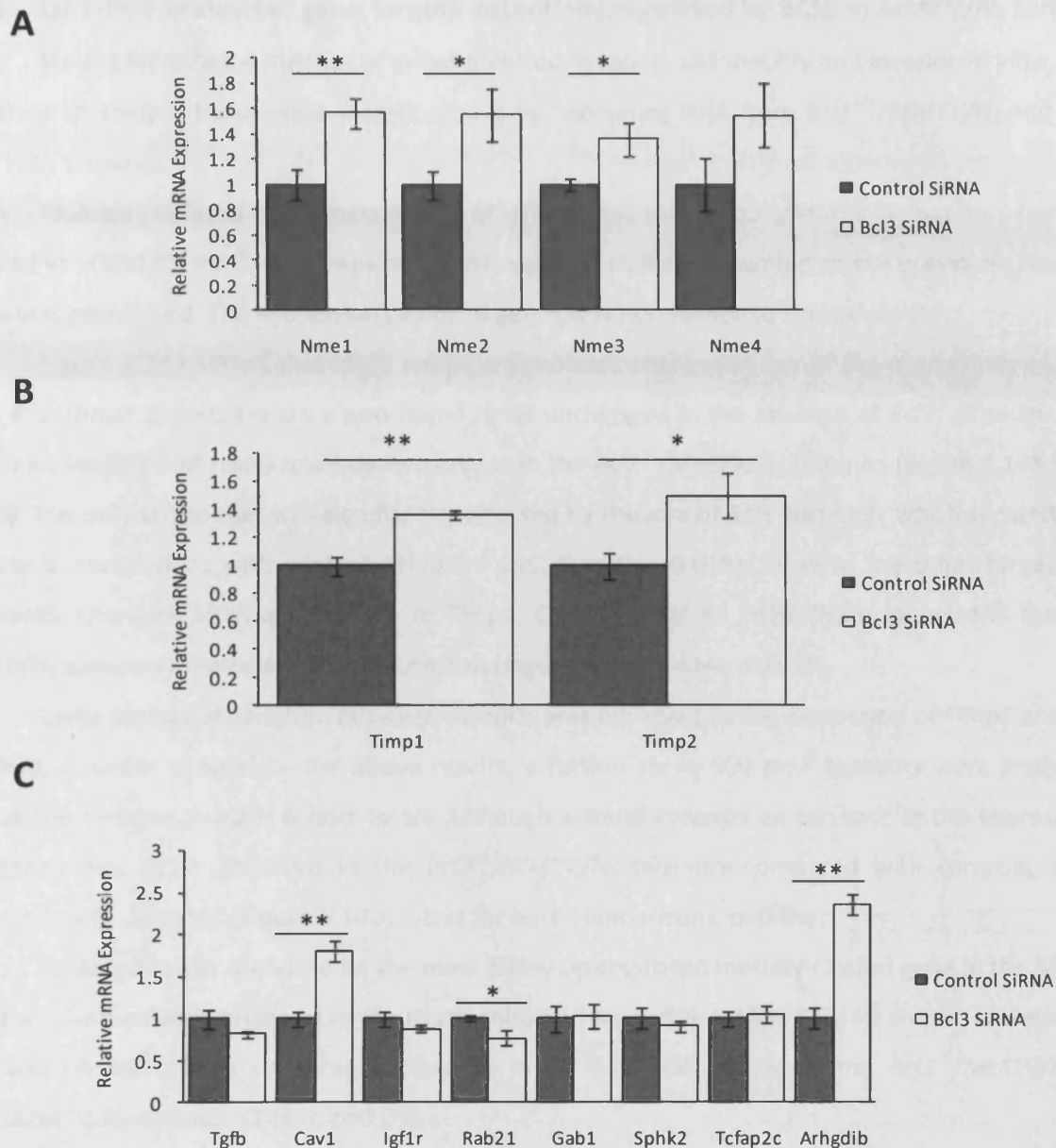


**Figure 5.13: BCL3 regulates the transcription of a variety of motility- and invasion-related genes** MG1361 cells were transfected with *Bcl3* or control SiRNA. QRT-PCR directed against targets identified by microarray analysis was performed. *Bcl3* suppression resulted in a significant up-regulation of *Nme1*, *Nme2*, and *Nme3* (A, T-test, \*\*= $p < 0.01$ , \*= $p < 0.05$ ) and of *Timp1* and *Timp2* (B, T-test, \*\*= $p < 0.01$ , \*= $p < 0.05$ ). Of the other targets analysed, only *Cav1* and *Arhgdib* were significantly up-regulated and *Rab21* was significantly down-regulated in response to *Bcl3* suppression (C, T-test, \*\*= $p < 0.01$ , \*= $p < 0.05$ ). Data are representative of three independent *Bcl3* transfection experiments. Error bars represent  $\pm$  SEM.

### 5.2.11 QRT-PCR analysis of gene targets potentially regulated by BCL3 in MMTV/N<sub>2</sub> tumours

Having identified a number of genes involved in cancer cell motility and invasion *in vitro*, it was of interest to analyse these same targets *in vivo* by harvesting RNA from *Bcl3*<sup>+/+</sup>/MMTV/N<sub>2</sub> and *Bcl3*<sup>-/-</sup>/MMTV/N<sub>2</sub> tumours.

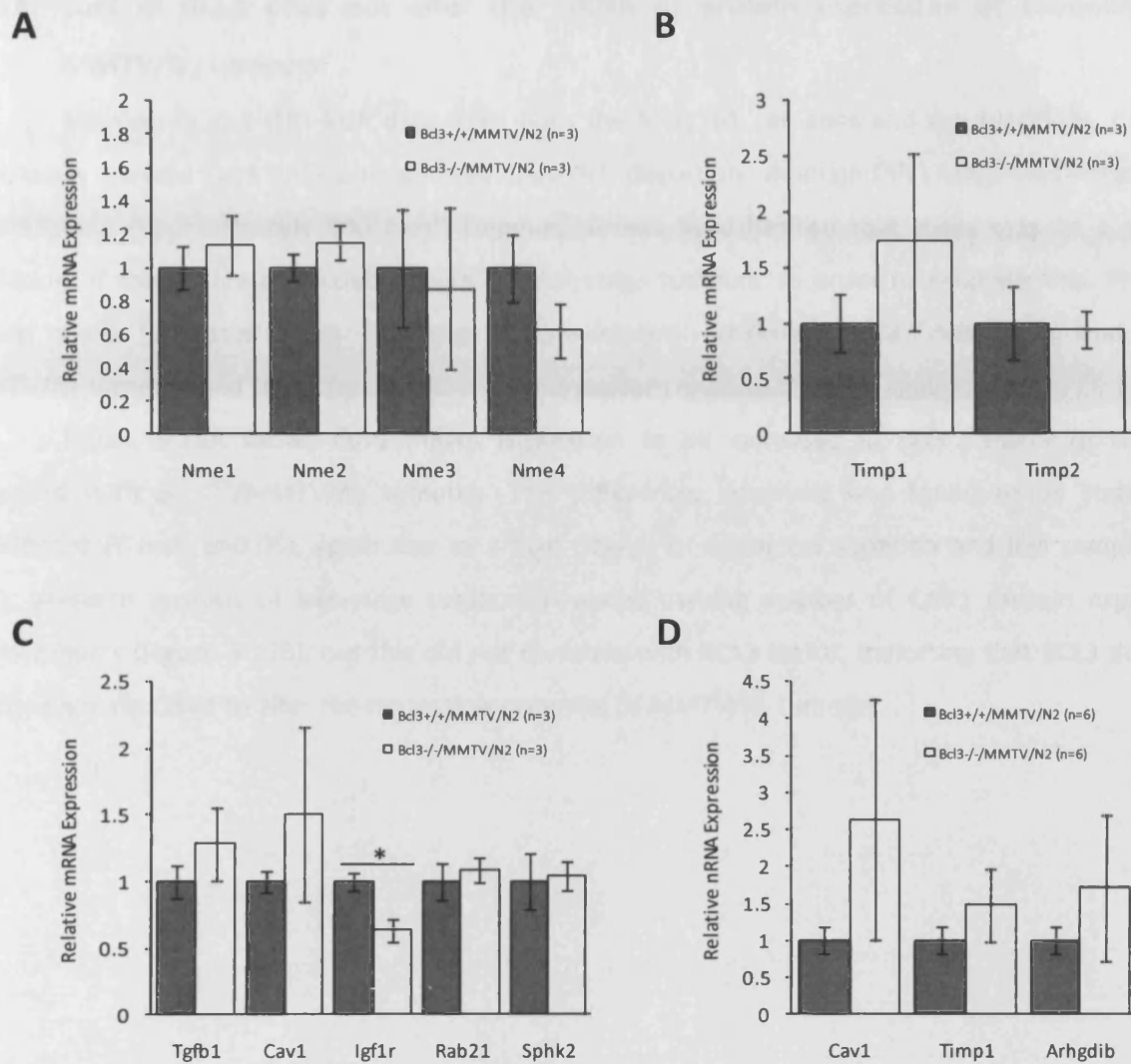
RNA was isolated from three *Bcl3*<sup>+/+</sup>/MMTV/N<sub>2</sub> and three *Bcl3*<sup>-/-</sup>/MMTV/N<sub>2</sub> tumours that were dissected at 500±13.5 mm<sup>3</sup>. cDNA was prepared, and QRT-PCR for a number of the previously identified targets was performed. The expression profile of genes was normalised to *cyclophilin B*.

Figure 5.14A shows that there were no significant changes in any of the *Nme* family of genes. *Timp1* and *Timp2* expression were also found to be unchanged in the absence of *Bcl3*, although *Timp1* showed an insignificant trend towards an increase in the *Bcl3*<sup>-/-</sup>/MMTV/N<sub>2</sub> tumours (Figure 5.14B, T-test, p>0.05). The only target that was significantly affected by the loss of *Bcl3* was *Igf1r* which showed a 37% decrease in comparison with controls (Figure 5.14C, T-test, p=0.018). None of the other targets were significantly changed, although similarly to *Timp1*, *Cav1* showed an insignificant increase in the *Bcl3*<sup>-/-</sup>/MMTV/N<sub>2</sub> tumours in comparison with controls (Figure 5.14C, T-test, p>0.05).

Large biological variation between samples was observed in the expression of *Timp1* and *Cav1*. Therefore, in order to validate the above results, a further three 500 mm<sup>3</sup> tumours were analysed to increase the number in each cohort to six. Although a trend towards an increase in the expression of both genes was again observed in the *Bcl3*<sup>-/-</sup>/MMTV/N<sub>2</sub> tumours compared with controls, still no significance was detected (Figure 5.14D, T-test for both comparisons, p>0.05).

As *Arhgdib* was shown to be the most highly up-regulated motility-related gene in the MG1361 cells, it was immediately analysed in the larger cohort of six samples. Figure 5.14D shows, however, that there was no statistically significant difference in its expression between the *Bcl3*<sup>-/-</sup>/MMTV/N<sub>2</sub> and *Bcl3*<sup>+/+</sup>/MMTV/N<sub>2</sub> tumours (T-test, p>0.05).

These results indicate that BCL3 deficiency does not alter the same set of motility-related genes in whole tumour samples. However, trends were observed which could indicate that BCL3 may have an effect on a smaller sub-population of cells within the tumour that have high metastatic potential.



**Figure 5.14: QRT-PCR analysis of motility- and invasion-related genes in MMTV/N<sub>2</sub> tumours**

RNA was extracted from *Bcl3*<sup>+/+</sup>/MMTV/N<sub>2</sub> and *Bcl3*<sup>-/-</sup>/MMTV/N<sub>2</sub> tumours and QRT-PCR directed against a number of previously identified motility- and invasion-related genes was performed. No significant differences were identified in the *Nme* family of genes (A, T-test,  $p > 0.05$ ). In a cohort of three, loss of *Bcl3* resulted in an insignificant increase in the expression of *Timp1* (B, T-test,  $p > 0.05$ ). *Igf1r* mRNA expression was significantly reduced in the absence of *Bcl3* (C, T-test,  $* = p < 0.05$ ). The expression of *Cav1*, *Timp1* and *Arhgdib* was analysed in a larger cohort of six tumours. Trends, but no significant differences in the expression of these genes were observed (D, T-test,  $p > 0.05$ ). Error bars represent  $\pm$  SEM.

### 5.2.12 Loss of BCL3 does not alter the mRNA or protein expression of Caveolin 1 in *MMTV/N<sub>2</sub>* tumours

Microarray and QRT-PCR data from both the MG1361 cell lines and the *MMTV/N<sub>2</sub>* tumours consistently showed *Cav1* to be up-regulated upon *Bcl3* depletion, although this change was insignificant in early-stage (approximately 500 mm<sup>3</sup>) tumours. It was hypothesised that there may be a greater regulation of this metastases-related gene in later-stage tumours. In order to establish this, RNA and protein were harvested from late-stage (approximately 4000mm<sup>3</sup>) *Bcl3<sup>+/+</sup>/MMTV/N<sub>2</sub>* and *Bcl3<sup>-/-</sup>/MMTV/N<sub>2</sub>* tumours and subjected to QRT-PCR and western analysis directed against Cav1.

Figure 5.15A shows *Cav1* mRNA expression to be increased in *Bcl3<sup>-/-</sup>/MMTV/N<sub>2</sub>* tumours compared with *Bcl3<sup>+/+</sup>/MMTV/N<sub>2</sub>* tumours. This difference, however, was found to be statistically insignificant (T-test,  $p > 0.05$ ), again due to a high degree of biological variation and low sample sizes ( $n=3$ ). Western analysis of late-stage tumours revealed varying degrees of CAV1 protein expression within cohorts (Figure 5.15B), but this did not correlate with BCL3 status, indicating that BCL3 does not directly regulate CAV1 to alter the metastatic potential of *MMTV/N<sub>2</sub>* tumours.

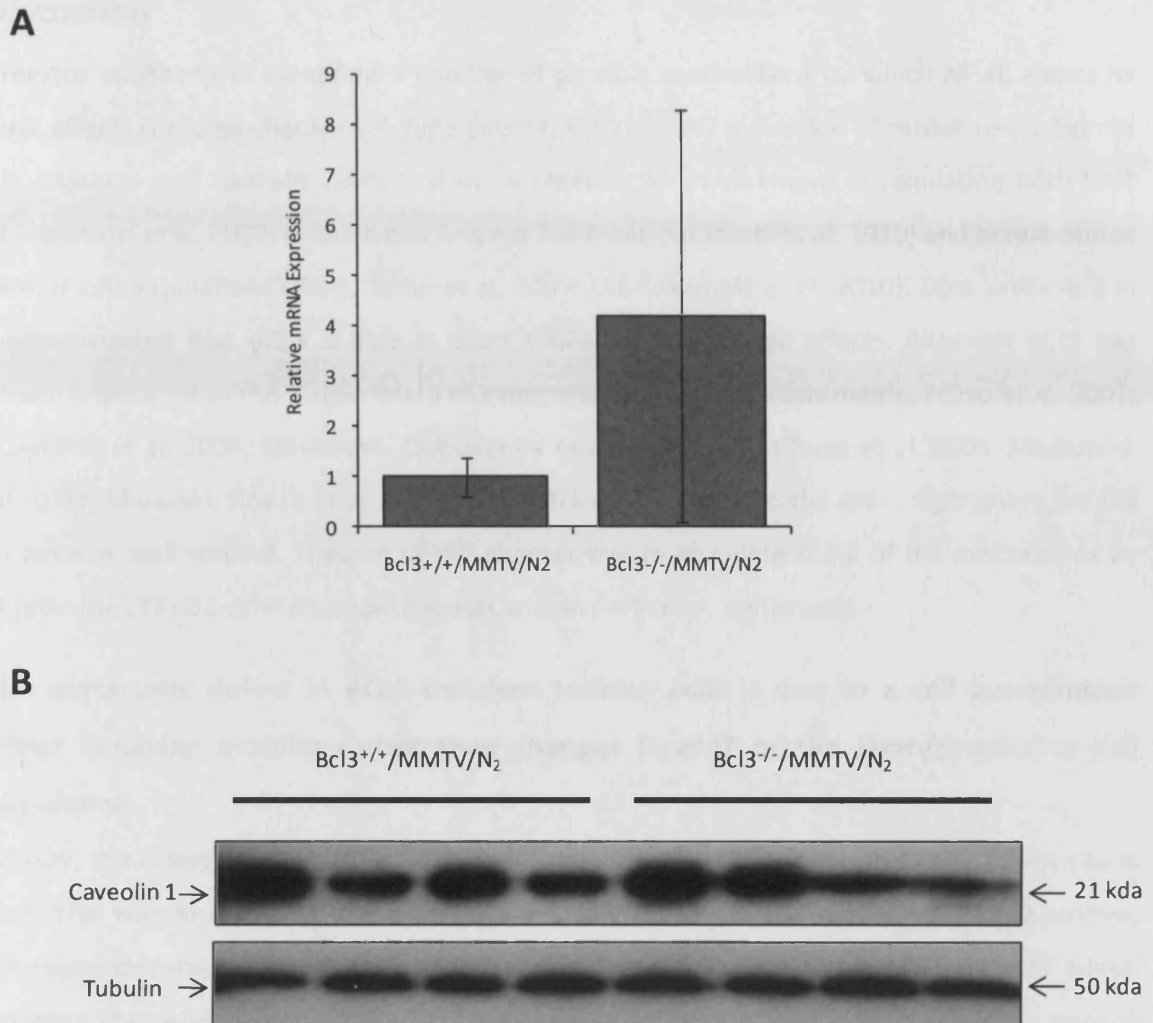


**Figure 5.15: BCL3 does not regulate Caveolin 1 in late stage MMTV/N<sub>2</sub> tumours**

RNA and protein was extracted from Bcl3<sup>+/+</sup>/MMTV/N<sub>2</sub> and Bcl3<sup>-/-</sup>/MMTV/N<sub>2</sub> tumours and QRT-PCR and western analysis directed against Caveolin 1 was performed. No significant differences in Cav1 mRNA expression were observed (A, n=3, error bars represent ± SEM, T-test, p>0.05). High variation in the protein expression of Caveolin 1 was observed but this did not correlate with BCL3 status (B). Equal loading was confirmed by Tubulin.

### 5.3 Discussion

Previous studies have identified a number of possible mechanisms by which NF- $\kappa$ B exerts its pro-oncogenic effect. These mechanisms include direct transcriptional regulation of cancer-related genes (reviewed in Basseres and Baldwin 2006) and more recently an involvement in regulating both EMT (Chua, Bhat-Nakshatri et al. 2007; Criswell and Arteaga 2007; Liu, Sakamaki et al. 2010) and breast cancer stem/progenitor cell populations (Pratt, Tibbo et al. 2009; Liu, Sakamaki et al. 2010). Data presented in chapter 4 demonstrated that BCL3 is able to exert similar pro-oncogenic effects. Although BCL3 has previously been implicated in the transcription of cancer-related genes (Westerheide, Mayo et al. 2001; Kashatus, Cogswell et al. 2006; Massoumi, Chmielarska et al. 2006; Park, Chung et al. 2006; Massoumi, Kuphal et al. 2009; Miyazaki, Simizu et al. 2010), in depth investigation into the exact mechanism behind this has not been as well studied. The aim of this chapter was to elucidate some of the mechanisms by which BCL3 promotes ERBB2-driven tumourigenesis and, in particular, metastases.

#### 5.3.1 The metastatic defect in BCL3 deficient tumour cells is due to a cell autonomous effect involving motility rather than changes in EMT or the stem/progenitor cell population

Initially, the question of whether BCL3, like NF- $\kappa$ B, was over-expressed in ERBB2-positive cells was analysed. This was found to be the case (Figure 5.1) and lead to the use of the ERBB2-positive, *MMTV/NK* tumour derived, MG1361 cells in this study. The key findings from MG1361 *Bcl3* SiRNA experiments were that while suppression of BCL3 had no effect on the proliferation of cells in normal growth conditions (Figure 5.3), it did have a profound effect on the metastatic properties of cells as demonstrated by both *in vivo* and *in vitro* experimental metastases models (Figure 5.4&5.5).

In order for cancer cells to successfully colonize a secondary site, they must detach from the primary tumour using extracellular matrix-degrading proteases, intravasate and survive in the blood stream, and then extravasate out of the vasculature to seed and grow in the target tissue. In an attempt to understand which of these stages are regulated by BCL3, intravenous tail vein experiments were performed. In this experimental metastases model, the anoikis resistance and invasive properties of tumour cells are critical for their survival and extravasation out of the blood stream, primarily during the first few hours after injection into the circulation. Based on the kinetics of SiRNA gene knock-down, transfected cells were likely to have maximal *Bcl3* silencing immediately after injection into the blood stream. Therefore, the use of transient SiRNA restricted the suppression of BCL3 activity to the crucial window of survival in the blood stream and extravasation out of it, with a release of this inhibition during the later stages of colonization and secondary tumour growth in the lungs. Thus, the role of BCL3

specifically in anoikis resistance and extravasation, rather than the subsequent steps was primarily addressed in this experiment.

Results revealed that *Bcl3*-suppressed cells produced less metastatic lung lesions than controls (Figure 5.4A) which indicated a requirement for BCL3 in either the anoikis resistance or extravasation stages of the metastatic process. Subsequent *in vitro* experiments demonstrated that BCL3 had no effect on the ability of cells to avoid anoikis (Figure 5.6), suggesting that it has a more crucial role to play in promoting the extravasation of cells out of blood vessels and into secondary tissue sites. Interestingly, when *Bcl3* suppressed cells did form metastases, they were larger in size than controls (Figure 5.4B). It is possible that the *Bcl3*-depleted cells that were actually able to extravasate from the blood stream were highly aggressive with up-regulated alternative survival pathways. In comparison to controls, these cells may be more readily able to colonise and grow at secondary sites, particularly following the release of *Bcl3* inhibition. Subsequent *in vitro* Boyden chamber experiments demonstrated that *Bcl3* suppression reduced both the migratory and invasive capacity of MG1361 cells (Figure 5.5), which taken together with results from tail vein and anoikis resistance experiments suggests that BCL3 promotes the extravasation of cells by enhancing their intrinsic migratory and invasive capacity.

Collectively, these data imply that the reduced ability of BCL3-deficient cells to metastasise to the lungs is, at least in part, due to a cell autonomous effect that is independent of the tumour microenvironment. Whether BCL3 also regulates broader processes such as angiogenesis and inflammation to mediate disease progression remains inconclusive. Intriguingly, however, loss of STAT3 has previously been shown to delay the metastatic progression of ERBB2-positive tumours via both direct cell autonomous mechanisms and through effects on the tumour microenvironment (Ranger, Levy et al. 2009). Like NF- $\kappa$ B, STAT3 is pro-apoptotic during mammary involution (Chapman, Lourenco et al. 1999) but is paradoxically up-regulated in many malignancies including breast cancer (Hsieh, Cheng et al. 2005; reviewed in Yu and Jove 2004). As *Bcl3* is a downstream transcriptional target of STAT3, it is possible that the two co-operate to promote a metastatic phenotype and that BCL3 may also influence the tumour microenvironment to mediate disease progression. It would be interesting to investigate this further in the future.

As NF- $\kappa$ B has previously been implicated in promoting the process of EMT (Chua, Bhat-Nakshatri et al. 2007; Criswell and Arteaga 2007), the question of whether BCL3 may also exert some of its pro-metastatic effects via regulating this process was investigated. To this end, the protein levels of some key markers of EMT were assessed. No BCL3-dependent differences in the protein expression of E-cadherin, Snail or Vimentin were identified in the MG1361 cells and furthermore, Vimentin and E-cadherin were not found to be regulated by BCL3 in *MMTV/N<sub>2</sub>* tumours. NF- $\kappa$ B has been shown to regulate a number of other genes involved in the EMT process such as the transcription factors SLUG,

TWIST, SIP, ZEB1 and ZEB2 (Chua, Bhat-Nakshatri et al. 2007; Criswell and Arteaga 2007). However, microarray analysis of MG1361 cells subjected to *Bcl3* suppression did not reveal differential expression of any of these genes (data not shown). Taken together these data suggest that BCL3 does not exert any of its pro-metastatic effect by mediating an EMT switch in this cell type.

Recently, a great deal of interest has surrounded the study of cancer stem cells and their role in tumourigenesis and metastases. The cancer stem cell hypothesis proposes that cancer originates from stem or progenitor cells through de-regulation of their normally tightly controlled self-renewal pathways, generating tumours that are driven by a small subset of tumour initiating cells (TICs). Researchers have recently shown that these cells also display increased invasion and migration (Hammond, Helbig et al. 2003; Helbig, Valmaggia et al. 2003). Both ERBB2 and NF- $\kappa$ B signalling have been implicated in promoting cancer stem cell properties (Korkaya, Paulson et al. 2008; Pratt, Tibbo et al. 2009; Liu, Sakamaki et al. 2010; Storci, Sansone et al. 2010) and so the effect of BCL3 on this population of cells was analysed using the functional mammosphere assay and known TIC markers. Transient suppression of *Bcl3* did not significantly reduce the percentage of either primary or secondary mammosphere forming units present in MG1361 cells (Figure 5.8). A major caveat to this work, however, is that, as mentioned above, suppression of *Bcl3* by siRNA is only temporary. In fact, transcript levels were shown to return to 50% of controls as early as day 5 (Figure 5.2) indicating that by the end of this 14 day experiment both control and *Bcl3* siRNA treated cells were likely to have equivalent *Bcl3* expression. Data from this experiment can therefore only serve to evaluate the effects of BCL3 on the initial anoikis-resistant cell population and the subsequent consequences that this early inhibition has on their self-renewal ability. This makes it only possible to conclude that suppression of *Bcl3* does not affect the size of the initial anoikis-resistant, TIC population or the early ability of these cells to self-renew. In contrast, permanent global inhibition of NF- $\kappa$ B has previously been shown to reduce the capacity of primary ERBB2-positive murine tumour cells to undergo self-renewal and form secondary mammospheres (Cao, Luo et al. 2007). It is possible that permanent suppression of BCL3 may lead to a similar phenotype. A comparable experiment whereby *Bcl3*<sup>+/-</sup>/MMTV/N<sub>2</sub> and *Bcl3*<sup>-/-</sup>/MMTV/N<sub>2</sub> primary tumour and pre-neoplastic cells were analysed for their mammosphere-forming abilities was in fact, attempted. Unfortunately however, neither cell type formed mammospheres on any occasion, preventing any conclusions from being drawn. Further evaluation using a technique to permanently suppress BCL3 in cell lines should be performed in the future.

Surprisingly, *Bcl3* suppression resulted in a significant increase in cells displaying the stem/TIC marker CD24. Both this study and previous reports have demonstrated that selection of cells expressing CD24 enriches for TICs as demonstrated by increased mammosphere formation (Figure 5.10; Liu, Deng et al. 2007). However, CD24-positivity is clearly not the exclusive factor that defines whether a cell becomes a TIC. This is demonstrated by the fact that selection of CD24-positive parental MG1361 cells did not

result in 100% mammosphere formation, but instead it simply enriched for this phenotype (Figure 5.10). This implies that although the majority of TICs may be CD24-positive, all CD24-positive cells are not necessarily TICs. It is therefore possible that as observed, *Bcl3* suppression does promote cells to become CD24-positive, but the percentage of TICs within this population remains unaltered. This hypothesis seems likely as *Bcl3* suppression did not result in an increase in mammosphere formation (Figure 5.8) or in the percentage of cells displaying another TIC marker, ALDH1 (Figure 5.9). Further analysis of the effect of BCL3 on TIC populations is beyond the scope of this thesis, however, future experiments utilising a more comprehensive range of markers on both cell lines and primary tumour cells could be performed. The gold standard experiment to determine the effect of a particular variable on TICs involves assessing the ability of cells to re-establish an entire tumour cell population upon serial dilution when injected back into a mammary fat pad. It would be interesting to conduct this experiment with BCL3 depleted cell lines or primaries to gain a more conclusive insight into whether it regulates the TIC population.

### **5.3.2 Gene expression profiling of *Bcl3*-deficient tumour cells reveals a combination of differentially expressed motility and invasion related genes**

Gene expression profiling of MG1361 cells subjected to *Bcl3* suppression revealed differential expression of a variety of genes involved in regulating motility and invasion (Table 5.1). QRT-PCR analysis confirmed a significant up-regulation in the expression of the first three members of the *Nme* family of anti-motility genes. Although putative NF- $\kappa$ B DNA binding sites were found in the promoters of these genes, transcriptional modulation of *Nme* genes by NF- $\kappa$ B has not previously been reported and possibly reflects a novel NF- $\kappa$ B/BCL3 mediated pro-motility pathway in this cell type.

*Timp1* and *Timp2* were also significantly up-regulated in response to *Bcl3* suppression. Indeed, inhibition of NF- $\kappa$ B has previously been shown to result in an up-regulation of *Timp1* expression in human gastric cancer cell lines (Jin, Pan et al. 2007). TIMPs act to inhibit the activity of MMPs which break down extracellular membranes enabling cancer cells to intravasate into the blood circulation or to extravasate out of it (reviewed in Kim, Yu et al. 1998; Deryugina and Quigley 2006; Zhang, Yang et al. 2010). Analysis of microarray data revealed that the MMPs themselves were not regulated at the transcriptional level by BCL3 (data not shown). However, as TIMPs inhibit MMPs post-transcriptionally (Murphy, Houbrechts et al. 1991; Willenbrock and Murphy 1994; Huang, Meng et al. 1997) it is likely that changes in their activity would only be identified at the protein level. The functional output of the BCL3-mediated regulation of *Timp* genes could be studied in the future by utilising zymography techniques to analyse the activity of MMPs in response to BCL3 suppression. Overall, the regulation of *Timp* gene expression suggests that BCL3 promotes metastatic properties of cells by indirectly up-regulating MMPs.

This further supports the previously proposed hypothesis that it plays a major role in mediating the extravasation stage of the metastatic process in which MMPs are so vital.

Disappointingly, none of the motility-related genes identified on the microarray were also significantly regulated by BCL3 in *MMTV/N<sub>2</sub>* tumours, although there was a trend towards an increase in *Timp1*, *Cav1* and *Arhgdib* in the *Bcl3<sup>-/-</sup>/MMTV/N<sub>2</sub>* tumours. It is possible that larger changes in the expression of these genes may occur in small tumour cell populations, for example, in those invading cells at the edge of the tumour. This hypothesis is difficult to prove although possible future experiments could involve analysis of the protein expression of possible targets on whole tumour sections by IHC.

### 5.3.3 Summary

In summary, the data presented in this chapter has established that, in accordance with previous *in vivo* studies in chapter 4, suppression of BCL3 results in a reduction in the motility and invasive capacity of murine ERBB2-positive tumour cells *in vitro*. The data suggests that in the *MMTV/N<sub>2</sub>* model, BCL3 may directly mediate the ability of tumour cells to metastasize to the lung in a cell autonomous manner. Any additional effects that BCL3 has on the on tumour microenvironment, such as inflammation or angiogenesis remain to be elucidated and deserve further attention in the future.

All data up to this point has been collected from mouse models of ERBB2-positive breast cancer. To evaluate more effectively whether BCL3 is likely to have similar effects in humans, it is essential to use models, such as human tumour-derived cell lines, that more closely recapitulate the genetic complexities of the human disease. This will therefore be the primary focus of chapter 6.

**Chapter 6:**  
**Analysis of BCL3 Deficiency in Human**  
**Breast Cancer Cell Lines**

## 6.1 Introduction

In the previous two chapters, BCL3 was shown to have a profound effect on ERBB2-driven mammary carcinogenesis in both an *in vivo* mouse model of breast cancer and in a mouse mammary tumour cell line. While this provides substantial evidence that it has a pro-oncogenic role to play in the initiation and progression of breast cancer, there are several limitations in the use of any mouse model system to recapitulate the human disease. One such limitation stems from the fact that mammary tumours arising in genetically engineered mouse models are, by definition, largely genetically homogeneous and fail to adequately capture the substantial genetic heterogeneity of the human disease. Generally speaking, any given mouse model can mimic only one, or at best a small subset, of the different types of breast cancer that have been found to occur in humans. This is certainly the case in the *MMTV/N<sub>2</sub>* model. Mammary tumours driven by the *MMTV/N<sub>2</sub>* transgene are histologically comparable to human Ductal Carcinoma *in situ* (DCIS) (Cardiff and Wellings 1999), in which ERBB2 is over-expressed in 40-60% of high grade cases (Lodato, Maguire et al. 1990; Somerville, Clarke et al. 1992). While this observation indicates that it is a suitable model for studying the effects of BCL3 on ERBB2-positive DCIS, it would be inappropriate to use data generated from *MMTV/N<sub>2</sub>* models to draw conclusions about its potential oncogenic role in any other subtype of the disease. A second limitation in using the *MMTV/N<sub>2</sub>* mouse model and tumour cell lines derived from it, is that expression of the *Neu* transgene is driven by a strong viral promoter which does not effectively imitate the endogenous human ERBB2 promoter and has doubtful physiological relevance to the human disease. Furthermore, there are inherent interspecies differences between mice and humans that may or may not directly impact the disease. One such example is ER, which, in some subtypes of the human disease, is highly expressed (Perou, Sorlie et al. 2000) but, in contrast, is generally low or absent in tumours from most mouse models (Herschkowitz, Simin et al. 2007). Many of these limitations can be overcome by the use of human breast cancer cell lines.

Cultured human tumour-derived cell lines have previously been shown to have genetic alterations that reflect the primary tumour from which they came (Neve, Chin et al. 2006), rendering them a useful tool to investigate the molecular mechanisms involved in different subtypes of the human disease. Breast cancer is commonly sub-divided into five different types, namely normal-like, luminal A, luminal B, basal-like or ERBB2-positive, according to certain gene expression profiles assessed by microarrays (Sotiriou, Neo et al. 2003). These different subtypes can be used to predict clinical outcome, with luminal A cancers having the best prognosis and ERBB2-positive and basal-like tumours being more aggressive with a worse prognosis (Sotiriou, Neo et al. 2003).

As previously discussed, NF- $\kappa$ B activation is associated with both EGFR and ERBB2 signalling (Biswas, Cruz et al. 2000; Biswas, Shi et al. 2004). More recently, it has been shown to be highly active in

a large proportion of basal breast cancer cell lines (Yamaguchi, Ito et al. 2009) and also in some human basal breast tumours (Biswas, Shi et al. 2004). Basal tumours often over-express EGFR (Nielsen, Hsu et al. 2004; Livasy, Karaca et al. 2006) and are generally negative for ERBB2 and for the oestrogen and progesterone receptors, in which case they are designated 'triple negative' tumours (reviewed in Chacon and Costanzo 2010). The shortage of molecular therapeutic targets makes basal-like, triple-negative tumours difficult to treat (reviewed in De Laurentiis, Cianniello et al. 2010), thus identification of new therapeutic targets to treat patients with these aggressive tumours is highly desirable.

Having previously demonstrated that inhibition of BCL3 had anti-metastatic effects in ERBB2-driven murine models of breast cancer, the overall aim of this chapter was to establish whether these effects might also be observed in a panel of human breast cancer cell lines. The cell lines investigated were chosen to represent the ERBB2-positive and EGFR-positive, disease subtypes in which NF- $\kappa$ B activation has previously been found to be most prevalent. In particular, the MDA-MB-231 cells were chosen as a model of the difficult to treat basal-like, and triple negative breast cancer subtype.

## 6.2 Results

### 6.2.1 *BCL3* is highly expressed in ERBB2-positive human breast cancer cell lines

As discussed previously, NF- $\kappa$ B activity has been shown to be strongly associated with EGFR receptor family signalling in breast cancer. Work from chapter 4 further demonstrated that *Bcl3* was highly expressed in ERBB2-positive murine mammary cells. In order to determine whether this was also the case in human breast cancer cells, a panel of human cell lines displaying different ERBB2 and EGFR protein levels were analysed for *BCL3* expression.

Firstly, to confirm the ERBB2 and EGFR status of each cell line, whole cell protein lysates were prepared for subsequent western analysis. This revealed that in accordance with previous reports (Clinchy, Gazdar et al. 2000; Neve, Chin et al. 2006), high ERBB2 protein levels were detected in the HCC1954 and SKBR3 cell lines, whereas very low levels were detected in the ZR-75-1 cells and it was completely absent in the MDA-MB-231 cell line (Figure 6.1A). In contrast, the ZR-75-1 and MDA-MB-231 cells expressed very high EGFR protein levels, whereas lower levels were present in the HCC1954 cells and it was undetectable in the SKBR3 cells. Equal loading of protein between samples was confirmed by visualising levels of the housekeeping protein, Tubulin (Figure 6.1A). This analysis confirmed that the four cell lines have differing combinations of ERBB2 and EGFR receptor expression, representing different subclasses of breast cancer.

In order to establish the relative *BCL3* expression in these cell lines, QRT-PCR was performed. Four separate wells of each cell line were grown to 70% confluency and RNA was isolated for subsequent cDNA preparation and *BCL3* QRT-PCR analysis. Gene expression was normalised to the house keeping gene  $\beta$ -*ACTIN*. Figure 6.1B shows that the ERBB2-positive, HCC1954 and SKBR3 cell lines, have almost 7 fold higher *BCL3* expression in comparison to the ERBB2-negative, MDA-MB-231 and ZR-75-1 cells. This indicates that high *BCL3* expression correlates with ERBB2 but not EGFR positivity.

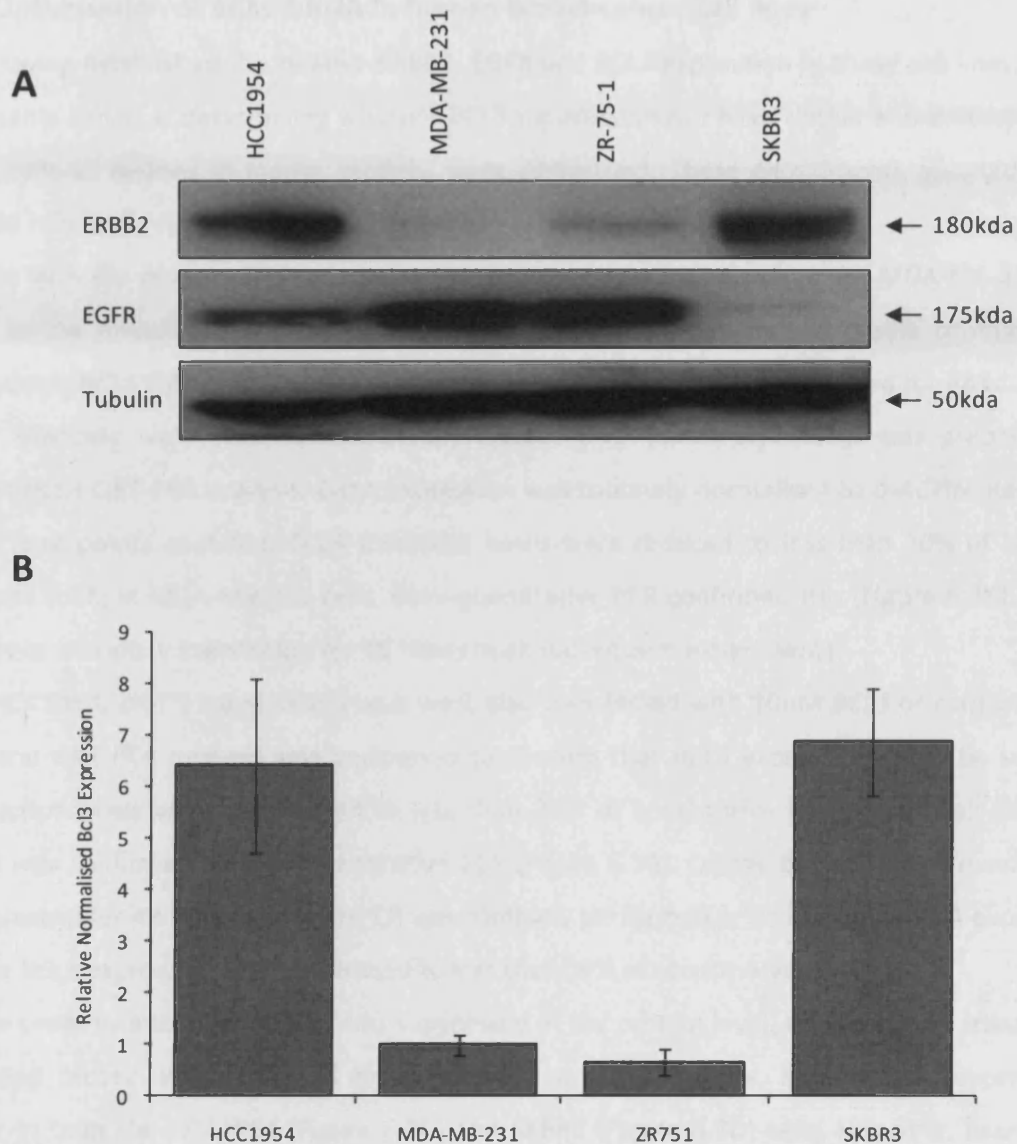


**Figure 6.1: *BCL3* expression correlates with high *ERBB2* rather than *EGFR* protein levels**

Total protein was extracted from HCC1954, MDA-MB-231, ZR-75-1 and SKBR3 cells and subjected to western analysis (A). HCC1954 and SKBR3 cells had high *ERBB2* protein levels whereas it was almost absent in the ZR-75-1 cells and completely absent in MDA-MB-231 cells. *EGFR* protein levels were highly expressed in MDA-MB-231 and ZR-75-1 cells whereas lower levels were found in the HCC1954 cells and it was completely absent in the SKBR3 cells. Equal loading was confirmed by Tubulin (A). RNA was harvested from the same cell lines for subsequent QRT-PCR analysis (B). The *ERBB2*-positive HCC1954 and SKBR3 cells had almost 7 fold more *BCL3* mRNA than the *ERBB2*-negative MDA-MB-231 and ZR-75-1 cells. Data represent samples harvested from 4 separate wells and error bars represent  $\pm$  SEM. *BCL3* mRNA expression was normalised to  $\beta$ -*ACTIN* mRNA expression.

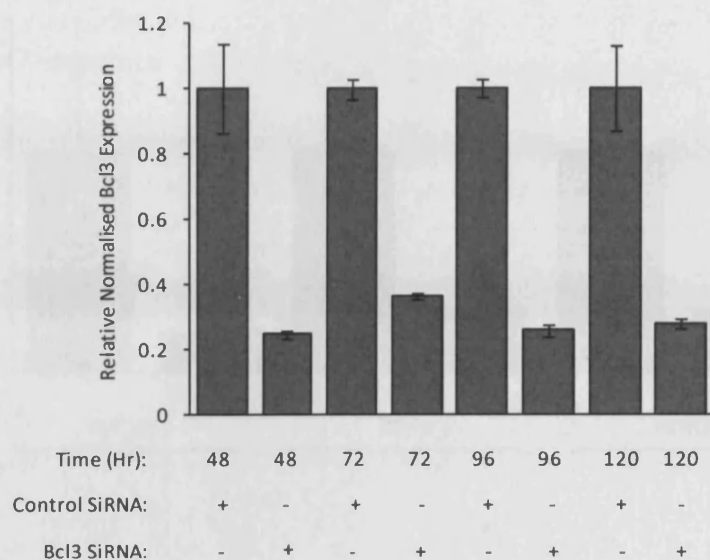
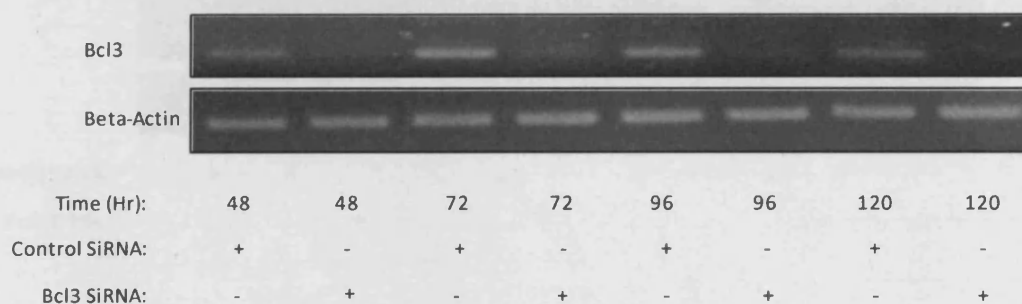
### 6.2.2 Optimisation of *BCL3* SiRNA in human breast cancer cell lines

Having established the relative ERBB2, EGFR and *BCL3* expression in these cell lines, a number of experiments aimed at determining whether *BCL3* suppression can have similar anti-metastatic effects in human cells as it does in mouse models, were performed. These experiments adopted an SiRNA approach to efficiently suppress *BCL3*.

As with the mouse cell lines, the SiRNA technique was optimised on the MDA-MB-231 cell line according to the manufacturer's protocol. Cells were plated in transfection media containing either 10nM of human *BCL3* SiRNA or 10nM of control, non-targeting SiRNA and incubated for 48 to 120 hours. RNA from triplicate wells was isolated at appropriate time points and cDNA was prepared before subsequent *BCL3* QRT-PCR analysis. Gene expression was routinely normalised to  $\beta$ -*ACTIN*. Results show that at all time points analysed, *BCL3* transcript levels were reduced to less than 30% of constitutive levels (Figure 6.2A) in MDA-MB-231 cells. Semi-quantitative PCR confirmed this (Figure 6.2B). MDA-MB-231 cells were therefore transfected for 48 hours in all subsequent experiments.

HCC1954, ZR-75-1 and SKBR3 cells were also transfected with 10nM *BCL3* or control SiRNA for 48 hours and QRT-PCR analysis was performed to confirm that *BCL3* expression could be suppressed. *BCL3* transcript levels were suppressed to less than 30% of constitutive levels in all cell lines (Figure 6.3A). This was confirmed by semi-quantitative PCR (Figure 6.3B). On the basis of these results, all cells were transfected for 48 hours and QRT-PCR was routinely performed prior to every SiRNA experiment to ensure that *BCL3* expression was suppressed to less than 30% of constitutive levels.

In order to ensure that *BCL3* was suppressed at the protein level, cell lines were transfected for 48 hours and protein was harvested for subsequent western analysis. *BCL3* protein expression was clearly lost in both the HCC1954 (Figure 6.3C) and SKBR3 (Figure 6.3D) cells. However, base-line *BCL3* protein expression was completely undetectable by western blotting with three separate antibodies in the ERBB2-negative MDA-MB-231 and ZR-75-1 cells (data not shown) and so the effect of *BCL3* SiRNA at the protein level in these cell lines could not be established.

**A****B**

**Figure 6.2: BCL3 SiRNA efficiently suppresses BCL3 mRNA expression in MDA-MB-231 cells**

MDA-MB-231 cells were transfected for 48-120 hours with 10nM *BCL3* or control SiRNA before being harvested for QRT-PCR analysis. *BCL3* mRNA expression was efficiently suppressed to less than 30% of constitutive levels at all time-points analysed (A, error bars represent  $\pm$  SEM of triplicate wells, data is represented as *BCL3* mRNA expression relative to  $\beta$ -*ACTIN* mRNA expression). This was confirmed by semi-quantitative PCR (B).

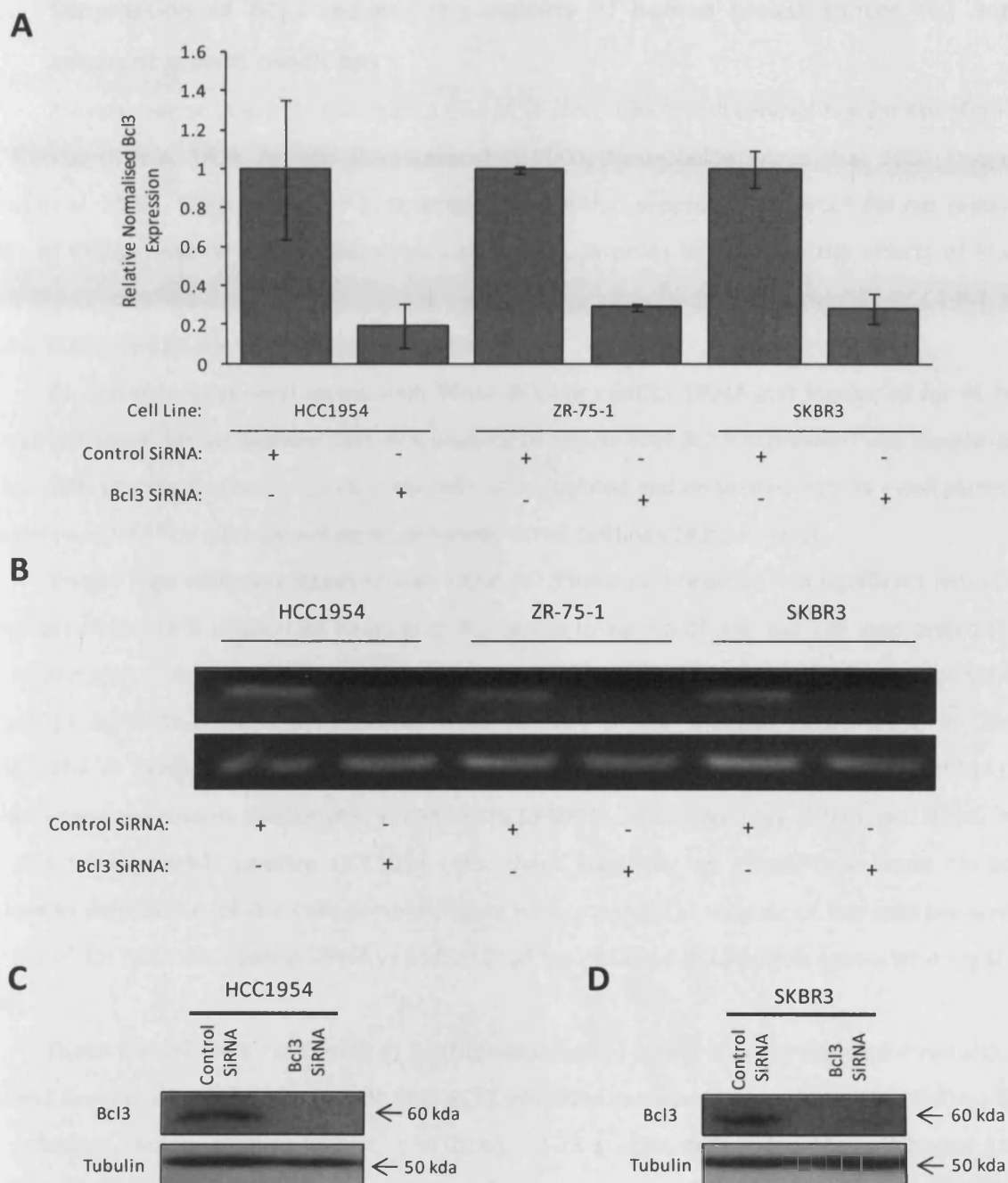


**Figure 6.3: BCL3 SiRNA efficiently suppresses BCL3 expression in HCC1954, ZR-75-1 and SKBR3 cells**

HCC1954, ZR-75-1 and SKBR3 cells were transfected with 10nM *BCL3* or control SiRNA for 48 hours before being harvested for QRT-PCR analysis. *BCL3* mRNA expression was efficiently suppressed to less than 30% of constitutive levels in all three cell lines (A, error bars represent  $\pm$  SEM of triplicate wells, data is represented as *BCL3* mRNA expression relative to  $\beta$ -ACTIN mRNA expression). This was confirmed by semi-quantitative PCR (B). Total proteins were also harvested from cell lines transfected with *BCL3* SiRNA for 48 hours and subjected to western analysis. *BCL3* SiRNA efficiently suppressed *BCL3* protein levels in HCC1954 (C) and SKBR3 (D) cells. Equal loading was confirmed by Tubulin.

### 6.2.3 Suppression of *BCL3* reduces the viability of human breast cancer cell lines in adherent growth conditions

Previous reports have demonstrated that *BCL3* can promote cell survival in a variety of contexts (Ong, Hackbarth et al. 1998; Rebollo, Dumoutier et al. 2000; Westerheide, Mayo et al. 2001; Dolgachev, Thomas et al. 2007). Work in chapter 5, however, showed that suppression of *BCL3* did not reduce the viability of ERBB2-positive murine mammary cancer cells. In order to establish the effects of *BCL3* on human ERBB2- or EGFR-positive breast cancer cells, viability assays were performed on HCC1954, MDA-MB-231, SKBR3 and ZR-75-1 cells subjected to *BCL3* SiRNA.

All cell lines were transfected with 10nM *BCL3* or control SiRNA and incubated for 48 hours. RNA was harvested for subsequent QRT-PCR analysis to ensure that *BCL3* expression was suppressed to less than 30% of constitutive levels. All other cells were counted and re-seeded into 96 –well plates. Live cell counts and CellTiter-Blue assays were performed on all cell lines 24 hours later.

Trypan blue exclusion counts revealed that *BCL3* inhibition resulted in a significant reduction in the number of live cells present 24 hours after seeding in three out of the four cell lines tested (Figure 6.4A, mean±SEM number of live cells per well was: 72350±4127 for MDA-MB-231 control SiRNA vs 41642±2414 for MDA-MB-231 *BCL3* SiRNA, Mann-Whitney U-Test,  $p=0.000$ ; 50357±2150 for ZR-75-1 control SiRNA vs 35285±2376 for ZR-75-1 *BCL3* SiRNA, Mann-Whitney U-Test,  $p=0.0002$  and 25714±1711 for SKBR3 control SiRNA vs 18428±1461 for SKBR3 *BCL3* SiRNA, Mann-Whitney U-Test,  $p=0.0298$ ). In the EGFR and ERBB2-double positive HCC1954 cells, there was only an insignificant trend towards a reduction in the number of live cells present (Figure 6.4A, mean±SEM number of live cells per well was 43777±2614 for HCC1954 control SiRNA vs 36111±2465 for HCC1954 *BCL3* SiRNA, Mann-Whitney U-Test,  $p>0.05$ ).

These results were confirmed in CellTiter-Blue assays which showed significant reductions in the overall number of viable cells present after *BCL3* inhibition compared to controls in the MDA-MB-231 (23% reduction, Mann-Whitney U-Test,  $p=0.0106$ ), ZR-75-1 (42% reduction, Mann-Whitney U-Test,  $p=0.002$ ) and SKBR3 cells (32% reduction, Mann-Whitney U-Test,  $p=0.0051$ ) but not in the HCC1954 cells (2% increase, Mann-Whitney U-Test,  $p>0.05$ ; Figure 6.4B).

CYCLIN D1 has previously been implicated in mediating NF- $\kappa$ B and *BCL3*-dependent changes in cell proliferation (Westerheide, Mayo et al. 2001). In order to establish whether this was the mechanism responsible for the observed changes in cell viability, *CYCLIN D1* QRT-PCR was performed on human cell lines subjected to *BCL3* SiRNA. No significant changes in the expression of this gene were observed in any of the cell lines tested (Figure 6.4C, T-test for all comparisons,  $p>0.05$ ) indicating that *CYCLIN D1* is not specifically responsible for *BCL3* dependent changes in the viability of these cell lines.

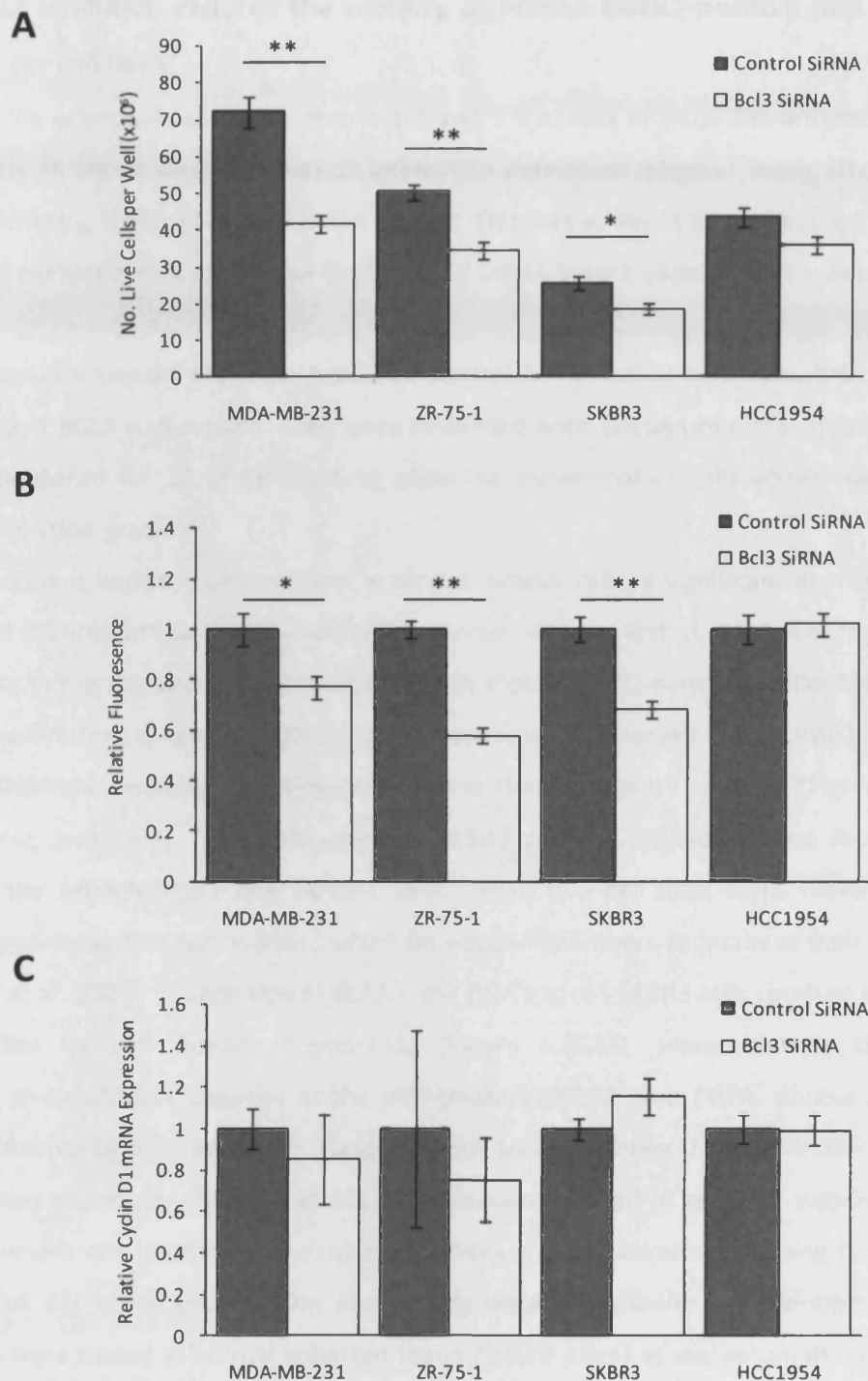


**Figure 6.4: BCL3 suppression reduces the viability of MDA-MB-231, ZR-75-1 and SKBR3 cells**  
 MDA-MB-231, ZR-75-1, SKBR3 and HCC1954 cells were transfected with *BCL3* or control SiRNA for 48 hours before either being harvested for RNA and subsequent QRT-PCR analysis or being subjected to viability assays. After 24 hours in normal adherent growth conditions, suppression of *BCL3* resulted in significantly reduced viability of MDA-MB-231, ZR-75-1 and SKBR3 but not HCC1954 cells as determined by live cell counts (A) and CellTiter-Blue assays (B, Mann-Whitney U-test, \*= $p < 0.05$ , \*\*= $p < 0.01$ ). Data represent 6 independent wells. *CYCLIN D1* mRNA expression was assessed by QRT-PCR and was found to be unchanged in all cell lines after *BCL3* suppression (C, T-test for all comparisons,  $p > 0.05$ ). Data is represented as *CYCLIN D1* mRNA levels relative to  $\beta$ -ACTIN mRNA levels. Error bars represent  $\pm$  SEM.

#### 6.2.4 *BCL3* inhibition reduces the motility of human ERBB2-positive and negative breast cancer cell lines

Having previously shown in chapters 4 and 5 that loss of *BCL3* has anti-metastatic effects in mouse models of breast cancer, it was of interest to determine whether these effects might also be observed in differing subtypes of the human disease. This was achieved by subjecting ERBB2-positive and EGFR-positive human breast cancer cell lines to *BCL3* SiRNA before performing Boyden chamber motility assays.

Cells were treated with 10nM *BCL3* or control SiRNA for 48 hours and RNA was harvested to ensure sufficient *BCL3* suppression. Cells were re-seeded onto Boyden motility chambers in low serum media and incubated for 24 or 48 hours to allow the movement of cells across membranes down a serum concentration gradient.

Consistent with the observations in mouse tumour cells, a significant decrease in cell motility was observed in three of the four human breast cancer cell lines tested. *BCL3* suppression resulted in a 56% reduction in the migratory capacity of the highly motile ERBB2-negative, MDA-MB-231 cells (Figure 6.5A&B, Mann-Whitney U-test,  $p=0.0008$ ). Similar results were observed in the ERBB2-low, ZR-75-1 cells, with *BCL3* inhibition resulting in a 49% reduction in their migratory capacity (Figure 6.5C&D, Mann-Whitney U-test,  $p=0.0002$ ). The ERBB2-positive, SKBR3 and HCC1954 cells were found to be far less motile than the MDA-MB-231 and ZR-75-1 cells. These two cell lines were therefore treated with hepatocyte growth/scatter factor (HGF) whilst on Boyden chambers to increase their base-line motility (Arihiro, Oda et al. 2000). Suppression of *BCL3* in the HGF treated-SKBR3 cells resulted in a 47% reduction in cell motility through Boyden membranes (Figure 6.6C&D, Mann-Whitney U-test,  $p=0.0304$ ). Interestingly, the migratory capacity of the HGF-treated, ERBB2- and EGFR- double positive HCC1954 cells was unaffected by *BCL3* inhibition (Figure 6.6A&B, Mann-Whitney U-test,  $p>0.05$ ).

Having previously shown that *BCL3* suppression resulted in reduced viability of some of the human cell lines, it was important to ensure that changes in cell numbers crossing the membranes was not simply due decreased proliferation of the cells resulting in lower cell numbers. To achieve this, parallel wells were plated in normal adherent tissue culture plates in low serum media for the duration of the experiments and counted at the same time as the Boyden chambers were fixed. In these low serum conditions there were only slight but insignificant decreases in cell numbers that were not big enough to account for the observed changes in motility (Figure 6.5B&D second set of bars, Figure 6.6B&D second set of bars).

These results demonstrate that in accordance with previous data from mouse models, suppression of *BCL3* has pronounced anti-motility effects on human cell lines and that these effects are not restricted to ERBB2-positive cells only.

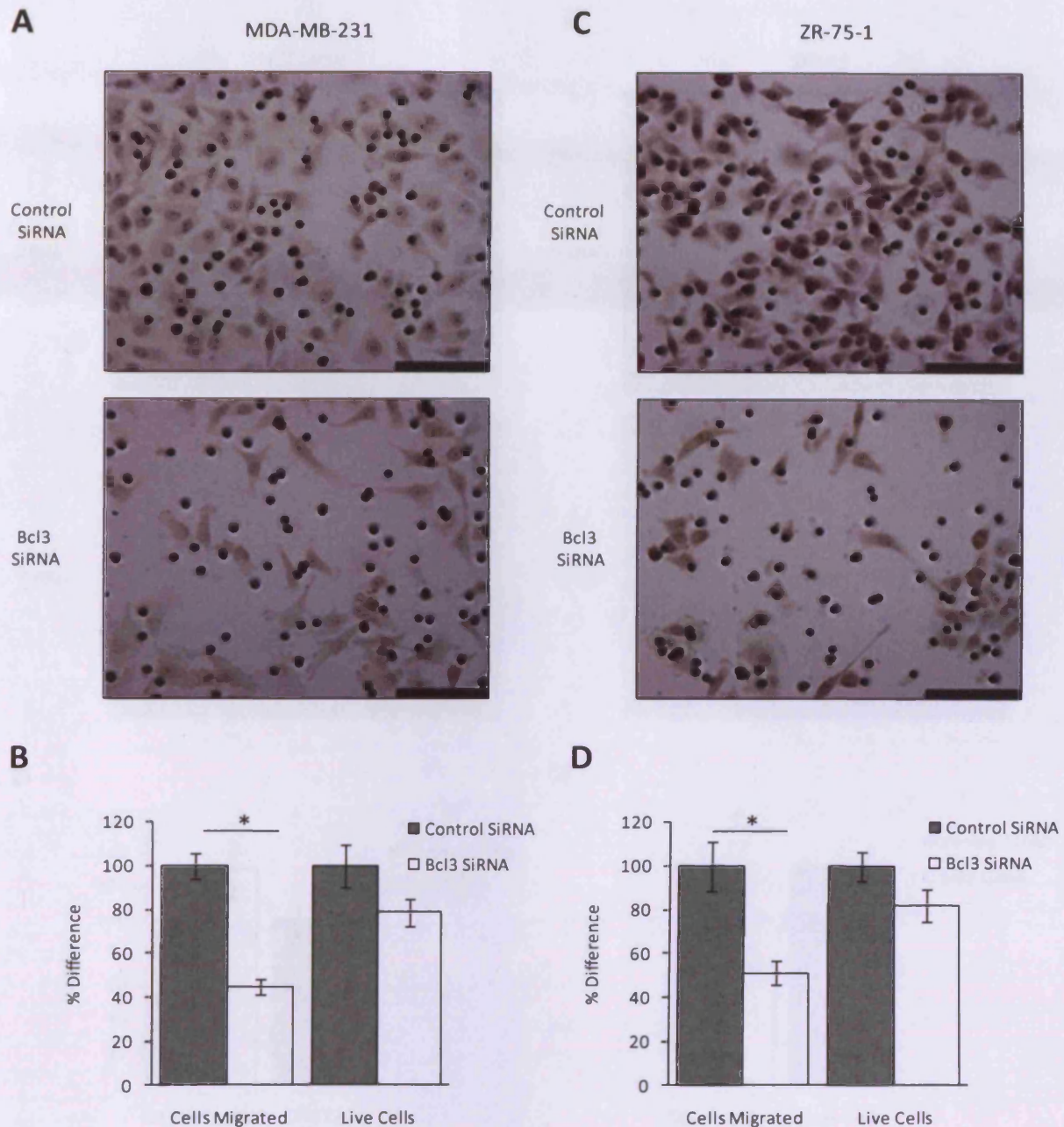


**Figure 6.5** *BCL3* suppression reduces the migratory capacity of ERBB2-negative, EGFR-positive human breast cancer cell lines

MDA-MB-231 and ZR-75-1 cells were transfected with *BCL3* or control SiRNA for 48 hours before being re-plated onto Boyden motility chambers. Cells were left for 24 hours before being fixed and stained on Boyden chamber membranes. Representative images of migrated MDA-MB-231 (A) and ZR-75-1 (C) cells on Boyden chamber membranes are shown. Scale bars indicate 100 $\mu$ m. Migrated cells (B&D, first set of bars) were counted from three fields of view of each of three replicate Boyden chambers and graphically represented as a percentage of the number of control cells counted. Three parallel wells were plated for the duration of the experiments in normal adherent growth conditions in low serum media. Live cell counts were performed at the end of each experiment and represented as a percentage of the number of live control cells present (B&D, second set of bars). Suppression of *BCL3* resulted in a significant reduction in the percentage of cells migrating through Boyden chambers in both the MDA-MB-231 (B, \*=Mann-Whitney U-test,  $p=0.0008$ ) and ZR-75-1 (D, \*=Mann-Whitney U-test,  $p=0.0002$ ) cell lines. The number of live cells present in parallel wells at the end of the experiment was not significantly affected by *BCL3* suppression in either cell line (B&D, Mann-Whitney U-test,  $p>0.05$ ). Error bars represent  $\pm$  SEM of triplicate Boyden chamber experiments.

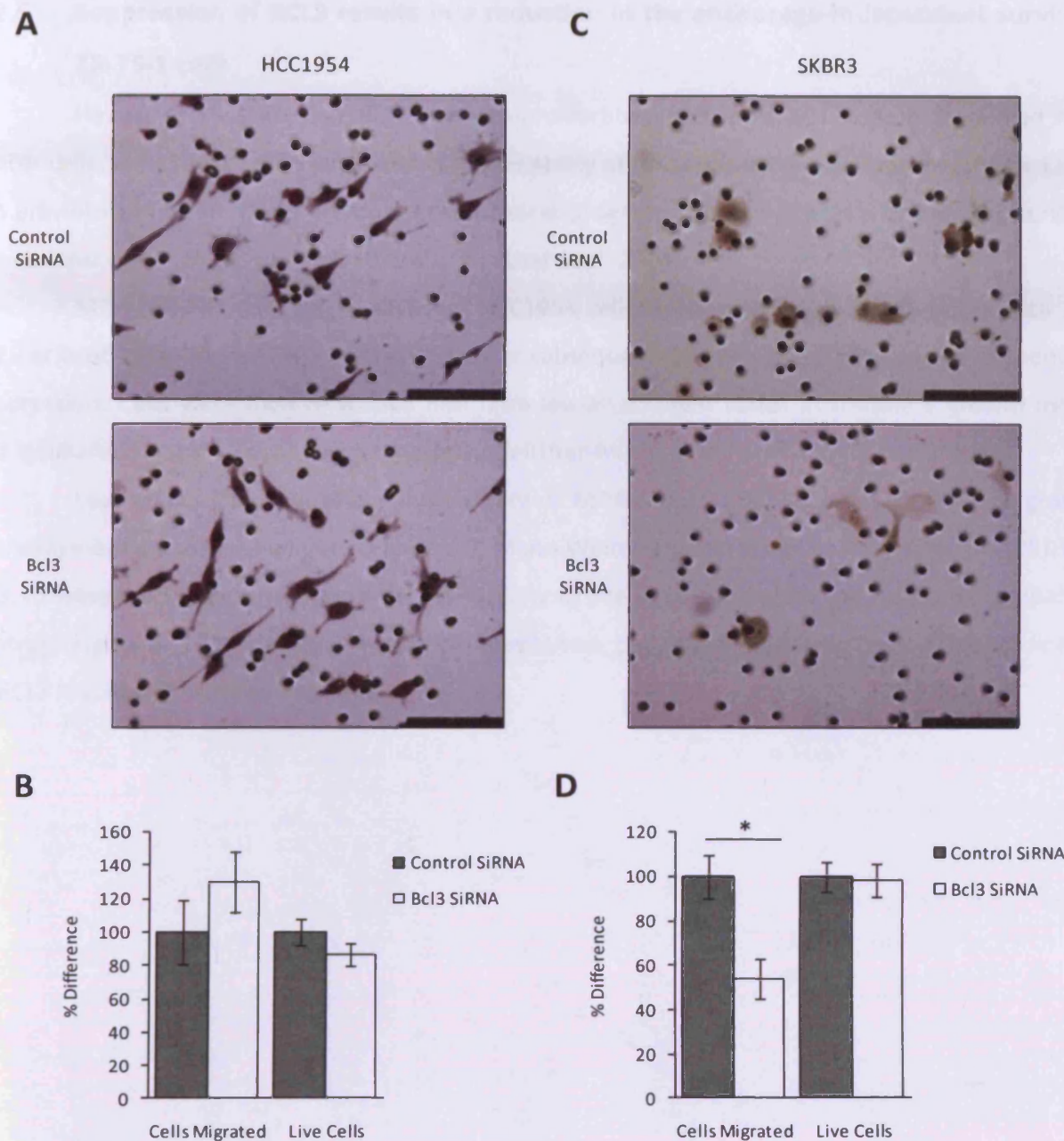


**Figure 6.6: BCL3 suppression reduces the migratory capacity of SKBR3 cells but not HCC1954 cells**

SKBR3 and HCC1954 cells were transfected with *BCL3* or control SiRNA for 48 hours before being re-plated onto Boyden motility chambers in the presence of HGF. Cells were left for 48 hours before being fixed and stained on Boyden chamber membranes. Representative images of migrated HCC1954 (A) and SKBR3 (B) cells on Boyden chamber membranes are shown. Scale bars indicate 100 $\mu$ m. Migrated cells (B&D, first set of bars) were counted from three fields of view of each of three replicate Boyden chambers and graphically represented as percentage of the number of control cells counted. Three parallel wells were plated for the duration of the experiments in normal adherent growth conditions in low serum media. Live cell counts were performed at the end of each experiment and represented as a percentage of the number of live control cells present (B&D, second set of bars). *BCL3* suppression did not significantly affect the motility of HCC1954 cells (B, Mann-Whitney U-test,  $p > 0.05$ ) but resulted in a significant reduction in the motility of SKBR3 cells (D, \* = Mann-Whitney U-test,  $p = 0.0304$ ). The number of viable cells present in low serum conditions at the end of the experiment was not significantly affected by *BCL3* suppression in either cell line (B&D, Mann-Whitney U-test,  $p > 0.05$ ). Error bars represent  $\pm$  SEM of triplicate Boyden chamber experiments.

### 6.2.5 Suppression of BCL3 results in a reduction in the anchorage-independent survival of ZR-75-1 cells

Having established that BCL3 has pro-proliferative and motility functions in human breast cancer cells, the affect of *BCL3* suppression on the ability of cells to resist anoikis was investigated as this has previously been shown to promote breast cancer progression and metastasis by enabling survival in the vascular or lymphatic channels (Douma, Van Laar et al. 2004).

MDA-MB-231, ZR-75-1, SKBR3 and HCC1954 cells were transfected for 48 hours with 10nM *BCL3* or control SiRNA and RNA was harvested for subsequent QRT-PCR analysis to ensure efficient *BCL3* suppression. Cells were then re-seeded into ultra-low-attachment plates in complete growth medium and incubated for 24 hours at which time-point CellTiter-Blue viability assays were performed.

Loss of *BCL3* did not affect the viability of MDA-MB-231, SKBR3 or HCC1954 cells grown in anchorage-independent conditions (Figure 6.7, Mann-Whitney U-test for all comparisons,  $p > 0.05$ ). There was, however, a significant decrease in the viability of the *BCL3* suppressed ZR-75-1 cells compared to controls (Figure 6.7, 33% decrease, Mann-Whitney U-test,  $p = 0.0022$ ), indicating that, in this cell line, loss of *BCL3* resulted in increased anoikis.

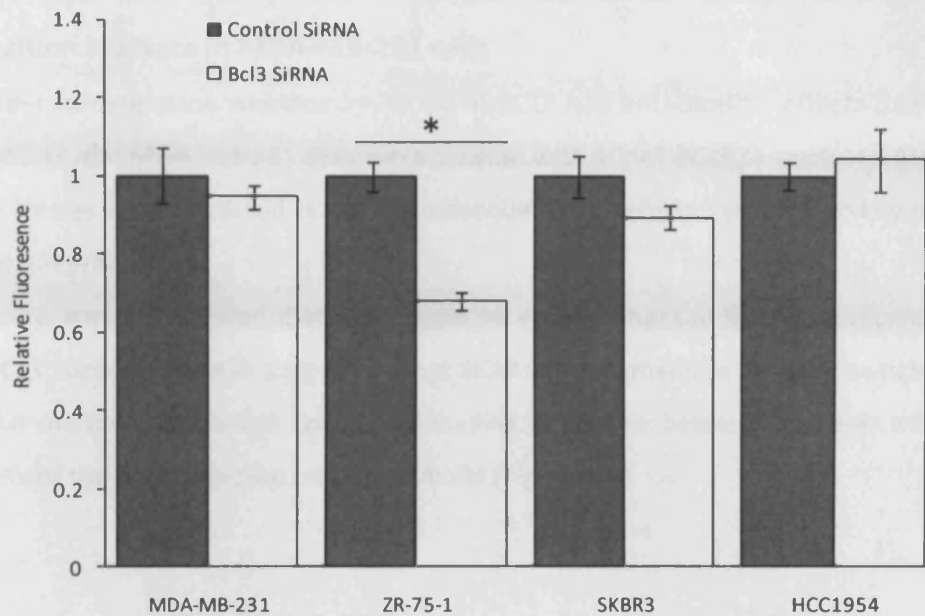


**Figure 6.7: BCL3 suppression results in a significant reduction in the viability of ZR-75-1 cells in anchorage-independent conditions**

MDA-MB-231, ZR-75-1, SKBR3 and HCC1954 cell lines were transfected with *BCL3* or control SiRNA for 48 hours before being re-plated in anchorage independent conditions. CellTiter-Blue assays were performed 24 hours later. *BCL3* suppression significantly reduced the viability of ZR-75-1 cells in non-adherent conditions (\*=Mann-Whitney U-test,  $p=0.0022$ ) whereas it had no effect on the other cell lines tested (Mann-Whitney U-test for all comparisons,  $p>0.05$ ). Data represent results from 6 wells of the same transfection experiment. Error bars represent  $\pm$  SEM.

### 6.2.6 *BCL3* suppression does not alter the expression of epithelial-to-mesenchymal transition markers in MDA-MB-231 cells

In order to determine whether inhibition of *BCL3* had anti-motility effects due to suppression of the EMT process, the MDA-MB-231 cells were treated with 10nM *BCL3* or control SiRNA for 48 hours, and whole cell lysates were extracted on ice for subsequent western analysis of two key markers of EMT, E-cadherin and Vimentin.

Western analysis revealed that there were no clear changes in the expression of E-cadherin or Vimentin in *BCL3* suppressed cells suggesting that *BCL3* did not mediate an EMT switch, as defined by these molecular markers, in this cell line. Equal loading of protein between samples was confirmed by visualising levels of the housekeeping protein, Tubulin (Figure 6.8).

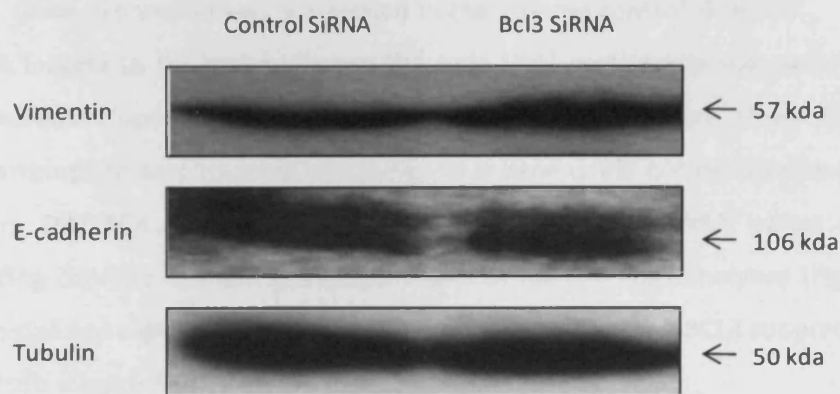


**Figure 6.8:** *BCL3* suppression has no effect on the expression EMT markers in MDA-MB-231 cells. MDA-MB-231 cells were transfected with *BCL3* or control SiRNA for 48 hours. Cells were then harvested for total proteins and subjected to western analysis. No changes were observed in the protein expression of E-cadherin or Vimentin. Equal loading was confirmed by Tubulin.

### 6.2.7 Analysis of motility-related gene targets potentially regulated by BCL3

Work in this chapter has so far shown that loss of BCL3 inhibits the motility of the EGFR-positive, ZR-75-1 and MDA-MB-231 cells, and the ERBB2-positive, SKBR3 cells. In order to determine whether BCL3 regulated the same set of motility-related genes in these human breast cancer cell lines as it did in MG1361 murine tumour cells, the expression of motility-related gene targets identified from the MG1361 microarray analysis (see Chapter 5, sections 5.2.9&5.2.10) were assessed. As a comparison, the expression of these genes was also assessed in the ERBB2- and EGFR-positive HCC1954 cells, the motility of which was unaffected by *BCL3* suppression.

Human cell lines were transfected with 10nM *BCL3* or control siRNA for 48 hours. The HCC1954 and SKBR3 cells were treated with HGF during the last 24 hours of transfection to increase their base-line motility and to recapitulate the conditions in which Boyden chamber motility experiments were previously performed. Triplicate wells of RNA were harvested for cDNA preparation and subsequent QRT-PCR analysis. Gene expression was normalised to the internal control,  $\beta$ -ACTIN.

The first targets to be analysed were the four *NME* metastases suppressor genes that were identified to be increased upon *BCL3* suppression in MG1361 cells. Of note, three different primer sets were used in an attempt to amplify *NME3*. However, this gene could not be detected in any cell line by any set of primers. QRT-PCR analysis directed against the other three *NME* genes showed that there were no outstanding changes in their expression in any of the cell lines analysed (Figure 6.9), although there was a very small but significant increase in *NME2* expression in the *BCL3* suppressed HCC1954 cells compared to controls (Figure 6.9D, 25% increase, T-test,  $p=0.0154$ ).

Next, *TIMP1* and *TIMP2* were analysed. Interestingly, *BCL3* suppression resulted in a significant up-regulation of *TIMP1* in comparison to control cells in three of the four cell lines tested, including the HCC1954 cells whose motility was unaffected by *BCL3* suppression (Figure 6.10A,B&D, MDA-MB-231 cells: 74% increase, T-test,  $p=0.0013$ ; ZR-75-1 cells: 81% increase, T-test,  $p=0.0002$  and HCC1954 cells 77% increase, T-test,  $p=0.0108$ ). It was also increased by 43% in the *BCL3* siRNA treated SKBR3 cells compared to controls but this change was found to be insignificant (Figure 6.10C, T-test,  $p>0.05$ ). Furthermore, *BCL3* inhibition resulted in a significant 20% up-regulation of *TIMP2* in the SKBR3 cells (Figure 6.10C, T-test,  $p=0.03$ ). This, however, was not observed in any of the other cell lines tested. These data indicate that, similarly to observations made in the MG1361 murine cell line (see Chapter 5, section 5.2.10), suppression of *BCL3* resulted in the up-regulation of members of the *TIMP* family of genes in both ERBB2- and EGFR-positive human breast cancer cell lines. This up-regulation did not necessarily correlate with the *BCL3*-mediated motility phenotype as up-regulation of *TIMP1* was also observed in the HCC1954 cells.

A number of the other targets identified in the MG1361 microarray were also analysed in the human cell lines. There were no significant changes in any of the targets analysed in the ERBB2-negative, MDA-MB-231 or ZR-75-1 cells (Figure 6.11A&B, T-test for all comparisons,  $p > 0.05$ ). In the HCC1954 and SKBR3 cells, very small but significant changes were observed in the expression of the Rho GDP dissociation inhibitor, *ARHGDIB* that has previously been shown to be a metastases inhibitor in human cancer (Gildea, Seraj et al. 2002) (Figure 6.11C&D). However, the changes were inconsistent across the two cell lines, with *BCL3* suppression resulting in an increase in *ARHGDIB* in the HCC1954 cells (Figure 6.11D) and a decrease in the SKBR3 cells (Figure 6.11C), indicating that changes in the expression of this gene are unlikely to be responsible for the observed *BCL3*-dependent motility phenotype. A significant increase in *SPHK2* was also observed in the HCC1954 cells (Figure 6.11D). However, as this gene has only previously been shown to enhance EGF-stimulated motility and as HCC1954 cells did not demonstrate a *BCL3*-mediated motility phenotype, it is unlikely to be involved in regulating motility in response to *BCL3* suppression.

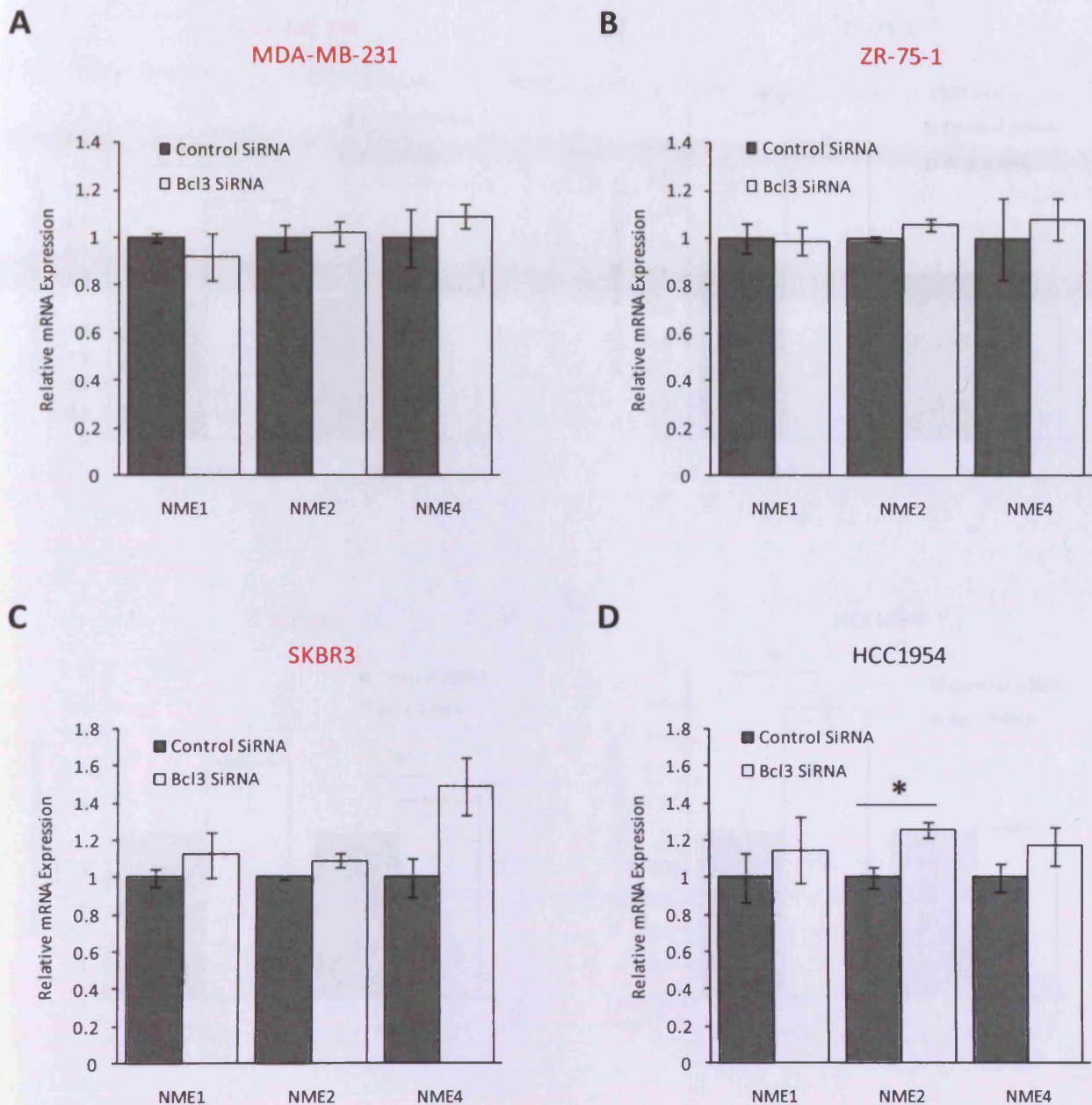


**Figure 6.9: QRT-PCR analysis of NME genes in BCL3 suppressed human breast cancer cell lines**

RNA was harvested from MDA-MB-231, ZR-75-1, SKBR3 and HCC1954 cells that had been transfected with *BCL3* or control SiRNA for 48 hours. QRT-PCR analysis directed against *NME1*, *NME2*, and *NME4* was performed. *BCL3* suppression had no significant effect on the mRNA expression of any of the genes analysed in the MDA-MB-231 (A), ZR-75-1 (B) or SKBR3 (C) cell lines. *BCL3* suppression resulted in a significant increase in *NME2* mRNA expression in the HCC1954 cells (\*=T-test,  $p=0.0154$ ). Data represent three independent transfection experiments and error bars represent  $\pm$  SEM. Graphs highlighted with a red title indicate cell lines in which suppression of *BCL3* was previously shown to induce a motility phenotype.

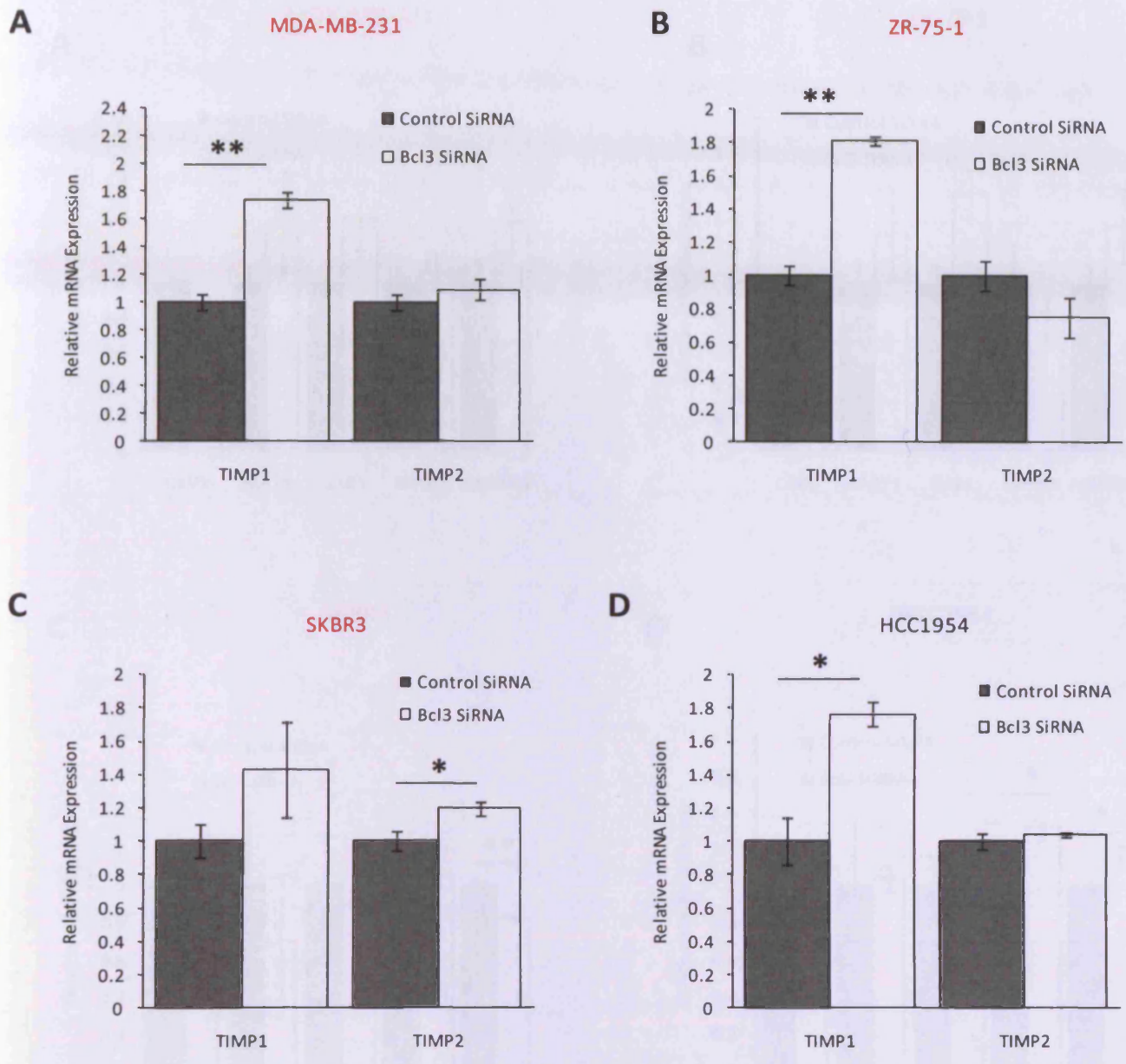


**Figure 6.10: BCL3 suppression increases the mRNA expression of TIMP genes in human breast cancer cell lines**

RNA was harvested from MDA-MB-231, ZR-75-1, SKBR3 and HCC1954 cells that had been transfected with *BCL3* or control SiRNA for 48 hours. QRT-PCR analysis directed against *TIMP1* and *TIMP2* was performed. *BCL3* suppression resulted in a significant increase in *TIMP1* mRNA expression in the MDA-MB-231 (A), ZR-75-1 (B) and HCC1954 (D) cells (T-test,  $*=p<0.05$ ,  $**=p<0.01$ ) but not in the SKBR3 cells (C, T-test,  $p>0.05$ ). *TIMP2* mRNA expression was significantly increased in response to *BCL3* suppression in the SKBR3 (C, T-test,  $*=p<0.05$ ) cells but not in any other cell line tested (A, B & D, T-test,  $p>0.05$ ). Data represent three independent transfection experiments and error bars represent  $\pm$  SEM. Graphs highlighted with a red title indicate cell lines in which suppression of *BCL3* was previously shown to induce a motility phenotype.

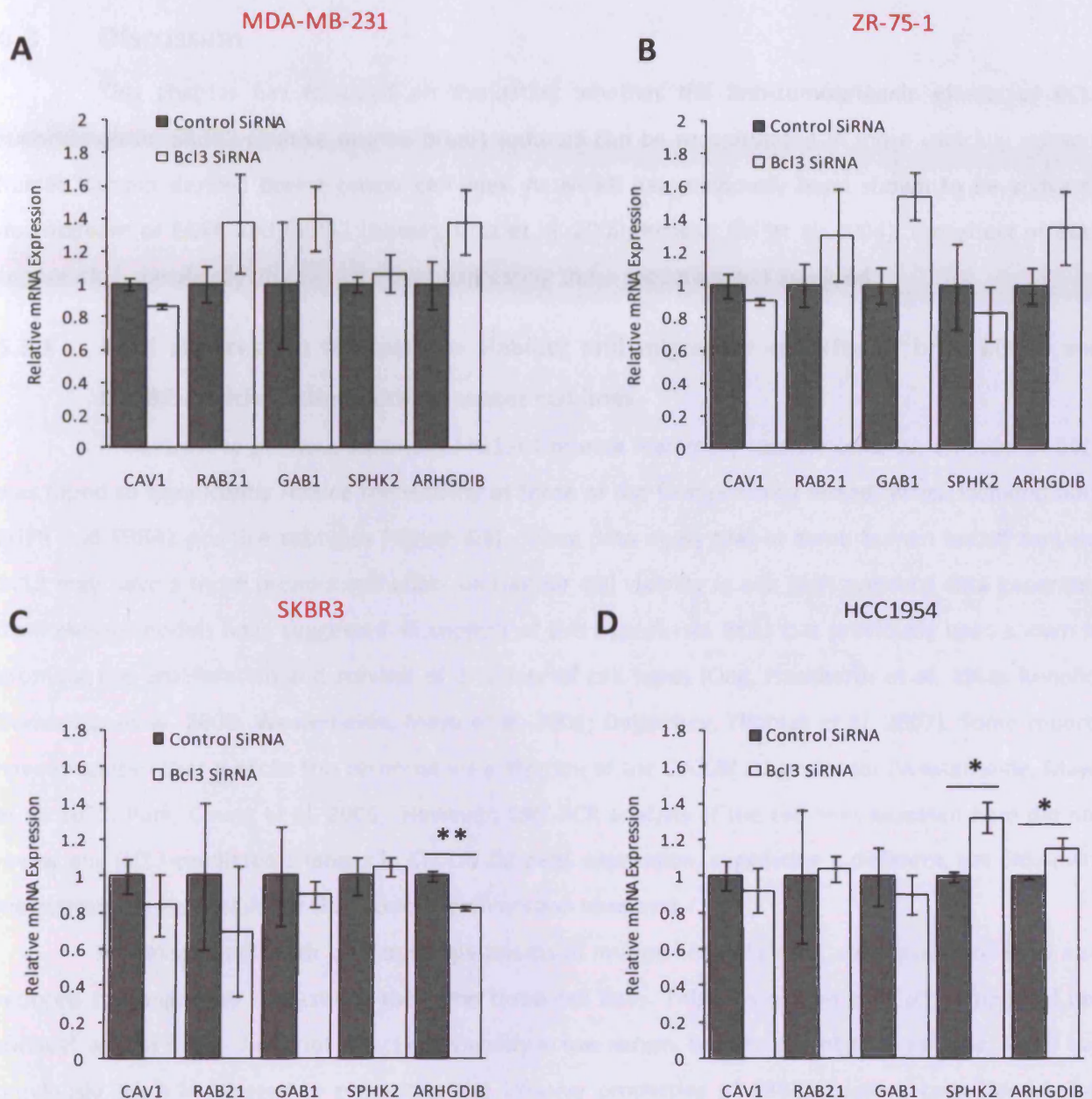


**Figure 6.11: QRT-PCR analysis of motility-related genes in *BCL3* suppressed human breast cancer cell lines**

RNA was harvested from MDA-MB-231, ZR-75-1, SKBR3 and HCC1954 cells that had been transfected with *BCL3* or control SiRNA for 48 hours. QRT-PCR analysis directed against motility-related genes that had previously been identified in chapter 5 was performed. *BCL3* suppression had no significant effects on any of the genes analysed in the MDA-MB-231 (A) or ZR-75-1 (B) cells (T-test for all comparisons,  $p > 0.05$ ). A significant reduction *ARHGDI B* mRNA expression was observed in SKBR3 cells in response to *BCL3* suppression (C, T-test,  $** = p < 0.01$ ). In the HCC1954 cells, *BCL3* suppression resulted in a significant increase *SPHK2* and *ARHGDI B* (D, T-test,  $* = p < 0.05$ ). Data represent three independent transfection experiments and error bars represent  $\pm$  SEM. Graphs highlighted with a red title indicate cell lines in which suppression of *BCL3* was previously shown to induce a motility phenotype.

## 6.3 Discussion

This chapter has focussed on evaluating whether the anti-tumourigenic effects of *BCL3* suppression on ERBB2-positive murine breast tumours can be recapitulated in more clinically relevant human tumour-derived breast cancer cell lines. As NF- $\kappa$ B has previously been shown to be activated downstream of EGFR and ERBB2 (Biswas, Cruz et al. 2000; Biswas, Shi et al. 2004), the effect of *BCL3* suppression specifically on cell types over-expressing these receptors was analysed.

### 6.3.1 *BCL3* suppression reduces the viability and migratory capacity of both EGFR- and ERBB2-positive human breast cancer cell lines

In contrast to previous studies in MG1361 murine mammary tumour cells, suppression of *BCL3* was found to significantly reduce the viability of three of the four cell lines tested, which included both EGFR and ERBB2-positive subtypes (Figure 6.4). These data imply that in some human breast cancers, *BCL3* may have a more pronounced effect on tumour cell viability *in situ* than previous data generated from mouse models have suggested. In support of this hypothesis, *BCL3* has previously been shown to promote the proliferation and survival of a variety of cell types (Ong, Hackbarth et al. 1998; Rebollo, Dumoutier et al. 2000; Westerheide, Mayo et al. 2001; Dolgachev, Thomas et al. 2007). Some reports have proposed that it elicits this response via activation of the *CYCLIN D1* promoter (Westerheide, Mayo et al. 2001; Park, Chung et al. 2006). However, QRT-PCR analysis of the cell lines assessed here did not reveal any *BCL3*-mediated changes in *CYCLIN D1* gene expression, suggesting a different, yet unknown, mechanism is responsible for the reduced proliferation observed.

In concordance with previous experiments in murine MG1361 cells, suppression of *BCL3* also reduced the migratory capacity of the same three cell lines. This was not an artefact of reduced cell survival, as loss of *BCL3* did not affect cell viability in low serum, Boyden chamber conditions. NF- $\kappa$ B has previously been implicated in promoting the invasive properties of ERBB2-positive cells (Merkhofer, Cogswell et al. 2010). However, this is the first time that *BCL3* has been shown to modulate the motility of human breast cancer cells, although it was recently shown to promote the migration of human melanoma cells via activation of the N-cadherin promoter (Massoumi, Kuphal et al. 2009). Effects on this promoter have not been evaluated in the present study but could be assessed in the future as a potential *BCL3*-mediated mechanism to induce cell migration.

Having identified that suppression of *BCL3* had anti-metastatic effects on human cell lines, QRT-PCR analysis of metastases-related targets identified in the microarray from chapter 5 was performed. This revealed that, similarly to the MG1361 murine mammary tumour cell line, either *TIMP1* or *TIMP2* were consistently up-regulated in response to *BCL3* suppression across all the cell lines analysed, suggesting a possible mechanism by which *BCL3* mediates a pro-invasive phenotype. In order

to investigate this possibility further, a number of future experiments could be performed, including ChIP on the *TIMP* promoters to establish which BCL3 mediated changes in NF- $\kappa$ B DNA binding are observed or SiRNA suppression of both *BCL3* and *TIMPs* to determine whether this abolishes the BCL3-mediated phenotype.

Of note, both the viability and invasive capacity of HCC1954 cells were consistently unaffected in response to *BCL3* suppression. A number of possible reasons for this could be proposed. Firstly as these cells were shown to have relatively high *BCL3* expression (Figure 6.1), it is feasible that a 70% suppression of *BCL3* from such high constitutive levels is not enough to result in a noticeable phenotype. Secondly, it is possible that although these cells have high levels of *BCL3* mRNA and express both EGFR and ERBB2 receptors, they may have very low levels of NF- $\kappa$ B subunits for BCL3 to co-operate with. This, however, is an unlikely hypothesis, as a previous study demonstrated that HCC1954 cells have a similar NF- $\kappa$ B DNA binding activity to SKBR3 cells (Yamaguchi, Ito et al. 2009) which were shown to respond to *BCL3* suppression. A final possibility is that ERBB2 may preferentially signal via alternative pathways to elicit growth and motility responses in these cells. Indeed, ERBB2 has previously been shown to induce proliferation via activation of the PI3K pathway independently of NF- $\kappa$ B signalling (Merkhofer, Cogswell et al. 2010).

One of the major observations from data presented in this chapter was that BCL3 mediated a profound effect on the proliferation and motility of both ERBB2- and EGFR-positive cell lines. Of particular interest was the significant response to BCL3 inhibition displayed by 'triple negative' MDA-MB-231 cells, a disease subtype that has a poor prognosis and is currently difficult to treat (reviewed in De Laurentiis, Cianniello et al. 2010). This effect was particularly remarkable considering the comparatively low constitutive expression of *BCL3* in these cells (Figure 6.1). Work from Pratt et al. (2009) suggested that human ERBB2-positive luminal cancers preferentially express NF- $\kappa$ B subunits involved in the canonical pathway whereas a large percentage of basal tumours, which are generally EGFR-positive, express constituents of the non-canonical pathway. It is possible that due to its involvement in both NF- $\kappa$ B signalling pathways, BCL3 may be able to influence the progression of both of these disease subtypes.

### 6.3.2 Summary

In summary, this chapter has established that suppression of BCL3 can reduce the viability and motility of both ERBB2- and EGFR-positive human breast cancer cell lines. Resistance to current therapies such as trastuzumab, the first-line therapy for ERBB2-positive breast cancer, is prevalent (Cobleigh, Vogel et al. 1999; Vogel, Cobleigh et al. 2001; Vogel, Cobleigh et al. 2002; reviewed in Nahta and Esteva 2006) Mechanisms involved in this resistance can include the up-regulation of other members of the EGF-family of receptors (Ritter, Perez-Torres et al. 2007; Dua, Zhang et al. 2010). Results from this chapter demonstrate that therapeutic inhibition of BCL3 could potentially block the downstream effects of both

the ERBB2 and EGFR oncogenic pathways, reducing the possibility of resistance. Taken together with data from all previous chapters, these results make BCL3 a very attractive therapeutic target for both ERBB2-positive and EGFR-positive breast cancers.

# **Chapter 7:**

## **General Discussion**

## 7.1 General Discussion

The mammary gland is a highly specialised organ that undergoes well co-ordinated cycles of cell proliferation, differentiation and programmed cell death with each successive pregnancy. However, partly due to its function during pregnancy, this organ is also highly susceptible to cancer with one in nine women in the western world developing breast cancer at some point in their life-time (Bray, McCarron et al. 2004).

NF- $\kappa$ B is up-regulated in a number of human malignancies, including breast cancer. This family of transcription factors regulate genes involved in many pro-oncogenic processes including cell proliferation, cell survival, angiogenesis, motility and invasion, and as such there has been much interest in the use of NF- $\kappa$ B inhibitors in the treatment of cancer. However, sustained global inhibition of NF- $\kappa$ B is likely to have serious adverse consequences on normal tissues, particularly those of the immune system. An ideal treatment strategy would be to selectively block the cancer-promoting functions of NF- $\kappa$ B whilst ensuring that its normal physiological functions are retained. One possible way of achieving this could be to target modifying NF- $\kappa$ B co-factors, such as BCL3.

With this in mind, the aim of this thesis was to: (1) determine the effect of BCL3 deletion on normal mammary tissue in the context of the pregnancy cycle, with particular emphasis on involution where it has previously been shown to be up-regulated; (2) evaluate the role of BCL3 in the initiation and progression of ERBB2-driven murine mammary carcinogenesis; and (3) assess the effect of BCL3 suppression on human breast cancer cell lines representing different subtypes of the disease.

## 7.2 The role of BCL3 during the murine pregnancy cycle

Results from chapter 3 of this thesis demonstrated that although *Bcl3* is a downstream transcriptional target of the principle initiator of involution, STAT3, deletion of this NF- $\kappa$ B co-factor had very little effect on the gross morphology or function of the mammary gland throughout the pregnancy cycle. A subtle BCL3 dose-dependent effect was observed during involution whereby *Bcl3*<sup>+/-</sup> mice had increased apoptotic bodies in comparison with both *Bcl3*<sup>+/+</sup> and *Bcl3*<sup>-/-</sup> mice, but this was very transient and had no lasting effect on the morphology or function of the gland. From these results, it would appear that the transient, STAT3 mediated, increase in *Bcl3* expression observed at the onset of involution (Chapter 3; Clarkson, Wayland et al. 2004) is a redundant pathway that can probably be compensated for by the altered DNA binding and transcriptional activation of various NF- $\kappa$ B subunits. Alterations in the protein expression of p50 and p52 were not observed by IHC in the absence of BCL3, in comparison with heterozygous mice, but it is highly likely that changes in BCL3 expression could perturb the DNA-binding activities of these subunits. The idea of compensatory mechanisms occurring following

the loss of involution regulators is not hugely surprising as even in the absence of STAT3 itself, involution was still able to proceed, albeit with considerably delayed kinetics (Chapman, Lourenco et al. 1999).

It has previously been shown that constitutive knock out of several members or upstream regulators of the NF- $\kappa$ B family results in severe morphological disruption across a number of organs and in some cases embryonic lethality (for review Gerondakis, Grumont et al. 2006). In the mammary gland specifically, inhibition of NF- $\kappa$ B activity has been shown to have considerable effects on lobuloalveolar development during pregnancy (Cao, Bonizzi et al. 2001) and delayed apoptosis during involution (Baxter, Came et al. 2006). Furthermore, experiments involving the up-regulation of NF- $\kappa$ B signalling have shown that this transcription factor is essential for maintaining the normal epithelial architecture during ductal development (Brantley, Chen et al. 2001). These genetically engineered mouse models provide substantial evidence that therapeutic targeting of NF- $\kappa$ B in disease could have severe consequences on normal tissues. Mice lacking BCL3 are viable with only minor immunological defects rendering them more susceptible to certain pathogens (Franzoso, Carlson et al. 1997; Schwarz, Krimpenfort et al. 1997). This observation, together with results from chapter 3 of this thesis, suggests that, unlike global inhibition of NF- $\kappa$ B, loss of BCL3 has little effect on normal tissues.

### 7.3 The role of BCL3 in breast carcinogenesis

Having established that depletion of BCL3 had only very mild effects on normal mammary epithelium, the role of BCL3 in breast cancer initiation and progression was investigated in the hope that inhibiting this NF- $\kappa$ B co-factor would block the tumour-promoting function of NF- $\kappa$ B, whilst allowing it to retain most of its normal physiological functions. To examine this notion, the effect of BCL3 deletion on ERBB2-driven mammary tumour initiation and progression was examined.

#### 7.3.1 BCL3 and murine ERBB2-driven mammary tumour initiation

The first observation that became apparent from studies utilising *MMTV/N<sub>2</sub>* tumour models was that loss of BCL3 resulted in a considerable delay in the formation of ERBB2-driven mammary tumours (Chapter 4). This finding is significant as it implies that BCL3 activity is essential for optimal ERBB2-mediated cell transformation. As BCL3 has been shown to promote cell proliferation in a number of contexts (see Chapter 1: General Introduction, section 1.4.5.2), this delay in tumour latency was initially thought to be due to a BCL3-dependent decrease in cell proliferation via reduced CYCLIN D1 activity. However, this was found not to be the case as no alterations in pre-neoplastic cell proliferation, apoptosis or *Cyclin D1* gene expression were observed.

Although the precise mechanism behind this BCL3-mediated delay in mammary tumour initiation was not established in this thesis, a number of hypotheses could be proposed to explain it (see Figure 7.1 for proposed model). Firstly, it is possible that loss of BCL3 delays the tyrosine kinase

activation of the wild-type *Neu* transgene. Mammary tumours induced by the wild-type *Neu* (*MMTV/N<sub>2</sub>*) transgene have increased NEU intrinsic tyrosine kinase activity in comparison with adjacent tissue, and it is thought that this activation is the rate limiting step in tumour induction (Guy, Webster et al. 1992). It has subsequently been shown that activation of NEU in transgenic mice often occurs through a somatic mutation located within the transgene itself (Siegel, Dankort et al. 1994). However, 35% of tumours lack these somatic mutations and yet still possess intrinsic NEU tyrosine kinase activity suggesting that activation can also occur via a different mechanism such as up-regulation of EGFR family ligands (Siegel, Dankort et al. 1994). Interestingly, a positive feedback loop involving the activation of NF- $\kappa$ B by ERBB2/NEU and a subsequent NF- $\kappa$ B-dependent transcriptional up-regulation of the EGFR family ligand, heregulin, has been previously identified (Frensing, Kaltschmidt et al. 2008). NEU/ERBB2 activation is often mediated by heterodimerisation with other ligand-bound EGFR family members, such as ERBB3 (Carraway, Sliwkowski et al. 1994; Sliwkowski, Schaefer et al. 1994) which has been found to be over-expressed in conjunction with NEU/ERBB2 in both the *MMTV/N<sub>2</sub>* model and human breast cancer (Siegel, Ryan et al. 1999). It is therefore feasible that loss of BCL3 could prevent the NF- $\kappa$ B-mediated up-regulation of EGFR family ligands such as heregulin, resulting in reduced ERBB2(NEU)/ERBB3 heterodimerisation and thus delayed constitutive ERBB2/NEU kinase activation and mammary tumour formation (Figure 7.1). This notion is supported by the observation that although BCL3 deletion resulted in a striking delay in the initiation of mammary tumours in wild-type *Neu* (*MMTV/N<sub>2</sub>*)-expressing mice, no comparable delay was found in the initiation of tumours driven by the activated form of the transgene (*MMTV/NK*). The discrepancies between the two models could be accounted for if the primary function of BCL3 was to promote the kinase activation of the *N<sub>2</sub>* transgene. This hypothesis is purely speculative and further experiments analysing the effect of BCL3 on the kinase activity of NEU/ERBB2 and the transcriptional regulation of EGFR family ligands should be performed in the future to investigate it further.

A second possible hypothesis to explain the delay in tumour initiation is that BCL3 depletion may perturb NF- $\kappa$ B-mediated effects on stem or progenitor cell populations within pre-neoplastic tissue. Mammary stem cells are functionally defined as those cells that are able to regenerate full glands after transplantation into a cleared fat pad whereas progenitors are usually committed to a specific cell lineage (luminal or myoepithelial) (Kordon and Smith 1998; Stingl, Eaves et al. 2001; Stingl, Eirew et al. 2006). Mammary stem or progenitor cells are considered likely targets for oncogenic transformation enabling them to initiate tumours that resemble the progenitor or stem cell from which they were derived (reviewed in Stingl and Caldas 2007). In the *MMTV/N<sub>2</sub>* mouse model, virtually all epithelial tumour cells have been shown to exhibit the luminal progenitor marker, CD61, suggesting that the target cell for malignant transformation in this model is the luminal progenitor (Vaillant, Asselin-Labat et al.

2008). It is possible that depletion of BCL3 alters NF- $\kappa$ B signalling to reduce the size of this population and thus reduce the number of potential cell targets in which further oncogenic events, such as the acquisition of constitutive NEU kinase activity, can occur (Figure 7.1). In support of this idea, NF- $\kappa$ B has previously been shown to be activated in the luminal progenitor cell population (Pratt, Tibbo et al. 2009). Furthermore, inhibition of canonical NF- $\kappa$ B activity specifically reduced the formation of luminal ERBB2-positive neoplasias, but had no effect on the formation of basally derived lesions following a chemical carcinogenesis protocol (Pratt, Tibbo et al. 2009). These findings suggest that NF- $\kappa$ B signalling is of prime importance in luminal progenitor cells and that depletion of an NF- $\kappa$ B co-factor, such as BCL3, could disturb the maintenance of this cell population. This hypothesis is currently being investigated in the laboratory by performing *in vitro* colony-forming cell assays on pre-neoplastic primary cells from *Bcl3*<sup>-/-</sup>/*MMTV*/*N*<sub>2</sub> and *Bcl3*<sup>+/+</sup>/*MMTV*/*N*<sub>2</sub> mice. This assay identifies progenitor cells that produce discrete colonies of mammary cells in low density adherent cultures (Stingl, Eaves et al. 2001 Stingl, Eirew 2006) and can therefore be used to establish the effect of BCL3 on this cell population.

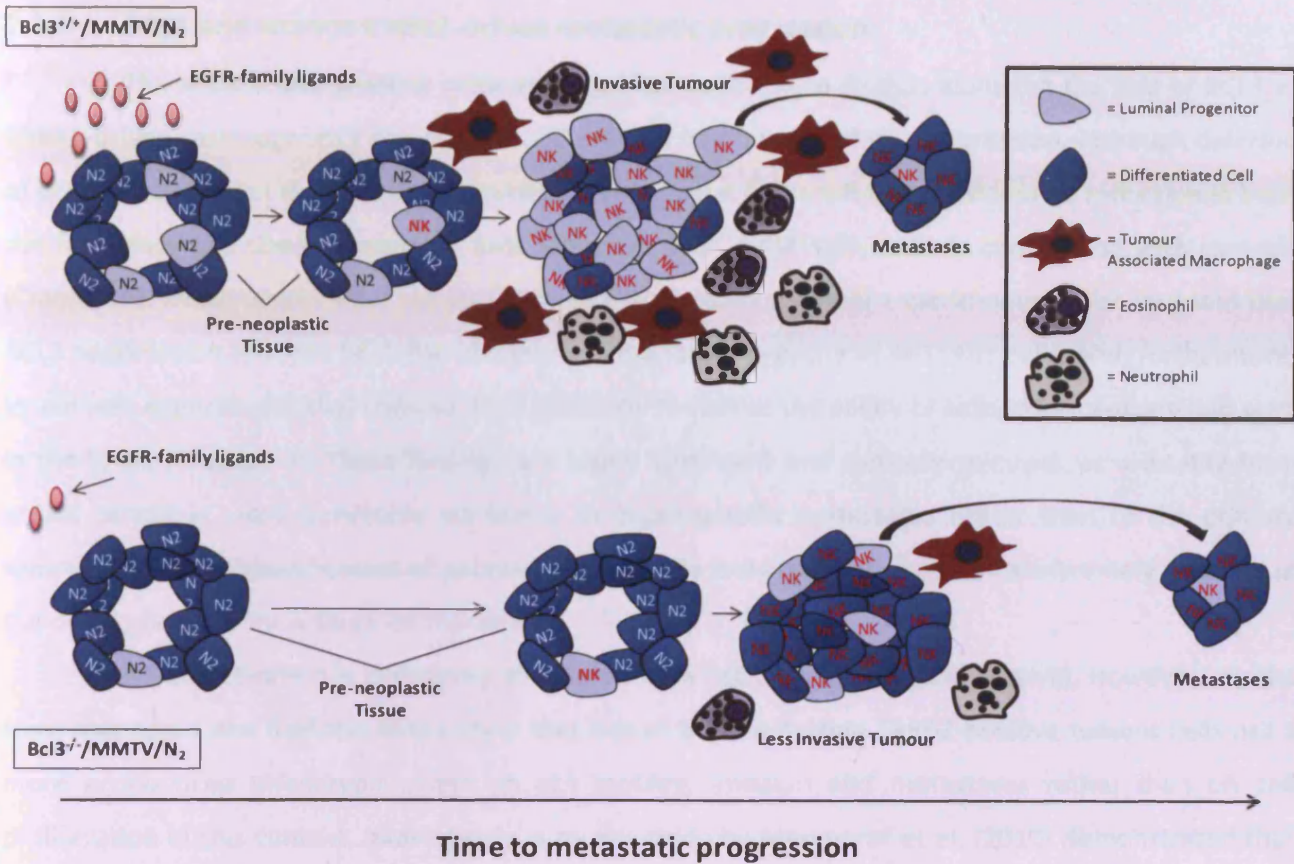


**Figure 7.1: Proposed model for the BCL3 mediated effects on breast cancer initiation and progression**

$Bcl3^{-/-}/MMTV/N_2$  tumours show delayed initiation in comparison to  $Bcl3^{+/+}/MMTV/N_2$  tumours. This could be due to delayed NEU kinase activation within the luminal progenitor pool. When BCL3 is present (top set of diagrams), NF- $\kappa$ B-mediated transcriptional up-regulation of EGFR-family ligands can occur to promote constitutive NEU kinase activation (from  $N_2$  cells to  $NK$  cells). Furthermore, a normal sized luminal progenitor cell population (light blue cells) is maintained in which kinase activation can occur, resulting in the initiation and growth of a kinase active tumour. However, loss of BCL3 (bottom set of diagrams), could result in a reduced tumour initiating luminal progenitor cell pool and reduced transcriptional up-regulation of EGFR-family ligands which, as a result, may delay constitutive luminal progenitor kinase activation and subsequent tumour initiation. In addition,  $Bcl3^{-/-}/MMTV/N_2$  tumours show delayed metastatic progression in comparison to  $Bcl3^{+/+}/MMTV/N_2$  tumours. This may be due to multiple effects of BCL3 on the tumour cells and the tumour microenvironment. When BCL3 is present, the luminal progenitor pool, from which metastases are likely to originate, continues to be well maintained (light blue cells). Also, BCL3 promotes the intrinsic motility and invasive properties of tumour cells and furthermore, it may promote the NF- $\kappa$ B-mediated recruitment of metastases promoting inflammatory cells to the tumour microenvironment. However, loss of BCL3 reduces the intrinsic motility and invasive properties of tumour cells. In addition, it may also reduce the luminal progenitor cell pool and suppress a metastases-promoting inflammatory tumour microenvironment, collectively resulting in delayed metastatic disease progression.

### 7.3.2 BCL3 and murine ERBB2-driven metastatic progression

The second and possibly most exciting observation from studies assessing the role of BCL3 in ERBB2-driven carcinogenesis was the marked effect it had on metastatic progression. Although deletion of BCL3 did not affect the growth of established tumours, it did result in a considerable reduction in both the frequency and size of metastatic lung lesions in *Bcl3*<sup>-/-</sup>/MMTV/*N*<sub>2</sub> mice in comparison with controls (Chapter 4). These results were supported by *in vitro* Boyden chamber experiments, which revealed that BCL3 suppression reduced both the invasive and migratory capacity of MG1361 cells, and, furthermore, by tail vein experiments that showed BCL3 inhibition to reduce the ability of cells to extravasate and seed in the lungs (Chapter 5). These findings are highly significant and clinically relevant, as mortality from breast cancer is most commonly attributed to organ-specific metastases rather than to the primary tumour. Thus, the identification of pathways involved in metastatic progression is extremely valuable in the development of new targeted therapies.

NF- $\kappa$ B activation is commonly associated with cell proliferation and survival. However, results from chapters 4 and 5 of this thesis show that loss of BCL3 in murine ERBB2-positive tumour cells has a more pronounced phenotypic effect on cell motility, invasion and metastases rather than on cell proliferation in this context. Interestingly, a recent study by Merkhofer et al. (2010) demonstrated that down-regulation of canonical NF- $\kappa$ B activity in ERBB2-positive human breast cancer cells specifically resulted in a decrease in cancer cell invasion, but had no effect on cell proliferation (Merkhofer, Cogswell et al. 2010). It is possible that a similar mechanism may occur in the murine tumour cells utilised in this thesis, whereby inhibition of BCL3 alters canonical NF- $\kappa$ B transcriptional activity to specifically suppress motility, invasion and metastases without having a noticeable effect on proliferation. Interestingly, however, BCL3 suppression in one human ERBB2-positive cell line resulted in the inhibition of both proliferation and motility (Chapter 6 and see section 7.3.3 below), indicating that, in some contexts, modulation of NF- $\kappa$ B downstream of ERBB2 can have effects on both of these processes.

Both *In vitro* and *in vivo* experiments performed in chapter 5 showed that the reduced ability of BCL3-deficient cells to metastasize to the lung was, at least in part, due to an intrinsic cell autonomous effect that was independent of the tumour microenvironment. However, the question of whether BCL3 may also regulate broader processes such as cancer-related inflammation to mediate disease progression remains unanswered. This is an important clinical question, as inflammatory breast cancer is an aggressive form of invasive breast cancer that has poor prognosis (reviewed in Robertson, Bondy et al. 2010).

During cancer-related inflammation, transcription factors are up-regulated that mediate the production of pro-inflammatory cytokines and chemokines in tumour cells which recruit and activate various inflammatory cells. The resulting inflammatory tumour microenvironment facilitates cancer

progression by promoting processes such as angiogenesis, cell migration, invasion and metastases (reviewed in Mantovani, Allavena et al. 2008). Studies targeting NF- $\kappa$ B have demonstrated that this signalling pathway is heavily involved in promoting an inflammatory tumour microenvironment and therefore disease progression in various cancer models (Greten, Eckmann et al. 2004; Luo, Maeda et al. 2004; Pikarsky, Porat et al. 2004). Recently, inhibition of NF- $\kappa$ B specifically in mammary epithelial cells was shown to reduce the proportion of infiltrating tumour associated macrophages (TAMs) in an ERBB2-driven murine breast cancer model (Liu, Sakamaki et al. 2010). The recruitment of TAMs has previously been shown to promote the metastatic progression of murine mammary tumours via a suggested mechanism involving the enhancement of angiogenesis (Lin, Nguyen et al. 2001; Lin and Pollard 2007). It is possible that loss of BCL3 may also inhibit the NF- $\kappa$ B-mediated recruitment of TAMs or other immune cells to delay mammary tumour progression (Figure 7.1). Moreover, as BCL3 was constitutively deleted in all cells in the mouse models utilised in this thesis, it is likely that NF- $\kappa$ B signalling intrinsic to immune cells would also be de-regulated, which could further delay the normal metastatic progression of mammary tumours.

Experiments performed in *MMTV/N<sub>2</sub>* or *MMTV/NK* mouse models have addressed the effect of global constitutive deletion of BCL3 across all tissues within the animal. Although these experiments have provided substantial evidence to implicate BCL3 in mammary tumour initiation and progression, they do not determine the effect of BCL3 inhibition on discrete stages during tumour development and progression. This leaves unanswered the question of whether short-term inhibition of BCL3 in late stages of tumour development can prevent the progression to metastatic disease, which is clinically relevant as it addresses the situation in which a patient is likely to present. Furthermore, although some mammary epithelial cell specific effects have been demonstrated *in vitro* and in tail vein experiments, the *in vivo* experiments presented in this thesis were unable to discriminate between the effects of BCL3 on mammary epithelial cells versus the surrounding inflammatory cells. One experiment that could potentially address both of these issues would be to create an inducible transgenic model in which *Bcl3* expression could be inhibited specifically in mammary epithelial cells at defined times during tumourigenesis. Such a model has recently been developed to determine the effect of inducible NF- $\kappa$ B inhibition in the context of PyVT-driven mammary tumourigenesis (Connelly, Barham et al. 2010). This model demonstrated that inhibition of NF- $\kappa$ B for a single week after primary tumours had developed resulted in reduced tumour burden, providing evidence that modulation of this signalling pathway could be an effective therapeutic treatment strategy for patients presenting with established breast tumours.

The discovery that global deletion of BCL3 reduces the occurrence of metastatic lung lesions in an ERBB2-driven murine breast cancer model is extremely exciting. However, a major limitation to the use of this model is its inability to accurately reflect all of the known sites of metastases in human breast

cancer, such as the brain, liver and in particular bone. In fact there is a distinct lack of models available in which to investigate the effect of a particular variable on bone metastases. Carefully selected sub-lines of cells generated from some spontaneous murine mammary carcinomas have been shown to have a high incidence of bone metastasis upon transplantation into the mammary fat pad (Lelekakis, Moseley et al. 1999; Li, Schem et al. 2008). Alternatively, intracardiac injection of human breast cancer cell lines into mice has also been shown to produce bone metastases. Although the latter method has the added advantage of enabling the investigator to use human cells representing an appropriate subtype of the disease (Yoneda 2000), intracardiac metastasis models are limited in that they do not encompass the early stages of the metastatic process. The future development of new ERBB2-driven mouse models of breast cancer that metastasize to the bone could aid in determining whether BCL3 contributes to this clinically relevant process.

### 7.3.3 BCL3 and human breast cancer

Having demonstrated that BCL3 plays a prominent role in promoting the initiation and progression of ERBB2-driven murine breast carcinoma, the question of whether it could have similar pro-tumourigenic effects in human breast cancer cells was addressed. Similarly to *in vitro* studies in murine MG1361 cell lines, suppression of BCL3 resulted in a reduction in the motility of three out of the four cell lines tested. Additionally, in contrast with both *in vitro* and *in vivo* murine studies, depletion of BCL3 also resulted in a considerable reduction in the viability of the same three cell lines indicating that therapeutic BCL3 inhibition *in situ* may have more pronounced effects on early tumourigenesis than previous data generated in murine models have suggested. The discrepancies between results in murine and human cell lines highlight the importance of substantiating observations in animal models with experiments on human tissues and indicate that further *in vitro* and *in vivo* studies utilising human cells are warranted to establish a better understanding of BCL3 in human disease.

A key observation from chapter 6 was that suppression of BCL3 inhibited the proliferative and migratory capacity of both ERBB2-positive and EGFR-positive human breast cancer cells, suggesting that it may be a useful target in the treatment of both subtypes of the disease. Excitingly, the basal-like, 'triple-negative' MDA-MB-231 cell line responded particularly well to BCL3 inhibition. This is a significant observation, as triple-negative breast cancers are extremely difficult to treat because of their lack of classical molecular therapeutic targets (reviewed in Gluz, Liedtke et al. 2009; De Laurentiis, Cianniello et al. 2010). It would be of great value to substantiate this preliminary observation by performing both orthotopic and tail vein transplants with MDA-MB-231 cells in the presence or absence of BCL3. Indeed, these experiments could be performed with cell lines displaying a variety of molecular and diagnostic markers in order to gain a greater understanding of the breadth of breast cancer subtypes that BCL3 may be able to modulate.

### 7.3.4 BCL3 and the transcriptional regulation of TIMPs

Having identified that BCL3 was able to regulate metastatic properties of both murine and human breast cancer cells, microarray analysis and subsequent QRT-PCR experiments were performed in an attempt to identify metastases-related gene targets of BCL3. These studies identified *TIMP1* and *TIMP2* to be consistently up-regulated following the inhibition of BCL3 in most cell lines tested. TIMPs act to inhibit MMPs that are known to promote breast cancer invasion and metastases (Talvensaarimattila, Paakko et al. 1998; Li, Cao et al. 2004; Wu, Wu et al. 2008; Zhang, Cao et al. 2008; Garcia, Gonzalez-Reyes et al. 2010; reviewed in Duffy, Maguire et al. 2000). Furthermore, they are critical regulators of matrix turnover at different stages of mammary gland development, including post-lactational involution (Talhouk, Bissell et al. 1992; Fata, Leco et al. 1999).

Previous analysis of the role of TIMPs in breast cancer has revealed a complex association with the disease. Over-expression of systemic TIMP1 in the context of two established murine mammary carcinogenesis models resulted in reduced tumour burden and metastases whereas mammary specific over-expression was ineffective against mammary tumourigenesis (Yamazaki, Akahane et al. 2004). Up-regulation of TIMP2 in the murine mammary gland resulted in reduced MMTV/Wnt1-induced mammary tumourigenesis and angiogenesis (Blavier, Lazaryev et al. 2006). In spite of the inhibitory effect of TIMPs on MMPs, high expression of TIMP1 or TIMP2 in primary human breast tumours has been found to correlate with increased metastases and poor prognosis (Gonzalez, Pidal et al. 2007; Vizoso, Gonzalez et al. 2007). This paradox could merely be due to co-upregulation of TIMPs and MMPs in breast cancer. However, as well as inhibiting MMPs, TIMP1 has also been shown to have other pro-tumourigenic functions on cell proliferation, survival and angiogenesis. Thus, the overall clinical relevance of the association between BCL3 and TIMPs observed in this thesis remains to be determined.

## 7.4 Future perspectives: targeting BCL3 as a therapeutic treatment in breast cancer?

Currently ERBB2-positive breast cancers are routinely treated with the ERBB2 monoclonal antibody trastuzumab (Herceptin). However, resistance to this treatment is prevalent resulting in a clinical need for new or adjuvant therapies for the disease. Data presented in this thesis provide compelling evidence for the use of the NF- $\kappa$ B co-factor, BCL3, as a therapeutic target in the treatment of metastatic ERBB2-positive breast cancer. Additionally, work performed in human breast cancer cell lines suggests that inhibition of BCL3 in the clinic may also have anti-tumourigenic effects on EGFR-positive tumours, including those characterised as aggressive triple-negative breast cancer, which are currently very difficult to treat. These observations are especially appealing in the light of findings that depletion

of BCL3 in otherwise normal mammary tissue had minimal effects on the gross morphology or function of the gland throughout the pregnancy cycle.

Therapeutic targeting of BCL3 alone may be of some benefit to patients presenting with certain tumour subtypes. However, it is likely that inhibition of BCL3 would be of most benefit as an adjuvant treatment in combination with other established targeted therapies, such as trastuzumab. Furthermore, as NF- $\kappa$ B has previously been shown to be activated in response to both chemotherapy (Piret and Piette 1996; Wang, Mayo et al. 1996; Das and White 1997; Wang, Abbruzzese et al. 1999; Dong, Scwabas et al. 2002; Nakanishi and Toi 2005) and hormonal treatments (Zhou, Yau et al. 2007; reviewed in Zhou, Eppenberger-Castori et al. 2005), future investigation into the therapeutic efficacy of adjuvant BCL3 inhibition to prevent resistance to such treatments is warranted. In addition, as BCL3 suppression appears to have therapeutic effects on both the initiation and metastatic progression of the disease, determination of which tumour stage would most benefit from BCL3 blockade requires thorough investigation in the future.

The overall feasibility of designing drugs to target BCL3 in human breast cancer is at present unknown. However, work currently being undertaken in the laboratory is focused on developing inhibitors of BCL3-p53 interactions in the hope of blocking the pro-carcinogenic functions of NF- $\kappa$ B whilst having minimal effects on the function of normal tissues. Evaluation of the efficacy and toxicity of these compounds *in vitro* and *in vivo* will help provide insight into the overall potential of the use of BCL3 inhibitors in the future treatment of breast cancer.

# **Appendices**

Accession	Definition	Symbol	Fold Change	Adj.P.Val
NM_010518.2	Mus musculus insulin-like growth factor binding protein 5 (Igfbp5), mRNA.	Igfbp5	2.97133279	6.03E-09
NM_001034870.2	Mus musculus serine (or cysteine) peptidase inhibitor, clade A, member 3H (Serpina3h), mRNA.	Serpina3h	2.41783564	7.07E-09
NM_133859.2	Mus musculus olfactomedin-like 3 (Olfml3), mRNA.	Olfml3	2.12292535	2.38E-07
XM_620286.3	PREDICTED: Mus musculus sterile alpha motif domain containing 9-like, transcript variant 1 (Samd9l), mRNA.	Samd9l	2.08956242	1.01E-07
NM_010357.1	Mus musculus glutathione S-transferase, alpha 4 (Gsta4), mRNA.	Gsta4	2.05521505	1.64E-07
XM_001471686.1	PREDICTED: Mus musculus hypothetical protein LOC100038882 (LOC100038882), mRNA.	LOC100038882	2.05061997	6.7E-08
NM_011909.1	Mus musculus ubiquitin specific peptidase 18 (Usp18), mRNA.	Usp18	2.04878197	1.73E-08
NM_009525.2	Mus musculus wntless-related MMTV integration site 5B (Wnt5b), mRNA.	Wnt5b	2.00367246	1.69E-08
NM_018734.2	Mus musculus guanylate nucleotide binding protein 3 (Gbp3), mRNA.	Gbp3	1.89624311	1.21E-07
NM_011909.1	Mus musculus ubiquitin specific peptidase 18 (Usp18), mRNA.	Usp18	1.87007214	2.75E-07
NM_011905.2	Mus musculus toll-like receptor 2 (Tlr2), mRNA.	Tlr2	1.85170934	1.9E-08
NM_015760.4	Mus musculus NADPH oxidase 4 (Nox4), mRNA.	Nox4	1.83705572	3.52E-08
NM_010476.3	Mus musculus hydroxysteroid (17-beta) dehydrogenase 7 (Hsd17b7), mRNA.	Hsd17b7	1.83588125	1.38E-05
NM_010260.1	Mus musculus guanylate nucleotide binding protein 2 (Gbp2), mRNA.	Gbp2	1.83593557	2.75E-07
NM_018734.3	Mus musculus guanylate nucleotide binding protein 3 (Gbp3), mRNA.	Gbp3	1.81971394	4.56E-06
XM_001480051.1	PREDICTED: Mus musculus similar to ubiquitin specific protease UBP43 (LOC100048346), mRNA.	LOC100048346	1.79704349	7.75E-07
NM_009831.2	Mus musculus cyclin G1 (Ccng1), mRNA.	Ccng1	1.77702745	5.46E-07
XM_001476984.1	PREDICTED: Mus musculus similar to CKLF-like MARVEL transmembrane domain containing 3 (LOC100046883), mRNA.	LOC100046883	1.76722793	1.9E-08
NM_010501.1	Mus musculus interferon-induced protein with tetratricopeptide repeats 3 (Ifit3), mRNA.	Ifit3	1.76463698	6.86E-05
NM_009242.1	Mus musculus secreted acidic cysteine rich glycoprotein (Sparc), mRNA.	Sparc	1.75497040	3.65E-07
NM_008176.1	Mus musculus chemokine (C-X-C motif) ligand 1 (Cxcl1), mRNA.	Cxcl1	1.73927182	1.14E-06
NM_145980.1	Mus musculus RIKEN cDNA 8430408G22 gene (8430408G22Rik), mRNA.	8430408G22Rik	1.73876121	2.75E-07
NM_011701.3	Mus musculus vimentin (Vim), mRNA.	Vim	1.73720397	3.01E-06
NM_011653.1	Mus musculus tubulin, alpha 1A (Tuba1a), mRNA.	Tuba1a	1.73132655	0.000145
NM_011315.3	Mus musculus serum amyloid A 3 (Saa3), mRNA.	Saa3	1.72597098	3.97E-08
NM_007987.1	Mus musculus Fas (TNF receptor superfamily member 6) (Fas), mRNA.	Fas	1.713925	7.5E-07
NM_009242.1	Mus musculus secreted acidic cysteine rich glycoprotein (Sparc), mRNA.	Sparc	1.68534646	3.99E-07
NM_008538.2	Mus musculus myristoylated alanine rich protein kinase C substrate (Marcks), mRNA.	Marcks	1.68201040	1.66E-07
NM_016979.1	Mus musculus protein kinase, X-linked (Prkx), mRNA.	Prkx	1.68089838	1.82E-07
NM_011358.1	Mus musculus splicing factor, arginine/serine-rich 2 (Sfrs2), mRNA.	Sfrs2	1.66087302	6.68E-06
NM_009338.3	Mus musculus acetyl-Coenzyme A acetyltransferase 2 (Acat2), mRNA.	Acat2	1.66072993	9.85E-05
NM_008137.3	Mus musculus guanine nucleotide binding protein, alpha 14 (Gna14), mRNA.	Gna14	1.65204690	2.16E-06
NM_016979.1	Mus musculus protein kinase, X-linked (Prkx), mRNA.	Prkx	1.65102362	9.44E-08
NM_011852.2	Mus musculus 2'-5' oligoadenylate synthetase 1G (Oas1g), mRNA.	Oas1g	1.64491530	5.06E-05
NM_172659.2	Mus musculus solute carrier family 2 (facilitated glucose transporter), member 6 (Slc2a6), mRNA.	Slc2a6	1.63792834	1.8E-06
NM_026178.2	Mus musculus monocyte to macrophage differentiation-associated (Mmd), mRNA.	Mmd	1.63170217	9.44E-08
NM_009749.1	Mus musculus brain expressed X-linked 2 (Bex2), mRNA.	Bex2	1.62918940	1.33E-06
NM_010169.3	Mus musculus coagulation factor II (thrombin) receptor (F2r), mRNA.	F2r	1.62838591	2.45E-07

Accession	Definition	Symbol	Fold Change	Adj.P.Val
NM_029662.1	Mus musculus major facilitator superfamily domain containing 2 (Mfsd2), mRNA.	Mfsd2	1.61818558	4.83E-06
NM_019440.2	Mus musculus interferon inducible GTPase 2 (Iigp2), mRNA.	Iigp2	1.60666438	1.97E-05
NM_021301.1	Mus musculus solute carrier family 15 (H+/peptide transporter), member 2 (Slc15a2), mRNA.	Slc15a2	1.60124172	2.97E-07
NM_178697.4	Mus musculus chloride channel calcium activated 5 (Clca5), mRNA.	Clca5	1.59354163	0.000395
NM_016850.2	Mus musculus interferon regulatory factor 7 (Irf7), mRNA.	Irf7	1.58855323	6.8E-06
NM_007898.2	Mus musculus phenylalkylamine Ca <sup>2+</sup> antagonist (emopamil) binding protein (Ebp), mRNA.	Ebp	1.58180773	5.6E-06
NM_008332.2	Mus musculus interferon-induced protein with tetratricopeptide repeats 2 (Ifit2), mRNA.	Ifit2	1.57294217	7.96E-06
NM_011854.1	Mus musculus 2'-5' oligoadenylate synthetase-like 2 (Oasl2), mRNA.	Oasl2	1.57120421	0.000188
NM_011358.1	Mus musculus splicing factor, arginine/serine-rich 2 (Sfrs2), mRNA.	Sfrs2	1.57098753	0.00057
NM_145569.2	Mus musculus methionine adenosyltransferase II, alpha (Mat2a), mRNA.	Mat2a	1.56974192	0.000479
NM_026464.2	Mus musculus WD repeat domain 55 (Wdr55), mRNA.	Wdr55	1.54201664	1.19E-06
NM_009223.2	Mus musculus stannin (Snn), mRNA.	Snn	1.54185649	2.54E-06
NM_027127.2	Mus musculus RIKEN cDNA 2310016C16 gene (2310016C16Rik), mRNA.	2310016C16Rik	1.54092402	7.14E-05
NM_009750.1	Mus musculus nerve growth factor receptor (TNFRSF16) associated protein 1 (Ngfrap1), mRNA.	Ngfrap1	1.52939660	3.2E-07
NM_008987.2		Ptx3	1.52783719	1.08E-06
NM_139144.2	Mus musculus O-linked N-acetylglucosamine (GlcNAc) transferase (UDP-N-acetylglucosamine:polypeptide-N-acetylglucosaminyl transferase) (Ogt), mRNA.	Ogt	1.52611585	7.87E-06
NM_018738.3	Mus musculus interferon gamma induced GTPase (Igtp), mRNA.	Igtp	1.52353419	6.86E-05
NM_011852.2	Mus musculus 2'-5' oligoadenylate synthetase 1G (Oas1g), mRNA.	Oas1g	1.51872619	0.000133
NM_018865.2	Mus musculus WNT1 inducible signaling pathway protein 1 (Wisp1), mRNA.	Wisp1	1.50788748	1.14E-06
NM_008908.1	Mus musculus peptidylprolyl isomerase C (Ppic), mRNA.	Ppic	1.50524768	1.37E-06
NM_175319.2	Mus musculus RIKEN cDNA C330005M16 gene (C330005M16Rik), mRNA.	C330005M16Rik	1.50289505	1.74E-05
NM_016753.4	Mus musculus latexin (Lxn), mRNA.	Lxn	1.49648075	1.1E-05
NM_025703.2	Mus musculus transcription elongation factor A (SII)-like 8 (Tceal8), mRNA.	Tceal8	1.49563819	2.64E-05
NM_020010.2	Mus musculus cytochrome P450, family 51 (Cyp51), mRNA.	Cyp51	1.49060967	8.85E-05
NM_001037279.1	Mus musculus RIKEN cDNA 2700094K13 gene (2700094K13Rik), transcript variant 2, mRNA.	2700094K13Rik	1.48399067	1.19E-06
NM_029619.2	Mus musculus methionine sulfoxide reductase B2 (Msrb2), mRNA.	Msrb2	1.47544783	8.96E-07
XM_001478939.1	PREDICTED: Mus musculus similar to human protein homologous to DROER protein (LOC100042777), mRNA.	LOC100042777	1.46823359	1.39E-06
NM_009283.3	Mus musculus signal transducer and activator of transcription 1 (Stat1), mRNA.	Stat1	1.46653524	2.67E-05
NM_021604.2	Mus musculus agrin (Agrn), mRNA.	Agrn	1.46204424	3.13E-05
NM_001013025.2	Mus musculus transforming growth factor, beta receptor associated protein 1 (Tgfbrap1), mRNA.	Tgfbrap1	1.45907682	6.59E-06
NM_173374.3	Mus musculus splicing factor, arginine/serine-rich 1 (ASF/SF2) (Sfrs1), transcript variant 1, mRNA.	Sfrs1	1.45808209	0.000505
NM_025365.2	Mus musculus prickle homolog 4 (Drosophila) (Prickle4), mRNA.	Prickle4	1.45769414	0.000447
NM_172641.2	Mus musculus RIKEN cDNA 9930023K05 gene (9930023K05Rik), mRNA.	9930023K05Rik	1.45752667	1.23E-05
NM_018770		Igsf4a	1.45291781	1.78E-05
NM_009160.1	Mus musculus surfactant associated protein D (Sftpd), mRNA.	Sftpd	1.45229249	3.53E-06
NM_009226.4	Mus musculus small nuclear ribonucleoprotein D1 (Snrpd1), mRNA.	Snrpd1	1.45015453	3.68E-05
NM_018815.1	Mus musculus nucleoporin 210 (Nup210), mRNA.	Nup210	1.44780234	1.73E-05
NM_175565.3	Mus musculus carnitine deficiency-associated gene expressed in ventricle 3 (Cdv3), transcript variant CDV3A, mRNA.	Cdv3	1.44498734	0.000895

Accession	Definition	Symbol	Fold Change	Adj.P.Val
NM_027878.2	Mus musculus RIKEN cDNA 1200002N14 gene (1200002N14Rik), mRNA.	1200002N14Rik	1.44285751	2.59E-06
NM_027127.1	Mus musculus RIKEN cDNA 2310016C16 gene (2310016C16Rik), mRNA.	2310016C16Rik	1.44209610	0.00013
NM_011014.2	Mus musculus opioid receptor, sigma 1 (Oprs1), mRNA.	Oprs1	1.44133286	0.000133
NM_025284.3	Mus musculus thymosin, beta 10 (Tmsb10), mRNA.	Tmsb10	1.43578153	0.000117
NM_011150.2	Mus musculus lectin, galactoside-binding, soluble, 3 binding protein (Lgals3bp), mRNA.	Lgals3bp	1.43273450	5.79E-05
NM_175401.3	Mus musculus F-box and WD-40 domain protein 17 (Fbxw17), mRNA.	Fbxw17	1.43270636	2.06E-05
NM_009320.3	Mus musculus solute carrier family 6 (neurotransmitter transporter, taurine), member 6 (Slc6a6), mRNA.	Slc6a6	1.42872470	0.000347
NM_175103.2	Mus musculus bolA-like 2 (E. coli) (Bola2), mRNA.	Bola2	1.42642792	1.22E-05
NM_025866.3	Mus musculus cell division cycle associated 7 (Cdca7), mRNA.	Cdca7	1.42177050	0.000357
NM_027127.2	Mus musculus RIKEN cDNA 2310016C16 gene (2310016C16Rik), mRNA.	2310016C16Rik	1.42115487	1.87E-05
NM_027342.1	Mus musculus RIKEN cDNA 2310056P07 gene (2310056P07Rik), mRNA.	2310056P07Rik	1.41611108	8.32E-06
NM_015807.1	Mus musculus 5',3'-nucleotidase, cytosolic (Nt5c), mRNA.	Nt5c	1.41357951	6.49E-05
NM_033270.1	Mus musculus E2F transcription factor 6 (E2f6), mRNA.	E2f6	1.41221845	2.3E-05
NM_007951.1	Mus musculus enhancer of rudimentary homolog (Drosophila) (Erh), mRNA.	Erh	1.41081835	7.56E-05
NM_009964.1	Mus musculus crystallin, alpha B (Cryab), mRNA.	Cryab	1.40993264	9.69E-05
NM_133888.2	Mus musculus sphingomyelin phosphodiesterase, acid-like 3B (Smpd13b), mRNA.	Smpd13b	1.40729464	4.09E-05
NM_020557.3		Tyki	1.40471196	3.43E-05
NM_001001979.1	Mus musculus multiple EGF-like-domains 10 (Megf10), mRNA.	Megf10	1.40345666	4.19E-05
NM_206958.1	Mus musculus latent transforming growth factor beta binding protein 1 (Ltbp1), transcript variant 2, mRNA.	Ltbp1	1.40329585	0.000157
NM_026405.3	Mus musculus RAB32, member RAS oncogene family (Rab32), mRNA.	Rab32	1.40311396	1.5E-06
NM_013640.2	Mus musculus proteasome (prosome, macropain) subunit, beta type 10 (Psmb10), mRNA.	Psmb10	1.40277209	0.000324
NM_008113.3	Mus musculus Rho GDP dissociation inhibitor (GDI) gamma (Arhgdig), mRNA.	Arhgdig	1.39840941	1.36E-05
NM_007527.2	Mus musculus Bcl2-associated X protein (Bax), mRNA.	Bax	1.39755720	8.3E-06
NM_028798.2	Mus musculus cysteine-rich C-terminal 1 (Crct1), mRNA.	Crct1	1.39632536	4.57E-05

#### Appendix 1: Top 100 largest fold increases in gene expression following Bcl3 suppression

Statistical differences in microarray data were determined by T-tests to obtain adjusted p-values. Data that achieved significance at  $p \leq 0.01$  (1691 genes) were ranked according to fold change. Table represents the top 100 largest fold increases in gene expression following *Bcl3* suppression.

Accession	Definition	Symbol	Fold Change	Adj.P.Val
NM_011931.3	Mus musculus ring finger and WD repeat domain 2 (Rfwd2), mRNA.	Rfwd2	0.700836811	2.32E-06
NM_146247		BC024814	0.700329214	1.4E-05
NM_001037136.1	Mus musculus centaurin, gamma 2 (Centg2), transcript variant 2, mRNA.	Centg2	0.700186671	0.000268
NM_011261.2	Mus musculus reelin (Reln), mRNA.	Reln	0.700089841	2.39E-05
NM_176933.3	Mus musculus dual specificity phosphatase 4 (Dusp4), mRNA.	Dusp4	0.698987264	0.000119
NM_008970.2	Mus musculus parathyroid hormone-like peptide (Pthlh), mRNA.	Pthlh	0.698620159	1.1E-05
NM_011949.3	Mus musculus mitogen-activated protein kinase 1 (Mapk1), transcript variant 1, mRNA.	Mapk1	0.698007364	1.22E-05
NM_178143.1	Mus musculus protein kinase, AMP-activated, alpha 2 catalytic subunit (Prkaa2), mRNA.	Prkaa2	0.697439604	1.55E-05
NM_009711.3	Mus musculus artemin (Artn), mRNA.	Artn	0.697368865	0.000315
NM_011690.2	Mus musculus valyl-tRNA synthetase (Vars), mRNA.	Vars	0.697349947	1.36E-05
NM_019703.3	Mus musculus phosphofructokinase, platelet (Pfkp), mRNA.	Pfkp	0.696954938	2.32E-06
NM_007669.3	Mus musculus cyclin-dependent kinase inhibitor 1A (P21) (Cdkn1a), mRNA.	Cdkn1a	0.695655894	2.64E-05
NM_033149.2	Mus musculus UDP-Gal:betaGlcNAc beta 1,3-galactosyltransferase, polypeptide 5 (B3galt5), mRNA.	B3galt5	0.695064007	1.73E-06
NM_008813.2	Mus musculus ectonucleotide pyrophosphatase/phosphodiesterase 1 (Enpp1), mRNA.	Enpp1	0.693475568	0.000122
NM_019738.1	Mus musculus nuclear protein 1 (Nupr1), mRNA.	Nupr1	0.692882883	0.00253
NM_177700.3	Mus musculus ATM interactor (Atmin), mRNA.	Atmin	0.691091469	3.93E-06
NM_026708.1	Mus musculus TLC domain containing 1 (Tlcd1), mRNA.	Tlcd1	0.690931482	1.37E-06
NM_028800.2	Mus musculus serine/threonine kinase 40 (Stk40), mRNA.	Stk40	0.690583076	2.65E-05
NM_028792.2	Mus musculus Josephin domain containing 1 (Josd1), mRNA.	Josd1	0.689936154	5.37E-07
NM_011065.2	Mus musculus period homolog 1 (Drosophila) (Per1), mRNA.	Per1	0.689232835	4.2E-05
NM_145447.2	Mus musculus feline leukemia virus subgroup C cellular receptor family, member 2 (Flvcr2), mRNA.	Flvcr2	0.687823971	3.01E-06
NM_177474.4	Mus musculus DNA segment, Chr 19, Brigham & Women's Genetics 1357 expressed (D19Bwg1357e), mRNA.	D19Bwg1357e	0.687695199	4.48E-06
NM_020625.3	Mus musculus zinc finger and BTB domain containing 22 (Zbtb22), mRNA.	Zbtb22	0.687138009	2.44E-06
NM_008488.1	Mus musculus Rho guanine nucleotide exchange factor (GEF) 1 (Arhgef1), mRNA.	Arhgef1	0.687039628	4.54E-05
NM_021389.4	Mus musculus SH3-domain kinase binding protein 1 (Sh3kbp1), mRNA.	Sh3kbp1	0.68623856	3.53E-06
NM_019990.4	Mus musculus START domain containing 10 (Stard10), mRNA.	Stard10	0.686059288	0.000226
NM_019703.3	Mus musculus phosphofructokinase, platelet (Pfkp), mRNA.	Pfkp	0.685854901	2.12E-05
NM_033601.1	Mus musculus B-cell leukemia/lymphoma 3 (Bcl3), mRNA.	Bcl3	0.685150317	6.49E-06
NM_001081170.1	Mus musculus phosphofurin acidic cluster sorting protein 2 (Pacs2), mRNA.	Pacs2	0.685027721	0.000114
NM_009801.3	Mus musculus carbonic anhydrase 2 (Car2), mRNA.	Car2	0.683701875	1.59E-05
NM_008813.3	Mus musculus ectonucleotide pyrophosphatase/phosphodiesterase 1 (Enpp1), mRNA.	Enpp1	0.683462757	7.08E-05
NM_144792.2		Tmem23	0.682853068	8.99E-05
NM_181323.2	Mus musculus RIKEN cDNA C130090K23 gene (C130090K23Rik), mRNA.	C130090K23Rik	0.681467093	5.14E-07
NM_008681		Ndr1	0.680753991	1.59E-05
NM_177700.3	Mus musculus ATM interactor (Atmin), mRNA.	Atmin	0.679744904	7.01E-06
NM_009075.2	Mus musculus ribose 5-phosphate isomerase A (Rpia), mRNA.	Rpia	0.679578242	1.85E-06
NM_009943.2	Mus musculus cytochrome c oxidase, subunit VI a, polypeptide 2 (Cox6a2), nuclear gene encoding mitochondrial protein, mRNA.	Cox6a2	0.679086681	8.19E-05
NM_016797.4	Mus musculus syntaxin 7 (Stx7), mRNA.	Stx7	0.678871722	2.69E-06
NM_144500.3	Mus musculus oxysterol binding protein-like 2 (Osbp12), mRNA.	Osbp12	0.678063267	1.13E-05
NM_030706.1	Mus musculus tripartite motif protein 2 (Trim2), mRNA. XM_984114 XM_984144 XM_984172 XM_984200 XM_984238 XM_984275 XM_984313	Trim2	0.670811372	2.48E-06
NM_011319.2	Mus musculus seryl-aminoacyl-tRNA synthetase (Sars), mRNA.	Sars	0.670135938	1.16E-05

Accession	Definition	Symbol	Fold Change	Adj.P.Val
NM_133898.3	Mus musculus RIKEN cDNA B230342M21 gene (B230342M21Rik), mRNA.	B230342M21Rik	0.66497052	1.46E-05
XM_001478602.1	PREDICTED: Mus musculus similar to FOG (LOC100047651), mRNA.	LOC100047651	0.664444308	1.22E-05
NM_053093.1	Mus musculus tachykinin 4 (Tac4), mRNA.	Tac4	0.661766682	2.75E-07
NM_001039089.1	Mus musculus sel-1 suppressor of lin-12-like (C. elegans) (Sel1l), transcript variant 1, mRNA.	Sel1l	0.661523227	5.83E-05
NM_024189.5	Mus musculus YY1 associated factor 2 (Yaf2), mRNA.	Yaf2	0.660863464	5.14E-07
NM_026407.2	Mus musculus transmembrane protein 39a (Tmem39a), mRNA.	Tmem39a	0.660246118	1.49E-06
NM_146017.3	Mus musculus gamma-aminobutyric acid (GABA-A) receptor, pi (Gabrp), mRNA.	Gabrp	0.659560984	7.87E-06
NM_029999.3	Mus musculus limb-bud and heart (Lbh), mRNA.	Lbh	0.656620181	1.29E-05
NM_007671.2	Mus musculus cyclin-dependent kinase inhibitor 2C (p18, inhibits CDK4) (Cdkn2c), mRNA.	Cdkn2c	0.65577269	7.62E-06
NM_007836.1	Mus musculus growth arrest and DNA-damage-inducible 45 alpha (Gadd45a), mRNA.	Gadd45a	0.655468024	0.003813
NM_175682.2	Mus musculus RIKEN cDNA 9930021D14 gene (9930021D14Rik), mRNA.	9930021D14Rik	0.653137082	1.39E-05
NM_013842.2	Mus musculus X-box binding protein 1 (Xbp1), mRNA.	Xbp1	0.65256871	2.15E-05
XM_001476512.1	PREDICTED: Mus musculus similar to aquaporin 5 (LOC100046616), mRNA.	LOC100046616	0.652065529	3.14E-07
NM_026270.3	Mus musculus AKT1 substrate 1 (proline-rich) (Akt1s1), mRNA.	Akt1s1	0.651461739	5.37E-07
NM_145525.2	Mus musculus oxysterol binding protein-like 6 (Osbp16), mRNA.	Osbp16	0.649423786	2.15E-05
NM_008609.3	Mus musculus matrix metalloproteinase 15 (Mmp15), mRNA. XM_001002221	Mmp15	0.648857872	9.42E-06
NM_019581.2	Mus musculus GTP binding protein 2 (Gtpbp2), mRNA.	Gtpbp2	0.645780581	5.08E-05
NM_031185.2	Mus musculus A kinase (PRKA) anchor protein (gravin) 12 (Akap12), mRNA.	Akap12	0.64338736	0.000218
NM_176933.4	Mus musculus dual specificity phosphatase 4 (Dusp4), mRNA.	Dusp4	0.641765708	2.69E-06
NM_025371.1	Mus musculus aminoacylase 1 (Acy1), mRNA.	Acy1	0.639844887	2.94E-06
NM_009996.2		Cyp24a1	0.638027453	1.09E-05
NM_009067.3	Mus musculus ralA binding protein 1 (Ralbp1), mRNA.	Ralbp1	0.637552358	5.25E-05
NM_177725.3	Mus musculus leucine rich repeat containing 8A (Lrrc8a), mRNA.	Lrrc8a	0.636764017	2.35E-05
NM_016865.2	Mus musculus HIV-1 tat interactive protein 2, homolog (human) (Htatip2), mRNA.	Htatip2	0.630846189	2.45E-07
NM_177725.2		Lrrc8	0.62980998	5.08E-05
NM_012037.2	Mus musculus vesicle amine transport protein 1 homolog (T californica) (Vat1), mRNA.	Vat1	0.62944579	1.22E-05
NM_026551.3	Mus musculus dephospho-CoA kinase domain containing (Dcakd), mRNA.	Dcakd	0.629215025	1.5E-07
NM_016865.2	Mus musculus HIV-1 tat interactive protein 2, homolog (human) (Htatip2), mRNA.	Htatip2	0.628100399	6.68E-06
NM_146017.3	Mus musculus gamma-aminobutyric acid (GABA-A) receptor, pi (Gabrp), mRNA.	Gabrp	0.623849993	6E-07
NM_139200.4	Mus musculus pleckstrin homology, Sec7 and coiled-coil domains, binding protein (Pscdbp), mRNA.	Pscdbp	0.623443765	7.09E-07
NM_029999.3	Mus musculus limb-bud and heart (Lbh), mRNA.	Lbh	0.621850147	4.52E-07
NM_029631.2	Mus musculus abhydrolase domain containing 14b (Abhd14b), mRNA.	Abhd14b	0.617769673	4.22E-07
NM_011177.1	Mus musculus kallikrein related-peptidase 6 (Klk6), mRNA.	Klk6	0.617232496	4.34E-05
NM_016916.3	Mus musculus bladder cancer associated protein homolog (human) (Blcap), mRNA.	Blcap	0.6156729	3.43E-07
NM_146028.4	Mus musculus SH3 and cysteine rich domain 2 (Stac2), mRNA.	Stac2	0.615165971	2.63E-06
XM_128174.2		2310001L23Rik	0.611471068	2.75E-07
NM_054087.2	Mus musculus solute carrier family 19 (thiamine transporter), member 2 (Slc19a2), mRNA.	Slc19a2	0.601620614	3.53E-07
NM_153114.2	Mus musculus otospiralin (Otos), mRNA.	Otos	0.600159002	2.21E-06
NM_133977.2	Mus musculus transferrin (Trf), mRNA.	Trf	0.600055342	0.000108
NM_008077.2		Gad1	0.600044412	4.61E-06
NM_019990.4	Mus musculus START domain containing 10 (Stard10), mRNA.	Stard10	0.57952738	2.48E-06

Accession	Definition	Symbol	Fold Change	Adj.P.Val
NM_153163.3	Mus musculus Ca <sup>2+</sup> -dependent activator protein for secretion 2 (Cadps2), mRNA.	Cadps2	0.575340229	1.38E-07
NM_028048.2	Mus musculus solute carrier family 25, member 35 (Slc25a35), mRNA.	Slc25a35	0.571399095	3.38E-08
NM_007913.5	Mus musculus early growth response 1 (Egr1), mRNA.	Egr1	0.570325872	4.48E-06
NM_026514.2	Mus musculus CDC42 effector protein (Rho GTPase binding) 3 (Cdc42ep3), mRNA.	Cdc42ep3	0.56449874	1.23E-07
NM_011690.2	Mus musculus valyl-tRNA synthetase (Vars), mRNA.	Vars	0.563426171	3.14E-07
NM_015786.1	Mus musculus histone cluster 1, H1c (Hist1h1c), mRNA.	Hist1h1c	0.555481545	3.97E-08
NM_015828.2	Mus musculus glucosamine (Gne), mRNA.	Gne	0.55258075	6.2E-08
NM_008597.3	Mus musculus matrix Gla protein (Mgp), mRNA.	Mgp	0.538368212	3.98E-07
NM_008077.4	Mus musculus glutamic acid decarboxylase 1 (Gad1), mRNA.	Gad1	0.526076848	2.16E-06
NM_016974.1	Mus musculus D site albumin promoter binding protein (Dbp), mRNA.	Dbp	0.521269471	7.52E-07
NM_022964.3	Mus musculus linker for activation of T cells family, member 2 (Lat2), transcript variant 2, mRNA.	Lat2	0.512946377	1.86E-08
NM_177613.2	Mus musculus cell division cycle 34 homolog ( <i>S. cerevisiae</i> ) (Cdc34), mRNA. XM_922814 XM_922817	Cdc34	0.455351144	1.73E-08
NM_030175.3	Mus musculus RIKEN cDNA 4930507C10 gene (4930507C10Rik), mRNA.	4930507C10Rik	0.453174903	3.14E-07
NM_021564.2	Mus musculus fetuin beta (Fetub), transcript variant 1, mRNA.	Fetub	0.442456892	4.16E-10
NM_029148.1	Mus musculus thioredoxin domain containing 13 (Txndc13), mRNA. XM_902134 XM_902137 XM_925631 XM_925632 XM_925633	Txndc13	0.433792905	3.48E-10
NM_022020.2	Mus musculus retinol binding protein 7, cellular (Rbp7), mRNA.	Rbp7	0.427226393	4.16E-10
NM_029148.1	Mus musculus thioredoxin domain containing 13 (Txndc13), mRNA. XM_902134 XM_902137 XM_925631 XM_925632 XM_925633	Txndc13	0.394442169	2.8E-09
NM_053078.3	Mus musculus DNA segment, human D4S114 (DOH4S114), mRNA.	DOH4S114	0.382487875	3.48E-10
XM_001478127.1	PREDICTED: Mus musculus similar to Cell division cycle 34 homolog ( <i>S. cerevisiae</i> ) (LOC100046898), mRNA.	LOC100046898	0.261074911	2.02E-11

### Appendix 2: Top 100 largest fold decreases in gene expression following *Bcl3* suppression

Statistical differences in microarray data were determined by T-tests to obtain adjusted p-values. Data that achieved significance at  $p \leq 0.01$  (1691 genes) were ranked according to fold change. Table represents the top 100 largest fold decreases in gene expression following *Bcl3* suppression.

# **Bibliography**

- Abdel-Latif, M. M., J. O'Riordan, et al. (2004). "NF-kappaB activation in esophageal adenocarcinoma: relationship to Barrett's metaplasia, survival, and response to neoadjuvant chemoradiotherapy." Ann Surg **239**(4): 491-500.
- Abell, K., A. Bilancio, et al. (2005). "Stat3-induced apoptosis requires a molecular switch in PI(3)K subunit composition." Nat Cell Biol **7**(4): 392-398.
- Aggarwal, B. B., S. Shishodia, et al. (2005). "Curcumin suppresses the paclitaxel-induced nuclear factor-kappaB pathway in breast cancer cells and inhibits lung metastasis of human breast cancer in nude mice." Clin Cancer Res **11**(20): 7490-7498.
- Aggarwal, S., H. Ichikawa, et al. (2006). "Curcumin (diferuloylmethane) down-regulates expression of cell proliferation and antiapoptotic and metastatic gene products through suppression of I kappa B alpha kinase and Akt activation." Mol Pharmacol **69**(1): 195-206.
- Ahmed, S. U. and J. Milner (2009). "Basal cancer cell survival involves JNK2 suppression of a novel JNK1/c-Jun/Bcl-3 apoptotic network." PLoS One **4**(10): e7305.
- Aktas, B., M. Tewes, et al. (2009). "Stem cell and epithelial-mesenchymal transition markers are frequently overexpressed in circulating tumor cells of metastatic breast cancer patients." Breast Cancer Res **11**(4): R46.
- Al-Hajj, M., M. S. Wicha, et al. (2003). "Prospective identification of tumorigenic breast cancer cells." Proc Natl Acad Sci U S A **100**(7): 3983-3988.
- Ali, S. and A. J. Clark (1988). "Characterization of the gene encoding ovine beta-lactoglobulin. Similarity to the genes for retinol binding protein and other secretory proteins." J Mol Biol **199**(3): 415-426.
- Arihiro, K., H. Oda, et al. (2000). "Cytokines facilitate chemotactic motility of breast carcinoma cells." Breast Cancer **7**(3): 221-230.
- Ashkenazi, A. and V. M. Dixit (1998). "Death receptors: signaling and modulation." Science **281**(5381): 1305-1308.
- Au, W. Y., D. E. Horsman, et al. (2002). "Bcl-3/IgH translocation (14;19)(q32;q13) in non-Hodgkin's lymphomas." Leuk Lymphoma **43**(4): 813-816.
- Awada, A., J. Albanell, et al. (2008). "Bortezomib/docetaxel combination therapy in patients with anthracycline-pretreated advanced/metastatic breast cancer: a phase I/II dose-escalation study." Br J Cancer **98**(9): 1500-1507.
- Badve, S., D. Turbin, et al. (2007). "FOXA1 expression in breast cancer--correlation with luminal subtype A and survival." Clin Cancer Res **13**(15 Pt 1): 4415-4421.
- Baldwin, A. S. (2001). "Control of oncogenesis and cancer therapy resistance by the transcription factor NF-kappaB." J Clin Invest **107**(3): 241-246.
- Bargou, R. C., F. Emmerich, et al. (1997). "Constitutive nuclear factor-kappaB-RelA activation is required for proliferation and survival of Hodgkin's disease tumor cells." J Clin Invest **100**(12): 2961-2969.
- Barre, B. and N. D. Perkins (2010). "The Skp2 promoter integrates signaling through the NF-kappaB, p53, and Akt/GSK3beta pathways to regulate autophagy and apoptosis." Mol Cell **38**(4): 524-538.
- Basseres, D. S. and A. S. Baldwin (2006). "Nuclear factor-kappaB and inhibitor of kappaB kinase pathways in oncogenic initiation and progression." Oncogene **25**(51): 6817-6830.

- Bassetti, M. F., J. White, et al. (2009). "Transgenic Bcl-3 slows T cell proliferation." Int Immunol **21**(4): 339-348.
- Battle, E., E. Sancho, et al. (2000). "The transcription factor snail is a repressor of E-cadherin gene expression in epithelial tumour cells." Nat Cell Biol **2**(2): 84-89.
- Bauer, A., A. Villunger, et al. (2006). "The NF-kappaB regulator Bcl-3 and the BH3-only proteins Bim and Puma control the death of activated T cells." Proc Natl Acad Sci U S A **103**(29): 10979-10984.
- Baxter, F. O., P. J. Came, et al. (2006). "IKKbeta/2 induces TWEAK and apoptosis in mammary epithelial cells." Development **133**(17): 3485-3494.
- Beg, A. A., W. C. Sha, et al. (1995). "Embryonic lethality and liver degeneration in mice lacking the RelA component of NF-kappa B." Nature **376**(6536): 167-170.
- Beinke, S. and S. C. Ley (2004). "Functions of NF-kappaB1 and NF-kappaB2 in immune cell biology." Biochem J **382**(Pt 2): 393-409.
- Bertucci, F., N. Borie, et al. (2004). "Identification and validation of an ERBB2 gene expression signature in breast cancers." Oncogene **23**(14): 2564-2575.
- Bertwistle, D. and A. Ashworth. (1998). "Functions of the BRCA1 and BRCA2 genes." Curr Opin Genet Dev **8**:14-20.
- Bhat-Nakshatri, P., H. Appaiah, et al. (2010). "SLUG/SNAI2 and tumor necrosis factor generate breast cells with CD44+/CD24- phenotype." BMC Cancer **10**: 411.
- Biswas, D. K., A. P. Cruz, et al. (2000). "Epidermal growth factor-induced nuclear factor kappa B activation: A major pathway of cell-cycle progression in estrogen-receptor negative breast cancer cells." Proc Natl Acad Sci U S A **97**(15): 8542-8547.
- Biswas, D. K. and J. D. Iglehart (2006). "Linkage between EGFR family receptors and nuclear factor kappaB (NF-kappaB) signaling in breast cancer." J Cell Physiol **209**(3): 645-652.
- Biswas, D. K., Q. Shi, et al. (2004). "NF-kappa B activation in human breast cancer specimens and its role in cell proliferation and apoptosis." Proc Natl Acad Sci U S A **101**(27): 10137-10142.
- Blavier, L., A. Lazaryev, et al. (2006). "Matrix metalloproteinases play an active role in Wnt1-induced mammary tumorigenesis." Cancer Res **66**(5): 2691-2699.
- Boissan, M., D. Wendum, et al. (2005). "Increased lung metastasis in transgenic NM23-Null/SV40 mice with hepatocellular carcinoma." J Natl Cancer Inst **97**(11): 836-845.
- Bolos, V., H. Peinado, et al. (2003). "The transcription factor Slug represses E-cadherin expression and induces epithelial to mesenchymal transitions: a comparison with Snail and E47 repressors." J Cell Sci **116**(Pt 3): 499-511.
- Bombonati, A. and D. C. Sgroi (2011). "The molecular pathology of breast cancer progression." J Pathol **223**(2): 307-317.
- Bonnet, D. and J. E. Dick (1997). "Human acute myeloid leukemia is organized as a hierarchy that originates from a primitive hematopoietic cell." Nat Med **3**(7): 730-737.
- Bortner, D. M. and M. P. Rosenberg (1997). "Induction of mammary gland hyperplasia and carcinomas in transgenic mice expressing human cyclin E." Mol Cell Biol **17**(1): 453-459.

- Bours, V., G. Franzoso, et al. (1993). "The oncoprotein Bcl-3 directly transactivates through kappa B motifs via association with DNA-binding p50B homodimers." *Cell* **72**(5): 729-739.
- Brantley, D. M., C. L. Chen, et al. (2001). "Nuclear factor-kappaB (NF-kappaB) regulates proliferation and branching in mouse mammary epithelium." *Mol Biol Cell* **12**(5): 1445-1455.
- Brantley, D. M., F. E. Yull, et al. (2000). "Dynamic expression and activity of NF-kappaB during post-natal mammary gland morphogenesis." *Mech Dev* **97**(1-2): 149-155.
- Brasier, A. R., M. Lu, et al. (2001). "NF-kappa B-inducible BCL-3 expression is an autoregulatory loop controlling nuclear p50/NF-kappa B1 residence." *J Biol Chem* **276**(34): 32080-32093.
- Bray, F., P. McCarron, et al. (2004). "The changing global patterns of female breast cancer incidence and mortality." *Breast Cancer Res* **6**(6): 229-239.
- Brenne, A. T., U. M. Fagerli, et al. (2009). "High expression of BCL3 in human myeloma cells is associated with increased proliferation and inferior prognosis." *Eur J Haematol* **82**(5): 354-363.
- Brocke-Heidrich, K., B. Ge, et al. (2006). "BCL3 is induced by IL-6 via Stat3 binding to intronic enhancer HS4 and represses its own transcription." *Oncogene* **25**(55): 7297-7304.
- Buchau, A. S., D. T. MacLeod, et al. (2009). "Bcl-3 acts as an innate immune modulator by controlling antimicrobial responses in keratinocytes." *J Invest Dermatol* **129**(9): 2148-2155.
- Bundy, D. L. and T. W. McKeithan (1997). "Diverse effects of BCL3 phosphorylation on its modulation of NF-kappaB p52 homodimer binding to DNA." *J Biol Chem* **272**(52): 33132-33139.
- Caamano, J. H., P. Perez, et al. (1996). "Constitutive expression of Bcl-3 in thymocytes increases the DNA binding of NF-kappaB1 (p50) homodimers in vivo." *Mol Cell Biol* **16**(4): 1342-1348.
- Caamano, J. H., C. A. Rizzo, et al. (1998). "Nuclear factor (NF)-kappa B2 (p100/p52) is required for normal splenic microarchitecture and B cell-mediated immune responses." *J Exp Med* **187**(2): 185-196.
- Caldas, C. and S. A. Aparicio (2002). "The molecular outlook." *Nature* **415**(6871): 484-485.
- Campbell, K. J. and N. D. Perkins (2004). "Post-translational modification of RelA(p65) NF-kappaB." *Biochem Soc Trans* **32**(Pt 6): 1087-1089.
- CancerResearchUK (2007). "Cancers at a glance  
<http://info.cancerresearchuk.org/cancerandresearch/cancers/breast/>."
- Cano, A., M. A. Perez-Moreno, et al. (2000). "The transcription factor snail controls epithelial-mesenchymal transitions by repressing E-cadherin expression." *Nat Cell Biol* **2**(2): 76-83.
- Canoz, O., G. Z. Rassidakis, et al. (2004). "Immunohistochemical detection of BCL-3 in lymphoid neoplasms: a survey of 353 cases." *Mod Pathol* **17**(8): 911-917.
- Cao, Y., G. Bonizzi, et al. (2001). "IKKalpha provides an essential link between RANK signaling and cyclin D1 expression during mammary gland development." *Cell* **107**(6): 763-775.
- Cao, Y. and M. Karin (2003). "NF-kappaB in mammary gland development and breast cancer." *J Mammary Gland Biol Neoplasia* **8**(2): 215-223.

- Cao, Y., J. L. Luo, et al. (2007). "IkappaB kinase alpha kinase activity is required for self-renewal of ErbB2/Her2-transformed mammary tumor-initiating cells." Proc Natl Acad Sci U S A **104**(40): 15852-15857.
- Cardiff, R. D. (1984). "Protoneoplasia: the molecular biology of murine mammary hyperplasia." Adv Cancer Res **42**: 167-190.
- Cardiff, R. D. and S. R. Wellings (1999). "The comparative pathology of human and mouse mammary glands." J Mammary Gland Biol Neoplasia **4**(1): 105-122.
- Carmody, R. J., Q. Ruan, et al. (2007). "Negative regulation of toll-like receptor signaling by NF-kappaB p50 ubiquitination blockade." Science **317**(5838): 675-678.
- Carraway, K. L., 3rd and L. C. Cantley (1994). "A new acquaintance for erbB3 and erbB4: a role for receptor heterodimerization in growth signalling." Cell **78**(1): 5-8.
- Carraway, K. L., 3rd, M. X. Sliwkowski, et al. (1994). "The erbB3 gene product is a receptor for heregulin." J Biol Chem **269**(19): 14303-14306.
- Carter, P., L. Presta, et al. (1992). "Humanization of an anti-p185HER2 antibody for human cancer therapy." Proc Natl Acad Sci U S A **89**(10): 4285-4289.
- Cavalli, L. R., B Singh, et al. (2004). "Loss of heterozygosity in normal breast epithelial tissue and benign breast lesions in BRCA1/2 carriers with breast cancer." Cancer Genet Cytogenet **149**:38-43.
- Cazals, V., E. Nabeyrat, et al. (1999). "Role for NF-kappa B in mediating the effects of hyperoxia on IGF-binding protein 2 promoter activity in lung alveolar epithelial cells." Biochim Biophys Acta **1448**(3): 349-362.
- Chacon, R. D. and M. V. Costanzo (2010). "Triple-negative breast cancer." Breast Cancer Res **12 Suppl 2**: S3.
- Chakraborti, S., M. Mandal, et al. (2003). "Regulation of matrix metalloproteinases: an overview." Mol Cell Biochem **253**(1-2): 269-285.
- Chapiro, E., I. Radford-Weiss, et al. (2008). "The most frequent t(14;19)(q32;q13)-positive B-cell malignancy corresponds to an aggressive subgroup of atypical chronic lymphocytic leukemia." Leukemia **22**(11): 2123-2127.
- Chapman, R. S., P. C. Lourenco, et al. (1999). "Suppression of epithelial apoptosis and delayed mammary gland involution in mice with a conditional knockout of Stat3." Genes Dev **13**(19): 2604-2616.
- Charafe-Jauffret, E., C. Ginestier, et al. (2010). "Aldehyde dehydrogenase 1-positive cancer stem cells mediate metastasis and poor clinical outcome in inflammatory breast cancer." Clin Cancer Res **16**(1): 45-55.
- Cheang, M. C., S. K. Chia, et al. (2009). "Ki67 index, HER2 status, and prognosis of patients with luminal B breast cancer." J Natl Cancer Inst **101**(10): 736-750.
- Chen, C., L. C. Edelstein, et al. (2000). "The Rel/NF-kappaB family directly activates expression of the apoptosis inhibitor Bcl-x(L)." Mol Cell Biol **20**(8): 2687-2695.
- Chen, L., W. Fischle, et al. (2001). "Duration of nuclear NF-kappaB action regulated by reversible acetylation." Science **293**(5535): 1653-1657.

- Chen, L. F. and W. C. Greene (2004). "Shaping the nuclear action of NF-kappaB." Nat Rev Mol Cell Biol 5(5): 392-401.
- Chen, X., K. Kandasamy, et al. (2003). "Differential roles of RelA (p65) and c-Rel subunits of nuclear factor kappa B in tumor necrosis factor-related apoptosis-inducing ligand signaling." Cancer Res 63(5): 1059-1066.
- Chilton, P. M. and T. C. Mitchell (2006). "CD8 T cells require Bcl-3 for maximal gamma interferon production upon secondary exposure to antigen." Infect Immun 74(7): 4180-4189.
- Chin, K., S DeVries, et al. (2006). "Genomic and transcriptional aberrations linked to breast cancer pathophysiologies." Cancer Cell 10:529-541.
- Chin, S. F., A. E. Teschendorff, et al (2007). "High-resolution acgh and expression profiling identifies a novel genomic subtype of er negative breast cancer." Genome Biol 8:R215.
- Chittenden, T. W., E. A. Howe, et al. (2008). "Functional classification analysis of somatically mutated genes in human breast and colorectal cancers." Genomics 91:508-511.
- Choi, C. Y., K. Reimers, et al. (2007). "Inhibition of apoptosis by expression of antiapoptotic proteins in recombinant human keratinocytes." Cell Transplant 16(6): 663-674.
- Choi, H. J., J. M. Lee, et al. (2010). "Bcl3-dependent stabilization of CtBP1 is crucial for the inhibition of apoptosis and tumor progression in breast cancer." Biochem Biophys Res Commun 400(3): 396-402.
- Chua, H. L., P. Bhat-Nakshatri, et al. (2007). "NF-kappaB represses E-cadherin expression and enhances epithelial to mesenchymal transition of mammary epithelial cells: potential involvement of ZEB-1 and ZEB-2." Oncogene 26(5): 711-724.
- Clarkson, R. W., M. P. Boland, et al. (2006). "The genes induced by signal transducer and activators of transcription (STAT)3 and STAT5 in mammary epithelial cells define the roles of these STATs in mammary development." Mol Endocrinol 20(3): 675-685.
- Clarkson, R. W., J. L. Heeley, et al. (2000). "NF-kappaB inhibits apoptosis in murine mammary epithelia." J Biol Chem 275(17): 12737-12742.
- Clarkson, R. W., M. T. Wayland, et al. (2004). "Gene expression profiling of mammary gland development reveals putative roles for death receptors and immune mediators in post-lactational regression." Breast Cancer Res 6(2): R92-109.
- Claudio, E., K. Brown, et al. (2002). "BAFF-induced NEMO-independent processing of NF-kappa B2 in maturing B cells." Nat Immunol 3(10): 958-965.
- Claus, E. B., N. J. Risch, et al. (1990). "Age at onset as an indicator of familial risk of breast cancer." Am J Epidemiol 131: 961-972.
- Clinchy, B., A. Gazdar, et al. (2000). "The growth and metastasis of human, HER-2/neu-overexpressing tumor cell lines in male SCID mice." Breast Cancer Res Treat 61(3): 217-228.
- Cobleigh, M. A., C. L. Vogel, et al. (1999). "Multinational study of the efficacy and safety of humanized anti-HER2 monoclonal antibody in women who have HER2-overexpressing metastatic breast cancer that has progressed after chemotherapy for metastatic disease." J Clin Oncol 17(9): 2639-2648.

- Cogswell, P. C., D. C. Guttridge, et al. (2000). "Selective activation of NF-kappa B subunits in human breast cancer: potential roles for NF-kappa B2/p52 and for Bcl-3." Oncogene **19**(9): 1123-1131.
- Cohen, S., H. Achbert-Weiner, et al. (2004). "Dual effects of IkappaB kinase beta-mediated phosphorylation on p105 Fate: SCF(beta-TrCP)-dependent degradation and SCF(beta-TrCP)-independent processing." Mol Cell Biol **24**(1): 475-486.
- Conaway, R. C., C. S. Brower, et al. (2002). "Emerging roles of ubiquitin in transcription regulation." Science **296**(5571): 1254-1258.
- Connelly, L., W. Barham, et al. (2010). "Inhibition of NF-kappa B activity in mammary epithelium increases tumor latency and decreases tumor burden." Oncogene.
- Coope, H. J., P. G. Atkinson, et al. (2002). "CD40 regulates the processing of NF-kappaB2 p100 to p52." Embo J **21**(20): 5375-5385.
- Corn, R. A., C. Hunter, et al. (2005). "Opposing roles for RelB and Bcl-3 in regulation of T-box expressed in T cells, GATA-3, and Th effector differentiation." J Immunol **175**(4): 2102-2110.
- Coussens, L., T. L. Yang-Feng, et al. (1985). "Tyrosine kinase receptor with extensive homology to EGF receptor shares chromosomal location with neu oncogene." Science **230**(4730): 1132-1139.
- Criswell, T. L. and C. L. Arteaga (2007). "Modulation of NFkappaB activity and E-cadherin by the type III transforming growth factor beta receptor regulates cell growth and motility." J Biol Chem **282**(44): 32491-32500.
- Crocker, B. A., L. A. Mielke, et al. (2008). "Socs3 maintains the specificity of biological responses to cytokine signals during granulocyte and macrophage differentiation." Exp Hematol **36**(7): 786-798.
- Dai, R., R. A. Phillips, et al. (2007). "Despite inhibition of nuclear localization of NF-kappa B p65, c-Rel, and RelB, 17-beta estradiol up-regulates NF-kappa B signaling in mouse splenocytes: the potential role of Bcl-3." J Immunol **179**(3): 1776-1783.
- Das, K. C. and C. W. White (1997). "Activation of NF-kappaB by antineoplastic agents. Role of protein kinase C." J Biol Chem **272**(23): 14914-14920.
- De Laurentiis, M., D. Cianniello, et al. (2010). "Treatment of triple negative breast cancer (TNBC): current options and future perspectives." Cancer Treat Rev **36 Suppl 3**: S80-86.
- Dechend, R., F. Hirano, et al. (1999). "The Bcl-3 oncoprotein acts as a bridging factor between NF-kappaB/Rel and nuclear co-regulators." Oncogene **18**(22): 3316-3323.
- Dejardin, E., G. Bonizzi, et al. (1995). "Highly-expressed p100/p52 (NFKB2) sequesters other NF-kappa B-related proteins in the cytoplasm of human breast cancer cells." Oncogene **11**(9): 1835-1841.
- Dejardin, E., N. M. Droin, et al. (2002). "The lymphotoxin-beta receptor induces different patterns of gene expression via two NF-kappaB pathways." Immunity **17**(4): 525-535.
- Deryugina, E. I. and J. P. Quigley (2006). "Matrix metalloproteinases and tumor metastasis." Cancer Metastasis Rev **25**(1): 9-34.
- Dolgachev, V., M. Thomas, et al. (2007). "Stem cell factor-mediated activation pathways promote murine eosinophil CCL6 production and survival." J Leukoc Biol **81**(4): 1111-1119.

- Dong, Q. G., G. M. Scwab, et al. (2002). "The function of multiple I $\kappa$ B : NF- $\kappa$ B complexes in the resistance of cancer cells to Taxol-induced apoptosis." Oncogene **21**(42): 6510-6519.
- Dontu, G., W. M. Abdallah, et al. (2003). "In vitro propagation and transcriptional profiling of human mammary stem/progenitor cells." Genes Dev **17**(10): 1253-1270.
- Dontu, G., K. W. Jackson, et al. (2004). "Role of Notch signaling in cell-fate determination of human mammary stem/progenitor cells." Breast Cancer Res **6**(6): R605-615.
- Douma, S., T. Van Laar, et al. (2004). "Suppression of anoikis and induction of metastasis by the neurotrophic receptor TrkB." Nature **430**(7003): 1034-1039.
- Dua, R., J. Zhang, et al. (2010). "EGFR over-expression and activation in high HER2, ER negative breast cancer cell line induces trastuzumab resistance." Breast Cancer Res Treat **122**(3): 685-697.
- Duffy, M. J., T. M. Maguire, et al. (2000). "Metalloproteinases: role in breast carcinogenesis, invasion and metastasis." Breast Cancer Res **2**(4): 252-257.
- Easton, D., D. Ford, et al. (1993). "Inherited susceptibility to breast cancer." Cancer Surv **18**:95-113.
- Fata, J. E., K. J. Leco, et al. (1999). "Timp-1 is important for epithelial proliferation and branching morphogenesis during mouse mammary development." Dev Biol **211**(2): 238-254.
- Feinman, R., J. Koury, et al. (1999). "Role of NF- $\kappa$ B in the rescue of multiple myeloma cells from glucocorticoid-induced apoptosis by bcl-2." Blood **93**(9): 3044-3052.
- Fillmore, C. M. and C. Kuperwasser (2008). "Human breast cancer cell lines contain stem-like cells that self-renew, give rise to phenotypically diverse progeny and survive chemotherapy." Breast Cancer Res **10**(2): R25.
- Finco, T. S., J. K. Westwick, et al. (1997). "Oncogenic Ha-Ras-induced signaling activates NF- $\kappa$ B transcriptional activity, which is required for cellular transformation." J Biol Chem **272**(39): 24113-24116.
- Fischer, C., S. Page, et al. (1999). "Differential effects of lipopolysaccharide and tumor necrosis factor on monocytic I $\kappa$ B kinase signalsome activation and I $\kappa$ B proteolysis." J Biol Chem **274**(35): 24625-24632.
- Folco, E. J., V. Z. Rocha, et al. (2009). "Adiponectin inhibits pro-inflammatory signaling in human macrophages independent of interleukin-10." J Biol Chem **284**(38): 25569-25575.
- Fong, A., M. Zhang, et al. (2002). "S9, a 19 S proteasome subunit interacting with ubiquitinated NF- $\kappa$ B2/p100." J Biol Chem **277**(43): 40697-40702.
- Fransen, K., M. C. Visschedijk, et al. (2010). "Analysis of SNPs with an effect on gene expression identifies UBE2L3 and BCL3 as potential new risk genes for Crohn's disease." Hum Mol Genet **19**(17): 3482-3488.
- Franzoso, G., V. Bours, et al. (1993). "The oncoprotein Bcl-3 can facilitate NF- $\kappa$ B-mediated transactivation by removing inhibiting p50 homodimers from select kappa B sites." Embo J **12**(10): 3893-3901.
- Franzoso, G., V. Bours, et al. (1992). "The candidate oncoprotein Bcl-3 is an antagonist of p50/NF- $\kappa$ B-mediated inhibition." Nature **359**(6393): 339-342.

- Franzoso, G., L. Carlson, et al. (1998). "Mice deficient in nuclear factor (NF)-kappa B/p52 present with defects in humoral responses, germinal center reactions, and splenic microarchitecture." J Exp Med **187**(2): 147-159.
- Franzoso, G., L. Carlson, et al. (1997). "Critical roles for the Bcl-3 oncoprotein in T cell-mediated immunity, splenic microarchitecture, and germinal center reactions." Immunity **6**(4): 479-490.
- Freiman, R. N. and R. Tjian (2003). "Regulating the regulators: lysine modifications make their mark." Cell **112**(1): 11-17.
- Frensing, T., C. Kaltschmidt, et al. (2008). "Characterization of a neuregulin-1 gene promoter: positive regulation of type I isoforms by NF-kappaB." Biochim Biophys Acta **1779**(2): 139-144.
- Fritz, R. D. and G. Radziwill (2010). "CNK1 promotes invasion of cancer cells through NF-kappaB-dependent signaling." Mol Cancer Res **8**(3): 395-406.
- Fujita, T., G. P. Nolan, et al. (1993). "The candidate proto-oncogene bcl-3 encodes a transcriptional coactivator that activates through NF-kappa B p50 homodimers." Genes Dev **7**(7B): 1354-1363.
- Garcia, M. F., S. Gonzalez-Reyes, et al. (2010). "Comparative study of the expression of metalloproteases and their inhibitors in different localizations within primary tumours and in metastatic lymph nodes of breast cancer." Int J Exp Pathol **91**(4): 324-334.
- Gasparini, G., M. Gion, et al. (2007). "Randomized Phase II Trial of weekly paclitaxel alone versus trastuzumab plus weekly paclitaxel as first-line therapy of patients with Her-2 positive advanced breast cancer." Breast Cancer Res Treat **101**(3): 355-365.
- Gavert, N., A. Ben-Shmuel, et al. (2010). "Nuclear factor-kappaB signaling and ezrin are essential for L1-mediated metastasis of colon cancer cells." J Cell Sci **123**(Pt 12): 2135-2143.
- Ge, B., O. Li, et al. (2003). "NF-kappa B regulates BCL3 transcription in T lymphocytes through an intronic enhancer." J Immunol **171**(8): 4210-4218.
- Gerondakis, S., R. Grumont, et al. (2006). "Unravelling the complexities of the NF-kappaB signalling pathway using mouse knockout and transgenic models." Oncogene **25**(51): 6781-6799.
- Geyer, C. E., J. Forster, et al. (2006). "Lapatinib plus capecitabine for HER2-positive advanced breast cancer." N Engl J Med **355**(26): 2733-2743.
- Gildea, J. J., M. J. Seraj, et al. (2002). "RhoGDI2 is an invasion and metastasis suppressor gene in human cancer." Cancer Res **62**(22): 6418-6423.
- Gilmore, T. D. and M. Herscovitch (2006). "Inhibitors of NF-kappaB signaling: 785 and counting." Oncogene **25**(51): 6887-6899.
- Ginestier, C., M. H. Hur, et al. (2007). "ALDH1 is a marker of normal and malignant human mammary stem cells and a predictor of poor clinical outcome." Cell Stem Cell **1**(5): 555-567.
- Gluz, O., C. Liedtke, et al. (2009). "Triple-negative breast cancer--current status and future directions." Ann Oncol **20**(12): 1913-1927.
- Gonzalez, L. O., I. Pidal, et al. (2007). "Overexpression of matrix metalloproteinases and their inhibitors in mononuclear inflammatory cells in breast cancer correlates with metastasis-relapse." Br J Cancer **97**(7): 957-963.

- Grange, C., S. Lanzardo, et al. (2008). "Sca-1 identifies the tumor-initiating cells in mammary tumors of BALB-neuT transgenic mice." Neoplasia **10**(12): 1433-1443.
- Green, K. A. and L. R. Lund (2005). "ECM degrading proteases and tissue remodelling in the mammary gland." Bioessays **27**(9): 894-903.
- Greenman, C., P. Stephens, et al. (2007). "Patterns of somatic mutation in human cancer genomes." Nature **446**:153-158.
- Greten, F. R., L. Eckmann, et al. (2004). "IKKbeta links inflammation and tumorigenesis in a mouse model of colitis-associated cancer." Cell **118**(3): 285-296.
- Grumont, R. J., I. J. Rourke, et al. (1998). "B lymphocytes differentially use the Rel and nuclear factor kappaB1 (NF-kappaB1) transcription factors to regulate cell cycle progression and apoptosis in quiescent and mitogen-activated cells." J Exp Med **187**(5): 663-674.
- Guan, Y., H. Yao, et al. (2010). "MiR-125b targets BCL3 and suppresses ovarian cancer proliferation." Int J Cancer.
- Guttridge, D. C., C. Albanese, et al. (1999). "NF-kappaB controls cell growth and differentiation through transcriptional regulation of cyclin D1." Mol Cell Biol **19**(8): 5785-5799.
- Guy, C. T., M. A. Webster, et al. (1992). "Expression of the neu protooncogene in the mammary epithelium of transgenic mice induces metastatic disease." Proc Natl Acad Sci U S A **89**(22): 10578-10582.
- Haffner, M. C., C. Berlato, et al. (2006). "Exploiting our knowledge of NF-kappaB signaling for the treatment of mammary cancer." J Mammary Gland Biol Neoplasia **11**(1): 63-73.
- Hagihara, K., T. Nishikawa, et al. (2005). "Essential role of STAT3 in cytokine-driven NF-kappaB-mediated serum amyloid A gene expression." Genes Cells **10**(11): 1051-1063.
- Hammarskjold, M. L. and M. C. Simurda (1992). "Epstein-Barr virus latent membrane protein transactivates the human immunodeficiency virus type 1 long terminal repeat through induction of NF-kappa B activity." J Virol **66**(11): 6496-6501.
- Hanahan, D. and R. A. Weinberg (2000). "The hallmarks of cancer." Cell **100**(1): 57-70.
- Hatada, E. N., A. Nieters, et al. (1992). "The ankyrin repeat domains of the NF-kappa B precursor p105 and the protooncogene bcl-3 act as specific inhibitors of NF-kappa B DNA binding." Proc Natl Acad Sci U S A **89**(6): 2489-2493.
- Hayden, M. S. and S. Ghosh (2004). "Signaling to NF-kappaB." Genes Dev **18**(18): 2195-2224.
- Heinrich, P. C., I. Behrmann, et al. (1998). "Interleukin-6-type cytokine signalling through the gp130/Jak/STAT pathway." Biochem J **334**( Pt 2): 297-314.
- Helbig, G., K. W. Christopherson, 2nd, et al. (2003). "NF-kappaB promotes breast cancer cell migration and metastasis by inducing the expression of the chemokine receptor CXCR4." J Biol Chem **278**(24): 21631-21638.
- Hernandez, L., S. C. Hsu, et al. (2010). "Activation of NF-kappaB signaling by inhibitor of NF-kappaB kinase beta increases aggressiveness of ovarian cancer." Cancer Res **70**(10): 4005-4014.
- Herschkowitz, J. I., K. Simin, et al. (2007). "Identification of conserved gene expression features between murine mammary carcinoma models and human breast tumors." Genome Biol **8**(5): R76.

- Heusch, M., L. Lin, et al. (1999). "The generation of nfkb2 p52: mechanism and efficiency." Oncogene **18**(46): 6201-6208.
- Hirano, F., H. Tanaka, et al. (1998). "Functional interference of Sp1 and NF-kappaB through the same DNA binding site." Mol Cell Biol **18**(3): 1266-1274.
- Hishiki, T., T. Ohshima, et al. (2007). "BCL3 acts as a negative regulator of transcription from the human T-cell leukemia virus type 1 long terminal repeat through interactions with TORC3." J Biol Chem **282**(39): 28335-28343.
- Hoffmann, A., G. Natoli, et al. (2006). "Transcriptional regulation via the NF-kappaB signaling module." Oncogene **25**(51): 6706-6716.
- Horak, C. E., J. H. Lee, et al. (2007). "Nm23-H1 suppresses tumor cell motility by down-regulating the lysophosphatidic acid receptor EDG2." Cancer Res **67**(15): 7238-7246.
- Hou, S., H. Guan, et al. (2003). "Phosphorylation of serine 337 of NF-kappaB p50 is critical for DNA binding." J Biol Chem **278**(46): 45994-45998.
- Hovelmeyer, N., F. T. Wunderlich, et al. (2007). "Regulation of B cell homeostasis and activation by the tumor suppressor gene CYLD." J Exp Med **204**(11): 2615-2627.
- Howell, A., C. K. Osborne, et al. (2000). "ICI 182,780 (Faslodex): development of a novel, "pure" antiestrogen." Cancer **89**(4): 817-825.
- Hsieh, F. C., G. Cheng, et al. (2005). "Evaluation of potential Stat3-regulated genes in human breast cancer." Biochem Biophys Res Commun **335**(2): 292-299.
- Huang, T. T., S. M. Wuerzberger-Davis, et al. (2003). "Sequential modification of NEMO/IKKgamma by SUMO-1 and ubiquitin mediates NF-kappaB activation by genotoxic stress." Cell **115**(5): 565-576.
- Huang, W., Q. Meng, et al. (1997). "Mutational study of the amino-terminal domain of human tissue inhibitor of metalloproteinases 1 (TIMP-1) locates an inhibitory region for matrix metalloproteinases." J Biol Chem **272**(35): 22086-22091.
- Huber, M. A., N. Azoitei, et al. (2004). "NF-kappaB is essential for epithelial-mesenchymal transition and metastasis in a model of breast cancer progression." J Clin Invest **114**(4): 569-581.
- Humphreys, R. C., B. Bierie, et al. (2002). "Deletion of Stat3 blocks mammary gland involution and extends functional competence of the secretory epithelium in the absence of lactogenic stimuli." Endocrinology **143**(9): 3641-3650.
- Huo, J., S. Xu, et al. (2009). "Genetic deletion of faim reveals its role in modulating c-FLIP expression during CD95-mediated apoptosis of lymphocytes and hepatocytes." Cell Death Differ **16**(7): 1062-1070.
- Huxford, T., D. B. Huang, et al. (1998). "The crystal structure of the IkappaBalpha/NF-kappaB complex reveals mechanisms of NF-kappaB inactivation." Cell **95**(6): 759-770.
- Ikeda, F. and I. Dikic (2006). "CYLD in ubiquitin signaling and tumor pathogenesis." Cell **125**(4): 643-645.
- Inoue, J., T. Takahara, et al. (1993). "Bcl-3, a member of the I kappa B proteins, has distinct specificity towards the Rel family of proteins." Oncogene **8**(8): 2067-2073.
- Irvin, W. J., Jr., R. Z. Orlowski, et al. (2010). "Phase II study of bortezomib and pegylated liposomal doxorubicin in the treatment of metastatic breast cancer." Clin Breast Cancer **10**(6): 465-470.

- Jacobs, M. D. and S. C. Harrison (1998). "Structure of an I kappa B alpha/NF-kappa B complex." Cell **95**(6): 749-758.
- Jamaluddin, M., S. Choudhary, et al. (2005). "Respiratory syncytial virus-inducible BCL-3 expression antagonizes the STAT/IRF and NF-kappa B signaling pathways by inducing histone deacetylase 1 recruitment to the interleukin-8 promoter." J Virol **79**(24): 15302-15313.
- Jin, H., Y. Pan, et al. (2007). "p75 neurotrophin receptor inhibits invasion and metastasis of gastric cancer." Mol Cancer Res **5**(5): 423-433.
- Jin, Z. and W. S. El-Deiry (2005). "Overview of cell death signaling pathways." Cancer Biol Ther **4**(2): 139-163.
- Jonkers, J. and P. W. Derksen (2007). "Modeling metastatic breast cancer in mice." J Mammary Gland Biol Neoplasia **12**(2-3): 191-203.
- Jordan, V. C. (2006). "Tamoxifen (ICI46,474) as a targeted therapy to treat and prevent breast cancer." Br J Pharmacol **147**(suppl1): S269-276.
- Ju, X., S. Katiyar, et al. (2007). "Akt1 governs breast cancer progression in vivo." Proc Natl Acad Sci U S A **104**(18): 7438-7443.
- Kabuta, T., F. Hakuno, et al. (2010). "Insulin receptor substrate-3, interacting with Bcl-3, enhances p50 NF-kappa B activity." Biochem Biophys Res Commun **394**(3): 697-702.
- Kamens, J., P. Richardson, et al. (1990). "Oncogenic transformation by vrel requires an amino-terminal activation domain." Mol Cell Biol **10**(6): 2840-2847.
- Kashatus, D., P. Cogswell, et al. (2006). "Expression of the Bcl-3 proto-oncogene suppresses p53 activation." Genes Dev **20**(2): 225-235.
- Kasof, G. M., J. J. Lu, et al. (2001). "Tumor necrosis factor-alpha induces the expression of DR6, a member of the TNF receptor family, through activation of NF-kappa B." Oncogene **20**(55): 7965-7975.
- Kato, T., Jr., M. Delhase, et al. (2003). "CK2 Is a C-Terminal I kappa B Kinase Responsible for NF-kappa B Activation during the UV Response." Mol Cell **12**(4): 829-839.
- Kelly, R. J., D. Wright, et al. (2008). "t(14;19)(q32;q13) incidence and significance in B-cell lymphoproliferative disorders." Br J Haematol **141**(4): 561-563.
- Kerr, L. D., C. S. Duckett, et al. (1992). "The proto-oncogene bcl-3 encodes an I kappa B protein." Genes Dev **6**(12A): 2352-2363.
- Keutgens, A., K. Shostak, et al. (2010). "The repressing function of the oncoprotein BCL-3 requires CtBP, while its polyubiquitination and degradation involve the E3 ligase TBLR1." Mol Cell Biol **30**(16): 4006-4021.
- Keutgens, A., X. Zhang, et al. (2010). "BCL-3 degradation involves its polyubiquitination through a FBW7-independent pathway and its binding to the proteasome subunit PSMB1." J Biol Chem **285**(33): 25831-25840.
- Kim, J., W. Yu, et al. (1998). "Requirement for specific proteases in cancer cell intravasation as revealed by a novel semiquantitative PCR-based assay." Cell **94**(3): 353-362.
- Kim, J. H., B. Kim, et al. (2005). "Transcriptional regulation of a metastasis suppressor gene by Tip60 and beta-catenin complexes." Nature **434**(7035): 921-926.

- King, C. R., I. Borrello, et al. (1988). "Egf binding to its receptor triggers a rapid tyrosine phosphorylation of the erbB-2 protein in the mammary tumor cell line SK-BR-3." Embo J **7**(6): 1647-1651.
- Kojima, M., T. Morisaki, et al. (2004). "Increased nuclear factor-kB activation in human colorectal carcinoma and its correlation with tumor progression." Anticancer Res **24**(2B): 675-681.
- Kordon, E. C. and G. H. Smith (1998). "An entire functional mammary gland may comprise the progeny from a single cell." Development **125**(10): 1921-1930.
- Korkaya, H., A. Paulson, et al. (2008). "HER2 regulates the mammary stem/progenitor cell population driving tumorigenesis and invasion." Oncogene **27**(47): 6120-6130.
- Kraus, M. H., W. Issing, et al. (1989). "Isolation and characterization of ERBB3, a third member of the ERBB/epidermal growth factor receptor family: evidence for overexpression in a subset of human mammary tumors." Proc Natl Acad Sci U S A **86**(23): 9193-9197.
- Kreisel, D., S. Sugimoto, et al. (2011). "Bcl3 prevents acute inflammatory lung injury in mice by restraining emergency granulopoiesis." J Clin Invest **121**(1): 265-276.
- Kreuzaler, P. A., A. D. Stanisiewska, et al. (2011). "Stat3 controls lysosomal-mediated cell death in vivo." Nat Cell Biol **13**(3): 303-309.
- Kritikou, E. A., A. Sharkey, et al. (2003). "A dual, non-redundant, role for LIF as a regulator of development and STAT3-mediated cell death in mammary gland." Development **130**(15): 3459-3468.
- Kucharczak, J., M. J. Simmons, et al. (2003). "To be, or not to be: NF-kappaB is the answer--role of Rel/NF-kappaB in the regulation of apoptosis." Oncogene **22**(56): 8961-8982.
- Kung, C. P. and N. Raab-Traub (2008). "Epstein-Barr virus latent membrane protein 1 induces expression of the epidermal growth factor receptor through effects on Bcl-3 and STAT3." J Virol **82**(11): 5486-5493.
- Kurylowicz, A. and J. Nauman (2008). "The role of nuclear factor-kappaB in the development of autoimmune diseases: a link between genes and environment." Acta Biochim Pol **55**(4): 629-647.
- Kuwata, H., Y. Watanabe, et al. (2003). "IL-10-inducible Bcl-3 negatively regulates LPS-induced TNF-alpha production in macrophages." Blood **102**(12): 4123-4129.
- Lee, Y. T. (1983). "Breast carcinoma: pattern of metastasis at autopsy." J Surg Oncol **23**(3): 175-180.
- Lelekakis, M., J. M. Moseley, et al. (1999). "A novel orthotopic model of breast cancer metastasis to bone." Clin Exp Metastasis **17**(2): 163-170.
- Lemoine, N. R., D. M. Barnes, et al. (1992). "Expression of the ERBB3 gene product in breast cancer." Br J Cancer **66**(6): 1116-1121.
- Lemoine, N. R., S. Staddon, et al. (1990). "Absence of activating transmembrane mutations in the c-erbB-2 proto-oncogene in human breast cancer." Oncogene **5**(2): 237-239.
- Leung, T. H., A. Hoffmann, et al. (2004). "One nucleotide in a kappaB site can determine cofactor specificity for NF-kappaB dimers." Cell **118**: 453-464.
- Li, B., Y. Y. Li, et al. (2009). "Targeting NF-kappaB signaling pathway suppresses tumor growth, angiogenesis, and metastasis of human esophageal cancer." Mol Cancer Ther **8**(9): 2635-2644.

- Li, H. C., D. C. Cao, et al. (2004). "Prognostic value of matrix metalloproteinases (MMP-2 and MMP-9) in patients with lymph node-negative breast carcinoma." Breast Cancer Res Treat **88**(1): 75-85.
- Li, Q., C. Eppolito, et al. (2006). "IL-12-programmed long-term CD8+ T cell responses require STAT4." J Immunol **177**(11): 7618-7625.
- Li, Q., D. Van Antwerp, et al. (1999). "Severe liver degeneration in mice lacking the I $\kappa$ B kinase 2 gene." Science **284**(5412): 321-325.
- Li, Z., C. Schem, et al. (2008). "Increased COX2 expression enhances tumor-induced osteoclastic lesions in breast cancer bone metastasis." Clin Exp Metastasis **25**(4): 389-400.
- Lin, E. Y., A. V. Nguyen, et al. (2001). "Colony-stimulating factor 1 promotes progression of mammary tumors to malignancy." J Exp Med **193**(6): 727-740.
- Lin, E. Y. and J. W. Pollard (2007). "Tumor-associated macrophages press the angiogenic switch in breast cancer." Cancer Res **67**(11): 5064-5066.
- Lin, J., C. M. Gan, et al. (2007) "A multidimensional analysis of genes mutated in breast and colorectal cancers." Genome Res **17**:1304-1318.
- Lin, L., G. N. DeMartino, et al. (1998). "Cotranslational biogenesis of NF-kappaB p50 by the 26S proteasome." Cell **92**(6): 819-828.
- Lin, L. and S. Ghosh (1996). "A glycine-rich region in NF-kappaB p105 functions as a processing signal for the generation of the p50 subunit." Mol Cell Biol **16**(5): 2248-2254.
- Lipnik, K., H. Petznek, et al. (2005). "A 470 bp WAP-promoter fragment confers lactation independent, progesterone regulated mammary-specific gene expression in transgenic mice." Transgenic Res **14**(2): 145-158.
- Liu, J. C., T. Deng, et al. (2007). "Identification of tumorsphere- and tumor-initiating cells in HER2/Neu-induced mammary tumors." Cancer Res **67**(18): 8671-8681.
- Liu, M., X. Ju, et al. (2009). "Nuclear factor-kappaB enhances ErbB2-induced mammary tumorigenesis and neoangiogenesis in vivo." Am J Pathol **174**(5): 1910-1920.
- Liu, M., T. Sakamaki, et al. (2010). "The canonical NF-kappaB pathway governs mammary tumorigenesis in transgenic mice and tumor stem cell expansion." Cancer Res **70**(24): 10464-10473.
- Liu, X., G. W. Robinson, et al. (1996). "Activation of Stat5a and Stat5b by tyrosine phosphorylation is tightly linked to mammary gland differentiation." Mol Endocrinol **10**(12): 1496-1506.
- Liu, X., G. W. Robinson, et al. (1997). "Stat5a is mandatory for adult mammary gland development and lactogenesis." Genes Dev **11**(2): 179-186.
- Livasy, C. A., G. Karaca, et al. (2006). "Phenotypic evaluation of the basal-like subtype of invasive breast carcinoma." Mod Pathol **19**(2): 264-271.
- Lodato, R. F., H. C. Maguire, Jr., et al. (1990). "Immunohistochemical evaluation of c-erbB-2 oncogene expression in ductal carcinoma in situ and atypical ductal hyperplasia of the breast." Mod Pathol **3**(4): 449-454.
- Lombardo, L. J., F. Y. Lee, et al. (2004). "Discovery of N-(2-chloro-6-methyl- phenyl)-2-(6-(4-(2-hydroxyethyl)- piperazin-1-yl)-2-methylpyrimidin-4- yl amino)thiazole-5-carboxamide (BMS-

- 354825), a dual Src/Abl kinase inhibitor with potent antitumor activity in preclinical assays." J Med Chem **47**(27): 6658-6661.
- Lopez-Tarruella, S. and M. Martin (2009). "Recent advances in systemic therapy: advances in adjuvant systemic chemotherapy of early breast cancer." Breast Cancer Res **11**(2): 204.
- Luftig, M., T. Yasui, et al. (2004). "Epstein-Barr virus latent infection membrane protein 1 TRAF-binding site induces NIK/IKK alpha-dependent noncanonical NF-kappaB activation." Proc Natl Acad Sci U S A **101**(1): 141-146.
- Lund, L. R., J. Romer, et al. (1996). "Two distinct phases of apoptosis in mammary gland involution: proteinase-independent and -dependent pathways." Development **122**(1): 181-193.
- Luo, J. L., S. Maeda, et al. (2004). "Inhibition of NF-kappaB in cancer cells converts inflammation- induced tumor growth mediated by TNFalpha to TRAIL-mediated tumor regression." Cancer Cell **6**(3): 297-305.
- Luo, M., H. Fan, et al. (2009). "Mammary epithelial-specific ablation of the focal adhesion kinase suppresses mammary tumorigenesis by affecting mammary cancer stem/progenitor cells." Cancer Res **69**(2): 466-474.
- Lynch, E. D., E. A Ostermeyer, et al. (1997). "Inherited mutations in PTEN that are associated with breast cancer, cowden disease, and juvenile polyposis." Am J Hum Genet **61**:1254-1260.
- Malek, S., Y. Chen, et al. (2001). "IkappaBbeta, but not IkappaBalpha, functions as a classical cytoplasmic inhibitor of NF-kappaB dimers by masking both NF-kappaB nuclear localization sequences in resting cells." J Biol Chem **276**(48): 45225-45235.
- Malek, S., D. B. Huang, et al. (2003). "X-ray crystal structure of an IkappaBbeta x NF-kappaB p65 homodimer complex." J Biol Chem **278**(25): 23094-23100.
- Mani, S. A., J. Yang, et al. (2007). "Mesenchyme Forkhead 1 (FOXC2) plays a key role in metastasis and is associated with aggressive basal-like breast cancers." Proc Natl Acad Sci U S A **104**(24): 10069-10074.
- Mantovani, A., P. Allavena, et al. (2008). "Cancer-related inflammation." Nature **454**(7203): 436-444.
- Marti, A., P. M. Ritter, et al. (2001). "Mouse mammary gland involution is associated with cytochrome c release and caspase activation." Mech Dev **104**(1-2): 89-98.
- Martin-Subero, J. I., R. Ibbotson, et al. (2007). "A comprehensive genetic and histopathologic analysis identifies two subgroups of B-cell malignancies carrying a t(14;19)(q32;q13) or variant BCL3-translocation." Leukemia **21**(7): 1532-1544.
- Martin-Subero, J. I., I. Wlodarska, et al. (2006). "Chromosomal rearrangements involving the BCL3 locus are recurrent in classical Hodgkin and peripheral T-cell lymphoma." Blood **108**(1): 401-402; author reply 402-403.
- Massoumi, R. (2009). "The central role of Bcl-3 in atopic dermatitis." J Invest Dermatol **129**(9): 2088-2090.
- Massoumi, R., K. Chmielarska, et al. (2006). "Cyld inhibits tumor cell proliferation by blocking Bcl-3-dependent NF-kappaB signaling." Cell **125**(4): 665-677.
- Massoumi, R., S. Kuphal, et al. (2009). "Down-regulation of CYLD expression by Snail promotes tumor progression in malignant melanoma." J Exp Med **206**(1): 221-232.

- Massoumi, R. and R. Paus (2007). "Cylindromatosis and the CYLD gene: new lessons on the molecular principles of epithelial growth control." Bioessays **29**(12): 1203-1214.
- Mastrorarde, J. G., B. He, et al. (1996). "Induction of interleukin (IL)-8 gene expression by respiratory syncytial virus involves activation of nuclear factor (NF)-kappa B and NF-IL-6." J Infect Dis **174**(2): 262-267.
- Mathas, S., K. Johrens, et al. (2005). "Elevated NF-kappaB p50 complex formation and Bcl-3 expression in classical Hodgkin, anaplastic large-cell, and other peripheral T-cell lymphomas." Blood **106**(13): 4287-4293.
- McDaniel, S. M., K. K. Rumer, et al. (2006). "Remodeling of the mammary microenvironment after lactation promotes breast tumor cell metastasis." Am J Pathol **168**(2): 608-620.
- McDermott, W. G., M. Boissan, et al. (2008). "Nm23-H1 homologs suppress tumor cell motility and anchorage independent growth." Clin Exp Metastasis **25**(2): 131-138.
- McKeithan, T. W., H. Ohno, et al. (1990). "Identification of a transcriptional unit adjacent to the breakpoint in the 14;19 translocation of chronic lymphocytic leukemia." Genes Chromosomes Cancer **1**(3): 247-255.
- McKeithan, T. W., H. Ohno, et al. (1994). "Genomic structure of the candidate proto-oncogene BCL3." Genomics **24**(1): 120-126.
- McKeithan, T. W., G. S. Takimoto, et al. (1997). "BCL3 rearrangements and t(14;19) in chronic lymphocytic leukemia and other B-cell malignancies: a molecular and cytogenetic study." Genes Chromosomes Cancer **20**(1): 64-72.
- Mercurio, F., J. A. DiDonato, et al. (1993). "p105 and p98 precursor proteins play an active role in NF-kappa B-mediated signal transduction." Genes Dev **7**(4): 705-718.
- Merkhofer, E. C., P. Cogswell, et al. (2010). "Her2 activates NF-kappaB and induces invasion through the canonical pathway involving IKKalpha." Oncogene **29**(8): 1238-1248.
- Michel, F., M. Soler-Lopez, et al. (2001). "Crystal structure of the ankyrin repeat domain of Bcl-3: a unique member of the IkappaB protein family." Embo J **20**(22): 6180-6190.
- Miki, Y., J. Swensen, et al. (1994). "A strong candidate for the breast and ovarian cancer susceptibility gene BRCA1." Science **266**: 66-71.
- Mishra, A., A. C. Bharti, et al. (2006). "Differential expression and activation of NF-kappaB family proteins during oral carcinogenesis: Role of high risk human papillomavirus infection." Int J Cancer **119**(12): 2840-2850.
- Mitchell, T. C., D. Hildeman, et al. (2001). "Immunological adjuvants promote activated T cell survival via induction of Bcl-3." Nat Immunol **2**(5): 397-402.
- Mitchell, T. C., T. K. Teague, et al. (2002). "Stronger correlation of bcl-3 than bcl-2, bcl-xL, costimulation, or antioxidants with adjuvant-induced T cell survival." Ann N Y Acad Sci **975**: 114-131.
- Mitchell, T. C., B. S. Thompson, et al. (2002). "A short domain within Bcl-3 is responsible for its lymphocyte survival activity." Ann N Y Acad Sci **975**: 132-147.
- Miyazaki, I., S. Simizu, et al. (2010). "A small-molecule inhibitor shows that pirin regulates migration of melanoma cells." Nat Chem Biol **6**(9): 667-673.

- Molyneux, G., F. C. Geyer, et al. (2010). "BRCA1 basal-like breast cancers originate from luminal epithelial progenitors and not from basal stem cells." Cell Stem Cell **7**(3): 403-417.
- Morimoto, K., S. J. Kim, et al. (2009). "Stem cell marker aldehyde dehydrogenase 1-positive breast cancers are characterized by negative estrogen receptor, positive human epidermal growth factor receptor type 2, and high Ki67 expression." Cancer Sci **100**(6): 1062-1068.
- Muhlbauer, M., P. M. Chilton, et al. (2008). "Impaired Bcl3 up-regulation leads to enhanced lipopolysaccharide-induced interleukin (IL)-23P19 gene expression in IL-10(-/-) mice." J Biol Chem **283**(21): 14182-14189.
- Muller, J. R. and U. Siebenlist (2003). "Lymphotoxin beta receptor induces sequential activation of distinct NF-kappa B factors via separate signaling pathways." J Biol Chem **278**(14): 12006-12012.
- Muller, W. J., E. Sinn, et al. (1988). "Single-step induction of mammary adenocarcinoma in transgenic mice bearing the activated c-neu oncogene." Cell **54**(1): 105-115.
- Murphy, G., A. Houbrechts, et al. (1991). "The N-terminal domain of tissue inhibitor of metalloproteinases retains metalloproteinase inhibitory activity." Biochemistry **30**(33): 8097-8102.
- Na, S. Y., H. S. Choi, et al. (1998). "Bcl3, an IkappaB protein, as a novel transcription coactivator of the retinoid X receptor." J Biol Chem **273**(47): 30933-30938.
- Na, S. Y., J. E. Choi, et al. (1999). "Bcl3, an IkappaB protein, stimulates activating protein-1 transactivation and cellular proliferation." J Biol Chem **274**(40): 28491-28496.
- Nabholtz, J. M., A. Buzdar, et al. (2000). "Anastrozole is superior to tamoxifen as first-line therapy for advanced breast cancer in postmenopausal women: results of a North American multicenter randomized trial. Arimidex Study Group." J Clin Oncol **18**(22): 3758-3767.
- Nahta, R. and F. J. Esteva (2006). "HER2 therapy: molecular mechanisms of trastuzumab resistance." Breast Cancer Res **8**(6): 215.
- Nair, A., M. Venkatraman, et al. (2003). "NF-kappaB is constitutively activated in high-grade squamous intraepithelial lesions and squamous cell carcinomas of the human uterine cervix." Oncogene **22**(1): 50-58.
- Nakanishi, C. and M. Toi (2005). "Nuclear factor-kappaB inhibitors as sensitizers to anticancer drugs." Nat Rev Cancer **5**(4): 297-309.
- Nakshatri, H., P. Bhat-Nakshatri, et al. (1997). "Constitutive activation of NF-kappaB during progression of breast cancer to hormone-independent growth." Mol Cell Biol **17**(7): 3629-3639.
- Nanni, P., S. M. Pupa, et al. (2000). "p185(neu) protein is required for tumor and anchorage-independent growth, not for cell proliferation of transgenic mammary carcinoma." Int J Cancer **87**(2): 186-194.
- Naumann, M., F. G. Wulczyn, et al. (1993). "The NF-kappa B precursor p105 and the proto-oncogene product Bcl-3 are I kappa B molecules and control nuclear translocation of NF-kappa B." Embo J **12**(1): 213-222.
- Nevanlinna, H. and J. Bartek, (2006). "The CHEK2 gene and inherited breast cancer susceptibility." Oncogene **25**:5912-5919.
- Neve, R. M., K. Chin, et al. (2006). "A collection of breast cancer cell lines for the study of functionally distinct cancer subtypes." Cancer Cell **10**(6): 515-527.

- Nielsen, T. O., F. D. Hsu, et al. (2004). "Immunohistochemical and clinical characterization of the basal-like subtype of invasive breast carcinoma." Clin Cancer Res **10**(16): 5367-5374.
- Nishikori, M., H. Ohno, et al. (2005). "Stimulation of CD30 in anaplastic large cell lymphoma leads to production of nuclear factor-kappaB p52, which is associated with hyperphosphorylated Bcl-3." Cancer Sci **96**(8): 487-497.
- Nolan, G. P., T. Fujita, et al. (1993). "The bcl-3 proto-oncogene encodes a nuclear I kappa B-like molecule that preferentially interacts with NF-kappa B p50 and p52 in a phosphorylation-dependent manner." Mol Cell Biol **13**(6): 3557-3566.
- Normanno, N., C. Bianco, et al. (2003). "Target-based agents against ErbB receptors and their ligands: a novel approach to cancer treatment." Endocr Relat Cancer **10**(1): 1-21.
- Normanno, N., A. Morabito, et al. (2009). "Target-based therapies in breast cancer: current status and future perspectives." Endocr Relat Cancer **16**(3): 675-702.
- Nowell, P. C. (1976). "The clonal evolution of tumor cell populations." Science **194**(4260): 23-28.
- O'Neil, B. H., P. Buzkova, et al. (2007). "Expression of nuclear factor-kappaB family proteins in hepatocellular carcinomas." Oncology **72**(1-2): 97-104.
- O'Shaughnessy, J. (2005). "Extending survival with chemotherapy in metastatic breast cancer." Oncologist **10** Suppl 3: 20-29.
- Ohno, H., M. Nishikori, et al. (2005). "Reappraisal of BCL3 as a molecular marker of anaplastic large cell lymphoma." Int J Hematol **82**(5): 397-405.
- Ohno, H., G. Takimoto, et al. (1990). "The candidate proto-oncogene bcl-3 is related to genes implicated in cell lineage determination and cell cycle control." Cell **60**(6): 991-997.
- Olayioye, M. A., R. M. Neve, et al. (2000). "The ErbB signaling network: receptor heterodimerization in development and cancer." Embo J **19**(13): 3159-3167.
- Ong, S. T., M. L. Hackbarth, et al. (1998). "Lymphadenopathy, splenomegaly, and altered immunoglobulin production in BCL3 transgenic mice." Oncogene **16**(18): 2333-2343.
- Orian, A., H. Gonen, et al. (2000). "SCF(beta)(-TrCP) ubiquitin ligase-mediated processing of NF-kappaB p105 requires phosphorylation of its C-terminus by I kappa B kinase." Embo J **19**(11): 2580-2591.
- Orian, A., A. L. Schwartz, et al. (1999). "Structural motifs involved in ubiquitin-mediated processing of the NF-kappaB precursor p105: roles of the glycine-rich region and a downstream ubiquitination domain." Mol Cell Biol **19**(5): 3664-3673.
- Orlowski, R. Z. and E. C. Dees (2003). "The role of the ubiquitination-proteasome pathway in breast cancer: applying drugs that affect the ubiquitin-proteasome pathway to the therapy of breast cancer." Breast Cancer Res **5**(1): 1-7.
- Osborn, L., S. Kunkel, et al. (1989). "Tumor necrosis factor alpha and interleukin 1 stimulate the human immunodeficiency virus enhancer by activation of the nuclear factor kappa B." Proc Natl Acad Sci U S A **86**(7): 2336-2340.
- Osorio, A., M. de la Hoya, et al. (2002). "Loss of heterozygosity analysis at the BRCA loci in tumor samples from patients with familial breast cancer." Int J Cancer **99**:305-309.

- Oyama, T., K. Iijima, et al. (2000). "Atypical cystic lobule of the breast: an early stage of low-grade ductal carcinoma in-situ." Breast Cancer **7**(4): 326-331.
- Oyama, T., H. Maluf, et al. (1999). "Atypical cystic lobules: an early stage in the formation of low-grade ductal carcinoma in situ." Virchows Arch **435**(4): 413-421.
- Page, D. L., W. D. Dupont, et al. (1985). "Atypical hyperplastic lesions of the female breast. A long-term follow-up study." Cancer **55**(11): 2698-2708.
- Pahl, H. L. (1999). "Activators and target genes of Rel/NF-kappaB transcription factors." Oncogene **18**(49): 6853-6866.
- Paik, S., R. Hazan, et al. (1990). "Pathologic findings from the National Surgical Adjuvant Breast and Bowel Project: prognostic significance of erbB-2 protein overexpression in primary breast cancer." J Clin Oncol **8**(1): 103-112.
- Pallares, J., J. L. Martinez-Guitarte, et al. (2004). "Abnormalities in the NF-kappaB family and related proteins in endometrial carcinoma." J Pathol **204**(5): 569-577.
- Palombella, V. J., O. J. Rando, et al. (1994). "The ubiquitin-proteasome pathway is required for processing the NF-kappa B1 precursor protein and the activation of NF-kappa B." Cell **78**(5): 773-785.
- Pan, J. and R. P. McEver (1995). "Regulation of the human P-selectin promoter by Bcl-3 and specific homodimeric members of the NF-kappa B/Rel family." J Biol Chem **270**(39): 23077-23083.
- Park, B. K., H. Zhang, et al. (2007). "NF-kappaB in breast cancer cells promotes osteolytic bone metastasis by inducing osteoclastogenesis via GM-CSF." Nat Med **13**(1): 62-69.
- Park, S. G., C. Chung, et al. (2006). "Up-regulation of cyclin D1 by HBx is mediated by NF-kappaB2/BCL3 complex through kappaB site of cyclin D1 promoter." J Biol Chem **281**(42): 31770-31777.
- Pellinen, T., A. Arjonen, et al. (2006). "Small GTPase Rab21 regulates cell adhesion and controls endosomal traffic of beta1-integrins." J Cell Biol **173**(5): 767-780.
- Pene, F., A. Paun, et al. (2011). "The I{kappa}B Family Member Bcl-3 Coordinates the Pulmonary Defense against Klebsiella pneumoniae Infection." J Immunol **186**(4): 2412-2421.
- Pereira, S. G. and F. Oakley (2008). "Nuclear factor-kappaB1: regulation and function." Int J Biochem Cell Biol **40**(8): 1425-1430.
- Perkins, N. D. (2006). "Post-translational modifications regulating the activity and function of the nuclear factor kappa B pathway." Oncogene **25**(51): 6717-6730.
- Perkins, N. D. (2007). "Integrating cell-signalling pathways with NF-kappaB and IKK function." Nat Rev Mol Cell Biol **8**(1): 49-62.
- Perkins, N. D. and T. D. Gilmore (2006). "Good cop, bad cop: the different faces of NF-kappaB." Cell Death Differ **13**(5): 759-772.
- Perou, C. M., T. Sorlie, et al. (2000). "Molecular portraits of human breast tumours." Nature **406**(6797): 747-752.
- Philp, J. A., T. G. Burdon, et al. (1996). "Differential activation of STATs 3 and 5 during mammary gland development." FEBS Lett **396**(1): 77-80.

- Pikarsky, E., R. M. Porat, et al. (2004). "NF-kappaB functions as a tumour promoter in inflammation-associated cancer." Nature **431**(7007): 461-466.
- Piret, B. and J. Piette (1996). "Topoisomerase poisons activate the transcription factor NF-kappaB in ACH-2 and CEM cells." Nucleic Acids Res **24**(21): 4242-4248.
- Plowman, G. D., J. M. Culouscou, et al. (1993). "Ligand-specific activation of HER4/p180erbB4, a fourth member of the epidermal growth factor receptor family." Proc Natl Acad Sci U S A **90**(5): 1746-1750.
- Ponti, D., A. Costa, et al. (2005). "Isolation and in vitro propagation of tumorigenic breast cancer cells with stem/progenitor cell properties." Cancer Res **65**(13): 5506-5511.
- Pratt, M. A., T. E. Bishop, et al. (2003). "Estrogen withdrawal-induced NF-kappaB activity and bcl-3 expression in breast cancer cells: roles in growth and hormone independence." Mol Cell Biol **23**(19): 6887-6900.
- Pratt, M. A., E. Tibbo, et al. (2009). "The canonical NF-kappaB pathway is required for formation of luminal mammary neoplasias and is activated in the mammary progenitor population." Oncogene **28**(30): 2710-2722.
- Prenzel, N., O. M. Fischer, et al. (2001). "The epidermal growth factor receptor family as a central element for cellular signal transduction and diversification." Endocr Relat Cancer **8**(1): 11-31.
- Puvvada, S. D., W. K. Funkhouser, et al. (2010). "NF-kB and Bcl-3 activation are prognostic in metastatic colorectal cancer." Oncology **78**(3-4): 181-188.
- Quaglino, A., M. Salierno, et al. (2009). "Mechanical strain induces involution-associated events in mammary epithelial cells." BMC Cell Biol **10**: 55.
- Quarrie, L. H., C. V. Addey, et al. (1996). "Programmed cell death during mammary tissue involution induced by weaning, litter removal, and milk stasis." J Cell Physiol **168**(3): 559-569.
- Rahman, N., S. Sea, et al. (2007). "PALB2, which encodes a BRCA2-interacting protein, is a breast cancer susceptibility gene." Nat Genet. **39**:165-167.
- Rangelova, S., S. Kirschnek, et al. (2008). "FADD and the NF-kappaB family member Bcl-3 regulate complementary pathways to control T-cell survival and proliferation." Immunology **125**(4): 549-557.
- Ranger, J. J., D. E. Levy, et al. (2009). "Identification of a Stat3-dependent transcription regulatory network involved in metastatic progression." Cancer Res **69**(17): 6823-6830.
- Rassidakis, G. Z., M. P. Oyarzo, et al. (2003). "BCL-3 overexpression in anaplastic lymphoma kinase-positive anaplastic large cell lymphoma." Blood **102**(3): 1146-1147.
- Ravi, R., G. C. Bedi, et al. (2001). "Regulation of death receptor expression and TRAIL/Apo2L-induced apoptosis by NF-kappaB." Nat Cell Biol **3**(4): 409-416.
- Rebollo, A., L. Dumoutier, et al. (2000). "Bcl-3 expression promotes cell survival following interleukin-4 deprivation and is controlled by AP1 and AP1-like transcription factors." Mol Cell Biol **20**(10): 3407-3416.
- Rehman, A. O. and C. Y. Wang (2009). "CXCL12/SDF-1 alpha activates NF-kappaB and promotes oral cancer invasion through the Carma3/Bcl10/Malt1 complex." Int J Oral Sci **1**(3): 105-118.

- Reis-Filho, J. S. and A. N. Tutt (2008). "Triple negative tumours: a critical review." Histopathology **52**(1): 108-118.
- Renwick, A., D. Thompson, et al. (2006). "ATM mutations that cause ataxia-telangiectasia are breast cancer susceptibility alleles." Nat. Genet. **38**:873-875.
- Reya, T., S. J. Morrison, et al. (2001). "Stem cells, cancer, and cancer stem cells." Nature **414**(6859): 105-111.
- Reynolds, B. A. and S. Weiss (1992). "Generation of neurons and astrocytes from isolated cells of the adult mammalian central nervous system." Science **255**(5052): 1707-1710.
- Rice, N. R., M. L. MacKichan, et al. (1992). "The precursor of NF-kappa B p50 has I kappa B-like functions." Cell **71**(2): 243-253.
- Richard, M., J. Louahed, et al. (1999). "Interleukin-9 regulates NF-kappaB activity through BCL3 gene induction." Blood **93**(12): 4318-4327.
- Richert, M. M., K. L. Schwertfeger, et al. (2000). "An atlas of mouse mammary gland development." J Mammary Gland Biol Neoplasia **5**(2): 227-241.
- Riemann, M., R. Endres, et al. (2005). "The IkappaB protein Bcl-3 negatively regulates transcription of the IL-10 gene in macrophages." J Immunol **175**(6): 3560-3568.
- Rietze, R. L. and B. A. Reynolds (2006). "Neural stem cell isolation and characterization." Methods Enzymol **419**: 3-23.
- Ritter, C. A., M. Perez-Torres, et al. (2007). "Human breast cancer cells selected for resistance to trastuzumab in vivo overexpress epidermal growth factor receptor and ErbB ligands and remain dependent on the ErbB receptor network." Clin Cancer Res **13**(16): 4909-4919.
- Robertson, F. M., M. Bondy, et al. (2010). "Inflammatory breast cancer: the disease, the biology, the treatment." CA Cancer J Clin **60**(6): 351-375.
- Rocha, S., M. D. Garrett, et al. (2005). "Regulation of NF-kappaB and p53 through activation of ATR and Chk1 by the ARF tumour suppressor." Embo J **24**(6): 1157-1169.
- Rocha, S., A. M. Martin, et al. (2003). "p53 represses cyclin D1 transcription through down regulation of Bcl-3 and inducing increased association of the p52 NF-kappaB subunit with histone deacetylase 1." Mol Cell Biol **23**(13): 4713-4727.
- Romieu-Mourez, R., E. Landesman-Bollag, et al. (2002). "Protein kinase CK2 promotes aberrant activation of nuclear factor-kappaB, transformed phenotype, and survival of breast cancer cells." Cancer Res **62**(22): 6770-6778.
- Rothstein, T. L. (2000). "Inducible resistance to Fas-mediated apoptosis in B cells." Cell Res **10**(4): 245-266.
- Rothwarf, D. M., E. Zandi, et al. (1998). "IKK-gamma is an essential regulatory subunit of the IkappaB kinase complex." Nature **395**(6699): 297-300.
- Rouzier, R., C. M. Perou, et al. (2005). "Breast cancer molecular subtypes respond differently to preoperative chemotherapy." Clin Cancer Res **11**(16): 5678-5685.
- Ruan, Q., S. J. Zheng, et al. (2010). "Roles of Bcl-3 in the pathogenesis of murine type 1 diabetes." Diabetes **59**(10): 2549-2557.

- Rusnak, D. W., K. Affleck, et al. (2001). "The characterization of novel, dual ErbB-2/EGFR, tyrosine kinase inhibitors: potential therapy for cancer." Cancer Res **61**(19): 7196-7203.
- Ryseck, R. P., P. Bull, et al. (1992). "RelB, a new Rel family transcription activator that can interact with p50-NF-kappa B." Mol Cell Biol **12**(2): 674-684.
- Sacco, M. G., L. Gribaldo, et al. (1998). "Establishment and characterization of a new mammary adenocarcinoma cell line derived from MMTV neu transgenic mice." Breast Cancer Res Treat **47**(2): 171-180.
- Sarrio, D., S. M. Rodriguez-Pinilla, et al. (2008). "Epithelial-mesenchymal transition in breast cancer relates to the basal-like phenotype." Cancer Res **68**(4): 989-997.
- Schedin, P. (2006). "Pregnancy-associated breast cancer and metastasis." Nat Rev Cancer **6**(4): 281-291.
- Schere-Levy, C., V. Buggiano, et al. (2003). "Leukemia inhibitory factor induces apoptosis of the mammary epithelial cells and participates in mouse mammary gland involution." Exp Cell Res **282**(1): 35-47.
- Schlessinger, J. (2000). "Cell signaling by receptor tyrosine kinases." Cell **103**(2): 211-225.
- Schlette, E., G. Z. Rassidakis, et al. (2005). "Expression of bcl-3 in chronic lymphocytic leukemia correlates with trisomy 12 and abnormalities of chromosome 19." Am J Clin Pathol **123**(3): 465-471.
- Schmid, P., D. Kuhnhardt, et al. (2008). "A phase I/II study of bortezomib and capecitabine in patients with metastatic breast cancer previously treated with taxanes and/or anthracyclines." Ann Oncol **19**(5): 871-876.
- Schmitz, M. L. and P. A. Baeuerle (1991). "The p65 subunit is responsible for the strong transcription activating potential of NF-kappa B." Embo J **10**(12): 3805-3817.
- Schoenenberger, C. A., A. C. Andres, et al. (1988). "Targeted c-myc gene expression in mammary glands of transgenic mice induces mammary tumours with constitutive milk protein gene transcription." Embo J **7**(1): 169-175.
- Schoonbroodt, S., V. Ferreira, et al. (2000). "Crucial role of the amino-terminal tyrosine residue 42 and the carboxyl-terminal PEST domain of I kappa B alpha in NF-kappa B activation by an oxidative stress." J Immunol **164**(8): 4292-4300.
- Schorr, K., M. Li, et al. (1999). "Gain of Bcl-2 is more potent than bax loss in regulating mammary epithelial cell survival in vivo." Cancer Res **59**(11): 2541-2545.
- Schwarz, E. M., P. Krimpenfort, et al. (1997). "Immunological defects in mice with a targeted disruption in Bcl-3." Genes Dev **11**(2): 187-197.
- Schwertfeger, K. L., M. M. Richert, et al. (2001). "Mammary gland involution is delayed by activated Akt in transgenic mice." Mol Endocrinol **15**(6): 867-881.
- Seal, S., D. Thomson, et al. (2006). "mutations in the Fanconi anemia J gene BRIP1 are low-penetrance breast cancer susceptibility alleles." Nat. Genet. **38**:1239-1241.
- Selbert, S., D. J. Bentley, et al. (1998). "Efficient BLG-Cre mediated gene deletion in the mammary gland." Transgenic Res **7**(5): 387-396.
- Sen, R. and D. Baltimore (1986). "Multiple nuclear factors interact with the immunoglobulin enhancer sequences." Cell **46**(5): 705-716.

- Senftleben, U., Y. Cao, et al. (2001). "Activation by IKK $\alpha$  of a second, evolutionary conserved, NF-kappa B signaling pathway." Science **293**(5534): 1495-1499.
- Sha, W. C., H. C. Liou, et al. (1995). "Targeted disruption of the p50 subunit of NF-kappa B leads to multifocal defects in immune responses." Cell **80**(2): 321-330.
- Shen, H. M. and V. Tergaonkar (2009). "NFkappaB signaling in carcinogenesis and as a potential molecular target for cancer therapy." Apoptosis **14**(4): 348-363.
- Siegel, P. M., D. L. Dankort, et al. (1994). "Novel activating mutations in the neu proto-oncogene involved in induction of mammary tumors." Mol Cell Biol **14**(11): 7068-7077.
- Siegel, P. M., E. D. Ryan, et al. (1999). "Elevated expression of activated forms of Neu/ErbB-2 and ErbB-3 are involved in the induction of mammary tumors in transgenic mice: implications for human breast cancer." Embo J **18**(8): 2149-2164.
- Slamon, D. J., G. M. Clark, et al. (1987). "Human breast cancer: correlation of relapse and survival with amplification of the HER-2/neu oncogene." Science **235**(4785): 177-182.
- Slamon, D. J., B. Leyland-Jones, et al. (2001). "Use of chemotherapy plus a monoclonal antibody against HER2 for metastatic breast cancer that overexpresses HER2." N Engl J Med **344**(11): 783-792.
- Sliwkowski, M. X., G. Schaefer, et al. (1994). "Coexpression of erbB2 and erbB3 proteins reconstitutes a high affinity receptor for heregulin." J Biol Chem **269**(20): 14661-14665.
- Smyth, G. K. (2004). "Linear models and empirical bayes methods for assessing differential expression in microarray experiments." Stat Appl Genet Mol Biol **3**: Article3.
- Sole, C., X. Dolcet, et al. (2004). "The death receptor antagonist FAIM promotes neurite outgrowth by a mechanism that depends on ERK and NF-kapp B signaling." J Cell Biol **167**(3): 479-492.
- Soma, L. A., S. M. Gollin, et al. (2006). "Splenic small B-cell lymphoma with IGH/BCL3 translocation." Hum Pathol **37**(2): 218-230.
- Somerville, J. E., L. A. Clarke, et al. (1992). "c-erbB-2 overexpression and histological type of in situ and invasive breast carcinoma." J Clin Pathol **45**(1): 16-20.
- Song, J., E. Sapi, et al. (2000). "Roles of Fas and Fas ligand during mammary gland remodeling." J Clin Invest **106**(10): 1209-1220.
- Sorlie, T., C. M. Perou, et al. (2001). "Gene expression patterns of breast carcinomas distinguish tumor subclasses with clinical implications." Proc Natl Acad Sci U S A **98**(19): 10869-10874.
- Sorlie, T., R. Tibshirani, et al. (2003). "Repeated observation of breast tumor subtypes in independent gene expression data sets." Proc Natl Acad Sci U S A **100**(14): 8418-8423.
- Sotiriou, C., S. Y. Neo, et al. (2003). "Breast cancer classification and prognosis based on gene expression profiles from a population-based study." Proc Natl Acad Sci U S A **100**(18): 10393-10398.
- Souvannavong, V., N. Saidji, et al. (2007). "Lipopolysaccharide from Salmonella enterica activates NF-kappaB through both classical and alternative pathways in primary B Lymphocytes." Infect Immun **75**(10): 4998-5003.
- Sovak, M. A., R. E. Bellas, et al. (1997). "Aberrant nuclear factor-kappaB/Rel expression and the pathogenesis of breast cancer." J Clin Invest **100**(12): 2952-2960.

- Srinivasan, R., C. E. Gillett, et al. (2000). "Nuclear expression of the c-erbB-4/HER-4 growth factor receptor in invasive breast cancers." Cancer Res **60**(6): 1483-1487.
- Stein, T., J. S. Morris, et al. (2004). "Involution of the mouse mammary gland is associated with an immune cascade and an acute-phase response, involving LBP, CD14 and STAT3." Breast Cancer Res **6**(2): R75-91.
- Stern, D. F. and M. Kamps (1988). "EGF-stimulated tyrosine phosphorylation of p185neu: a potential model for receptor interactions." Embo J **7**(4): 995-1001.
- Stern, D. F. (2000). "Tyrosine kinase signalling in breast cancer: ErbB family receptor tyrosine kinases." Breast Cancer Res **2**(3): 176-183.
- Stingl, J. and C. Caldas (2007). "Molecular heterogeneity of breast carcinomas and the cancer stem cell hypothesis." Nat Rev Cancer **7**(10): 791-799.
- Stingl, J., C. J. Eaves, et al. (2001). "Characterization of bipotent mammary epithelial progenitor cells in normal adult human breast tissue." Breast Cancer Res Treat **67**(2): 93-109.
- Stingl, J., P. Eirew, et al. (2006). "Purification and unique properties of mammary epithelial stem cells." Nature **439**(7079): 993-997.
- Storci, G., P. Sansone, et al. (2010). "TNFalpha up-regulates SLUG via the NF-kappaB/HIF1alpha axis, which imparts breast cancer cells with a stem cell-like phenotype." J Cell Physiol **225**(3): 682-691.
- Suh, J., F. Payvandi, et al. (2002). "Mechanisms of constitutive NF-kappaB activation in human prostate cancer cells." Prostate **52**(3): 183-200.
- Sun, S. C., P. A. Ganchi, et al. (1994). "Autoregulation of the NF-kappa B transactivator RelA (p65) by multiple cytoplasmic inhibitors containing ankyrin motifs." Proc Natl Acad Sci U S A **91**(4): 1346-1350.
- Suo, Z., B. Risberg, et al. (2002). "EGFR family expression in breast carcinomas. c-erbB-2 and c-erbB-4 receptors have different effects on survival." J Pathol **196**(1): 17-25.
- Sweeney, C. J., S. Mehrotra, et al. (2005). "The sesquiterpene lactone parthenolide in combination with docetaxel reduces metastasis and improves survival in a xenograft model of breast cancer." Mol Cancer Ther **4**(6): 1004-1012.
- Szymanowska, N., W. Klapper, et al. (2008). "BCL2 and BCL3 are recurrent translocation partners of the IGH locus." Cancer Genet Cytogenet **186**(2): 110-114.
- Talhouk, R. S., M. J. Bissell, et al. (1992). "Coordinated expression of extracellular matrix-degrading proteinases and their inhibitors regulates mammary epithelial function during involution." J Cell Biol **118**(5): 1271-1282.
- Talvensaari-Mattila, A., P. Paakko, et al. (1998). "Matrix metalloproteinase-2 immunoreactive protein: a marker of aggressiveness in breast carcinoma." Cancer **83**(6): 1153-1162.
- Tan, D. S., C. Marchio, et al. (2008). "Triple negative breast cancer: molecular profiling and prognostic impact in adjuvant anthracycline-treated patients." Breast Cancer Res Treat **111**(1): 27-44.
- Tanei, T., K. Morimoto, et al. (2009). "Association of breast cancer stem cells identified by aldehyde dehydrogenase 1 expression with resistance to sequential Paclitaxel and epirubicin-based chemotherapy for breast cancers." Clin Cancer Res **15**(12): 4234-4241.

- Tao, L., A. L. Roberts, et al. (2011). "Repression of mammary stem/progenitor cells by p53 is mediated by Notch and separable from apoptotic activity." Stem Cells **29**(1): 119-127.
- Thangaraju, M., M. Rudelius, et al. (2005). "C/EBPdelta is a crucial regulator of pro-apoptotic gene expression during mammary gland involution." Development **132**(21): 4675-4685.
- Thiery, J. P. (2002). "Epithelial-mesenchymal transitions in tumour progression." Nat Rev Cancer **2**(6): 442-454.
- Thornburg, N. J., R. Pathmanathan, et al. (2003). "Activation of nuclear factor-kappaB p50 homodimer/Bcl-3 complexes in nasopharyngeal carcinoma." Cancer Res **63**(23): 8293-8301.
- Tischkowitz, M., J. S. Brunet, et al. (2007). "Use of immunohistochemical markers can refine prognosis in triple negative breast cancer." BMC Cancer **7**: 134.
- Tonner, E., M. C. Barber, et al. (2002). "Insulin-like growth factor binding protein-5 (IGFBP-5) induces premature cell death in the mammary glands of transgenic mice." Development **129**(19): 4547-4557.
- Trinchieri, G. (2003). "Interleukin-12 and the regulation of innate resistance and adaptive immunity." Nat Rev Immunol **3**(2): 133-146.
- Turksen, K., T. Kupper, et al. (1992). "Interleukin 6: insights to its function in skin by overexpression in transgenic mice." Proc Natl Acad Sci U S A **89**(11): 5068-5072.
- Ueshima, Y., M. L. Bird, et al. (1985). "A 14;19 translocation in B-cell chronic lymphocytic leukemia: a new recurring chromosome aberration." Int J Cancer **36**(3): 287-290.
- Ullrich, A., L. Coussens, et al. (1984). "Human epidermal growth factor receptor cDNA sequence and aberrant expression of the amplified gene in A431 epidermoid carcinoma cells." Nature **309**(5967): 418-425.
- Ursini-Siegel, J., B. Schade, et al. (2007). "Insights from transgenic mouse models of ERBB2-induced breast cancer." Nat Rev Cancer **7**(5): 389-397.
- Usami, Y., S. Satake, et al. (2008). "Snail-associated epithelial-mesenchymal transition promotes oesophageal squamous cell carcinoma motility and progression." J Pathol **215**(3): 330-339.
- Vaillant, F., M. L. Asselin-Labat, et al. (2008). "The mammary progenitor marker CD61/beta3 integrin identifies cancer stem cells in mouse models of mammary tumorigenesis." Cancer Res **68**(19): 7711-7717.
- Valenzuela, J. O., C. D. Hammerbeck, et al. (2005). "Cutting edge: Bcl-3 up-regulation by signal 3 cytokine (IL-12) prolongs survival of antigen-activated CD8 T cells." J Immunol **174**(2): 600-604.
- van Lier, M. G. F., A. Wagner, et al. (2010). "High Cancer Risk in Peutz-Jeghers Syndrome: A Systematic Review and Surveillance Recommendations." The Am Journ Gast **105**:1258-1264.
- Venkitaraman, A. R. (2002). "Cancer susceptibility and the functions of BRCA1 and BRCA2." Cell **108**:171-182.
- Viani, G. A., S. L. Afonso, et al. (2007). "Adjuvant trastuzumab in the treatment of her-2-positive early breast cancer: a meta-analysis of published randomized trials." BMC Cancer **7**: 153.
- Viatour, P., E. Dejardin, et al. (2004). "GSK3-mediated BCL-3 phosphorylation modulates its degradation and its oncogenicity." Mol Cell **16**(1): 35-45.

- Viatour, P., M. P. Merville, et al. (2004). "Protein phosphorylation as a key mechanism for the regulation of BCL-3 activity." Cell Cycle **3**(12): 1498-1501.
- Viatour, P., M. P. Merville, et al. (2005). "Phosphorylation of NF-kappaB and I kappa B proteins: implications in cancer and inflammation." Trends Biochem Sci **30**(1): 43-52.
- Visvader, J. E. (2009). "Keeping abreast of the mammary epithelial hierarchy and breast tumorigenesis." Genes Dev **23**(22): 2563-2577.
- Vizoso, F. J., L. O. Gonzalez, et al. (2007). "Study of matrix metalloproteinases and their inhibitors in breast cancer." Br J Cancer **96**(6): 903-911.
- Vogel, C. L., M. A. Cobleigh, et al. (2001). "First-line Herceptin monotherapy in metastatic breast cancer." Oncology **61 Suppl 2**: 37-42.
- Vogel, C. L., M. A. Cobleigh, et al. (2002). "Efficacy and safety of trastuzumab as a single agent in first-line treatment of HER2-overexpressing metastatic breast cancer." J Clin Oncol **20**(3): 719-726.
- von Minckwitz, G., A. du Bois, et al. (2009). "Trastuzumab beyond progression in human epidermal growth factor receptor 2-positive advanced breast cancer: a german breast group 26/breast international group 03-05 study." J Clin Oncol **27** (12): 1999-2006.
- Walker, R. A. and S. J. Dearing (1999). "Expression of epidermal growth factor receptor mRNA and protein in primary breast carcinomas." Breast Cancer Res Treat **53**(2): 167-176.
- Walton, K. D., K. U. Wagner, et al. (2001). "Conditional deletion of the bcl-x gene from mouse mammary epithelium results in accelerated apoptosis during involution but does not compromise cell function during lactation." Mech Dev **109**(2): 281-293.
- Wang, C. Y., M. W. Mayo, et al. (1996). "TNF- and cancer therapy-induced apoptosis: potentiation by inhibition of NF-kappaB." Science **274**(5288): 784-787.
- Wang, C. Y., M. W. Mayo, et al. (1998). "NF-kappaB antiapoptosis: induction of TRAF1 and TRAF2 and c-IAP1 and c-IAP2 to suppress caspase-8 activation." Science **281**(5383): 1680-1683.
- Wang, F., Y. Shi, et al. (2010). "p52-Bcl3 complex promotes cyclin D1 expression in BEAS-2B cells in response to low concentration arsenite." Toxicology **273**(1-3): 12-18.
- Wang, K. H., A. P. Kao, et al. (2010). "Increasing CD44+/CD24(-) tumor stem cells, and upregulation of COX-2 and HDAC6, as major functions of HER2 in breast tumorigenesis." Mol Cancer **9**: 288.
- Wang, W., J. L. Abbruzzese, et al. (1999). "The nuclear factor-kappa B RelA transcription factor is constitutively activated in human pancreatic adenocarcinoma cells." Clin Cancer Res **5**(1): 119-127.
- Watanabe, N., T. Iwamura, et al. (1997). "Regulation of NFKB1 proteins by the candidate oncoprotein BCL-3: generation of NF-kappaB homodimers from the cytoplasmic pool of p50-p105 and nuclear translocation." Embo J **16**(12): 3609-3620.
- Watson, C. J. (2006). "Involution: apoptosis and tissue remodelling that convert the mammary gland from milk factory to a quiescent organ." Breast Cancer Res **8**(2): 203.
- Watson, C. J. (2006). "Post-lactational mammary gland regression: molecular basis and implications for breast cancer." Expert Rev Mol Med **8**(32): 1-15.

- Watson, C. J. and W. T. Khaled (2008). "Mammary development in the embryo and adult: a journey of morphogenesis and commitment." Development **135**(6): 995-1003.
- Weih, F., D. Carrasco, et al. (1995). "Multiorgan inflammation and hematopoietic abnormalities in mice with a targeted disruption of RelB, a member of the NF-kappa B/Rel family." Cell **80**(2): 331-340.
- Wellings, S. R. and H. M. Jensen (1973). "On the origin and progression of ductal carcinoma in the human breast." J Natl Cancer Inst **50**(5): 1111-1118.
- Wellings, S. R., H. M. Jensen, et al. (1975). "An atlas of subgross pathology of the human breast with special reference to possible precancerous lesions." J Natl Cancer Inst **55**(2): 231-273.
- Wendt, M. K., J. A. Smith, et al. (2010). "Transforming growth factor-beta-induced epithelial-mesenchymal transition facilitates epidermal growth factor-dependent breast cancer progression." Oncogene **29**(49): 6485-6498.
- Wessells, J., M. Baer, et al. (2004). "BCL-3 and NF-kappaB p50 attenuate lipopolysaccharide-induced inflammatory responses in macrophages." J Biol Chem **279**(48): 49995-50003.
- Westerheide, S. D., M. W. Mayo, et al. (2001). "The putative oncoprotein Bcl-3 induces cyclin D1 to stimulate G(1) transition." Mol Cell Biol **21**(24): 8428-8436.
- Wicha, M. S., S. Liu, et al. (2006). "Cancer stem cells: an old idea--a paradigm shift." Cancer Res **66**(4): 1883-1890; discussion 1895-1886.
- Willenbrock, F. and G. Murphy (1994). "Structure-function relationships in the tissue inhibitors of metalloproteinases." Am J Respir Crit Care Med **150**(6 Pt 2): S165-170.
- Williams, T. M., F. Medina, et al. (2004). "Caveolin-1 gene disruption promotes mammary tumorigenesis and dramatically enhances lung metastasis in vivo. Role of Cav-1 in cell invasiveness and matrix metalloproteinase (MMP-2/9) secretion." J Biol Chem **279**(49): 51630-51646.
- Willis, T. G. and M. J. Dyer (2000). "The role of immunoglobulin translocations in the pathogenesis of B-cell malignancies." Blood **96**(3): 808-822.
- Wood, L. D., D. W. Parsons, et al. (2007). "The genomic landscapes of human breast and colorectal cancers." Science **318**:1108-1113.
- Wooster, R., G. Bignell, et al. (1995). "Identification of the breast cancer susceptibility gene BRCA2." Nature **378**:789-792.
- Woronicz, J. D., X. Gao, et al. (1997). "IkappaB kinase-beta: NF-kappaB activation and complex formation with IkappaB kinase-alpha and NIK." Science **278**(5339): 866-869.
- Wright, M. H., A. M. Calcagno, et al. (2008). "Brca1 breast tumors contain distinct CD44+/CD24- and CD133+ cells with cancer stem cell characteristics." Breast Cancer Res **10**(1): R10.
- Wu, C. and S. Ghosh (2003). "Differential phosphorylation of the signal-responsive domain of I kappa B alpha and I kappa B beta by I kappa B kinases." J Biol Chem **278**(34): 31980-31987.
- Wu, Y., J. Deng, et al. (2009). "Stabilization of snail by NF-kappaB is required for inflammation-induced cell migration and invasion." Cancer Cell **15**(5): 416-428.
- Wu, Z. S., Q. Wu, et al. (2008). "Prognostic significance of MMP-9 and TIMP-1 serum and tissue expression in breast cancer." Int J Cancer **122**(9): 2050-2056.

- Wulczyn, F. G., M. Naumann, et al. (1992). "Candidate proto-oncogene bcl-3 encodes a subunit-specific inhibitor of transcription factor NF-kappa B." Nature **358**(6387): 597-599.
- Xiao, G., E. W. Harhaj, et al. (2001). "NF-kappaB-inducing kinase regulates the processing of NF-kappaB2 p100." Mol Cell **7**(2): 401-409.
- Xu, X., C. Prorock, et al. (1993). "Functional interaction of the v-Rel and c-Rel oncoproteins with the TATA-binding protein and association with transcription factor IIB." Mol Cell Biol **13**(11): 6733-6741.
- Yabumoto, K., H. Ohno, et al. (1994). "Involvement of the BCL3 gene in two patients with chronic lymphocytic leukemia." Int J Hematol **59**(3): 211-218.
- Yamaguchi, N., T. Ito, et al. (2009). "Constitutive activation of nuclear factor-kappaB is preferentially involved in the proliferation of basal-like subtype breast cancer cell lines." Cancer Sci **100**(9): 1668-1674.
- Yamazaki, M., T. Akahane, et al. (2004). "Long-term exposure to elevated levels of circulating TIMP-1 but not mammary TIMP-1 suppresses growth of mammary carcinomas in transgenic mice." Carcinogenesis **25**(9): 1735-1746.
- Yan, M., Q. Xu, et al. (2010). "Correlation of NF-kappaB signal pathway with tumor metastasis of human head and neck squamous cell carcinoma." BMC Cancer **10**: 437.
- Yang, J., R. S. Williams, et al. (2009). "Bcl3 interacts cooperatively with peroxisome proliferator-activated receptor gamma (PPARgamma) coactivator 1alpha to coactivate nuclear receptors estrogen-related receptor alpha and PPARalpha." Mol Cell Biol **29**(15): 4091-4102.
- Yeh, T. C., V. Marsh, et al. (2007). "Biological characterization of ARRY-142886 (AZD6244), a potent, highly selective mitogen-activated protein kinase kinase 1/2 inhibitor." Clin Cancer Res **13**(5): 1576-1583.
- Yoneda, T. (2000). "Cellular and molecular basis of preferential metastasis of breast cancer to bone." J Orthop Sci **5**(1): 75-81.
- Yu, H. and R. Jove (2004). "The STATs of cancer--new molecular targets come of age." Nat Rev Cancer **4**(2): 97-105.
- Yu, K., L. Toral-Barza, et al. (2001). "mTOR, a novel target in breast cancer: the effect of CCI-779, an mTOR inhibitor, in preclinical models of breast cancer." Endocr Relat Cancer **8**(3): 249-258.
- Zamora, R., M. Espinosa, et al. (2010). "Depletion of the oncoprotein Bcl-3 induces centrosome amplification and aneuploidy in cancer cells." Mol Cancer **9**: 223.
- Zandi, E., D. M. Rothwarf, et al. (1997). "The IkappaB kinase complex (IKK) contains two kinase subunits, IKKalpha and IKKbeta, necessary for IkappaB phosphorylation and NF-kappaB activation." Cell **91**(2): 243-252.
- Zhang, B., X. Cao, et al. (2008). "Tumor-derived matrix metalloproteinase-13 (MMP-13) correlates with poor prognoses of invasive breast cancer." BMC Cancer **8**: 83.
- Zhang, J., M. A. Warren, et al. (2007). "NFkappaB1/p50 is not required for tumor necrosis factor-stimulated growth of primary mammary epithelial cells: implications for NFkappaB2/p52 and RelB." Endocrinology **148**(1): 268-278.

- Zhang, M. Y., E. W. Harhaj, et al. (1998). "Bcl-3 expression and nuclear translocation are induced by granulocyte-macrophage colony-stimulating factor and erythropoietin in proliferating human erythroid precursors." Blood **92**(4): 1225-1234.
- Zhang, Q., J. A. Didonato, et al. (1994). "BCL3 encodes a nuclear protein which can alter the subcellular location of NF-kappa B proteins." Mol Cell Biol **14**(6): 3915-3926.
- Zhang, Q., M. Yang, et al. (2010). "The role of the intravascular microenvironment in spontaneous metastasis development." Int J Cancer **126**(11): 2534-2541.
- Zhang, X., J. Gureasko, et al. (2006). "An allosteric mechanism for activation of the kinase domain of epidermal growth factor receptor." Cell **125**(6): 1137-1149.
- Zhang, X., H. Wang, et al. (2007). "A role for the IkappaB family member Bcl-3 in the control of central immunologic tolerance." Immunity **27**(3): 438-452.
- Zhao, Y., A. Ramakrishnan, et al. (2005). "Regulation of Bcl-3 through interaction with the Lck tyrosine kinase." Biochem Biophys Res Commun **335**(3): 865-873.
- Zhong, H., M. J. May, et al. (2002). "The phosphorylation status of nuclear NF-kappa B determines its association with CBP/p300 or HDAC-1." Mol Cell **9**(3): 625-636.
- Zhong, H., H. SuYang, et al. (1997). "The transcriptional activity of NF-kappaB is regulated by the IkappaB-associated PKAc subunit through a cyclic AMP-independent mechanism." Cell **89**(3): 413-424.
- Zhong, H., R. E. Voll, et al. (1998). "Phosphorylation of NF-kappa B p65 by PKA stimulates transcriptional activity by promoting a novel bivalent interaction with the coactivator CBP/p300." Mol Cell **1**(5): 661-671.
- Zhou, J., H. Zhang, et al. (2008). "NF-kappaB pathway inhibitors preferentially inhibit breast cancer stem-like cells." Breast Cancer Res Treat **111**(3): 419-427.
- Zhou, Y., S. Eppenberger-Castori, et al. (2005). "The NFkappaB pathway and endocrine-resistant breast cancer." Endocr Relat Cancer **12** Suppl 1: S37-46.
- Zhou, Y., S. Eppenberger-Castori, et al. (2005). "Activation of nuclear factor-kappaB (NFkappaB) identifies a high-risk subset of hormone-dependent breast cancers." Int J Biochem Cell Biol **37**(5): 1130-1144.
- Zhou, Y., C. Yau, et al. (2007). "Enhanced NF kappa B and AP-1 transcriptional activity associated with antiestrogen resistant breast cancer." BMC Cancer **7**: 59.
- Zhu, J., H. Yamane, et al. (2006). "GATA-3 promotes Th2 responses through three different mechanisms: induction of Th2 cytokine production, selective growth of Th2 cells and inhibition of Th1 cell-specific factors." Cell Res **16**(1): 3-10.

